GAZİ ÜNİVERSİTESİ

Gazi

1926

A HIGH EFFICIENT AND ROBUST MPPT CONTROL OF A HYBRID SYSTEM

A THESIS SUBMITTED TO
THE GRADUATE SCHOOL OF NATURAL AND APPLIED SCIENCES
OF
GAZİ UNIVERSITY

BY

Ruhi Zafer ÇAĞLAYAN

IN PARTIAL FULFILLMENT OF THE REQUIREMENTS
FOR
THE DEGREE OF MASTER OF SCIENCE
IN
ELECTRICAL ELECTRONIC ENGINEERING

JUNE 2023

ETHICAL STATEMENT

I hereby declare that in this thesis study I prepared in accordance with thesis writing rules of Gazi University Graduate School of Natural and Applied Sciences;

- All data, information and documents presented in this thesis have been obtained within the scope of academic rules and ethical conduct,
- All information, documents, assessments and results have been presented in accordance with scientific ethical conduct and moral rules,
- All material used in this thesis that are not original to this work have been fully cited and referenced,
- No change has been made in the data used,
- The work presented in this thesis is original,

or else, I admit all loss of rights to be incurred against me.

Ruhi Zafer ÇAĞLAYAN
19/06/2023

A HIGH EFFICIENT AND ROBUST MPPT CONTROL OF A HYBRID SYSTEM

(M. Sc. Thesis)

Ruhi Zafer ÇAĞLAYAN

GAZİ UNIVERSITY

GRADUATE SCHOOL OF NATURAL AND APPLIED SCIENCES

June 2023

ABSTRACT

The energy is needed for all work done in daily life. This energy can be based on human power, mechanical power or electrical power. Power is the key point. For this reason, fossil fuels, nuclear energy, and other renewable sources are used to obtain the required power. In this thesis renewable energy sources are used to produce power. During literature review there is no PV, TEG, Fuel Cell combination with Super Twisting Sliding Mode Control based MPPT application. For this reason the PV,TEG and Fuel Cell is selected as source and Super Twisting Sliding Mode Control is selected as a control method. PV panel is used to convert the sun light or light energy as the electrical energy. PV is commonly used source in the literature. The other source is TEG (Thermoelectric Generator). TEG device uses temperature difference between two surfaces to generate electrical energy. The third source is Fuel Cell. The Fuel Cell used chemical reaction to produce electrical energy. In the system, Fuel Cell will be used as a source and by using reversable types of fuel cell or electrolyser, the fuel cell can be used as battery. Power and voltage characteristics of the mentioned three sources are different from linear power sources. The RES sources have Maximum Power Point (MPP) in the Power Voltage Characteristic. MPP can be obtained from using Maximum Power Point Tracking (MPPT) methods. In the thesis, Super Twisting Sliding Mode Control is selected. The aim is to obtain efficient, sustainable design. For this reason, the control method is very important. Super Twisting Sliding Mode control is reducing the disadvantages of the Sliding Mode Control Method. In the thesis MPPT control the three boost converter and Buck Converter. The system is connected 3 Phase Half Bridge based DC/AC inverter that controlled with Sinusoidal Pulse Width Modulation (SPWM). The aim is to obtain 50 Hz, 220 V_{rms} voltage on load side. The system is worked under two different load types as resistive, and motor load. The system behavior is tested under ideal condition (there are three different test in ideal condition) and under nonideal components (real switching units and components). The aim is to obtain efficiency greater than 98%. To obtain the advantages and disadvantages of the controller, Simulation is tested from using Super Twisting Sliding Mode (STSM) Control and Perturb and Observe Control (P&O). The aim of the test is to ensure the controller performance.

Science Code	:	90544, 90522
Key Words	:	Photovoltaic, Thermoelectric Generator, Fuel Cell, Super Twisting Sliding Mode, Maximum Power Point Tracking Method, Hybrid
Page Number	:	170
Supervisor	:	Assoc. Prof. Dr. Korhan KAYIŞLI

HİBRİT BİR SİSTEMİN YÜKSEK VERİMLİ VE DAYANIKLI MPPT DENETİMİ

(Yüksek Lisans Tezi)

Ruhi Zafer Çağlayan

GAZİ ÜNİVERSİTESİ

FEN BİLİMLERİ ENSTİTÜSÜ

Haziran 2023

ÖZET

Günlük hayatta yapılan tüm işler için enerjiye ihtiyaç vardır. Bu enerji insan gücüne, mekanik güce veya elektrik gücüne dayalı olabilir. Güç kilit noktadır. Bu nedenle gerekli gücü elde etmek için fosil yakıtlar, nükleer enerji ve diğer yenilenebilir kaynaklar kullanılmaktadır. Bu tezde yenilenebilir enerji kaynakları güç üretmek için kullanılmaktadır. Literatür taraması sırasında, Süper Bükümlü Kayan Mod Kontrolü tabanlı MPPT uygulamasına sahip PV, TEG, Yakıt Pili kombinasyonu yoktur. Bu nedenle kaynak olarak PV, TEG ve Yakıt Hücresi, kontrol yöntemi olarak Süper Bükümlü Kayan Mod Kontrolü seçilmiştir. Güneş ışığını veya ışık enerjisini elektrik enerjisine dönüştürmek için PV panel kullanılır. PV literatürde yaygın olarak kullanılan bir kaynaktır. Diğer kaynak ise TEG'dir (Termoelektrik Jeneratör). TEG cihazı, elektrik enerjisi üretmek için iki yüzey arasındaki sıcaklık farkını kullanır. Üçüncü kaynak, Yakıt Pili'dir. Yakıt Hücresi, elektrik enerjisi üretmek için kimyasal reaksiyon kullanır. Sistemde yakıt pili kaynak olarak kullanılacak ve tersinir tipte yakıt pili veya elektrolizör kullanılarak yakıt pili pil olarak kullanılabilir. Bahsedilen üç kaynağın güç ve gerilim özellikleri lineer güç kaynaklarından farklıdır. RES kaynakları, Güç Voltajı Karakteristiğinde Maksimum Güç Noktasına (MPP) sahiptir. MPP, Maksimum Güç Noktası İzleme (MPPT) yöntemleri kullanılarak elde edilebilir. Tezde Süper Bükümlü Kayar Mod Kontrolü seçilmiştir. Amaç verimli, sürdürülebilir tasarım elde etmektir. Bu nedenle kontrol yöntemi çok önemlidir. Süper Bükümlü Kayma Modu kontrolü, Kayan Mod Kontrol Yönteminin dezavantajlarını azaltmaktadır. Tezde MPPT, üç boost dönüştürücüyü ve Buck dönüştürücüyü kontrol eder. Sistem, Sinüzoidal Darbe Genişlik Modülasyonu (SPWM) ile kontrol edilen 3 Fazlı Yarım Köprü tabanlı DC/AC inverter bağlanmıştır. Amaç yük tarafında 50 Hz, 220 Vrms gerilim elde etmektir. Sistem rezistif ve motor yükü olmak üzere iki farklı yük altında çalışmaktadır. Sistem davranışı, ideal koşul altında (ideal durumda üç farklı test vardır) ve ideal olmayan bileşenler (gerçek anahtarlama birimleri ve bileşenleri) altında test edilir. Amaç %98'in üzerinde verim elde etmektir. Denetleyicinin avantajlarını ve dezavantajlarını elde etmek için Simülasyon, Süper Büküm Kayma Modu (STSM) Kontrolü ve Değiştir ve Gözlemle Control (P&O) kullanılarak test edilir. Testin amacı kontrolör performansını sağlamaktır.

Bilim Kodu	:	90544, 90522
Anahtar Kelimeler	:	Fotovoltaik, Termoelektrik Jeneratör, Yakıt Hücresi, Süper Bükümlü Kayma Mod Kontrol, Maksimum Güç Noktası Takip Metodu, Hibrit
Sayfa Adedi	:	170
Danışman	:	Doç. Dr. Korhan KAYIŞLI

ACKNOWLEDGEMENT

I express my thankfulness to my thesis advisor Associate Professor. Dr. Korhan KAYIŞLI who support me with his experience, his knowledge and guidance at every stage of my thesis.

I would like to thank my elders deceased Hüsame BİLGİN and Retired Judge Şemseddin BİLGİN to their moral support during my education life and Master of Science degree. I would like to thank my mother Retired Teacher Major F. Nilgün Bilgin ÇAĞLAYAN, and my father retired High Engineer Lieutenant Colonel Semih ÇAĞLAYAN.

CONTENT LIST

Page

Page

LIST OF TABLES

LIST OF FIGURES

Figures **Pages**

Figures **Pages**

Figures **Pages**

Figures **Pages**

Figures **Pages**

Figures **Pages**

SYMBOLS AND ABBREVIATIONS

Symbols	**Definitions**
&	And
%	Percentage
Δ	Delta
$\dot{V}$	First Derivative of the voltage
F()	Function
$\ddot{V}$	Second Derivative of the voltage
| |	Absolute Value
$\frac{d}{dt}$	Derivative of the function to time
$\sqrt{\ }$	Square Root
$\int$	Integral
s	S Domain Operator
Σ	Sigma Symbol (addition symbol)

Abbreviations	**Definitions**
α	Alpha
α	Alpha Angle Formula 4.58
α	For STSM alpha constant
A	In Matrix form the x's coefficient for derivative of x
AC	Alternating Current
ANN	Artificial Neural Network
β	Beta Angle Formula 4.59
β	For STSM beta constant
B	In Matrix form the d's coefficient for derivative of x
C	Current
C	Capacitance Value
C	In Matrix form the x's coefficient for Output Voltage
c	Light speed
$C_{Boltzman}$	Boltzmann Constant
$c_{cellshort}$,I_{coeff}	Cell's short circuit current temperature

Abbreviations	**Definitions**
CdTe	Cadmium Telluride
CIS	Copper Indium Diselenide
$\boldsymbol{C_p}$	Parasitic Junction Voltage Capacitance Formula 3.3 Coefficient
$\boldsymbol{\gamma}$	Gama
$\boldsymbol{D}$	Duty ratio
D	In Matrix form the d's coefficient for Output Voltage
$\boldsymbol{\tilde{d}}$	DC and AC total duty value.
$\boldsymbol{d}$	Small change of duty (AC part of the duty)
DC	Direct Current
$\boldsymbol{duty}$	Duty value
$\boldsymbol{duty_{AC}}$	Small change of Duty signal (AC part)
$\boldsymbol{duty_{DC}}$	DC Duty signal
D- STATCOM	Distribution Static Synchronous Compensator
ΔE	The Energy Change
$\boldsymbol{\Delta G}$	Gibbs Energy Change
$\boldsymbol{\Delta H^{o}}$	Standard enthalpy change
ΔH	Enthalpy change
$\boldsymbol{\Delta I_L}$	Delta Inductance Current Formula 4.7
Δn(Part 2.3.1)	Change in gasses molar
$\boldsymbol{\Delta S_{\mathrm{Environment}}}$	Environment's Entropy Change
$\boldsymbol{\Delta S_{\mathrm{System}}}$	System's Entropy Change
$\boldsymbol{\Delta S_{\mathrm{Total}}}$	Total Entropy Change
ΔT	Temperature Change or Delta Temperature
$\boldsymbol{\Delta V_o}$	Delta Output Voltage
ΔV	Voltage Change or Delta Voltage
$\boldsymbol{e^+}$	Positron
$\boldsymbol{e^-}$	Electron
E	Energy of the system
$\boldsymbol{e}$	Error
$\boldsymbol{e}$	Euler's Number
$\boldsymbol{E_{\mathrm{final}}}$	Systems final inner energy

Abbreviations	**Definitions**
$\mathbf{E_{initial}}$	Systems initial inner energy
eV	Electron Volt
$\boldsymbol{F}$	A constant that used formula 2.43
$\boldsymbol{f}$	Frequency
FC	Fuel Cell
FPGA	Field Programable Gate Arrays
$\boldsymbol{f_{switch}}$	Switching frequency
GaAs	Gallium Arsenide
$\boldsymbol{H_2O(s), H_2O(g)}$	Liquid water| Gas water
$\boldsymbol{H_2(g)}$	Gas Hydrogen
H	Enthalpy
H	Hydrogen Atom
He	Helium Atom
HOMER	Hypergeometric Optimization of Multiple Energy Resources
Hz	Hertz
I	Current
$\boldsymbol{i(0)}$	Initial Current
$\boldsymbol{i(t)}$	Current at t
$\boldsymbol{I_{ac_{peak}}}$	AC Peak Current
IC	Incremental Conductance
$\boldsymbol{i_c}$	Capacitance Current
$\boldsymbol{I_{coeff}}$	Temperature Coefficient of Short Circuit
$\mathbf{I_d}$	Diode Current
$\boldsymbol{I_{in}}$	Input Current
$\boldsymbol{I_L}$	In the main source the current name is not mentioned Formula 3.3
$\boldsymbol{i_L}$	Inductance Current
$\boldsymbol{I_L}$	DC Current of inductance value
$\boldsymbol{i_L}$	AC current of inductance value
$\boldsymbol{i_{L_{AC}}}$	AC Current Value of Inductance
$\boldsymbol{i_{L_{All}}}$	AC and DC Current of Inductance

Abbreviations	**Definitions**
$I_{L_{DC}}$	DC Current Value of Inductance
I_{Lim}	Limiting Current formula 2.43
$I_{L_{max}}$	Maximum Inductance Current
$I_{L_{min}}$	Minimum Inductance Current
I_{mpp}	Maximum Power Point Current
I_o	Output Current
I_p	Parallel Resistance Current
I_{ph}	Photovoltaic current
I_{photo}	photo voltaic Current
I_{PN}	PN Junction current
I_{PV}	Photovoltaic Output Current
$I_{R_{Load}}$	Series Load Current
$I_{R_{series}}$	Series Resistance Current
I_{sat}	Saturation Current
I_{short}	Short Circuit Current
I_{TEG}	TEG Current
J	Joule
L	Inductance Value
m	Mass of atom
MATLAB	Matrix Laboratory
MeV	Mega Electron Volt
MPP	Maximum Power Point
MPPT	Maximum Power Point Tracking
N	Positive doped Semiconductor
n	Neutron
n**(Part 2.3.1)**	gasses molar
n_{cell}	Number of Cell per PV module
n_elec	Electron number formula 2.43
$O_2(g)$	Gas Oxgyen
P	Positive doped Semiconductor
P (Part 2.3.1)	Pressure of the gas

Abbreviations	Definitions
p	Proton
P&O	Perturb and Observe
PEM	Proton-exchange membrane
P_{H_2}	Pressure of Hydrogen gasses formula 2.43
P_{H_2O}	Pressure of Water gasses formula 2.43
PI	Proportional Integral
PID	Proportional Integral Derivative
P_{in}	For Converters Power of Input
P_{O_2}	Pressure of Oxygen gasses formula 2.43
P_{out}	For Converters Power of Output
$P_{R_{Load}}$	Power of Load Resistance
$P_{R_{series}}$	Power of Series Resistance
PSO	Partial Swarm optimization
P_{TEG}	TEG Power
PV	Photovoltaic
PWM	Pulse Width Modulation
Q	Power Value (MeV or J)
q	Systems heat energy value
R	Resistance (All Circuit Part)
R**(Part 2.3.1)**	A constant which is used in ideal gas theorem
Ref	Reference value
R_{eq}	Equivalent Resistance
RES	Renewable Energy Source
R_{Load}	Load Resistance
$R_{Load_{in}}$	Load Resistance that reflects to input side
R_p	Parallel Resistance
R_s	Series Resistance
R_series	Series Resistance
S	Sun Value $\frac{W}{m^2}$
SM	Sliding Mode Control
SMC	Sliding Mode Control

Abbreviations	**Definitions**
SPWM	Sinusoidal Pulse Width Modulation
$\mathbf{S_{ref}}$	Reference Sun Value 1000 $\frac{W}{m^2}$
STATCOM	Static Synchronous Compensator
STSM	Super Twisting Sliding Mode
STSMC	Super Twisting Sliding Mode Control
T	Temperature
TEG	Thermoelectric Generator
$\mathbf{T_{ref}}$	Reference Temperature Kelvin
THD	Total Harmonic Distortion
$\boldsymbol{T_{switch}}$	Switching time
V	Voltage
V(Part 2.3.1)	Volume of the gasses
$\boldsymbol{v}$	Neutrino
$\mathbf{V(0)}$	Initial Voltage
$\boldsymbol{v(0)}$	Initial Voltage
$\boldsymbol{v(t)}$	Voltage at t
$\boldsymbol{V_{ac_{peak}}}$	AC Peak Voltage
$\boldsymbol{v_c}$	Capacitance Voltage
$\mathbf{V_d}$	Diode Voltage
$\mathbf{v_e}$	Electron Neutrino
$\boldsymbol{V_{in}}$	Input Voltage
$\boldsymbol{V_{in}}$	DC Voltage input
$\boldsymbol{v_{in}}$	AC Voltage input
$\boldsymbol{v_{in_{All}}}$	AC and DC Voltage of Input
$\boldsymbol{v_L}$	Inductance Voltage
$\mathbf{V_{Load}}$	Load Voltage
$\boldsymbol{v_{load}}$	DC and AC Load Voltage
$\boldsymbol{v_{Load_{AC}}, v_{load_{ac}}}$	AC Load Voltage
$\boldsymbol{V_{Load_{DC}}}$	DC Load Voltage
$\mathbf{V_{mpp}}$	Maximum Power Point Voltage
$\boldsymbol{V_o}$	DC Voltage output

Abbreviations	**Definitions**
$\boldsymbol{v_o}$	AC Voltage output
$\boldsymbol{v_{o_{All}}}$	AC and DC Voltage of Output
$\mathbf{V_{oc}}$	Open Circuit Voltage
$\boldsymbol{V_{o_{max}}}$	Maximum Output Voltage
$\boldsymbol{V_{o_{min}}}$	Minimum Output Voltage
$\mathbf{V_{open}}$	Open Circuit Voltage
$\boldsymbol{V_{out}}$	Output Voltage
$\boldsymbol{v_p}$	Parasitic Junction Voltage Formula 3.3
$\boldsymbol{V_{peak}}$	Peak Value of Voltage Signal
$\mathbf{V_{PN}}$	PN Junction Voltage
$\mathbf{V_{PV}}$	Photovoltaic Output Voltage
$\boldsymbol{V_{PV_{system}}}$	PV System Voltage
$\mathbf{V_{R_{Load}}}$	Series Load Voltage
$\mathbf{V_{rms}}$	Root Mean Square Voltage
$\mathbf{V_{R_{series}}}$	Series Resistance Voltage
$\boldsymbol{v_s}$	Source Voltage
$\boldsymbol{v_{s_{AC}}}$	AC part of Source Voltage
$\boldsymbol{V_{s_{DC}}}$	DC part of Source Voltage
$\boldsymbol{V\_t}$	Threshold Voltage
$\mathbf{V_{TEG}}$	Thermoelectric Generator Voltage
$\mathbf{V_{TEG_{out}}}$	Thermoelectric Generator Output Voltage
W	Watt
$\boldsymbol{w}$	Angular Speed ($2\pi f$)
w	Systems work done value (Thermodynamic laws)

1. INTRODUCTION

The usage of electricity has been increased during time. Especially todays, technology is supplied by the electrical energy and it is mainly produced by fossil fuels, hydroelectric power station, independent RESs and the nuclear power plants etc. The fossil fuel reserve of the world is limited and also it is not reusable, pollute the environment, and it is consumed away over time. The hydroelectrical power station is a RES but it is not possible to construct on every place. Also, they are limited sources because they need water level to generate the electricity by using potential difference between two places. The nuclear power plants are used nuclear elements and reactions. During these reactions, the radioactive wave forms are produced to heat and evaporate the water. The generators are fed by the water vapor with high pressure to generate electricity. The process contains radioactive activities, so each nuclear reaction contains dangerous and risky situations. From that knowledge, the independent RESs are very important to product electrical energy.

The RESs also need main source to product electricity. They have limitations and must be used efficiently; however, the RESs are saved and generally cleaned sources. One source produces the required power on the industrial applications. But using combination of the RESs, the power production and efficiency can be increased. In the renewable energy application, one losses factor (such as heat or byproduct of the system) may be source of other RES.

In this thesis, the Photovoltaic system (PV), Thermoelectric Generator (TEG) and Reversible Fuel Cell (FC) are used to produce electrical energy as RESs. PV and TEG device work continuously and the FC produce electrical power if the produced energy is greater than the demanded power. The electrolyser part is started to convert extra energy to the fuel of FC. If the energy production is higher than requirements, the fuel cell store electrical energy. If the energy production is lower than requirements, the fuel cell start to release the stored energy to the load.

In the literature, there is no research that examined these three RESs with Super Twisting Sliding Mode Control (STSMC) based Maximum Power Point Tracking (MPPT). The STSMC algorithm is a high order Sliding Mode (SM) algorithm and it is relatively new method from the other MPPT methods. It is aimed with this MPPT algorithm to obtain, the robust, reliable, highly efficient, clean power production.

Energy is very important for modern world, and all works depend on the energy which can be electrical, mechanical or other type. By the way, the global warming and the environmental (especially air) pollution are important issues for the modern world. In this thesis, the main aim is to investigate electrical energy production from RESs. For this reason, the literature review has also relatively older studies to.

Can was prepared a thesis that examine renewable microgrid system for optimal power planning with the metaheuristic techniques. The wind, PV, hydro and geothermal energy sources were investigated (Can, 2016). One thesis which was done by Keleş in 2017 researched energy and load management of the smart grid system which contains renewable energy systems. In the thesis, one optimization algorithm was proposed to optimize and manage of the electrical consumption of the house by using time rate multiphase amplitude modulation (Keleş, 2017). Another research about renewable energy was Koyuncuoğlu’s thesis which search the blockchain application on smart grid. Wind and solar energy were defined, an also other RESs were mentioned such as bio energy, geothermal energy hydroelectric etc. (Koyuncuoğlu, 2019).

Other application was used for multi objective optimization of household level hybrid renewable energy systems. In this paper, genetic algorithm was used to obtain environmental and economic analysis. (Mayer, Szilagyi and Grof, 2020). The other research was done by Ang et al. to classify, find challenges and give suggestions about usage of RESs. The mentioned energies are; Solar energy, wind energy, hydropower, tidal energy, bioenergy, biomass, biodiesel, geothermal energy, hydrogen energy (Ang, Salem, Kamarol, Das, Nazari and Prabaharan, 2022)

PV panel converts sun light or light to the electrical energy, if the light contains enough energy. For PV panel application this knowledge is important.

The first topic is related with PV panel used systems designed articles The first study was Simmons and Infield’s study about amorphous silicon photovoltaic array in 1996 (Simmons and Infield, 1996). Lloret et.al. presented a study that examine Hybrid PV (PV-

Thermal) system integrated Public Building in Barcelona Spain in 1998 (Andreu, Merten, Puigdollers, Aceves, Sabata, Chantant and Eicker, 1998). The other application example was performed by Nayar. The topic was control and integrate bidirectional inverter in off grid and weak grid using PV power system (Nayar, 2020). Another research was done for off grid residential PV system maintenance experience by Canada et.al. (Canada, Moore, Post and Strachan, 2005). Valcan et.al studied about an application of PV supplied micro grid system to the public grid (Valcan, Marinescu and Kaplanis, 2008). Similar application was performed by Kim et.al by using PV panel to obtain highly efficient low-cost series connected DC-DC converter system to connect PV panel as a supply (Kim, Kim, Yoo and Kim, 2009). A study was done by Qoaider and Steinbrecht and it was related with PV system application for agricultural communities, and examination of cost options to supply energy for off grid system was researched (Qoaider and Steinbrecht, 2010). Gupta et.al. modelled steady state condition of a hybrid energy system that examine off grid electrification for the villages (Gupta, Saini and Sharma, 2010). Saranrom and Polmai performed an application that increase the efficiency of the Series connected PV panels under partial shading condition for using per-panel DC/DC converter (Saranrom and Polmai, 2011). The other application was about lightning system by using solar controller and solar power at off grid condition (He and Chen, 2011).

In 2011, Çalışkan wrote a thesis that designed the DSP based solar converter application for using PV system (Çalışkan, 2011).Other application about smart grid for using PV inverters and voltage control performed by Fawzy et al. (Fawzy, Premm, Bletterie and Gorsek, 2011).Shah, et al. studied smart wireless dc micro-grid application with using PV panel in 2012 (Shah, Chen, Shwab, Shenai, Gouin-Davis and Downey, 2012). And also the inverter application was done like impedance source to the transformer-based Z source inverter fed by PV panel. (Mehdipour, Majdinasab, Khazraj and Kumar, 2012). The sustainability applications for renewable energy projects for off grid rural areas done in The Pangan Island Philippines in 2012 (Hong and Abe, 2012). In 2012, the newer (to their time) technology application which is done by Bandara et al. In the study, multilevel inverter technology was examined for off grid electrification and energy storage (Bandara, Sweet and Ekanayake, 2012). The other application was boosting half bridge PV based micro inverter connected to grid. The used MPPT technique was repetitive current control (Jiang, Cao, Peng and Li, 2012). The other application was classification and comparison application of PV panel supplied DC-DC converter concepts (Kasper, Bortis, Friedli and

Kolar, 2012). An application was performed to improve PV grid connected micro inverters by using active clamp interleaved flyback converters with digital controller (Mo, Chen, Zhang, Zhang and Qian, 2012).

As study was performed by using multifunction converter on Lyapunov function in PV systems to improved quality of the distribution generation (Nguyen and Luo, 2014). Other one was tried to improve PV voltages by using high step-up DC/DC converter. The proposed system was combination of Buck-Boost and flyback converter for high voltage gain (Shen, Lee, Su and Tsai, 2014). A multilevel DC/DC converter research was done by Hafez (Hafez, 2015). Another multilevel application was three phase multilevel inverter application for active filtering. (Sezen, 2015). In 2015, Hakimizad et al. reviewed the design approach of the urban park. The park designed by using renewable energy systems. (Hakimizad, Asl and Ghiai, 2015). The other study performed for the partial shading condition and to use adaptive fuzzy logic based MPPT system for PV panels (Choudhury and Rout, 2015). Başoğlu and Çakır examined a new MPPT method (for their time) which was based on incremental conductance, constant voltage, and look-up table approach and named as improved incremental conductance for PV modules (Başoğlu and Çakır, 2015). A research was done to develop and compare solar tracked PV panel by using improved incremental conductance algorithm (Huynh and Dunnigan, 2016). In 2016, Belkaid et al. presented an application that using modified P&O algorithm for PV application under variable solar radiation. The aim was to improve the performance and handle the disadvantages of the P&O using modified P&O control. (Belkaid, Colak and Kayisli, 2016).

An energy management application was proposed for the residential smart energy storage systems for supplied by hybrid renewable energy. (Alkan, 2016). Another thesis study was done by Koca. The topic of the thesis was cascade H-bridge inverter based multilevel inverter by using PV panel for grid connection (Koca, 2017). Another thesis study and management application about the micro grid system by using PV panel and lithium battery for different load conditions (Gözlükaya, 2018). Ekşi prepared a thesis which examined the Micro PV systems to smart grid applications (Ekşi, 2019).

Not only these applications were done but also the other MPPT techniques and converters were used in the applications. One application which used Cuk converter with direct duty cycle incremental conductance MPPT algorithm for PV Battery system (Belkaid, Colak, Kayıslı and Bayındır, 2019). One of the high efficiencies aimed application about PV panel used Fuzzy Logic Control based MPPT (Belkaid, Colak, Kayıslı and Bayındır, 2020). Other applications were energy conversion related studies. The cascaded DC-AC-AC converters grid connection was used study. The source was PV Panels and the system had AC-Link part (Barrios, Cardenas, Sandoval, Guerrero and Vazquez, 2021). The other research aimed to control a system with MPPT and no need to inverter that supplied electrical thermal load without grid connection. The used techniques were relatively new technique called load segmentation (Eldessouky, Mahmoud and Abdel-Salam, 2023).

The number of studies increasing day by day and this situation the importance of renewable energy source-based researches. There are also studies that analyses the system factors such as cost, efficiency etc. In 1996 Caamano, and Lorenzo did an analysis. In the paper analyses model was estimated PV systems energy performance and economic performance (Caamano and Lorenzo, 1996). Other analysis was performed the technical and economic analysis by using simulation on Grid connected PV systems in 1999 (Reinders, van Dijk, Wiemken and Turkenburg, 1999). The only analysis was not depended on this topic. The other analysis topic was Modeling, simulation and control for output on PV systems for using MATLAB (Fara and Craciunescu, 2017). The other study was performed by using new combine MPPT technique which was based on Incremental voltage step size algorithm and Adaptive Fixed Duty cycle algorithm comparative and experimental analyses. The analysis was done by Srikumar, and Saibabu in 2020 (Srikumar and Saibabu, 2020).

There is also the researched to solve PV connection problem. Their aim was to focus on the problem and tried to solve. Ropp, and Rohatgi wrote an article that tried to prevent islanding problem in grid connected PV systems (Ropp and Rohatgi, 1999). Another research was tried to solve grid connection problems like power quality, islanding mode, voltage distortion for short and long term, voltage fluctuation, harmonics, voltage imbalance and other grid related problems (Arıcı and İskender, 2020).

There are several topics are related to PV panel as a source. The modelling of the PV panel is important for all studies. They firstly needed a simulation model and then real time application was started. Sera et al. wrote a conference paper that modelling PV panel for using datasheet values. In the article the important formulas for the mathematical model and equivalent circuit for mathematical model were given (Sera, Teodorescu and Rodriguez, 2007). The other modelling was done by using Simscape tool to verify the result (Sahoo, Elamvazuthi, Nor, Sebastian and Lim, 2011). The other modelling study was performed with using one diode equivalent circuit model of PV modules. They also obtained the important formulas to convert real PV panel to mathematical equivalent and equivalent circuit model (Qi and Ming, 2012). Edouard and Njomo designed PV solar panel mathematical modelling and digital simulation with MATLAB. They defined the solar panel and derived the equations (Edouard and Njomo, 2013). There were also other studies that done by using PV panel topics. These modelling studies done by Rahman et al. The article published in 2014. (Rahman, Varma and Vanderheide, 2014). Aoun et al. was done another modelling study (Aoun, Chenni, Nahnan and Bouchouicha, 2014). The other study was optical and thermal model combination that predict electrical production study (Hoang, Bourdin, Liu, Caruso and Archambault, 2014). Other modelling study was aimed to found saturation current and ideality factor from open circuit voltage and shorth circuit current of PV model (Meyer, 2017). A thesis study aimed to model and simulate the PV battery power generation microgrid system (Algowairi, 2017). Vinod et al. wrote a paper that modelled the PV panel and simulated for renewable energy solutions (Vinod, Kumar and Singh, 2018). Another study was about polycrystalline silicon PV cell modelling and simulation by using MATLAB/Simulink (Belkaid, Colak, Kayisli, Sara and Bayindir, 2019).

The other important topic is modelling and application of proposed systems. The studies were both modelling PV panel and examining specifical condition. The Coppolaet al. presented a paper designed coupled inductor boost DC-AC Converter (Coppola, Daliento, Guerriero, Lauria and Napoli, 2012). Other one was aimed to obtain multimode operation capacity for PV panel fed an inverter system (Kale, Thale and Agarwal, 2013). Another inverter modelling and application was about micro inverter system application for solar home systems (Loba and Salim, 2013). About modelling and micro grid connection application was done by AbdelHady (AbdelHady, 2017). A PV panel related modelling and application study presented the PV array configurations such as series, series-parallel, honey Comb type connections under partial shading connection application (Pendem and Mikkili, 2018).

There is many different type of PV panel studies have been performed by researchers. Optimization of the systems based on PV panel is another hot topic in literature. Optimization means get better the system for efficiency, cost or other important issues to have more advantages compared to other systems. Kapser et al. prepared a conference paper about system optimization of the PV string under shading condition by using panel voltage equalizing converter and also the system to single converter with overcurrent protection (Kasper, Herden, Bortis and Kolar, 2014). Other optimization study was about sub-panel MPPT to remove the bypass capacitor and optimization the sub panels individually (Marti-Arbona, Mandal, Bakkaloglu and Kiaei, 2015). The Fuzzy logic based MPPT controlled PV was optimized in a thesis (Kocabaş, 2017). Another study was performed by Kayisli in 2023 and aim was parameter optimization of the Super Twisting Sliding mode based II fuzzy based MPPT control. The PV system was examined under variable irradiance condition (Kayisli, 2023).

The following topic is about comparison studies according to control and performance analysis. A thesis related with comparison of MPPT methods under partial shading condition by using MATLAB Simulink (Raof, 2020). And another study was performed to compare different MPPT strategies with using zeta converter used PV system (Başoğlu, 2021). The control topic is also important and a thesis aims to control power flowing, load and energy storage in large scale PV micro grid (Fazalyar, 2021). The last but not least important topic was performance analysis studies. Rastogi et al. wrote an article (not pressed yet) that examined two level reduced-switch D-STATCOM for grid tied PV array using stepped P and O MPPT and modified synchronous reference frame study (Rastogi, Ahmed and Bhat, 2021).

Thermoelectric generators (TEG) devices convert heat energy to the electrical energy. The system works based on Seebeck Effect, Peltier Effect, Thomson Effect, Joule Heating to produce electrical energy (some effects are investigated reverse phenomenon of the producing electricity). In this part, the literature review continues with TEG studies.

Hatzikraniotis et al. was written an article that examine the TEG systems during long term performance and stability under temperature and power cycling. The result shown that for long term usage the Seebeck coefficient was reduced and resistance was increased. (Hatzikraniotis, Zorbas, Samaras, Kyratsi and Paraskevopoulos, 2009). Other TEG related study was modelling a system that use TEG modules controlled by artificial neural networks. (Bilen, 2011). Another TEG related study was multiphase multilevel modular DC/DC converter with zero current switching capacitor dc-dc converter usage together. The aim was to obtain high current and high voltage gain with minimize the losses, such as the switching losses and reduce electromagnetic interference noise (Cao and Peng, 2011). Nagayoshi et al. presented a study that designed 100 W TEG with battery system and it was aimed to achieve high efficiency (96.7%) MPPT power conditioning (Nagayoshi, Nakabayashi, Maiwa and Kajikawa, 2011). Kanimba and Tian wrote a chapter that investigated the modelling of TEG device. The necessary examinations and the founding the important formulas done in the chapter (Kanimba and Tian, 2016). Other modelling study was performed by Belkaid et al. In the paper they modelled the TEG device and simulated the system and used SMC for boost converter. In the article, the comparison of P&O and SMC were done (Belkaid, Colak and Kayıslı, 2017). Yahya et al. prepared conference paper that aimed to improve MPPT performance in TEG system. Kalman filter was used to predict the following variable that reduce the disturbance in real time application. The preferred MPPT method was P&O based MPPT technique (Yahya, Bilgin, Erfidan and Çakir, 2018). Other TEG related application was performance analysis of TEG devices with grid connected photovoltaic inverter. The control mechanism was conventional P&O method with current limit control. (Bijukumar, Raam, Ganesan and Nagamani, 2020). Other TEG device research was phase change material for harvesting energy from changing ambient temperature study. (Tuoi, Toan, and Ono, 2020)

In a study, the TEG device was firstly modelled as mathematical model and it converted to the equivalent circuit. P&O was used to control of boost converter under changing load condition (Mamur and Çoban, 2020). In 2021, there was a review article that review the TEG technology and applications of the TEG devices (Jouhara, Zabnienska-Gora, Khordehgah, Doraghi, Ahmad, Norman, Axcell, Wrobel and Dai, 2021). One of the efficiency studies was Ataol’s thesis and it was aimed to examine the effects of TEG density on close hot air flowing geometries electrical power production efficiency. In this thesis, three-dimensional numerical approach was used. The result showed that if TEG density was increased TEG devices power production was increased (Ataol, 2021).

Vergragt, and Noort wrote an article about mobile hydrogen fuel cell. The long-term challenges and other thing about fuel cell technology were researched (Vergragt and van

Noort, 1996). He presented an article to analyze molten carbonate fuel cell systems numerically. System modelling, system definition and working principles of the system was mentioned (He, 1997). In 1998, He wrote an article about the dynamic performance of Molten carbonate fuel-cell system. The analysis was done by using computational fluid dynamic software as Phoneics, and speedup (He, 1998). One historical development and working principles study was done by Bıyıkoğlu in 2003. In the article review of the Fuel Cell history, working principles of fuel cell and types of fuel cells was presented (Bıyıkoglu, 2003). Another fuel cell application was performed by Obara in 2007. The system used wind power as another RES (Obara, 2007). Obara wrote an article that connect the micro grid with diesel power plant and solid polymer membrane fuel cell. (Obara, 2008). Ural and Gencoglu prepared a conference paper about modelling mathematically of PEM Fuel Cell and it was simulated by using MATLAB/Simulink (Ural, and Gencoglu, 2010). Another conference paper was prepared by Bhuyan et al. The paper aimed to investigate fuel cell connected to the grid via inverter and controlled by hysteresis current control method (Bhuyan and Mahapatra, 2012). Another study examined the fuel cell integrated micro combined heat and power unit on low voltage grid in Danish. The aim was to determine technical issues for different systems which was used fuel cell system for different levels of penetration (You, Marra and Træholt, 2012). In the Özden's thesis, the hybrid hydrogen-solar RESs and electrolysers were examined for standalone application. The simulation was done by using transient systems simulation against the reference system. The real time reference was taken according to Keçiören Research and Training Hospital in Ankara. For obtaining transient systems simulation data, ANSYS Fluent Solver was used (Özden, 2015). The other research study aimed to determine the proton exchange membra fuel cell's thermodynamic, components and application areas. In the article, the usage areas of the fuel cell and historical knowledge about fuel cell was mentioned (Karanfil, 2020). A paper related to mathematical modelling of proton-exchange membrane (PEM) fuel cell was prepared by Omranet al. (Omran, Lucchesi, Smith, Alaswad, Amiri, Wilberforce, Sodre and Olabi, 2021)

For renewable energy systems, the other important issue is storage systems. The renewable energy topic is depending on some external conditions. These external conditions will be discontinuous like wind energy, sun light etc., or continuous like fuel. For both cases, the storage of the power is very important to obtain continuous energy distribution. The storage related studies are written in this paragraph. Latif wrote a thesis to control microgrid RESs with multiple converters. In thesis, the writer mentioned control methods of the microgrid, renewable energy systems, the storage units like batteries, flywheels and supercapacitors (Latif, 2019). Other storage unit mentioned thesis include renewable energy and energy storage systems in smart DC microgrid (Moghanlou, 2020)

The main subject of this thesis is to get hybrid combination of RESs, and the aim is to design a sustainable and efficient system. The system must be new and must improve the literature studies to develop new technologies. In this part, the literature review about the hybrid systems is mentioned.

The first hybrid system type was PV-TEG based. This article researched PV/Thermal system modelling (Zakharchenko, Licea-Jimenez, Perez-Garcia, Vorobiev, Dehesa-Carrasco, Perez-Robles, Gonzalez-Hernandez and Vorobiev, 2004). Ammar et al. wrote a paper about PV/T system with ANN control to track optimum thermal and electrical power. (Ammar, Chaabene and Chotourou, 2013). Alhammad et al. prepared a conference paper to use TEG and thermoelectrical cooler with PV panel to improve the power efficiency. The used control was current control to improve coefficient of performance (Alhammad, Al-Azzawi and Tutunji, 2016). Belkaid, et al. presented a conference paper that used SMC to extract the maximum power from PV-TEG hybrid system (Belkaid, Colak, Kayıslı, Bayındır and Bulbul, 2018). Fini et al. wrote an article about mathematical, numerical and experimental approach to improve the efficiency of hybrid PV and TEG system (Fini, Gharapetian and Asgari, 2022). In 2022, a review study was written to examine of the PV-TEG system for critical factors and parameters. The explored factors and parameters were material properties and other important issues like geometrical structural parameters, solar irradiation, temperature, applied cooling technology, thermal interface material, thermo-mechanical stability, MPPT techniques. (Cotfas, Cotfas, Mahmoudinezhad and Louzazni, 2022)

The other combine system type was PV-Fuel hybrid system. Yu and Yuvarajan prepared a conference study about load sharing condition on hybrid PV- proton exchange membrane fuel cell with PI controller (Yu, Yuvarajan, 2006). Altanneh wrote a thesis study about to design and implementation of the electrical car battery charger system supplied with solar cell and hydrogen fuel cell. Battery systems, solar cells, fuel cells, motor selection and converter were mentioned (Altanneh, 2012). The other study related with optimization to grid connected PV-Fuel Cell- Ultra capacitor system with frequency control. The used optimization algorithm was Partial Swarm Optimization (PSO) algorithm (Hassanzadehfard, Moghaddas-Tafreshi and Hakimi, 2015).

Another hybrid system was about PV-Diesel hybrid system. According to this conference paper and the article study (Caglayan, Kayisli, Zhakiyev, Harrouz and Colak, 2022) diesel can be produced from organic materials, and this biodiesel will be used in diesel systems. In this case, it is possible to operate diesel systems with biodiesel.

Shaahid and El-Amin wrote an article to examine the techno-economic evaluation of the off-grid PV-Diesel battery systems for rural areas in Saudi Arabia (Shaahid and El-Amin, 2009). Yamegeu et al. presented a study about the electricity production of the PV/Diesel hybrid system without battery for off-grid places (Yamagueu, Azoumah, Py and Zongo, 2011). Another real time application study was Nour and Rohani's article and they designed a system and tried to find optimal standalone PV-Diesel hybrid system for rural area in Al Gharbia United Arab Emirates (Nour and Rohani, 2014). Another real time application was performed for Nigerian Oil Producing Communities based on PV-Battery-Diesel systems. In this article, HOMER program was used to optimize of Net Present Cost (Diemuodeke, Agbalagba and Okorho, 2014).

The following topic is about Wind-PV hybrid system. Brent and Rogers wrote a paper about the sustainability of mini hybrid off grid renewable energy systems for rural areas electrification for Africa in 2010 (Brent and Rogers, 2010). Oğuz et al. wrote an article to analyze of the hybrid system efficiency for laboratory illumination by using Wind PV hybrid renewable energy system (Oğuz, Oğuz, Yabanova, Oguz and Kırkbaş, 2012). Another article was integrated the renewable hybrid wind-PV-battery system with reduced number of power converter and fast control for off grid application (Ghoddami, Delghavi and Yazdani, 2012). Other off-grid hybrid wind-PV analyze was done for water pumping system by Vick and Neal (Vick and Neal ,2012). The other application was performed by Gongmeiet al. to examine of Hybrid Wind-PV system for Micro grid connected and islanding operation conditions (Dongmei, Nan and Yanhua, 2012). One thesis was done by Çiçek and RESs supplied from smart grid. The aim was to obtain demand response and optimize the supply (Çiçek, 2013). Other implementation was performed by using Buck converter to hybrid solar-wind system for off-grid condition (Rahman, Razak and Hassan, 2016). Sharma and Suhang presented an article to examine a special control strategy. The strategy includes optimal power point tracking algorithm for hybrid Wind-PV system and the storage units was connected to system via bidirectional Buck/Boost converter The storage units were battery and super capacitor (Sharma and Suhag, 2017). Yapıcı presented a thesis about a novel (to his time) optimization method. The method was integrated to the RESs (mentioned PV and wind), smart grid, and mentioned optimization algorithms as PSO, eagle strategy algorithm, salp swarm algorithm, firefly, and chaotic firefly. The used algorithm was improved PSO with eagle strategy (Yapıcı, 2019). Another optimization related thesis was done by Yılmaz in 2019. The aim was to optimize the power quality of the smart grid and integrated the RESs. In the thesis, ANN was used to predict the optimization conditions (Yılmaz, 2019). Other thesis was related to improve reliability of the Nigeria's electrical grid by using renewable energy systems. Wind, PV, and Pumped Hydro electrical systems were mentioned, but in the methodology part PV and Wind were used to improve of the grid reliability (Koyi, 2019).

One of the types of research was performed by Altun and Kılıç. This study was containing simulation of PV-Wind hybrid energy production. (Altun and Kılıç, 2019). In 2021, Qadir et al. wrote an article to predict the output energy of the PV-wind hybrid system using recursive feature elimination include cross-validation and the data trained by ANN. From the results, the opting feature selection technique had lower mean square error (Qadir, Khan, Khalaji, Munawar, Al-Turjman, Mahmud, Kouzani, and Le, 2021). Zafar et al. wrote an article and tried to predict the produced power to hybrid renewable PV-Wind system. In the article, the improvised dynamic group-based cooperative search mechanism with search radial basis function neural network was used to forecast short times (Zafar, Khan, Mansoor, Mirza, Moosavi and Sanfilippo,2022). The other PV-Wind based study was done by Chakir et al. examined the smart home using electrical vehicle and renewable energy study (Chakir, Abid, Tabaa and Hachimi,2022).

The other hybrid type is Wind-PV and diesel system. Liu et al. prepared a conference paper and they proposed a new (for its time) DC micro grid system that use renewable energy, electrical machines, ultra capacitors (Liu, Chau, Zhong, Zhang, Gao and Wu ,2010). Ullah wrote an article that about using Solar-Wind-Diesel and battery hybrid system. The aim was to reduce the CO_2 emission of diesel system by adding RESs (Ullah, 2013). Another study was done by Vakili et al. The article examined techno-economic feasibility of hybrid PV wind and diesel hybrid system for standalone and grid connected shipyard electrification of Italy (Vakili, Schönborn and Ölçer,2022).

The following hybrid system was PV- Wind and Fuel Cell system. Palizban et al. prepared a conference paper to control the active and reactive power of PV-Wind, Fuel Cell, Electrolyser, and super capacitor system for off-grid mode (Palizban, Rezaei and Mekhilef, 2011). Ganesan et al. wrote an article to model, control and get power management of the grid connected hybrid PV-Wind-Fuel Cell system. The system simulation performed by using MATLAB/Simulink (Ganesan, Dash and Samanta, 2016). Özdemir prepared a thesis to examine the reliability of the PV-Wind- Fuel hybrid system. The loss of load probability, loss of load expectation, energy expected Not Supplied, and energy index of reliability were calculated in the thesis (Özdemir, 2021).

The other hybrid type study was about PV-Wind and Hydro hybrid system. Bekele, and Tadesse performed a study to examine the feasibility of the Hydro-PV-Wind off grid electrification for rural area of Dejen district of Ethiopia. The study used optimization program called as HOMER to optimize the combinations (Bekele and Tadesse, 2012).

The following studies were mentioned more than one hybrid system and researches reviewed or compared the systems. Goel and Ali wrote a feasibility study and optimized the renewable system by using HOMER for remote area electrification in Odisha İndia (Goel and Ali, 2013). Rhaman wrote a study contains more than one hybrid system to obtain sustainable future of Bangladesh's energy system and Wind-Diesel-Battery, PV-Diesel-Battery, Wind-PV-Diesel-Battery systems were mentioned. (Rhaman, 2013). Other paper tried to find optimum configuration of RESs which was performed by Maleki and Askarzadeh. The combinations of the Fuel Cell, PV and wind system was examined by using hybrid metaheuristic technique based on chaotic search, harmony search, simulated annealing methods (Maleki and Askarzadeh, 2013). Beyarslan wrote a thesis about to find optimal solution of renewable energy system for micro grid design by using HOMER program (Beyarslan, 2021). Li et al. presented a study that explored the feasible hybrid renewable energy generation system for resource-based areas of China by using HOMER. The mentioned renewable systems were PW-Wind-Diesel Generator-Battery, PV-Wind Turbine-Battery (Li, Zhou, Zhang and Shan, 2022). Other review-based hybrid system was thermoelectric generator based renewable energy (Wehbi, Taher, Faraj, Castelain and Khaled, 2022).

Bishnoi, and Chaturvedi wrote an article that examined the optimized site for installing the renewable hybrid system to reduce the combustion gasses by using multi-criteria decision making (Bishnoi and Chaturvedi, 2022). Nur presented a thesis about the hybrid AC/DC energy system power flow analyses for smart grid. The aim was to obtain reliable, high quality, cost effective and uninterrupted power for consumption facilities. Newton-Raphson and Gauss-Seidel iteration methods were used for power flow analysis of the system (Nur, 2022).

In the electrical systems, the load is very important and the aim is to supply the load. The power demand should be satisfied, so the load is also important for hybrid system. Because of that, the load sharing topic is also important. For Hybrid systems each source need load for producing power, so the load is important not only one source, but also all system. Yu and Yuvarajan examined the load sharing principles of PV-Fuel Cell devices which was controlled by constant output voltage with PI controller. (Yu and Yuvarajan, 2006)

The power sources generally behave as non-linear. In the working limits of power and voltage or power and current are not linearly growing. There is one point that the derivative of the equation is equal to zero, this means that the maximum point is obtained. The main aim is to obtain this Maximum Power Point (MPP). In the literature, there is a special definition that defines some control algorithm which is track the MPP and called as Maximum Power Point Tracking Methods (MPPT). In the next part of literature review MPPT based studies are mentioned.

Bekker and Beukes investigated the optimal PV panel MPPT method and voltage controlled MPPT was examined (Bekker and Beukes, 2004). Onat and Ersöz wrote a conference paper about the Perturb & Observe (P&O), Constant Voltage, Constant Current, Incremental Conductance (IC), Parasitic Capacitance Algorithm for PV panel. A comparison table shown the efficiency of these algorithms (Onat and Ersöz, 2009). Another MPPT modelling and investigation was done by Roshua et al. In the study, voltage based MPPT with buck-boost converter was used. The result showed that the system more efficient than older (the older than this method) VMPPT based systems

(Roshau, Yuvarajan and Schulz, 2009). Korodi presented a conference paper that built the knowledge based (2 dimensional look up table was used) MPPT algorithm that tracked the MPP. The methods were knowledge-driven method and the classical search method. The classical search method was based on P&O algorithm. The results showed that the new method was faster and had no oscillation around MPP. (Korodi, 2012) Another comparison study about PV based MPPT algorithms was written by Dris and Djilani. The efficiency of fractional open circuit voltage method, P&O and IC algorithms were compared (Dris and Djilani,2013). A PV related study was performed by using Boost converter topology, and soft switching methods used as MPPT method (Erdoğan, Dinçler, Kuncan and Ertunç, 2014). Raj et al. wrote an article that compare ANN, P&O and IC algorithms for PV Panel as a source. The results showed that ANN had extracted same power value with lower oscillation. (Raj, Winston, Ramaraj, and Christabel, 2015). Kurak et al. presented a study about Constant Voltage Algorithm, IC Algorithm and P&O algorithm for PV application. The definitions of P&O algorithm were examined. (Kurak, Erdemir and Dursun, 2016) Belkaid et al. presented a conference paper to compare P&O, IC, SMC and Fuzzy MPPT methods. The results showed that SMC and fuzzy control were better according to efficiency, tracking time and simultaneous static oscillation (Belkaid, Colak and Kayisli, 2017).

The other application about MPPT for PV panel was based comparison of P&O, IC, Fractional Open Voltage, Fuzzy Control and ANN algorithms. (Mnati, Araujo, Abed and Bossche, 2018). Baba et al. wrote a review study about MPPT Methods (Baba, Liu and Chen, 2020). Other review and classification article was written by Mao et al. In the article the basic algorithms and intelligent algorithms were compared. The comparison was performed for cost, efficiency, accuracy (Mao, Cui, Zhang, Guo, Zhou and Huang, 2020). Another review article was written by Tozlu and Calik and they examined conventional Methods (Constant voltage, Fractional order open circuit voltage etc.) and intelligent methods (fuzzy logic, ANN etc.). A comparison was done according to stability, speed, cost, efficiency and other factors. (Tozlu and Calik, 2021). In a similar study, P&O and IC MPPT Methods were compared experimentally by using Field Programmable Gate Arrays (FPGA) under different radiation conditions. (Çelikel and Gündoğdu, 2021). Other article examined the twin rotor multiple input and multiple output system with different control algorithms which PID, Fractional order PID, SMC, STSMC, Fractional order STSMC and combination of both, Fractional order PID and Fractional order STSMC were used. The results showed that the combination method was suitable for these applications (Abukan and Almalı, 2023).

In this thesis, the selected MPPT method is an improved version of SMC, and it is classified as second order SMC. In this part, the SMC based studies are mentioned on the literature.

Levron and Shimilovitz was used SMC to control of the PV for high tracking efficiency, fast dynamics and all range stability. (Levron and Shmilovitz, 2013). The difference between traditional methods and SMC algorithm was examined for achieved the switching surface according to voltage, current and temperature (Vazquez, Azaf, Cervantes, Vazquez and Hernandez, 2015). The other application was done by using wind energy fed induction generator to obtain robust system. They designed special SMC algorithm called low-cost SMC (Djoudi, Chekireb, Berkouk and Bacha, 2015). Other SMC design was performed by Belkaid et al. In the application, solar system and battery was used and modified equivalent SMC is used as controller. The efficiency of the system was nearly 100% (99.6) (Belkaid, Colak and Kayisli, 2016).

Not only the DC-DC converter application was done related this topic, but also one of the DC-AC application by performed by Saheb and Gudey. The used SMC was called fractional order SMC. The results showed that lower steady state error and low total harmonic distortion (THD) was obtained (Saheb and Gudey, 2020). Also, the SMC based STSMC was used in inverter applications. This controller provided low THD and allowed usage of nonlinear load (Güler, 2021). One of the articles searched the Robust Model reference, and Adaptive STSMC and its Lyapunov stability analyses was done. The results showed that proposed system was globally stable and had high robust characteristic (Hollweg, Evald, Milbradt, Tambara and Gründling, 2022). The other study was performed by using Bidirectional converter for constant power load with STSMC. The results were compared with PI control under bounded perturbations. The result showed that system was robust under external system variations. (Hatlehol and Zadeh, 2022).

There are many researches have been presented about SMC based algorithms for especially the robustness, The other important issue is optimization of renewable energy. A thesis study by Yapıcı and he was aimed to propose a new optimization method for the RESs to smart grid integration (Yapıcı, 2019).

The mentioned topics are renewable sources like PV, TEG, Fuel cell, combine sources, MPPT method and the importance of optimization. There are also some studies that review related to renewable energy.

Kartite, and Cherkaoui presented a conference paper about the different structures of the hybrid energy systems. The mentioned hybrid systems were PV system with conventional source, wind system with conventional source, PV/wind/Diesel system, standalone systems, PV with storage, wind with storage, PV/Wind storage hybrid systems. The mentioned optimization algorithms are genetic algorithm, optimization based on degradation, and loss of power supply probability optimization (Kartite and Cherkaoui, 2019) and also, mentioned softwares were Hybrid2, HOMER and RAPSIM. Another study examined the hybrid renewable systems for off-grid electrification in developing countries. The most used sources and the optimization techniques were explored (Zebra, van der Windt, Nhumaio and Faaij, 2021). Naz et al. prepared a review study about hybrid energy controls, combination systems and principles. (Naz, Bou-Rabee, Shukrullah, Gungor and Sulaiman, 2021). Another article examined the renewable energy systems for building to heat, cool and electric production with thermal energy storage. The reference sources, problem studies, and the major results were presented. (Zhang, Oclon, Klemes, Michorczyk, Pielichowska and Pielichowski, 2022). The analysis of hybrid systems and recommendations about hybrid systems were offered (Farhat, Khaled, Faraj, Hachem, Taher and Castelain, 2022). Other study was about countries, hybrid system applications, cost of electrifications, and net present cost using tables (Sohail, Afrouzi, Mehranzamir, Ahmed, Siddique and Tabassum, 2022). The sizing, optimization, controlling and energy management of hybrid renewable energy systems were the subjects of a review study (Ammari, Belatrache, Touhami and Makhloufi, 2022).

All Power Electronic based systems need special circuit topologies. In this part the converter and inverter related studies (which was based on the renewable energy topic) are mentioned. The first topic is DC/DC converter-based studies. An important application report about boost converter was presented by Texas Instruments. In the report the analysis of Boost converter and the matrix form of the equations was obtained (Zaitsu, 2009). Rao, et al. wrote a paper about grid connected high voltage gain DC-DC converter supply asymmetrical multilevel inverter topology for renewable energy applications. (Rao, Kumar and Babu, 2018).

Khan wrote a thesis to examine new (for his time) AC/DC control method. PV Panel was used as a source and the proposed controller was droop (Khan, 2019)

The literature review is very important to determine the thesis topic. The results of this review shows that the renewable energy is very important issue to obtain clean, efficient, and sustainable energy. The researches contain different researchers' studies. There are also some studies which was prepared or presented by us. These sources topics are related to RES and MPPT. In this part, the prepared and presented studies which belongs to us are mentioned.

The conference paper was the case study of the standalone hybrid renewable energy systems and it examined the RESs briefly, and used MPPT techniques. The main objective was to review of the renewable energy combination as hybrid systems, applications and studies (Caglayan, Kayisli, Zhakiyev, Harrouz and Colak, 2022). Second study was a review article of hybrid renewable energy systems and MPPT method. In the article, renewable energy-based sources related studies, MPPT techniques, and the hybrid systems were reviewed and brief summary was presented (Caglayan, Kayisli, Zhakiyev, Harrouz and Colak, 2022). The third article was about Twisting SMC with PV which was used as renewable and nonlinear supply. The total system was examined and analysed based on MPPT dc dc boost converter (Kayisli and Caglayan, 2022).

Hypothesis

- The power sources of the systems are renewable energy-based sources. Not only one source is used, but also three different energy sources are used. (Sun Light, Heating Energy, and Fuel Sources (Hydrogen and other renewable fuels)).

- According to first hypothesis power sources are nonlinear power sources. Their Power – Voltage or Power - Current characteristics are not linear. The MPP should be determined. For this reason, the MPPT techniques are defined by reviewing the literature. In this system, the MPPT control is also used to obtain the MPP.

- The proposed hybrid system has DC-DC Converters fed a DC-AC Converter that supply the AC load. The output of DC-AC Systems will supply resistive, and motor. The examination must be done at least one linear load (resistive-based load) nonlinear load (motor) supplied and the output behavior must be examined.

- The maximum efficiency of renewable energy sources cannot be increased because the efficiency depends on the production technology. The important point is to use the RES on MPP under all conditions. To obtain MPP, the system should be controlled with an efficient of the MPPT Method. In this thesis, the proposed MPPT method is STSMC (one of the second order SMC). The aim is to obtain efficiency value higher than 98%.

- As for the reason to choose STSMC, the robustness and fast response of the method are the first things that come to mind. The aim is to obtain high efficient and sustainable hybrid system. Additionally, minimum one other MPPT method is used to compare with STSMC. The Efficiency Factor is calculated as RESs outputs (output side of boost converters) and the overall output (three phase load output power).

- The STSMC method minimize some disadvantages of the SMC and the selected MPPT Algorithm.

Assumptions

- In the design stage all components are ideal.
- The AC analyses was done by using ideal components.
- For obtaining nonideal condition efficiency the switching elements must be selected as real elements and the efficiency is obtained.
- PV, TEG and Fuel Cell have some limitations like power and voltage limits. In the design. These limitations must be considered.

Limitations

- The RESs like TEG, PV, Fuel Cell are nonlinear power sources. Their control is relatively different than the linear power sources, so the MPPT algorithms are used to control these sources.
- These sources are not ideal and they have losses, and the power extractions are relatively low according to full power (the conversion is not 100% efficient) especially PV panel.
- The TEG device needs heat difference, so the heat difference is obtained by the highest temperature rise element and heating losses of the system is used to generate electricity. For this case, the TEG device cannot start to generate electricity, until the temperature difference is obtained. If the TEG device uses heat energy of another systems, it causes that the other systems heat losses is a source of designed system, so the converted heat energy is greater than the designed systems heat losses, but losses of the other system is not converted to the same system.
- The Electrolyser is not working until the time when the systems power should be greater than limit power.
- The nonideal case is also limitation. It must examine and the efficiency must be found greater than 98%. In the thesis the aim is to obtain higher efficient system.

Definitions

Maximum power point tracking

This is one of the control methods that used for finding maximum power point from the working condition. This topic is used mostly in renewable energy application and nonlinear systems. There are several control methods are defined as Maximum Power Point Tracking Methods.

Super twisting sliding mode control

The Super Twisting Sliding Mode Control is second order sliding mode control methods. This method is defined as one of the Maximum Power Point Tracking Method.

Subatomic particles

The subatomic particles are matter or energy that are the fundamental parts of all materials. These particles will be negative charged like electron, positive charged like proton, and neutral like neutrons. The proton, neutron and electron does not only subatomic particles, also there are quarks, muons and neutrinos. There are also unusual antimatter particles that positron etc. (Sutton, Invictus, Augustyn, Curley, Gaur, Gregersen, Jain, Hosch, Lotha, Cunningham, Rodriguez, Setia, The Editors of Encyclopedia Britannica, 2023)

Free energy

In the thermodynamic, free energy is a word that will be define as the energy like property or state function related to the thermodynamical equilibrium of the system. It shows the work done of the system and change of the system. There are two forms of the free energy; Helmholtz free energy and Gibbs free energy. (The Editors of Encyclopaedia Britannica, Gregersen, Hosch, and Young, 2022)

Entropy

Entropy has different definitions. These definitions are; Entropy is a measure of molecules or systems disorder or randomness. The other definition is systems thermal energy per unit temperature. This was introduced by Rudolf Clausius according to Britannica encyclopedia’s entropy title. (Drake, Schreiber, Gaur, Gregersen, Hosch, Lotha, Manchanda, and The Editors of Encyclopaedia Britannica, 2023)

2. RENEWABLE ENERGY SOURCES

There are several RESs that can be used to produce electrical energy. Most of them is nonlinear energy sources. In this chapter, RESs are examined. There are several RESs can be used in applications, but in this thesis, there are three different types of RESs Photovoltaic (PV) Panels, Thermoelectric Generator (TEG) and, Fuel Cell are selected to use.

2.1. Photovoltaic Generator (PV Panels)

PV Panels are special devices that convert Sun light and heat to the electrical energy. The PV panels are constructed p-n junction areas and these areas consumes the sun power. If the energy of sun lights or light is equal or greater than the needed ionize power, PV device starts to produce electrical energy. In this part, the aim is to examine and define the production chain of electrical energy by using PV panel.

The first step is to define sun light, second is to define electron ejection, third is to obtain the equivalent model of the PV panels, and last is to list the types of PV panels.

2.1.1. Fusion and sunlight

There are several reactions defined in the science of chemistry. One of the reactions is called as nuclear reaction and it happens between nucleus and the subatomic particles.

One of the nuclear reactions is called as fusion. “The fusion reaction is occurred between the light nucleus. The reaction produces heavier elements”. (Mortimer, 1999: 441). According to (Serway and Beichner, 2011: 1483) “the light nucleus are the elements that mass number is less than 20”.

The fusion reaction examples:

$$ {}_{1}^{1}H + {}_{1}^{1}H \rightarrow {}_{1}^{2}H + {}_{1}^{0}e \quad (2.1)$$

$$ {}_{1}^{2}H + {}_{1}^{1}H \rightarrow {}_{2}^{3}He + \gamma \quad (2.2)$$

$$ {}_{2}^{3}He + {}_{2}^{3}He \rightarrow {}_{2}^{4}He + 2{}_{1}^{1}H \quad (2.3)$$

(Mortimer, 1999: 441)

And also

$${}_{1}^{1}H + {}_{2}^{3}He \rightarrow {}_{2}^{4}He + e^{+} + v \qquad (2.4)$$

(Serway and Beichner, 2011: 1484)

The fusion reactions also produce energy. The reaction examples and the produced energies are shown in Eq. 2.5, Eq 2.6, Eq 2.7.

According to (Serway and Beichner, 2011: 1484)

$${}_{1}^{2}H + {}_{1}^{2}H \rightarrow {}_{2}^{3}He + {}_{0}^{1}n \quad Q=3{,}27\ MeV \qquad (2.5)$$

$${}_{1}^{2}H + {}_{1}^{2}H \rightarrow {}_{1}^{3}He + {}_{1}^{1}H \quad Q=4{,}03\ MeV \qquad (2.6)$$

$${}_{1}^{2}H + {}_{1}^{3}H \rightarrow {}_{2}^{4}He + {}_{0}^{1}n \quad Q=17{,}59\ MeV \qquad (2.7)$$

According to (Serway and Beichner, 2011: E.2)

$$1eV = 1.602 * 10^{-19}J \qquad (2.8)$$

$$Q = 3{,}27\ MeV = 5.23854 * 10^{-13}\ J \qquad (2.9)$$

$$Q = 4{,}03\ MeV = 6.45606 * 10^{-13}J \qquad (2.10)$$

$$Q = 17{,}59\ MeV = 2.817918 * 10^{-12}J \qquad (2.11)$$

The sun is the source of life and the main power source of the photosynthetic reactions. It is nearly eternal power source. The energy of the sun is produced by the nuclear reaction called as fusion reactions. The fusion equation is shown below

$$4p \rightarrow {}^{4}He + 2e^{+} + 2v_{e} \qquad (2.12)$$

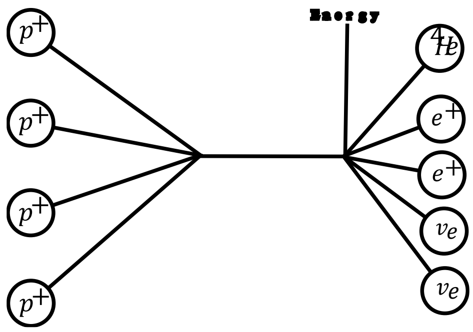

Figure 2.1. The proton used fusion reaction

For this reaction, 4 proton particles converted to 1 Helium atom, 2 positron, and 2 electron neutrinos. This reaction is a nuclear reaction and the result is produced radiation too (Mosteiro et. Al, 2015), (Office of Energy Efficiency & Renewable Energy, n.d.)
The energy quantity will be found by using the formula: Original formula is given in (Conn, 2023)

$$Energy = \left(4 * m_p - \left(m_{He} + 2 * m_e + 2 * m_{v_e}\right)\right) * c^2 \quad (2.13)$$

If the energy is positive the energy is given to output side. The amount of energy from a single reaction is very small, however if the atom amount is nearly tons of atoms, the energy of reaction is very high values.

2.1.2. P-N junction and electron ejection on PV panel

P-N junction

The PV panel has P-N junction surfaces and the sunlight hit the PV Panels surface. The system is made by using semiconductor materials. Atoms of this materials can be pure semiconductor or has some impurities.

If the placed material has greater than 4 valence electrons, the new material is called as n type semiconductor. The impurity atom is called as donor atom.

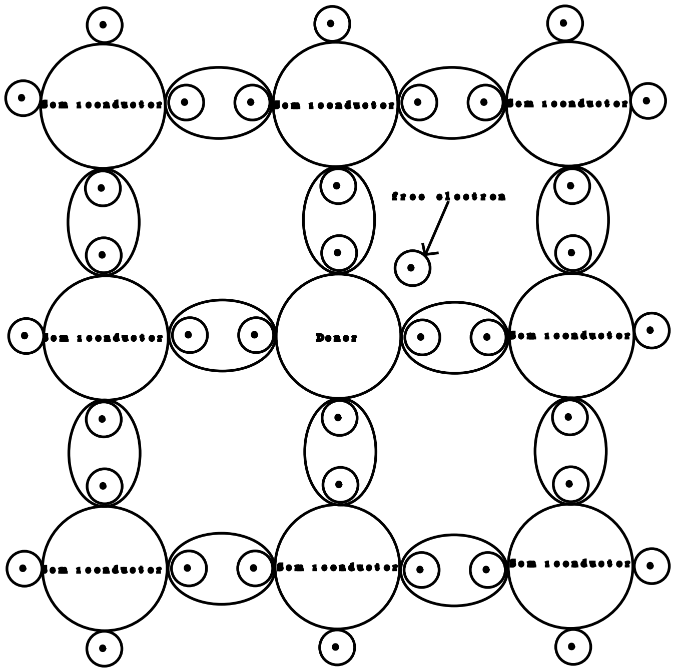

Figure 2.2. N type material

The number of electrons and the nucleus's protons are equal, but the in free space, there are a lot of free electrons of the material. For this type of materials, majority type of carries are electrons and the minority carriers are holes. (Boylestad and Nashelsky, 1998)

If the new element has less than 4 valence electrons, it is called p type material and the impurity element is called acceptor atom.

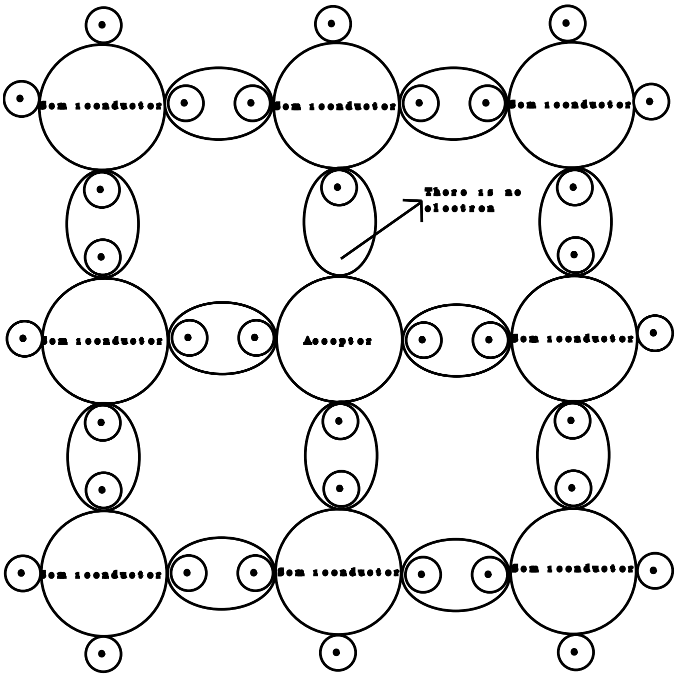

Figure 2.3. P type material

The electron and the proton numbers are equal, but one electron place is empty in the free space. For this type of materials majority type of carriers are holes, and minority carriers are electrons.

PV panel contains P and N type materials which bounded each other and the overall material called as P-N type materials. Diode material is one of the examples of P-N type materials. In diode there is a P-N Junction area and if the enough electrical energy is supplied to the diode, it starts to conduct. The generalization of the current in this type of material

$$I_{PN} = I_{sat} * (e^{\frac{c_{Boltzman} * V_{PN}}{T_{kelvin}}} - 1) \qquad (2.14)$$

The original formula is shown in (Boylestad and Nashelsky, 1998: 14)
This condition is created by using power source, but the only source is sun radiation and the temperature in the PV Panel (also the light is used, but it must be equal or higher than ionized power). For this reason, the electron ejection topic is important, too.

Electron ejection

The new topic is electron ejection from the atom. In 1913 Bohr was explained the Bohr atomic model. In this model there were placed (orbital) that the electron could be found. This placed was called orbitals which had energy. If one electron is changed its place, the energy difference is occurred. If its energy increase, the electron move other orbitals that far from the atoms nucleus. If the electron moves orbitals have lower energy, the electron must be reducing its energy. Energy dissipation is done by the electromagnetic radiation called as photon and the photons energy, and the frequency of photon, is changed by atom to atom. (McGrayne et al., 2023)

The symbolic atom and orbitals are described below. The assumption is that there are 4 orbitals in the atom. Further distance between electron and the outer orbital, the electron become free electron. The nucleus gravity force is decreased by the further distance. After 4th orbital, the electron become free when the nucleus gravity force is broken.

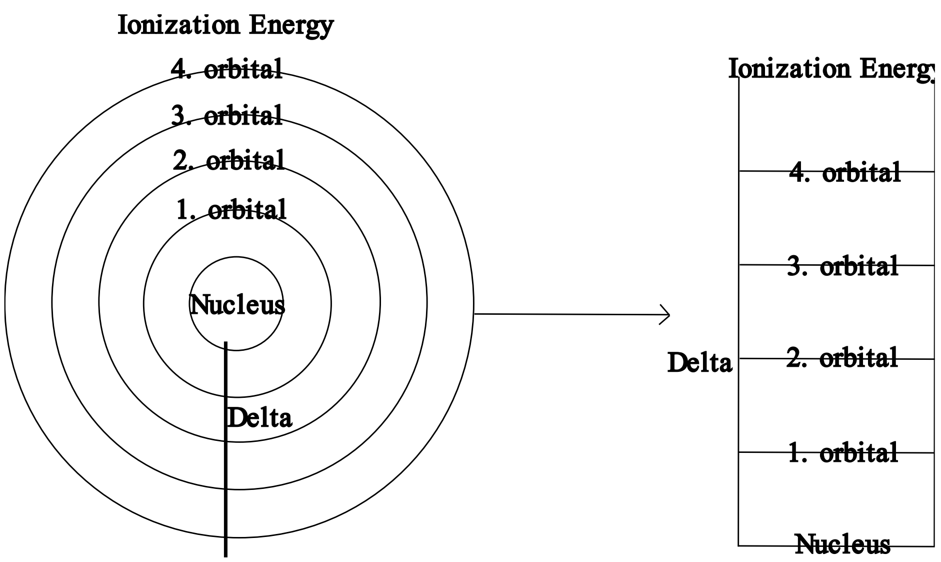

Figure 2.4. Atom and orbital

In figure 2.4, delta surface is selected for showing orbitals and explain the condition. The delta surface is defined as ε and this ε is too small to assume the circle area is nearly linear. The linear configuration shown in Figure 2.5. There are energy gaps between two orbitals the figure is also shown in Figure 2.5.

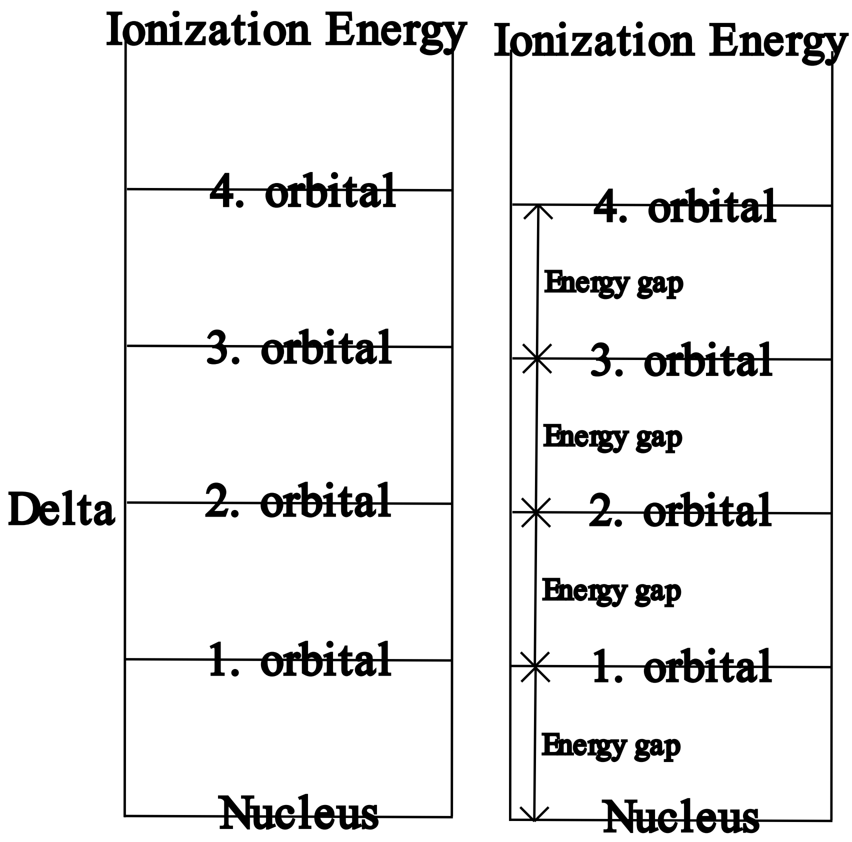

Figure 2.5. The Delta surface and Energy Gap

The electron energy conditions are shown in figure 2.6.

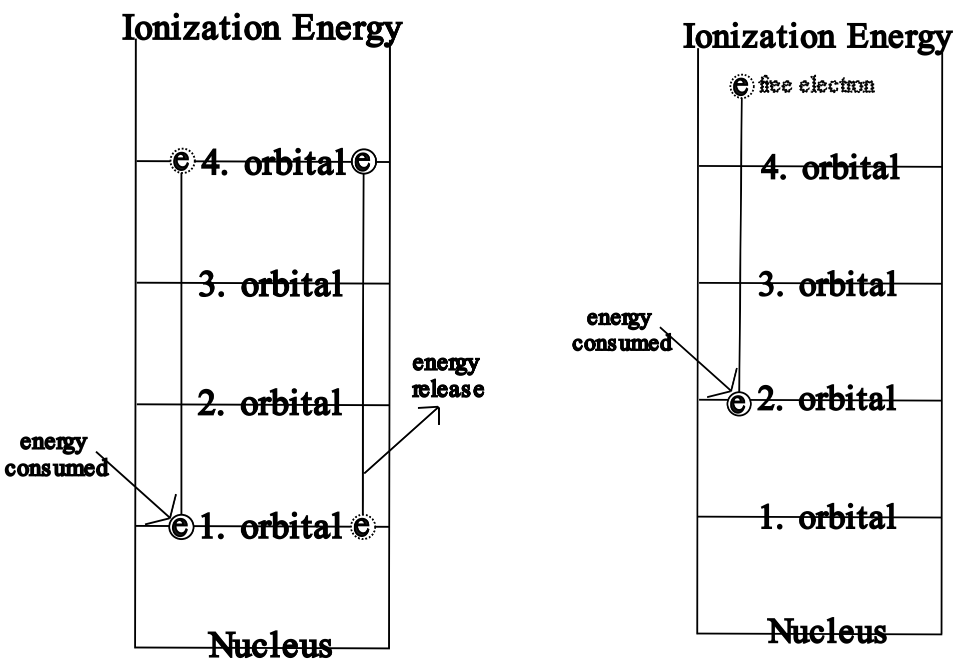

Figure 2.6. Electron movement on delta surface

The energy consumed arrow shown the energy consumption. The electron moves to the higher energy level. In the energy release arrow part, electron reduce its energy by producing photon and the electron move to lover energy level (orbital). The figure 2.6 right figure shows that electron emitted photon. The energy of emitted photon is higher than the energy gap between 4. And 2. orbitals, and the electron become free electron. In the figure 2.6 left figure energy consumed means electron consumes photon energy. The energy release means the electron produces photon to reduce its energy.

2.1.3. Modelling of PV panel

In the part 2.1, the PV panel is investigated totally and the modelling of the PV is mentioned. The PV panel is a special device that aimed to produce electrical energy form sun light. The PV panel has one P-N Junction area like diode and internal resistance like all circuit elements. So, the PV Panel is modelled by using one controlled current source, one diode, one shunt and one series resistance.

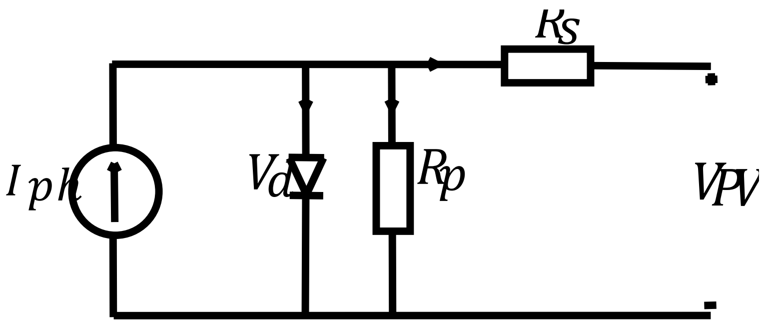

Figure 2.7. PV one diode model

The one diode model of the PV panel is shown in Figure 2.7. In this model one diode model is shown without defining the current names There is also two diode model of the PV, but in this thesis only one diode model of the PV panel is used.

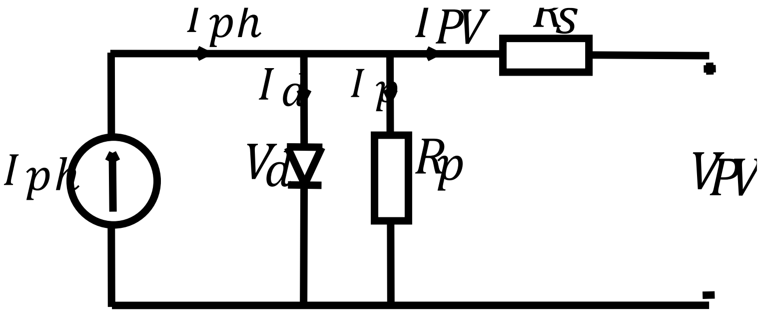

Figure 2.8. PV one diode model Current Model

There are 4 current flow as I_{Ph}, I_d, I_p, I_{PV} defined in the model in Eq 2.15 the relation between source current (I_{Ph}) and other current values are shown (I_d, I_p, I_{PV}).

$$I_{Ph} = I_d + I_p + I_{PV} \tag{2.15}$$

The I_{Ph} is controlled current source and the I_{Ph} value is found in Eq. 2.16:

$$I_{Ph} = \left[I_{short} * c_{cellshort} * \left(T - T_{ref}\right)\right] * \frac{S}{S_{ref}} \tag{2.16}$$

I_d is diode current and is found from Eq. 2.17:

$$I_{PN} = I_{sat} * (e^{\frac{c_{Boltzman} * V_{PN}}{T_{kelvin}}} - 1) \tag{2.17}$$

I_{sat} is dark saturation current and it is found using MATLAB PV model.

I_p is the current passing through R_p:

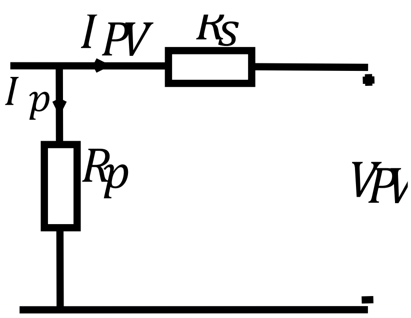

Figure 2.9. Resistance Diagram

$$V_{PV} = I_p * R_p - I_{PV} * R_s \tag{2.18}$$

$$V_{PV} + I_{PV} * R_s = I_p * R_p \tag{2.19}$$

$$I_p = \frac{V_{PV}+I_{PV}*R_s}{R_p} \tag{2.20}$$

From Eq. 2.17, Eq. 2.18, Eq. 2.19, Eq. 2.20 that I_{PV};

$$I_{Ph} = I_{sat} * (e^{\frac{c_{Boltzman}*V_{Ph}}{n_{cell}*T_{kelvin}}} - 1) + \frac{V_{PV}+I_{PV}*R_s}{R_p} + I_{PV} \tag{2.21}$$

$$I_{PV} = I_{Ph} - I_{sat} * \left(e^{\frac{c_{Boltzman}*V_{Ph}}{n_{cell}*T_{kelvin}}} - 1\right) - \frac{V_{PV}+I_{PV}*R_s}{R_p} \tag{2.22}$$

The original formulas (Edouard and Njomo, 2013: 26-27), (Sera, Teodorescu and Rodriguez, 2007: 2392-2393)

The important conditions are Open Circuit, Short Circuit, at Maximum Peak Point

<u>Open circuit</u>

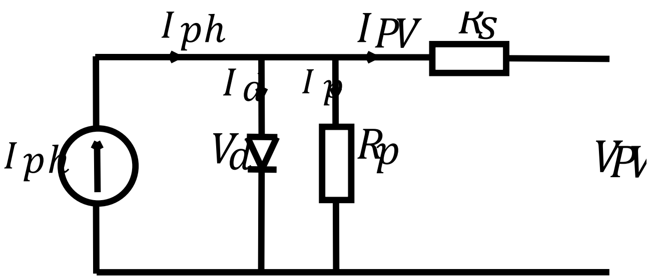

Figure 2.10. Open Circuit Model

$$I_{PV} = 0 \tag{2.23}$$

$$V_{PV} = V_{oc} \tag{2.24}$$

$$0 = I_{Ph} - I_{sat} * \left(e^{\frac{c_{Boltzman}*V_{oc}}{n_{cell}*T_{kelvin}}} - 1\right) - \frac{V_{oc}}{R_p} \tag{2.25}$$

Short circuit

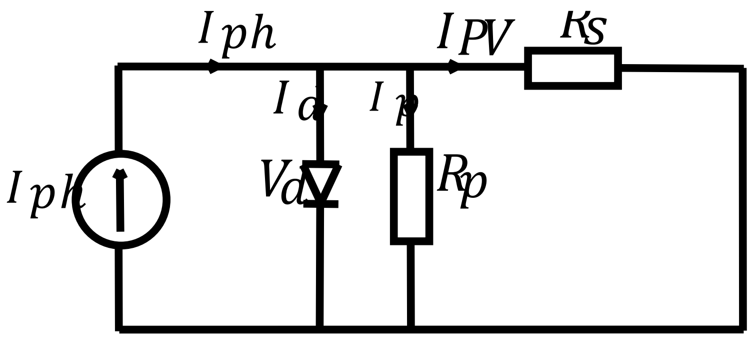

Figure 2.11. Short Circuit Model

$I_{PV} = I_{short}$ (2.26)

$V_{PV} = 0$ (2.27)

$$I_{short} = I_{Ph} - I_{sat} * \left(e^{\frac{c_{Boltzman} * I_{short} * R_S}{n_{cell} * T_{kelvin}}} - 1 \right) - \frac{I_{short} * R_S}{R_p} \quad (2.28)$$

Maximum power point

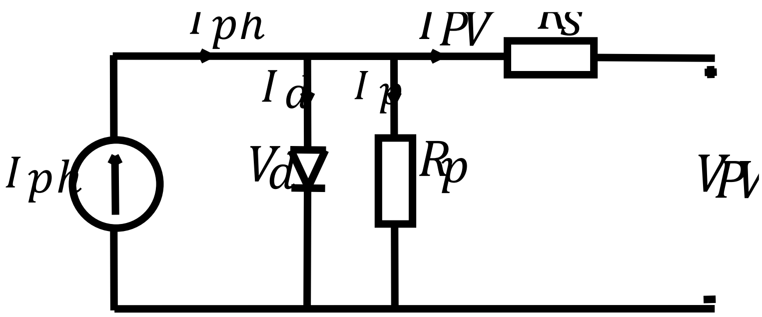

Figure 2.12. Maximum Power Point Model

$$I_{PV} = I_{Ph} - I_{sat} * \left(e^{\frac{c_{Boltzman} * (V_{MPP} + I_{MPP} * R_S)}{n_{cell} * T_{kelvin}}} - 1 \right) - \frac{V_{MPP} + I_{MPP} * R_S}{R_p} \quad (2.29)$$

2.1.4. Types of PV panel

PV panels conduction contains one of the following materials; “Silicon (Si), Gallium Arsenide (GaAs), Copper Indium Diselenide (CIS), Cadmium Telluride (CdTe)” [The more information is given in (Edouard and Njomo, 2013: 25)], “Ribbon Silicon, Amorphous Silicon" (Ekşi, 2019: 12), etc. From using these materials, the PV panel construct. The other classification is "monocrystalline Silicon, polycrystalline Silicon" (Çalışkan, 2011: 7), and "Thin Film PV's". (Can, 2016: 38), other similar studies that examine types of the PV (Ekşi, 2019), (Raof, 2020).

2.2. Thermoelectric Generator (TEG)

The Thermoelectric Generator device means that both convert thermal difference to electrical power and electrical power to thermal energy. The Thermoelectric Generator will use both producing electrical energy from using heat energy, and producing heat from using electrical energy. The Thermoelectric Power Generators has many types:

- Fossil Fuel Based Generators**:** This type of generators is used fossil fuel such as natural gas, wood etc. Their power values are limited between 10 and 100W.
- Solar Source Based Generators: Although this type of generators cannot compete with solar panels, there are areas where they are used.
- Nuclear-fueled generators: The fuel is nuclear fuel. The nuclear reaction of the nuclear element creates energy and the energy become electricity from using this type of Thermoelectric Power Generators. The power range is between 10^{-6} to 100 W (Strohl, Harpestre, President, Intek Inc., Westerville, Ohio, Hosch and The Editors of Encyclopedia Britannica, 2007)

In this experiment our heat energy is produced by our designs most heated element or the external head source. The TEG device is used some important principles;

- Seebeck effect
- Peltier effect
- Thomson effect
- Joule Heating

2.2.1. Seebeck effect

In 1794, Alessandro Volta designed an experiment that found that heated material was electrically attached. This is the first example of the Seebeck influence. (Jouhara, Zabnienska-Gora, Khordehgah, Doraghi, Ahmad, Norman, Axcell, Wrobel and Dai, 2021) In 1821, However, Thomas Johann Seebeck was firstly defined this effect. (Jouhara et al., 2021), (Strohl et al.,2007). The experiment shown that temperature difference between two different conduction material cause voltage difference and it also generate magnetic field. If the two different conductions, whose temperatures were different, was disconnected the current flow was stopped, but in open circuit condition the voltage difference was maintained (Jouhara et al., 2021), (Strohl, et al., 2007), (Kanimba and Tian, 2016)

In the Seebeck phenomenon, there are three variables. The first variable is voltage difference, The second is temperature difference, and the last one is Seebeck coefficient.

$$\Delta V = \alpha \Delta T \tag{2.30}$$

If the initial voltage value is V(0)=0, the formula becomes

$$V = \alpha \Delta T \tag{2.31}$$

(Kanimba and Tian, 2016: 462), (Strohl, et al. , 2007: Seebeck effect)

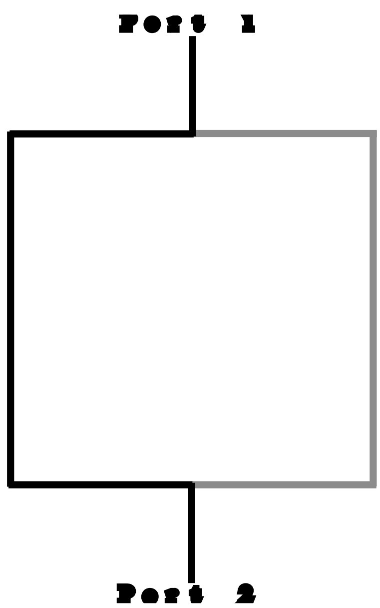

Figure 2.13. Example of TEG

In Figure 2.13, dark side shows hot surface, and grey side shows cold surface. The Port 1 and Port 2 show the entrance of the measurement elements or the circuit connection ports.

2.2.2. Peltier effect

In 1834, (Strohl, et al., 2007: Peltier effect) Jean Charles Athanase (Strohl, et al., 2007: Peltier effect) examined the Seebeck effect and he discovered that one junction of the system would be consumed heat energy, but on the contrary side of the system emitted. (Jouhara et al., 2021)

2.2.3. Thomson effect

In 1855, William Thomson (Lord Kelvin) defined Peltier effect related to junction current, and also, he defined the relation between Peltier and Joule effects (Strohl, et al., 2007). He also defines Celsius degree (known as Thomson coefficient). (Jouhara et al., 2021)

2.2.4. Joule heating

In 1840, Joule was done lots of experiment and examined the first law of thermodynamics. From the result relationship between electrical current and temperature (rising) was involved. (Jouhara et al., 2021)

2.2.5. Mathematical equivalent of the TEG device

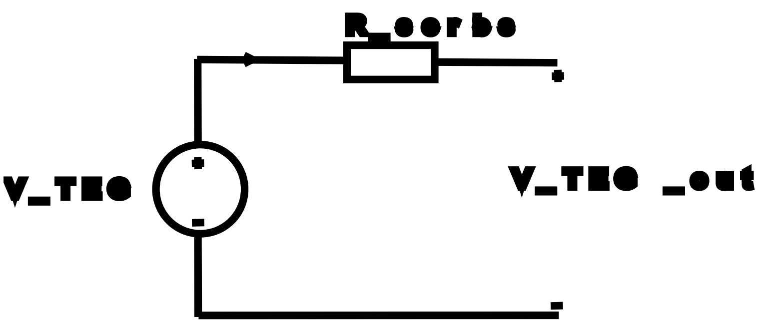

Figure 2.14. Equivalent Model of TEG

In Open Circuit Condition

$$V_{TEG} = \alpha * \Delta T \quad (2.32)$$

ΔT is temperature difference between two surfaces.

The circuit

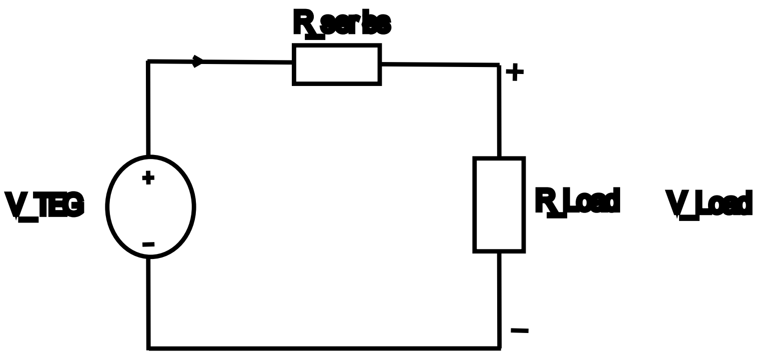

Figure 2.15. Example Circuit

The aim is to obtain maximum power transfer to R_Load. The system seems like Thevenin equivalent circuit of the system in the figure 2.15. The equivalent circuit of maximum power transfer is only the equal power conditions.

$$P_{R_{series}} = P_{R_{Load}} \tag{2.33}$$

$$V_{R_{series}} * I_{R_{series}} = V_{R_{Load}} * I_{R_{Load}} = \frac{P_{TEG}}{2} \tag{2.34}$$

$$V_{R_{series}} = V_{R_{Load}} \tag{2.35}$$

$$I_{R_{series}} = I_{R_{Load}} \tag{2.36}$$

It is assumed that P_{TEG} is constant.

$$V_{TEG} = V_{R_{series}} + V_{R_{Load}} \tag{2.37}$$

$$I_{TEG} = I_{R_{series}} = I_{R_{Load}} \tag{2.38}$$

In the same Thermal conditions,

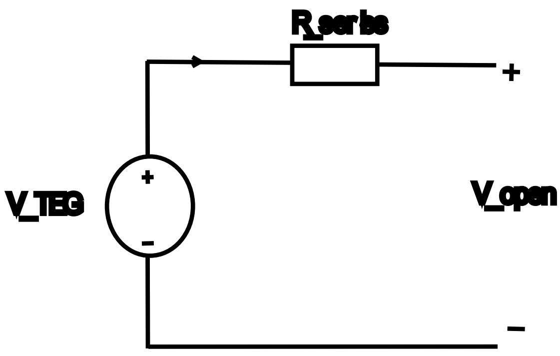

Figure 2.16. TEG Model of Open Circuit Condition

Open circuit equivalence

$$V_{TEG} = V_{open} \tag{2.39}$$

$$V_{TEG} = 2 * V_{R_{series}} \tag{2.40}$$

$$V_{R_{series}} = \frac{V_{TEG}}{2} = \frac{V_{open}}{2} \tag{2.41}$$

$$I_{TEG} = I_{R_{series}} = I_{R_{Load}} = 0 \tag{2.42}$$

$$V_{R_{series}} = \frac{V_{TEG}}{2} = \frac{V_{open}}{2} \tag{2.43}$$

Short circuit equivalent

In the same Thermal conditions

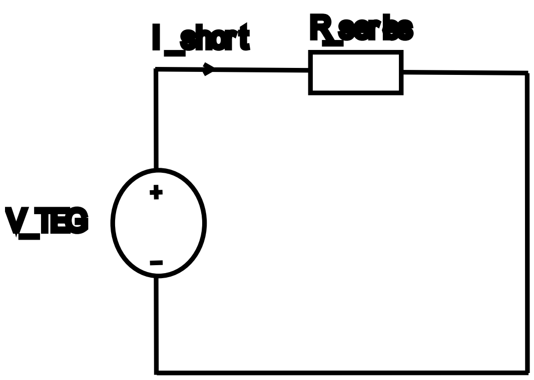

Figure 2.17. TEG Model of Short Circuit Condition

$$I_{short} = I_{TEG} \tag{2.44}$$

Maximum power point

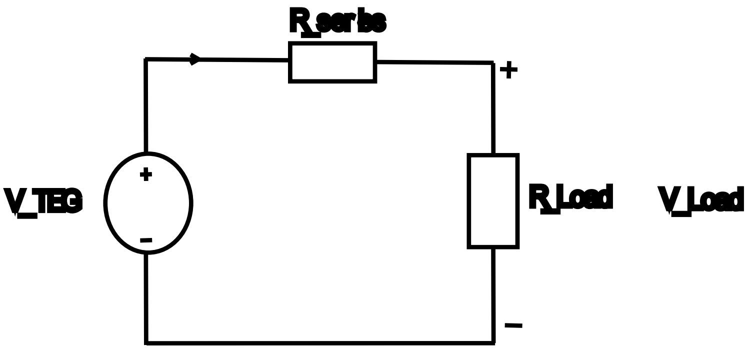

Figure 2.18. Maximum Power Point Circuit

$$I_{TEG} = I_{R_{series}} + I_{R_{Load}} \quad (2.45)$$

$$I_{short} = 2 * I_{R_{Load}} \quad (2.46)$$

$$I_{R_{Load}} = \frac{I_{short}}{2} \quad (2.47)$$

The related study about the Fuel Cell formulas is (Mamur and Çoban,2020)

2.3. Fuel Cell

The third RES is Fuel Cell. From above the sun light is converted to the electricity by using PV panel. The heat energy is converted to the electricity by using TEG device. The third conversion is chemical bound energy is converted to the electricity.

The fuel cell device is used to convert chemical bound energy to the electrical energy the fuel cell device has an advantage to other chemical energy to electrical energy device that the fuel cell has several types. Each type uses different sources. According to (Hydrogen and Fuel Cell Technologies Office, n.d., para. 1), if the hydrogen selected as fuel, the output is only heat, electricity, and water. The fuel cell device will be supply continuously for external sources, so it is long life time than batteries. Because of that the fuel cell will be used for space devices, space crafts, and some places like hospital, school, and other buildings. A fuel cell will design to work reversible. This type of application, the oxygen and hydrogen are produced water, and also the water can be produced the hydrogen and oxygen in working time (Schumm et al., 2023)).

2.3.1. Thermodynamical reaction

Each reaction has own dynamics. The Fuel Cells are devices that using hydrogen, carbon monoxide, and methane like materials in the combustion reactions and this combustion energy turns directly to the electrical energy. Theoretically in ideal conditions the %100 of the free energy is changed to the electrical energy. In reality the value is decreasing. (Mortimer, 2004: 441)

ΔH^o is the standard enthalpy change where at 1 atm (atmosphere pressure unit), at 25°C (Mortimer, 2004: 209). ΔH is represented the enthalpy change. ΔE is the change of the energy.

$$\Delta E = E_{final} - E_{initial} \tag{2.48}$$

If assume:

$$E_{final} = q \tag{2.49}$$

Positive value of q means absorb heat by system. Negative value of q means produce heat by system (Figure 2.24).

$$E_{initial} = w \tag{2.50}$$

And Positive value of w work done by system. Negative value of w means work done against the system. The definitions is given (Mortimer, 1999: 129) (Figure 2.25)

$$H = E + PV \tag{2.51}$$

(Mortimer, 1999: 130)

H: Enthalpy
E: Energy of the system
P: Pressure of the gas
V: Volume of the gasses

For the ideal gasses law

$$PV = nRT \tag{2.52}$$

(Mortimer, 2004: 236)

P: Pressure of the gas
V: Volume of the gasses
n: gasses mollar
T: Temperature

From this the equation become

$$\Delta H = \Delta E + (\Delta n)RT \tag{2.53}$$

(Mortimer, 1999: 132)

Where,

$$R = 8{,}3143 \frac{J}{K * mol}$$

In the thesis the system uses PEM Fuel Cell so the H_2O molecules calculations:
The formation enthalpy of the H_2O is:

$$\mathrm{H_2(g)} + \frac{1}{2}\mathrm{O_2(g)} \rightarrow \mathrm{H_2O(s)} \quad \Delta\mathrm{H^o} = -285{,}9\ \mathrm{kJ} \tag{2.54}$$

For gas formation

$$\mathrm{H_2(g)} + \frac{1}{2}\mathrm{O_2(g)} \rightarrow \mathrm{H_2O(g)} \quad \Delta\mathrm{H^o} = -241{,}8\ \mathrm{kJ} \tag{2.55}$$

(Mortimer, 2004: 209-210)

All chemical bounds contain energy to bound the elements each other. In the formula 2.56, these chemical bound energies are mentioned to $\frac{kj}{mol}$ unit.

H-H(g)→ $2H(g) \quad \Delta H = 435$ kJ

O-O(g)→ $2O(g) \quad \Delta H = 138$ kJ

$O_2(g) \rightarrow 2O(g) \quad \Delta H = 494$ kJ

H-O-H(g)→ $2H(g) + O(g) \quad \Delta H = 926$ kJ

O-H (g)→ $O(g) + H(g) \quad \Delta H = 425$ kJ

H-O-H (g)→ $H(g) + O - H(g) \quad \Delta H = 501$ kJ (2.56)

The bound of the Hydrogen, Oxygen, Hydroxy and Water molecules. Phase condition is also important for the reactions. (Mortimer, 1999: 134-136)

The Enthalpy is mentioned 2.3.1 part. The other important definition is the disorder or randomness of the system. This is called entropy.

<u>The entropy is</u>

$$\Delta S_{Total} = \Delta S_{System} - \Delta S_{Environment} \tag{2.57}$$

(Mortimer, 1999: 137-139)

The third important equation is Gibbs free Energy

$$\Delta G = \Delta H - T * \Delta S \tag{2.58}$$

At 25°C and 1 atm pressure the liquid water is produced:

$$2H_2(g) + O_2(g) \rightarrow H_2O(s) \quad \Delta G = -474{,}42 \text{ kJ} \tag{2.59}$$

(Mortimer, 1999: 144)

2.3.2. Working principle

The Fuel Cell system is a system that convert chemical reaction power to the electrical power.

Non_Reversible Chemical Reactions

Chemical1+Chemical2→ Chemical Product+ Electrical Energy

Reversible Chemical Reactions

$$\text{Chemical1+Chemical2} \rightleftarrows \text{Chemical Product+ Electrical Energy} \quad (2.60)$$

In the Fuel Cell reaction some fuel cell reactions will be reversible. It allows to be designed the system with fuel cell as storage unit. The Fuel Cell has four important parts. The first part is anode part, the second is cathode part, and the other part is catalyzer and the last part of the fuel cell (for example for PEM fuel cell the Proton Exchange Membrane part is this part.) In the thesis the fuel cell system is PEM Fuel Cell. For PEM system the reaction is become according to (Karanfil, 2020: 59):

The Anode reaction is:

Anode Reaction

$$H_2 \rightarrow 2H^+ + 2e^- \quad (2.61)$$

But the real reaction done by catalyzing the Platinum so the reaction will arrange.

Anode Reaction

$$H_2 \xrightarrow{\text{Platinum}} 2H^+ + 2e^- \quad (2.62)$$

The reaction is done by two time to obtain $4H^+$ to obtain the

$$2H_2 \rightarrow 4H^+ + 4e^- \tag{2.63}$$

(Bhuyan, Sao and Mahapatra, 2012: Description of Fuel Cell)

$$2H_2 \overset{\text{Platinum}}{\rightarrow} 4H^+ + 4e^- \tag{2.64}$$

The Catalyzer (Platinum), started the reaction and does not affect after reaction the Platinum is started the reaction catalyze the reaction. If the product is produced the Catalyzer also does not affect resultant part of the reaction.
The second reaction is Cathode reaction according to (Karanfil, 2020: 59):

Cathode Reaction

$$O_2 + 4H^+ + 4e^- \rightarrow 2H_2O \tag{2.65}$$

The Produced Hydrogen ions and electrons reacts with the oxygen and the 2 molecules of water atom are produced. The simple for of the reaction is:

$$2H^+ + \frac{1}{2}O_2 + 2e^- \rightarrow H_2O \tag{2.66}$$

(Bıyıkoğlu, 2003: 527)

The Total Reaction is:

$$2H_2 \overset{\text{Platinum}}{\rightarrow} 4H^+ + 4e^-$$

$$+$$

$$O_2 + 4H^+ + 4e^- \rightarrow 2H_2O$$

$$2H_2 + 2O_2 \rightarrow 2H_2O + \text{Heat energy} + \text{Electrical energy} \tag{2.67}$$

(Karanfil, 2020: 59)

In the reaction the oxygen and hydrogen become water. The electrical energy produced, but the heat energy and chemical bound energy are losses of the system.

2.3.3. Equivalent circuit

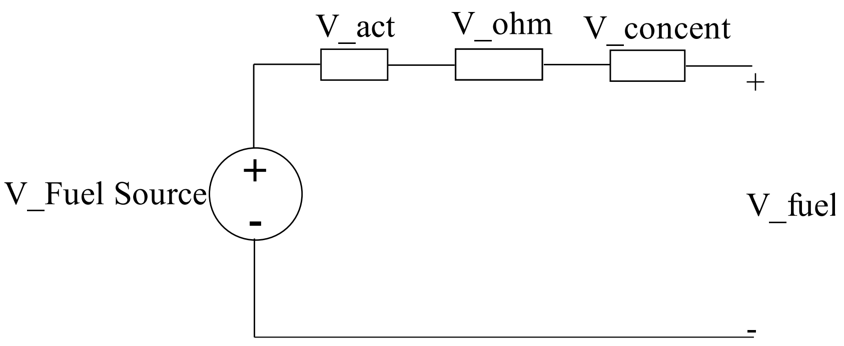

Figure 2.19. Fuel Cell Equivalent Circuit

$$V_{Fuel\,Source} = \frac{-\Delta G}{2*F} + \frac{R*T}{2*F} In(\frac{P_{H_2}\sqrt{P_{O_2}}}{P_{H_2O}}) \tag{2.68}$$

$$V_{act} = \frac{2{,}3*R*T}{\alpha*n_{elec}*F} * In(\frac{I_{FC}}{I_o}) \tag{2.69}$$

$$V_{ohm} = I_{FC} * R_{in} \tag{2.70}$$

$$V_{concent} = -\frac{R*T}{n_{elec}*F} * In(1 - \frac{I_{FC}}{I_L}) \tag{2.71}$$

<u>Open circuit voltage</u>

$$E_{open} = \frac{-\Delta G}{2*F} + \frac{R*T}{2*F} In\left(\frac{P_{H_2}\sqrt{P_{O_2}}}{P_{H_2O}}\right) - \frac{\Delta S}{2*F} * (T - 298{,}15) \tag{2.72}$$

$\mathrm{F} = 968445\ \frac{\mathrm{A.s}}{\mathrm{mol}}$

$\Delta\mathrm{G}$ = Delta free Gibbs Energy

$\mathrm{P_{H_2}}$ = Pressure of Hydrogen Gasses (atm)

$\mathrm{P_{O_2}}$ = Pressure of Oxygen Gasses (atm)

$\mathrm{P_{H_2O}}$ = Pressure of Water Gasses (atm)

$\mathrm{R} = 8{,}3145 \frac{\mathrm{J}}{\mathrm{mol.K}}$

T = Stack Temperature

α = Charge transfer coefficient

$\mathrm{n_{elec}}$ = number of electron

I_{FC} = Fuel Cell Current

I_o = Exchange Current

R_{in} =Total electron and proton resistance

I_L = Limiting Currrent

ΔS = entropy variation

The related studies to this topic (Karanfil, 2020), (Bhuyan, Sao and Mahapatra, 2012), (Bıyıkoğlu, 2003: 527), (Omran et al., 2021), (Ural and Gencoglu, 2010).

2.3.4. Types of fuel cell

Polymer electrolyte membrane fuel cell

Compared to other types, it is light and high powered. It produces electrical energy using hydrogen, oxygen and water. It uses solid polymer, platinum or platinum alloy as catalyst. It is more durable and operates at relatively low temperatures. It is sensitive to carbon monoxide.

Direct methanol fuel cell

It uses fuels such as methanol, ethanol, hydrocarbon. Methanol is the most used fuel.

Alkaline fuel cell

It is one of the oldest fuel cells. The reaction with metals is carried out as a catalyst to the potassium hydroxide solution in water. These types are similar to Polymer Electrolyte Membrane Fuel Cell in general features. It is sensitive to carbon dioxide.

Phosphoric acid fuel cells

These are fuel cells with liquid phosphoric acid as electrolytics and platinum catalyst. It is one of the oldest fuel cells like Alkaline Fuel cells. It is more resistant to poisoning than PEM Fuel cell.

Molten carbonate fuel cells

Uses a mixture of inert ceramic lithium, aluminum oxide suspended carbon salts for the reaction. These types use fuels such as natural gas and biogas as fuel without the need for an additional catalyst. They work at high temperatures such as 650 degrees.

Solid oxide fuel cells

Electrolytes are made of ceramic. They work at high temperatures such as 1000 degrees. It has a high tolerance to Sulphur. They are not affected by carbon monoxide.

Reversible fuel cells

Their fuels are hydrogen and oxygen. Heat and water are produced as products. The reaction is reversible. They can work reversibly with the help of renewable energy (Hydrogen and Fuel Cell Technologies Office, n.d.).

3. MAXIMUM POWER POINT TRACKING (MPPT)

Power Electronics aims to convert one type of electrical power to another type like DC/DC, DC/AC, AC/DC, AC/AC, electrical power to mechanical power, mechanical power to electrical power and other types, or other special topics like STATCOM, High Voltage DC etc.

In the energy conversion of the DC/DC, DC/AC, AC/DC, AC/AC, the source can be linear power sources or nonlinear power sources. The main aim of all the systems is to obtain efficient, low total harmonic distorted, reliable energy conversion. The conversion is done by using switching elements (Diode, BJT, MOSFET, IGBT etc.) which are mostly produced by using semiconductor elements and has special working principles. The power electronic branch uses these devices on special modes to convert energy efficiently. In order to obtain efficient and reliable system, these type of power circuits must be controlled.

From this information, the control techniques are very important and several control methods have been proposed and applied to the systems. There are two types of sources as linear and nonlinear. Linear systems have linear power increases or decreases. However, in the nonlinear system the power does not change linearly. After some conditions, it can rapidly increase, decrease or direction change. Voltage and current relation of the nonlinear systems changes related to the outer conditions. For this type of applications, the aim is to obtain the maximum power extraction/defining the MPP to the source. Optimize the system that follows the characteristic behavior and found MPP.

In this thesis, the sources are chosen as RESs, and they are also nonlinear power sources, so the aim is selected the control that extract maximum power from the source, and the conversion efficiency must be higher. For this aim, the MPPT control algorithms are searched and one system selected as control mechanism.

3.1. MPPT Algorithms

The aim of the MPPT Algorithm is to obtain MPP of the source. For this reason, MPPT algorithm are defined and examined. Some researches are classified according to their different features. Other researches examined the MPPT algorithms and found optimal usage areas. Some studies investigated the MPPT methods with controlling nonlinear sources. The RESs topic is used also nonlinear sources, so the MPPT is important for renewable energy research. The MPPT methods are discussed and described at this section.

3.1.1. Constant voltage method

This technique was mentioned in several researches. In some studies, the name was changed, but the technique was similar. According to the (Mao, Cui, Zhang, Guo, Zhou, and Huang, 2020), (Tozlu and Çalık, 2021), (Mnati, Araujo, Abed, and den Bossche, 2018) there were two techniques about constant voltage. One of them is called as open circuit theorem or fractional open circuit voltage. These resources said that the constant voltage method selected the voltage, and it was closed to actual Voltage MPP. The controller obtains the error and adjust the voltage level. The other method was called as Fractional Open-Circuit Voltage. In this method, the open circuit voltage is multiple with a constant between 0 to 1. The selected values are between 71%-80% (0.71 or 0.8), but the optimal usage was 76% (0.76) according to (Caglayan, Kayisli, Zhakiyev, Harrouz and Colak, 2022). The other sources assumes that these techniques are similar. The main point is that the voltage is constant, the selected voltage is different from open circuit voltage. The selected voltage was near to the MPP.

3.1.2. Constant current method

The similar condition is also valid. Some sources report that there are two different theorems (Constant Current or Short Circuit). The other theorem called Short Circuit Current Theorem. According to the (Caglayan, Kayisli, Zhakiyev, Harrouz and Colak, 2022), the constant range was 78%-92% (0,78-0,92), but the optimum usage was 86% (0,86).

3.1.3. Some special methods

The other theorems are Look-up-Table, Load current or Load Voltage Maximization, PV Output Senseless, Online MPP Search, DC-link Capacitor, (Tozlu and Calik, 2021), Feedback Voltage or Current method, Temperature gradient method, Linear current control method etc. (Baba, Liu and Chen, 2020). In the study (Baba, Liu and Chen, 2020), all the MPPT method classification is given.

3.1.4. Incremental conductance and perturb & observe methods

The most used MPPT methods are Incremental Conductance (IC) algorithm, Perturb and Observe (P&O) algorithm (Hill Climbing).

- Incremental Conductance (IC) algorithm use mathematical calculation to the found the MPP. The method uses this mathematical model which is given in Eq. 3.1.

$$\frac{\Delta I}{\Delta V} \rightarrow -\frac{I}{V} \tag{3.1}$$

$\rightarrow$: Relation of the model

If the $\frac{\Delta I}{\Delta V} < -\frac{I}{V}$ MPP is on the left. (right of MPP)
If the $\frac{\Delta I}{\Delta V} > -\frac{I}{V}$ MPP is on the right. (left of MPP)
If the $\frac{\Delta I}{\Delta V} = -\frac{I}{V}$ MPP is founded.

The related studies (Tozlu and Çalık, 2021), (Mnati et al., 2018), (Onat and Ersöz, 2009), (Kurak, Erdemir and Dursun, 2016: 4), (Çelikel and Gündoğdu, 2021)

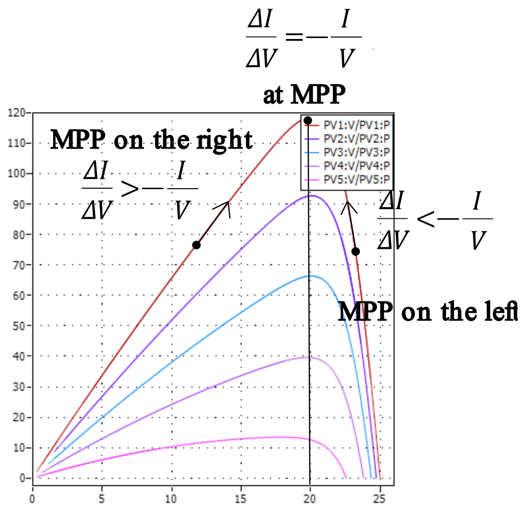

Figure 3.1. PV Panel with controlled by IC

- Perturb & Observe method is based on changes between voltage or duty and power values. Some sources assume that the Hill climbing is also Perturb and Observe (P&O). It was mentioned in (Mao et al., 2020) page 1315. The other assumes that there was difference between them (Baba., Liu and Chen, 2020). The main point is to change one parameter and track the difference to the other parameter.

The main algorithm: (Voltage selected.)

Table 3.1. The table of P&O Voltage Power Relation and Decision

Perturb and Observe Algorithm		
Voltage Change	Power Change	Next Step for Voltage
(1) Increase	(1’) Increase	Increase
(2) Increase	(2’) Decrease	Decrease
(3) Decrease	(3’) Increase	Increase
(4) Decrease	(4’) Decrease	Decrease

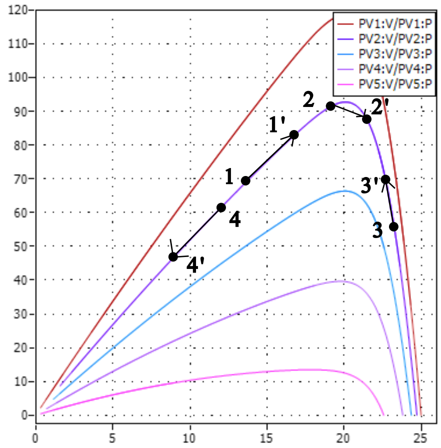

Figure 3.2. PV Panel Controlled by P&O

The related researches (Mao et al., 2020), (Baba, Liu and Chen, 2020), (Onat and Ersöz, 2009), (Çelikel and Gündoğdu, 2021), (Mnati et al., 2018), (Tozlu, and Çalık, 2021), (Dris and Djilani, 2013), (Raj et al., 2015), (Kurak, Erdemir and Dursun, 2016),

3.1.5. Parasitic capacitance method

This method uses the parasitic junction capacitance value to find MPP. The mathematical calculation ensures the MPP which is given in Formula 3.2.

$$I = I_{Photo} - I_o \left(e^{\frac{V_{OC} - I*R}{V_t}} - 1 \right) \tag{3.2}$$

To find the capacitance according to (Baba, Liu and Chen, 2020: Parasitic Capacitance), the equation become as;

$$I = I_L - I_o * \left[\exp\left(\frac{V_p + R_S * I}{a} \right) - 1 \right] + C_p * \frac{dv_p}{dt} = F(v_p) + C_p * \frac{dv_p}{dt} \tag{3.3}$$

For calculation:

$$\frac{dF(v_p)}{dt} + C_p * \left(\frac{\dot{V}}{V} + \frac{\ddot{V}}{\dot{V}} \right) + \frac{F(v_p)}{v_p} = 0 \tag{3.4}$$

(Baba, Liu and Chen, 2020, para. Parasitic Capacitance)

The related studies (Mao et al., 2020) , (Baba, Liu and Chen, 2020), (Tozlu and Çalık, 2021)

3.1.6. Soft switching techniques with MPPT

This is another option to get MPP. In one research, the soft switching techniques with MPPT was used to reduce the losses of switching. The Soft Switching techniques are “Zero Current Switching, Zero Voltage Switching, Zero Voltage Transition, Zero Current Transition” (Erdoğan et al., 2014: 1057).

3.1.7. Intelligent methods

These methods are based on artificial intelligence-based techniques. These techniques are Fuzzy logic, Artificial Neural Networks, Particle Swarm Optimization, Ant Colony Optimization, Grey Wolf Optimization (Tozlu and Çalık, 2021) etc. In the (Mao et al., 2020, fig. 1) the artificial intelligent topic was written two different subtitle one of them is MPPT techniques/Intelligent, and MPPT Techniques/MPPT under Partial Shading Conditions. In the second title, the Artificial Intelligent Controls would extend to Particle Swarm Optimization, Artificial Bee Colony, Salp Swarm Algorithm, Gray Wolf Optimizer, Genetic Algorithm, Differential Evolution. The other related studies for neural network topic (Raj et al., 2015)

3.1.8. Sliding mode based MPPT methods

The examples of the MPPT methods can be extended, but one MPPT model is selected for this thesis. This MPPT is called Super Twisting Sliding Mode Control (STSMC). This control is based on SMC and this is a second order SMC method.

<u>Sliding mode control</u>

According to (Kayışlı and Caglayan, 2022), the SMC is a nonlinear system control known as robust control. According to (Güler, 2021: 62), the SMC is nonlinear system, and not sensitive to the system. It has fast dynamics for instant changings; however, it has chattering problem, because of variable switching frequency, and this situation effects the efficiency of the system.

The sliding mode systems can be improved by using other systems, and other additional features. The order of the system can be greater. It can be classified as First Order SMC, Second Order SMC and High Order SMCs. In the thesis, one of the second order SMC is used to control. The aim is to obtain high efficient sustainable hybrid system. Additionally, this system is robust to dynamic, nonlinear, and disturbing attempts. Also, the proposed system is minimizing the chattering problem.

Super twisting SMC

STSMC is based on SMC and Super Twisting algorithm. This is classified as high order SMC (Hatlehol: Zadeh, 2022). The STSMC Model is shown in Figure 3.3.

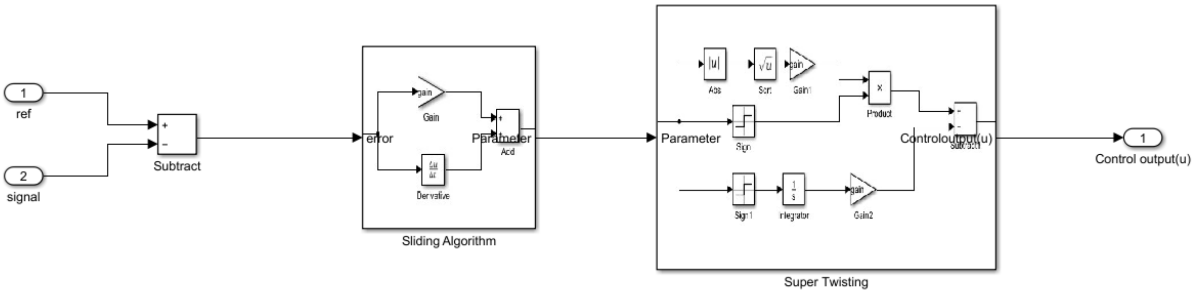

Figure 3.3. The algorithm of STSMC

error= Ref-Signal (3.5)

Parameter= gain*error+ $\frac{\mathrm{d(errror)}}{\mathrm{dt}}$ (3.6)

Control output (u)= $\left|\sqrt{Parameter}\right| * sign(Parameter) - gain * \int sign(Parameter)dt$ (3.7)

error= Ref-Signal(t) (3.8)

Parameter= gain*(Ref-Signal(t))+ $\frac{\mathrm{d(Ref-Signal(t))}}{\mathrm{dt}}$= Parameter= gain*(Ref-Signal(t))- $\frac{\mathrm{d(Signal(t))}}{\mathrm{dt}}$ (3.9)

Parameter= gain*(Ref-Signal(t))-$\frac{\mathrm{d(Signal(t))}}{\mathrm{dt}}$ = par (3.10)

Duty Signal= $\left|\sqrt{\mathrm{par}}\right| * sign(\mathrm{par}) - gain * \int sign(\mathrm{par})dt$ (3.11)

The result of the equation is shown above in here, the solution will be obtained.

$$u = \left|\sqrt{\text{gain} * (\text{Ref} - \text{Signal(t)}) - \frac{\text{d(Signal(t))}}{\text{dt}}}\right| * sign\left(\text{gain} * (\text{ Ref} - \text{Signal(t)}) - \frac{\text{d(Signal(t))}}{\text{dt}}\right) - gain * \int sign\left(\text{gain} * (\text{Ref} - \text{Signal(t)}) - \frac{\text{d(Signal(t))}}{\text{dt}}\right) dt \quad (3.12)$$

Open version of the equation is shown

If the signal is voltage the signal of the will replace with V(t)

$$u= \left|\sqrt{\text{gain} * (\text{Ref} - \text{V(t)}) - \frac{\text{d(V(t))}}{\text{dt}}}\right| * sign\left(\text{gain} * (\text{Ref} - \text{V(t)}) - \frac{\text{d(V(t))}}{\text{dt}}\right) - gain * \int sign\left(\text{gain} * (\text{Ref} - \text{V(t)}) - \frac{\text{d(V(t))}}{\text{dt}}\right) dt \quad (3.13)$$

For every RESs, V(t) formula is changed.

4. DC-DC CONVERTERS

There are several DC-DC type converters are used practically These converters can be classified as isolated converters and non-isolated converters. Isolated converters contain transformer device in the topology and thanks to the transformer, the input side and output side are separated from each other. Only the magnetic effect maintains the circuit’s energy flow.

4.1. Boost Converter

In this part, one of the non-isolated converters is examined. The main aim is to increase the average voltage level, but ideally the input power is equal to output power. The used boost converter topology is shown figure 4.1.

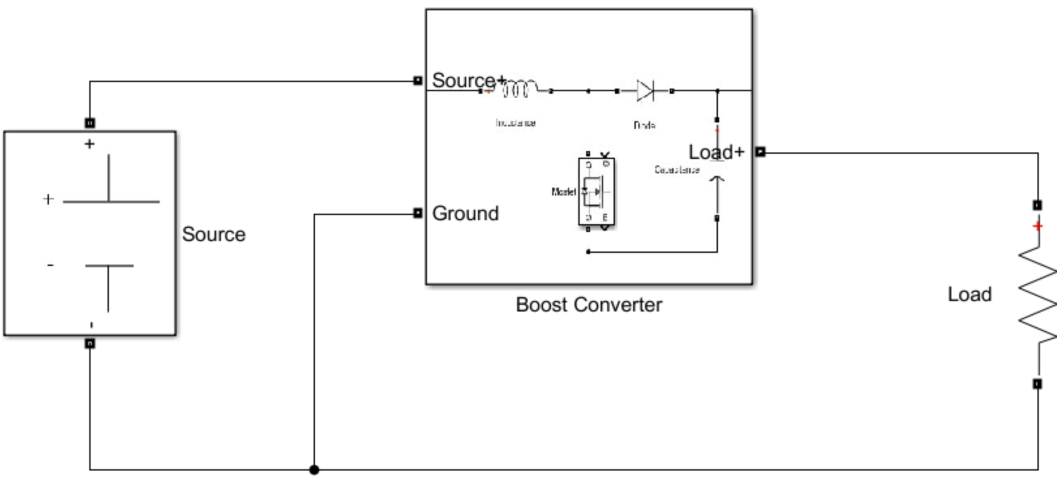

Figure 4.1. Boost Converter Topology

In this case the components are ideal, so the inner losses are neglected. The efficiency is assumed as 100%. The MOSFET and Diode are working in switching mode, so they are simple switches. For this reason, there are two stages in this circuit.

- First Stage is

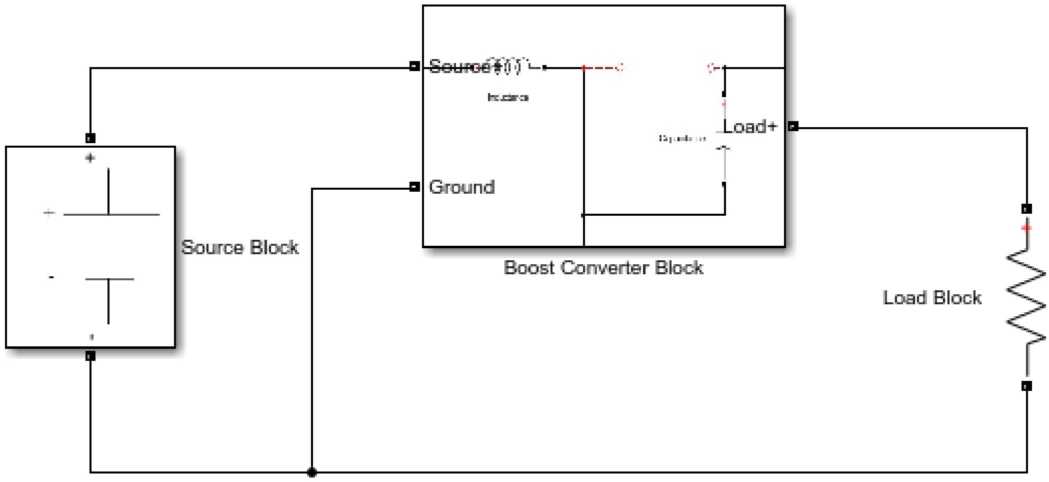

Figure 4.2. MOSFET is On. Diode is Off

MOSFET is OFF and diode is ON. In this mode, the capacitor is discharging and the inductance is charging.

$$i_c = C * \frac{dv_c}{dt} \quad (4.1)$$

$$dv_c = \frac{1}{C} * i_c * dt \quad (4.2)$$

$$\int_{-\infty}^{t} dv_c = \frac{1}{C} \int_{-\infty}^{t} i_c * dt \quad (4.3)$$

$$v_c(t) = \frac{1}{C} \int_{-\infty}^{t} i_c * dt = \frac{1}{C} * (\int_{-\infty}^{0} i_c * dt + \int_{0}^{t} i_c * dt) \quad (4.4)$$

$$\int_{-\infty}^{0} i_c * dt = v_c(0) \quad (4.5)$$

$$v_c(t) = \frac{1}{C} * \left(v_c(0) + \int_{0}^{t} i_c * dt\right) = v_c(0) + \frac{1}{C} \int_{0}^{t} i_c * dt \quad (4.6)$$

$v_c(0)$ is constant, $\frac{1}{C}$ is constant.

The original formula (Irwin, Nelms and Patnaik, 2015: 233-234)

<u>For inductance</u>

$$v_L = L * \frac{di_L}{dt} \quad (4.7)$$

$$di_L = \frac{1}{L} * v_L * dt \quad (4.8)$$

$$\int_{-\infty}^{t} di_L = \int_{-\infty}^{t} \frac{1}{L} * v_L * dt \tag{4.9}$$

$$i_L(t) = \frac{1}{L} * \int_{-\infty}^{t} v_L * dt = \frac{1}{L} * (\int_{-\infty}^{0} v_L * dt + \int_{0}^{t} v_L * dt) \tag{4.10}$$

$$\int_{-\infty}^{0} v_L * dt = i_L(0) \tag{4.11}$$

$$i_L(t) = \frac{1}{L} * (i_L(0) + \int_{0}^{t} v_L * dt) \tag{4.12}$$

$i_L(0)$ is constant, $\frac{1}{L}$ is constant.

$$i_L(t) = i_L(0) + \frac{1}{L} * \int_{0}^{t} v_L * dt \tag{4.13}$$

The original formula (Irwin, Nelms and Patnaik, 2015: 239)

From Eq. 4.13,

$$0 \leq t \leq D * T_{switch} \tag{4.14}$$

$$i_L(t) = i_L(0) + \frac{1}{L} * \int_{0}^{t} v_L * dt \tag{4.15}$$

$$i_L(0) = I_{L_{min}}, \, i_L(t) = I_{L_{max}} \tag{4.16}$$

$$I_{L_{max}} = I_{L_{min}} + \frac{1}{L} * \int_{0}^{t} v_L * dt \tag{4.17}$$

$$\Delta I_L = \frac{1}{L} * V_{in} * D * T_{Switch} \tag{4.18}$$

$$\Delta I_L = \frac{V_{in} * D}{L * f_{switch}} \tag{4.19}$$

$$v_c(t) = v_c(0) + \frac{1}{C} \int_{0}^{t} i_c * dt \tag{4.20}$$

$$v_c(t) = V_{o_{min}}, \; v_c(0) = V_{o_{max}}, i_c = -I_o \tag{4.21}$$

$$V_{o_{min}} = V_{o_{max}} + \frac{1}{C} \int_{0}^{t} -I_o * dt \tag{4.22}$$

$$\Delta V_o = \frac{1}{C} \int_{0}^{t} I_o * dt = \frac{1}{C} * I_o * D * T_{switch} \tag{4.23}$$

$$\Delta V_o = \frac{I_o * D}{C * f_{switch}} \tag{4.24}$$

- Second Stage is

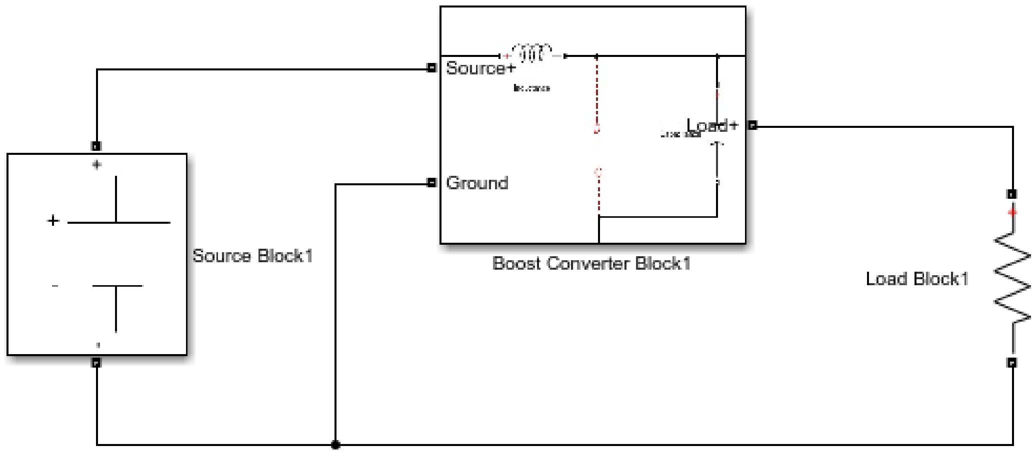

Figure 4.3. Second Stage MOSFET off. Diode on

MOSFET is OFF and diode is ON. In this mode, the capacitor is charging, and the inductance is discharging.

For inductance

$$v_L = L * \frac{di_L}{dt} \tag{4.25}$$

$$di_L = \frac{1}{L} * v_L * dt \tag{4.26}$$

$$\int_{-\infty}^{t} di_L = \int_{-\infty}^{t} \frac{1}{L} * v_L * dt \tag{4.27}$$

$$i_L(t) = \frac{1}{L} * \int_{-\infty}^{t} v_L * dt = \frac{1}{L} * (\int_{-\infty}^{0} v_L * dt + \int_{0}^{t} v_L * dt) \tag{4.28}$$

$$\int_{-\infty}^{0} v_L * dt = i_L(0) \tag{4.29}$$

$$i_L(t) = \frac{1}{L} * (i_L(0) + \int_{0}^{t} v_L * dt) \tag{4.30}$$

$i_L(0)$ is constant, $\frac{1}{L}$ is constant.

$$i_L(t) = i_L(0) + \frac{1}{L} * \int_{0}^{t} v_L * dt \tag{4.31}$$

The original formula (Irwin, Nelms and Patnaik, 2015: 239)

From this formula,

$$D * T_{switch} \leq t \leq T_{switch} \quad (4.32)$$

$$i_L(t) = i_L(D * T_{switch}) + \frac{1}{L} * \int_{D*T_{switch}}^{T_{switch}} v_L * dt \quad (4.33)$$

$$i_L(D * T_{switch}) = I_{L_{max}}, \; i_L(T) = I_{L_{min}} \quad (4.34)$$

$$I_{L_{min}} = I_{L_{max}} + \frac{1}{L} * \int_{D*T_{switch}}^{T_{switch}} v_L * dt \quad (4.35)$$

$$-\Delta I_L = \frac{1}{L} * v_L * (T_{switch} - D * T_{switch}) \quad (4.36)$$

$$v_L = V_{in} - V_{out} \quad (4.37)$$

$$-\Delta I_L = \frac{1}{L} * (V_{in} - V_{out}) * \frac{1-D}{f_{switch}} \quad (4.38)$$

$$\Delta I_L = \frac{(V_{in} - V_{out}) * (1-D)}{L * f_{switch}} \quad (4.39)$$

$$V_{in} = V_{out} * (1 - D) \quad (4.40)$$

$$\Delta I_L = \frac{(V_{out} * (1-D) - V_{out}) * (1-D)}{L * f_{switch}} \quad (4.41)$$

$$\Delta I_L = \frac{(V_{out}) * (D - D^2)}{L * f_{switch}} \quad (4.42)$$

The current and voltage equations of the boost converter should be used to control of the circuit and the transfer function should be obtained.

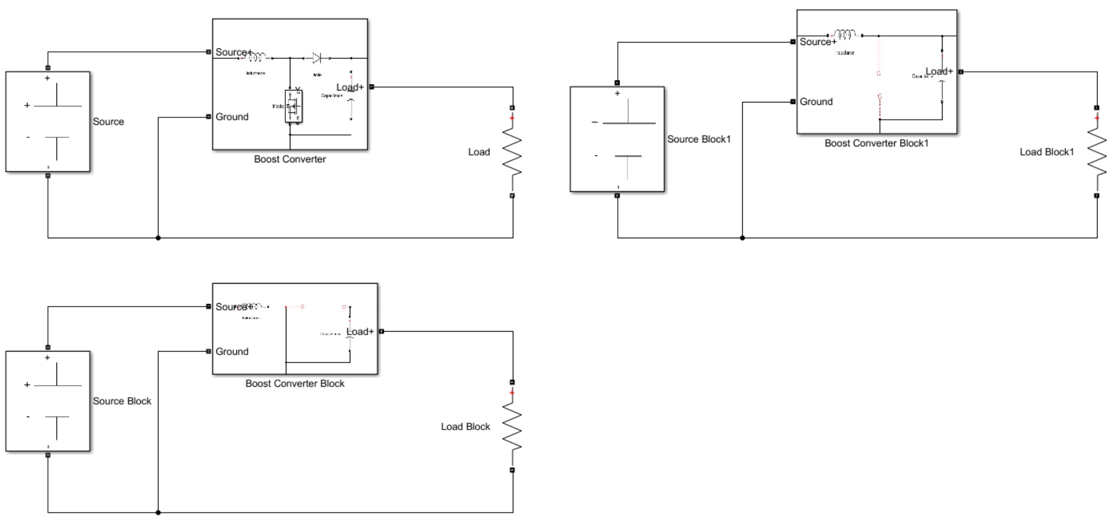

Figure 4.4. All conditions of Boost Converter

For Stage 1

$$L * \frac{di_{L_{All}}}{dt} = v_{in_{All}} \ , \ C * \frac{dv_{o_{All}}}{dt} = \frac{v_{o_{All}}}{R} \tag{4.43}$$

For Stage 2

$$L * \frac{di_{L_{All}}}{dt} = v_{in_{All}} - v_{o_{All}} \quad , C * \frac{dv_{o_{All}}}{dt} = i_{L_{All}} - \frac{v_{o_{All}}}{R} \tag{4.44}$$

<u>Total operation</u>

$$L * \frac{di_{L_{All}}}{dt} = \left(v_{in_{All}}\right) * \tilde{d} + \left(v_{in_{All}} - v_{o_{All}}\right) * (1 - \tilde{d}) \tag{4.45}$$

$$C * \frac{dv_{o_{All}}}{dt} = (i_{L_{All}}) * (1 - \tilde{d}) - \frac{v_{o_{All}}}{R} \tag{4.46}$$

DC and AC signal

$$i_{L_{All}} = I_L + i_L, \ v_{o_{All}} = v_o + V_o, v_{in_{All}} = V_{in} + v_{in} \ , \ \tilde{d} = D + d \tag{4.47}$$

$$L * \frac{d(I_L + i_L)}{dt} = (V_{in} + v_{in}) * (D + d) + (V_{in} + v_{in} - V_{out} - v_{out}) * (1 - D - d) \tag{4.48}$$

$$C * \frac{d(V_o + v_o)}{dt} = (I_L + i_L) * (1 - D - d) - \frac{V_o}{R} - \frac{v_o}{R} \tag{4.49}$$

DC

$$L * \frac{d(I_L)}{dt} = (V_{in}) * (D) + (V_{in} - V_{out}) * (1 - D) \tag{4.50}$$

$$L * \frac{d(I_L)}{dt} = V_{in} - V_o(1 - D) \tag{4.51}$$

$$0 = V_{in} - V_o(1 - D) \tag{4.52}$$

$$V_o = \frac{V_{in}}{(1 - D)} \tag{4.53}$$

$$C * \frac{d(V_o + v_o)}{dt} = (I_L + i_L) * (1 - D - d) - \frac{V_o}{R} - \frac{v_o}{R} \tag{4.54}$$

$$0 = (I_L) * (1 - D) - \frac{V_o}{R} \tag{4.55}$$

$$0 = I_L - I_L * D - \frac{V_o}{R} \tag{4.56}$$

$$\frac{V_o}{R} = (I_L) * (1 - D) = I_o \tag{4.57}$$

AC

$$L * \frac{d(I_L+i_L)}{dt} = (V_{in} + v_{in}) * (D + d) + (V_{in} + v_{in} - V_{out} - v_{out}) * (1 - D - d) \quad (4.58)$$

$$C * \frac{d(V_o+v_o)}{dt} = (I_L + i_L) * (1 - D - d) - \frac{V_o}{R} - \frac{v_o}{R} \quad (4.59)$$

$$L * \frac{d(i_L)}{dt} = (V_{in} + v_{in}) * (D + d) + (V_{in} + v_{in} - V_{out} - v_{out}) * (1 - D - d) \quad (4.60)$$

$$I_L - D * I_L - \frac{V_o}{R} = 0; I_L * (1 - D) = \frac{V_o}{R}; R(1 - D) = \frac{V_o}{I_L} \quad (4.61)$$

$$R = \frac{V_o}{I_o} = \frac{V_o}{I_L*(1-D)} \quad (4.62)$$

$$L * \frac{d(i_L)}{dt} = v_{in} - (V_{out} * v_{out}) * (1 - D - d) \quad (4.63)$$

$$L * \frac{d(i_L)}{dt} = v_{in} + V_{out} * d - v_{out} + v_{out} * D + v_{out} * d \quad (4.64)$$

$$s * L * i_L = v_{in} + V_{out} * d - v_{out} + v_{out} * D + v_{out} * d \quad (4.65)$$

$$C * \frac{d(V_o+v_o)}{dt} = (I_L + i_L) * (1 - D - d) - \frac{V_o}{R} - \frac{v_o}{R} \quad (4.66)$$

$$C * \frac{d(v_o)}{dt} = -I_L * d + i_L - i_L * D - i_L * d - \frac{v_o}{R} \quad (4.67)$$

$$s * C * v_o = -I_L * d + i_L - i_L * D - i_L * d - \frac{v_o}{R} \quad (4.68)$$

<u>Matrix form</u>

$$\dot{x} = \begin{bmatrix} \dot{v_o} \\ \dot{i_L} \end{bmatrix}, x = \begin{bmatrix} v_o \\ i_L \end{bmatrix}, \quad (4.69)$$

$$L * \frac{d(i_L)}{dt} = v_{in} + V_{out} * d - v_{out} + v_{out} * D + v_{out} * d \quad (4.70)$$

$$C * \frac{d(v_o)}{dt} = -I_L * d + i_L - i_L * D - i_L * d - \frac{v_o}{R} \quad (4.71)$$

$$\begin{bmatrix} C * \dot{v_o} \\ L * \dot{i_L} \end{bmatrix} = \begin{bmatrix} -I_L * d + i_L - i_L * D - i_L * d - \frac{v_o}{R} \\ V_{out} * d * \begin{bmatrix} 1 & 0 \\ 0 & 1 \end{bmatrix} + (v_{in} + V_{out} * d - v_{out} + v_{out} * D + v_{out} * d) * \begin{bmatrix} 1 & 0 \\ 0 & 1 \end{bmatrix} \end{bmatrix}$$

(4.72)

$$\begin{bmatrix} C * \dot{v_o} \\ L * \dot{i_L} \end{bmatrix} = \begin{bmatrix} i_L - i_L * D - \frac{v_o}{R} \\ +(-v_{out} + v_{out} * D) \end{bmatrix} + \begin{bmatrix} -I_L * d \\ V_{out} * d * \begin{bmatrix} 1 & 0 \\ 0 & 1 \end{bmatrix} + v_{out} * d \end{bmatrix} \quad (4.73)$$

From there

$$-i_L * d \cong 0 \quad (4.74)$$

$$v_{out} * d \cong 0 \tag{4.75}$$

$$v_{in} \cong 0 \tag{4.76}$$

$$\begin{bmatrix} C * \dot{v_o} \\ L * \dot{i_L} \end{bmatrix} = \begin{bmatrix} -\frac{1}{R} & 1 - D \\ -1 + D & 0 \end{bmatrix} * \begin{bmatrix} v_o \\ i_L \end{bmatrix} + \begin{bmatrix} -I_L \\ V_{out} \end{bmatrix} * d \tag{4.77}$$

$$\begin{bmatrix} C & 0 \\ 0 & L \end{bmatrix} * \begin{bmatrix} \dot{v_o} \\ \dot{i_L} \end{bmatrix} = \begin{bmatrix} -\frac{1}{R} & 1 - D \\ -1 + D & 0 \end{bmatrix} * \begin{bmatrix} v_o \\ i_L \end{bmatrix} + \begin{bmatrix} -I_L \\ V_{out} \end{bmatrix} * d \tag{4.78}$$

$$\begin{bmatrix} C & 0 \\ 0 & L \end{bmatrix} * \begin{bmatrix} \dot{v_o} \\ \dot{i_L} \end{bmatrix} = \begin{bmatrix} -\frac{1}{R} & 1 - D \\ -1 + D & 0 \end{bmatrix} * \begin{bmatrix} v_o \\ i_L \end{bmatrix} + \begin{bmatrix} -I_L \\ V_{out} \end{bmatrix} * d \tag{4.79}$$

$$\begin{bmatrix} \dot{v_o} \\ \dot{i_L} \end{bmatrix} = \frac{1}{C*L} * \begin{bmatrix} L & 0 \\ 0 & C \end{bmatrix} * \begin{bmatrix} -\frac{1}{R} & 1 - D \\ -1 + D & 0 \end{bmatrix} * \begin{bmatrix} v_o \\ i_L \end{bmatrix} + \frac{1}{C*L} * \begin{bmatrix} L & 0 \\ 0 & C \end{bmatrix} * \begin{bmatrix} -I_L \\ V_{out} \end{bmatrix} * d \tag{4.80}$$

$$\begin{bmatrix} \dot{v_o} \\ \dot{i_L} \end{bmatrix} = \frac{1}{C*L} \begin{bmatrix} -\frac{L}{R} & L - L * D \\ -C + C * D & 0 \end{bmatrix} * \begin{bmatrix} v_o \\ i_L \end{bmatrix} + \begin{bmatrix} -\frac{1}{C} & 0 \\ 0 & \frac{1}{L} \end{bmatrix} * \begin{bmatrix} I_L \\ V_{out} \end{bmatrix} * d \tag{4.81}$$

$$\begin{bmatrix} \dot{v_o} \\ \dot{i_L} \end{bmatrix} = \begin{bmatrix} -\frac{1}{C*R} & \frac{1-D}{C} \\ \frac{-1+D}{L} & 0 \end{bmatrix} * \begin{bmatrix} v_o \\ i_L \end{bmatrix} + \begin{bmatrix} -\frac{1}{C} & 0 \\ 0 & \frac{1}{L} \end{bmatrix} * \begin{bmatrix} I_L \\ V_{out} \end{bmatrix} * d \tag{4.82}$$

$$\dot{x} = A * x + B * d \tag{4.83}$$

Where,

$$A = \begin{bmatrix} -\frac{1}{C*R} & \frac{1-D}{C} \\ \frac{-1+D}{L} & 0 \end{bmatrix} \tag{4.84}$$

$$B = \begin{bmatrix} -\frac{1}{C} & 0 \\ 0 & \frac{1}{L} \end{bmatrix} * \begin{bmatrix} I_L \\ V_{out} \end{bmatrix} = \begin{bmatrix} \frac{-I_L}{C} \\ \frac{V_{out}}{L} \end{bmatrix} \tag{4.85}$$

$$y = \tilde{V}_{out} = v_{out} \tag{4.86}$$

$$y = \begin{bmatrix} 1 & 0 \end{bmatrix} \begin{bmatrix} v_{out} \\ i_L \end{bmatrix} \tag{4.87}$$

$$y = \acute{C} * x + 0 * d \tag{4.88}$$

$$y = \acute{C} * x \tag{4.89}$$

$$\acute{C} = \begin{bmatrix} 1 & 0 \end{bmatrix} \tag{4.90}$$

$$A = \begin{bmatrix} -\frac{1}{C*R} & \frac{1-D}{C} \\ \frac{-(1-D)}{L} & 0 \end{bmatrix} \tag{4.91}$$

$$B = \begin{bmatrix} \frac{-I_L}{C} \\ \frac{V_{out}}{L} \end{bmatrix} \tag{4.92}$$

$$\acute{C} = [1 \quad 0] \tag{4.93}$$

X'=AX+BU (4.94)

Y=CX+DU (4.95)

And other parameter analysis shown in the Texas Instrument Report (Zaitsu, 2009)

Load condition of the boost converter

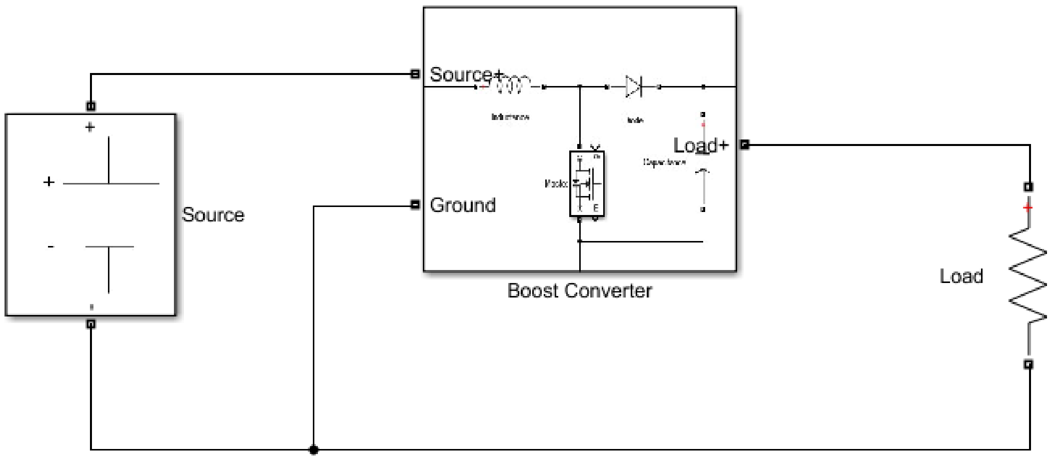

Figure 4.5. Boost Converter Topology

Boost Converter is controlled by the duty cycle which produced by the controller unit. The Boost converter ideally increase the voltage average value without changing power value. The input power is equal to output power, if the losses are neglected. For this part, there is an important equation:

$$V_o = \frac{V_{in}}{1-D} \tag{4.96}$$

From above calculation and enlighten to this knowledge:

$$P_{in} = P_{out} \tag{4.97}$$

$$P_{in} = V_{in} * I_{in} \tag{4.98}$$

$$P_{out} = V_{out} * I_{out} \tag{4.99}$$

$$P_{in} = V_{in} * I_{in} = V_{out} * I_{out} = P_{out} \tag{4.100}$$

$$V_{in} * I_{in} = V_{out} * I_{out} \quad (4.101)$$

$$V_{in} * I_{in} = (\frac{V_{in}}{1-D}) * I_{out} \quad (4.102)$$

$$I_{in} = \frac{I_{out}}{1-D} \quad (4.103)$$

$$V_{in} * I_{in} = V_{out} * I_{out} \quad (4.104)$$

$$V_{in} = R_{in} * I_{in} \quad (4.105)$$

$$V_{out} = R_{out} * I_{out} \quad (4.106)$$

$$R_{in} * I_{in} * I_{in} = R_{out} * I_{out} * I_{out} \quad (4.107)$$

$$R_{in} * \frac{I_{out}}{1-D} * \frac{I_{out}}{1-D} = R_{out} * I_{out} * I_{out} \quad (4.108)$$

$$R_{in} = R_{out} * (1 - D)^2 \quad (4.109)$$

The similar examination was done in (Omran et al., 2021: 4)

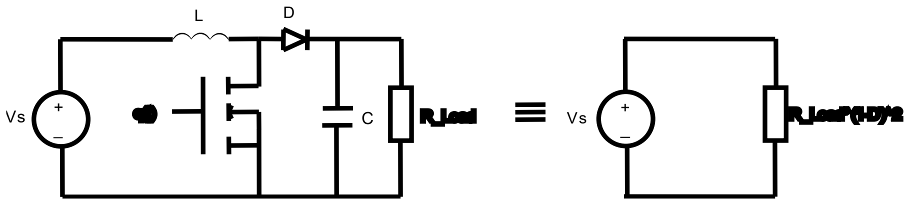

Figure 4.6. Equivalent Circuit of Boost Converter

4.2. Buck Converter

The Buck Converter is one of the non-isolated converters. This converter ideally reduces the average value of the output voltage and increase the average of the current value. In the ideal case the output power is equal to the input power supplies power value. In this case the components are ideal, so the inner losses are neglected. The efficiency is 100%. The MOSFET and Diode are working in switching mode, so they are simple switches. For this reason, there are two stages.

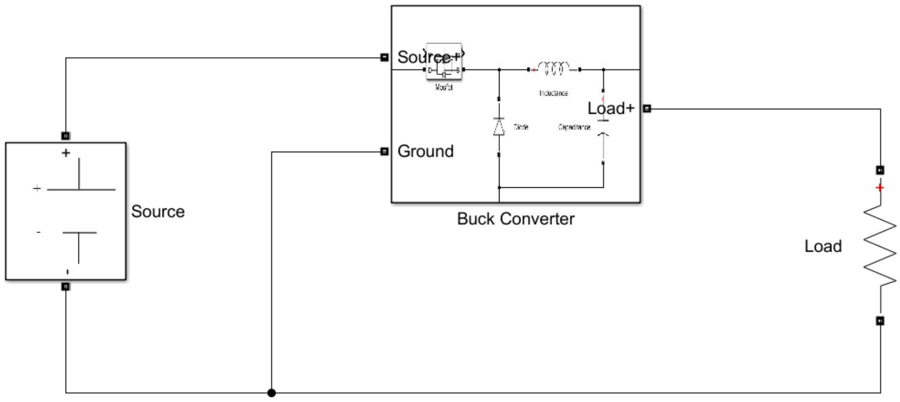

Figure 4.7. Buck Converter

- First Stage is

This stage is working during $0 < t < duty * t_{switch}$ interval. The inductor is charging in this stage.

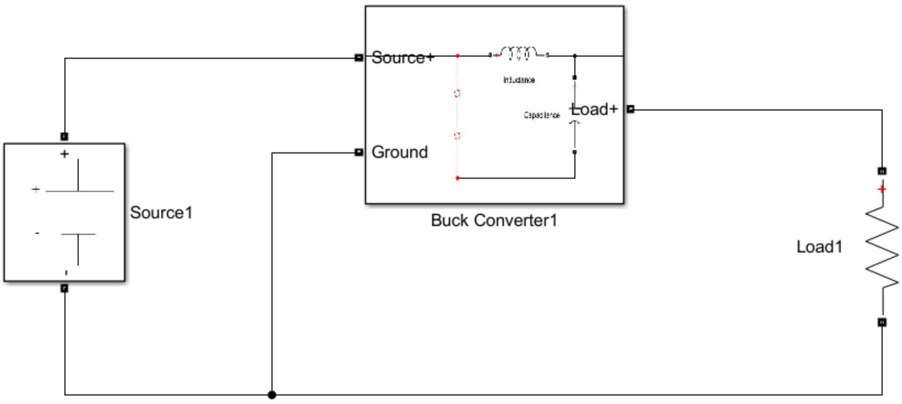

Figure 4.8. Buck Converter MOSFET off

$$v_L = L * \frac{di_L}{dt} \tag{4.110}$$

$$i_L = \frac{1}{L} * \int_{-\infty}^{t} v_L dt \tag{4.111}$$

The original formula is (Irwin, Nelms and Patnaik, 2015: 239)

$$\frac{\int_{-\infty}^{t}(v_S - v_{Load})dt}{L} = i_L \tag{4.112}$$

$$v_S(-\infty) = v_s(0) = 0 \tag{4.113}$$

$$v_{Load}(-\infty) = v_{Load}(0) = 0 \tag{4.114}$$

$$v_S(t) = v_s(duty * t_{switch}) = |v_s| \quad (4.115)$$

$$v_{Load}(t) = v_{Laod}(duty * t_{switch}) = |v_{Laod}| \quad (4.116)$$

$$v_S - v_{Load} = v_L = L * \frac{di_L}{dt} \quad (4.117)$$

$$i_C = C * \frac{dv_c}{dt} \quad (4.118)$$

$$v_c = \frac{1}{C} * \int_{-\infty}^{t} i_c \, dt \quad (4.119)$$

The original formula is (Irwin, Nelms and Patnaik, 2015: 233-234)

$$v_c = \frac{\int_{-\infty}^{t} (i_L - i_{Load}) dt}{C} \quad (4.120)$$

$$i_S(-\infty) = i_s(0) = 0 \quad (4.121)$$

$$i_{Load}(-\infty) = i_{Load}(0) = 0 \quad (4.122)$$

$$i_S(t) = i_s(duty * t_{switch}) = |i_s| \quad (4.123)$$

$$i_{Load}(t) = i_{Laod}(duty * t_{switch}) = |i_{Laod}| \quad (4.124)$$

$$i_L - i_{Load} = i_C = C * \frac{dv_C}{dt} \quad (4.125)$$

- Second Stage is;

It works only $duty * t_{switch} < t < t_{switch}$ interval. The inductor is discharging.

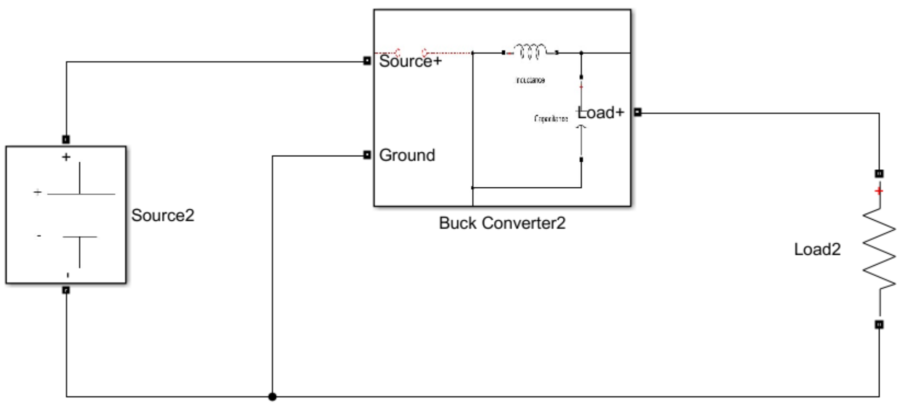

Figure 4.9. Buck Converter MOSFET on

For Inductance,

$$v_L = L * \frac{di_L}{dt} \tag{4.126}$$

$$i_L = \frac{1}{L} * \int_{-\infty}^{t} v_L dt \tag{4.127}$$

The original formula is (Irwin, Nelms and Patnaik, 2015: 239)

$$\frac{\int_{duty*t_{switch}}^{t_{switch}} (v_L)dt}{L} = i_L \tag{4.128}$$

$$v_L(t_{switch}) = 0\ , v_L(duty * t_{switch}) = |v_{Load}| \tag{4.129}$$

$$0 - v_{Load} = v_L = L * \frac{di_L}{dt} \tag{4.130}$$

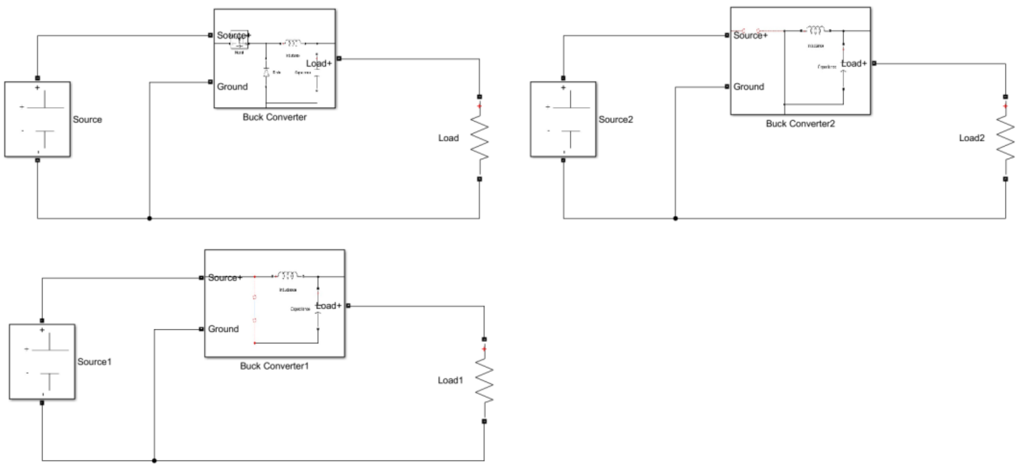

Figure 4.10. Buck Converter Topology and MOSFET Behavior

<u>From super position rule</u>

$$L * \frac{di_{L_{all}}}{dt} = \frac{(v_S - v_{Load}) * duty * t_{switch} + (-v_{Load}) * (1 - duty) * t_{switch}}{t_{switch}} \tag{4.131}$$

$$L * \frac{di_{L_{all}}}{dt} = (v_S - v_{Load}) * duty + (-v_{Load}) * (1 - duty) \tag{4.132}$$

$$L * \frac{di_{L_{all}}}{dt} = v_s * duty - v_{Load} \tag{4.133}$$

$$C * \frac{dv_{C_{all}}}{dt} = i_L - i_{Load} \tag{4.134}$$

$$i_{L_{all}} = i_{L_{AC}} + I_{L_{DC}} \tag{4.135}$$

$$v_s = v_{s_{AC}} + V_{s_{DC}} \tag{4.136}$$

$$v_c = v_{Load} \quad (4.137)$$

$$v_{Load} = v_{Load_{AC}} + V_{Load_{DC}} \quad (4.138)$$

$$i_{Load} = \frac{v_{load}}{R} \quad (4.139)$$

$$duty = duty_{AC} + duty_{DC} \quad (4.140)$$

$$L * \frac{di_{L_{all}}}{dt} = L * \frac{di_{L_{AC}}}{dt} + L * \frac{dI_{L_{DC}}}{dt} = \left(v_{s_{AC}} + V_{s_{DC}}\right) * (duty_{AC} + duty_{DC}) - (v_{Load_{AC}} + V_{Load_{DC}}) \quad (4.141)$$

$$C * \frac{dv_{C_{all}}}{dt} = C * \frac{dv_{Load_{AC}}}{dt} + C * \frac{dV_{Load_{DC}}}{dt} = \left(i_{L_{AC}} + I_{L_{DC}}\right) - \frac{v_{Load_{AC}} + V_{Load_{DC}}}{R} \quad (4.142)$$

Derivative of the DC components are zero because of the derivative of constant values.

$$L * \frac{di_{L_{AC}}}{dt} = \left(v_{s_{AC}} + V_{s_{DC}}\right) * (duty_{AC} + duty_{DC}) - (v_{Load_{AC}} + V_{Load_{DC}}) \quad (4.143)$$

$$C * \frac{dv_{Load_{AC}}}{dt} = \left(i_{L_{AC}} + I_{L_{DC}}\right) - \frac{v_{Load_{AC}} + V_{Load_{DC}}}{R} \quad (4.144)$$

For $L * \frac{di_{L_{AC}}}{dt}$

$$L * \frac{di_{L_{AC}}}{dt} = v_{s_{AC}} * duty_{AC} + v_{s_{AC}} * duty_{DC} + V_{s_{DC}} * duty_{AC} + V_{s_{DC}} * duty_{DC} - v_{Load_{AC}} - V_{Load_{DC}} \quad (4.145)$$

$$C * \frac{dv_{Load_{AC}}}{dt} = i_{L_{AC}} + I_{L_{DC}} - \frac{v_{Load_{AC}}}{R} - \frac{V_{Load_{DC}}}{R} \quad (4.146)$$

$$L * \frac{di_{L_{AC}}}{dt} = v_{s_{AC}} * duty_{AC} + v_{s_{AC}} * duty_{DC} + V_{s_{DC}} * duty_{AC} + V_{s_{DC}} * duty_{DC} - v_{Load_{AC}} - V_{Load_{DC}} \quad (4.147)$$

If the derivative of DC is zero pure DC part must be cancel

$$V_{s_{DC}} * duty_{DC} - V_{Load_{DC}} = 0 \quad (4.148)$$

$$V_{s_{DC}} * duty_{DC} = V_{Load_{DC}} \quad (4.149)$$

$$V_{in} * d = V_{out} \quad (4.150)$$

$$L * \frac{di_{L_{AC}}}{dt} = v_{s_{AC}} * duty_{AC} + v_{s_{AC}} * duty_{DC} + V_{s_{DC}} * duty_{AC} - v_{Load_{AC}} \quad (4.151)$$

$$C * \frac{dv_{Load_{AC}}}{dt} = i_{L_{AC}} + I_{L_{DC}} - \frac{v_{Load_{AC}}}{R} - \frac{V_{Load_{DC}}}{R} \quad (4.152)$$

$$I_{L_{DC}} = \frac{V_{Load_{DC}}}{R} \quad (4.153)$$

$$C* \frac{dv_{Load_{AC}}}{dt} = i_{L_{AC}} - \frac{v_{Load_{AC}}}{R} \quad (4.154)$$

$$L * \frac{di_{L_{AC}}}{dt} = v_{s_{AC}} * duty_{AC} + v_{s_{AC}} * duty_{DC} + V_{s_{DC}} * duty_{AC} - v_{Load_{AC}} \quad (4.155)$$

$$C* \frac{dv_{Load_{AC}}}{dt} = i_{L_{AC}} - \frac{v_{Load_{AC}}}{R} \quad (4.156)$$

Transform to s domain

$$L * s * i_{L_{AC}} = v_{s_{AC}} * duty_{AC} + v_{s_{AC}} * duty_{DC} + V_{s_{DC}} * duty_{AC} - v_{Load_{AC}} \quad (4.157)$$

$$C * s * v_{Load_{AC}} = i_{L_{AC}} - \frac{v_{Load_{AC}}}{R} \quad (4.158)$$

For simplification:

$$i_L = i_{L_{AC}},\ v_s = v_{s_{AC}},\ d = duty_{AC},\ D = duty_{DC},\ V_S = V_{s_{DC}} \quad (4.159)$$

$$v_{Load} = v_{Load_{AC}} \quad (4.160)$$

$$L * s * i_L = v_S * d + v_s * D + V_S * d - v_{Load} \quad (4.161)$$

$$C * s * v_{Load} = i_L - \frac{v_{Load}}{R} \quad (4.162)$$

$$L * i_L = \frac{v_S * d}{s} + \frac{v_s * D}{s} + \frac{V_S * d}{s} - \frac{v_{Load}}{s} \quad (4.163)$$

$$C * v_{Load} = \frac{i_L}{s} - \frac{v_{Load}}{R * s} \quad (4.164)$$

$v_S * d \cong$ so small value so it will be ignored, the source voltage assumed to the DC value so the input voltages ac component is zero. $v_s \cong 0$

$$L * i_L = + \frac{V_S * d}{s} - \frac{v_{Load}}{s} \quad (4.164)$$

To obtain i_L equivalent ;

$$i_L = \frac{V_S * d}{L * s} - \frac{v_{Load}}{L * s} \quad (4.165)$$

$$C * v_{Load} = \frac{\left(\frac{V_S * d}{L * s} - \frac{v_{Load}}{L * s}\right)}{s} - \frac{v_{Load}}{R * s} \quad (4.166)$$

$$C * v_{Load} = \frac{V_S * d}{L * s^2} - \frac{v_{Load}}{L * s^2} - \frac{v_{Load}}{R * s} \quad (4.167)$$

$$v_{Load} * \left(C + \frac{1}{L*s^2} + \frac{1}{R*s}\right) = \frac{V_S*d}{L*s^2} \tag{4.168}$$

To matrix form

$$L * \frac{di_{L_{AC}}}{dt} = v_{s_{AC}} * duty_{AC} + v_{s_{AC}} * duty_{DC} + V_{s_{DC}} * duty_{AC} - v_{Load_{AC}} \tag{4.169}$$

$$\mathrm{C}* \frac{dv_{Load_{AC}}}{dt} = i_{L_{AC}} - \frac{v_{Load_{AC}}}{R} \tag{4.170}$$

$$i_L = i_{L_{AC}},\ v_s = v_{s_{AC}},\ d = duty_{AC},\ D = duty_{DC},\ V_S = V_{s_{DC}} \tag{4.171}$$

$$v_{Load} = v_{Load_{AC}} \tag{4.172}$$

$$L * \frac{di_L}{dt} = v_S * d + v_s * D + V_S * d - v_{Load} \tag{4.173}$$

$$C * \frac{dv_{Load}}{dt} = i_L - \frac{v_{Load}}{R} \tag{4.174}$$

$$\begin{bmatrix} C * \dot{v}_{Load} \\ L * i_{\dot{v}_{Load}} \end{bmatrix} = \begin{bmatrix} v_S * d + v_s * D + V_S * d - v_{Load} \\ i_L - \frac{v_{Load}}{R} \end{bmatrix} \tag{4.175}$$

$$\begin{bmatrix} C & 0 \\ 0 & L \end{bmatrix} * \begin{bmatrix} \dot{v}_{Load} \\ i_{Load} \end{bmatrix} = \begin{bmatrix} v_S * d + v_s * D + V_S * d - v_{Load} \\ i_L - \frac{v_{Load}}{R} \end{bmatrix} \tag{4.176}$$

$$\begin{bmatrix} C & 0 \\ 0 & L \end{bmatrix} * \begin{bmatrix} \dot{v}_{Load} \\ i_{Load} \end{bmatrix} = \begin{bmatrix} v_S * d + V_S * d + v_s * D - v_{Load} \\ i_L - \frac{v_{Load}}{R} \end{bmatrix} \tag{4.177}$$

$$\begin{bmatrix} C & 0 \\ 0 & L \end{bmatrix} * \begin{bmatrix} \dot{v}_{Load} \\ i_{Load} \end{bmatrix} = \begin{bmatrix} v_s * D - v_{Load} \\ i_L - \frac{v_{Load}}{R} \end{bmatrix} + [V_S * d] \tag{4.178}$$

v_s means AC part of the source voltage. In this case the source is DC voltage source. There is no AC part,

$$\begin{bmatrix} C & 0 \\ 0 & L \end{bmatrix} * \begin{bmatrix} \dot{v}_{Load} \\ i_{Load} \end{bmatrix} = \begin{bmatrix} -v_{Load} \\ i_L - \frac{v_{Load}}{R} \end{bmatrix} + [V_S * d] \tag{4.179}$$

$$\begin{bmatrix} C & 0 \\ 0 & L \end{bmatrix} * \begin{bmatrix} \dot{v}_{Load} \\ i_{Load} \end{bmatrix} = \begin{bmatrix} -1 & 0 \\ -\frac{1}{R} & 1 \end{bmatrix} * \begin{bmatrix} v_{Load} \\ i_{Load} \end{bmatrix} + [V_S] * d \tag{4.180}$$

$$\begin{bmatrix} \dot{v}_{Load} \\ i_{Load} \end{bmatrix} = \frac{1}{C*L} * \begin{bmatrix} L & 0 \\ 0 & C \end{bmatrix} * \begin{bmatrix} -1 & 0 \\ -\frac{1}{R} & 1 \end{bmatrix} * \begin{bmatrix} v_{Load} \\ i_{Load} \end{bmatrix} + \frac{1}{C*L} * \begin{bmatrix} L & 0 \\ 0 & C \end{bmatrix} * [V_S] * d \tag{4.181}$$

$$\begin{bmatrix} L & 0 \\ 0 & C \end{bmatrix} * \begin{bmatrix} -1 & 0 \\ -\frac{1}{R} & 1 \end{bmatrix} = \begin{bmatrix} -L & 0 \\ -\frac{C}{R} & C \end{bmatrix} \tag{4.182}$$

$$\begin{bmatrix} \dot{v}_{Load} \\ i_{Load} \end{bmatrix} = \frac{1}{C*L} * \begin{bmatrix} -L & 0 \\ -\frac{C}{R} & C \end{bmatrix} * \begin{bmatrix} v_{Load} \\ i_{Load} \end{bmatrix} + \frac{V_S}{C*L} * \begin{bmatrix} L & 0 \\ 0 & C \end{bmatrix} * d \tag{4.183}$$

$$\begin{bmatrix} \dot{v}_{Load} \\ i_{Load} \end{bmatrix} = \begin{bmatrix} -\frac{1}{C} & 0 \\ -\frac{1}{L*R} & \frac{1}{L} \end{bmatrix} * \begin{bmatrix} v_{Load} \\ i_{Load} \end{bmatrix} + \begin{bmatrix} \frac{V_S}{C} & 0 \\ 0 & \frac{V_S}{L} \end{bmatrix} * d \quad (4.184)$$

$$\begin{bmatrix} \dot{v}_{Load} \\ i_{Load} \end{bmatrix} = \begin{bmatrix} -\frac{1}{C} & 0 \\ -\frac{1}{L*R} & \frac{1}{L} \end{bmatrix} * \begin{bmatrix} v_{Load} \\ i_{Load} \end{bmatrix} + \begin{bmatrix} \frac{V_S}{C} & 0 \\ 0 & \frac{V_S}{L} \end{bmatrix} * d \quad (4.185)$$

$$\dot{x} = A * x + B * d \quad (4.186)$$

$$A = \begin{bmatrix} -\frac{1}{C} & 0 \\ -\frac{1}{L*R} & \frac{1}{L} \end{bmatrix} \quad (4.187)$$

$$B = \begin{bmatrix} \frac{V_S}{C} & 0 \\ 0 & \frac{V_S}{L} \end{bmatrix} \quad (4.188)$$

$$y = v_{Load} = [1 \quad 0] * \begin{bmatrix} v_{Load} \\ i_{Load} \end{bmatrix} \quad (4.189)$$

$$y = C * x + 0 * d \quad (4.190)$$

$$C = [1 \quad 0] \quad (4.191)$$

Load condition of the buck converter

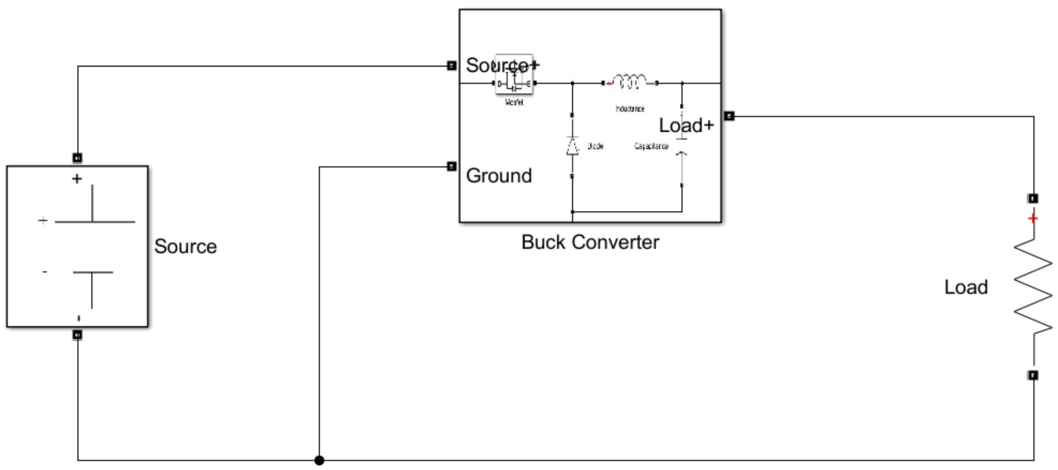

Figure 4.11. Buck Converter Topology

From Eq. 148, Eq. 149, Eq. 150 , the duty cycle input and output voltage relation found as follows:

$$V_{in} * d = V_{out} \quad (4.192)$$

Ideally the Buck Converter output and input power values are equal:

$$P_{in} = P_{out} \tag{4.193}$$

$$P_{in} = V_{in} * I_{in} \tag{4.194}$$

$$V_{in} = R_{in} * I_{in} \tag{4.195}$$

$$P_{out} = V_{out} * I_{out} \tag{4.196}$$

$$V_{out} = R_{out} * I_{out} \tag{4.197}$$

$$V_{in} * I_{in} = V_{out} * I_{out} \tag{4.198}$$

$$V_{in} * I_{in} = V_{in} * Duty * I_{out} \tag{4.199}$$

$$I_{in} = Duty * I_{out} \tag{4.200}$$

$$V_{in} * I_{in} = V_{out} * I_{out} \tag{4.201}$$

$$R_{in} * I_{in} * Duty * I_{out} = V_{out} * I_{out} \tag{4.202}$$

$$R_{in} * I_{in} * Duty = V_{out} \tag{4.203}$$

$$R_{in} * Duty * I_{out} * Duty = V_{out} \tag{4.204}$$

$$R_{in} * Duty^2 = \frac{V_{out}}{I_{out}} = R_{out} \tag{4.205}$$

$$R_{in} = \frac{R_{out}}{Duty^2} \tag{4.206}$$

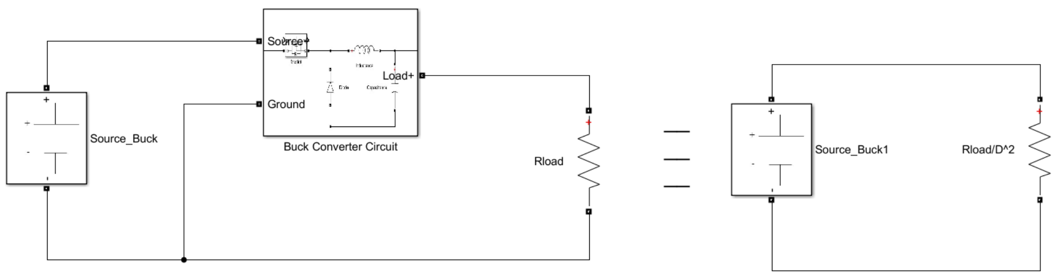

Figure 4.12. Buck Converter to Equivalent Model

5. THREE PHASE DC-AC CONVERTER AND SINUSOIDAL PULSE WIDTH MODULATION

The topology is shown in figure 5.1. The aim is to obtain 3 phase AC sinus wave from the output load. One branch of the 3 Phase inverter there are two MOSFET. Each MOSFET works inversely. Using special control method (PWM) the variable length pulse signal is produced. Using suitable filter this signal is converted to the AC signal. Product signal can be triangle, another pulse or sinus signal, but the signal has positive half cycle and negative half cycle. In thesis, the load side has 3 phases, because of that the inverter should be chosen as one of the 3 phase inverter topologies. The selected topology is 3 phase Half Bridge (H bridge) inverter.

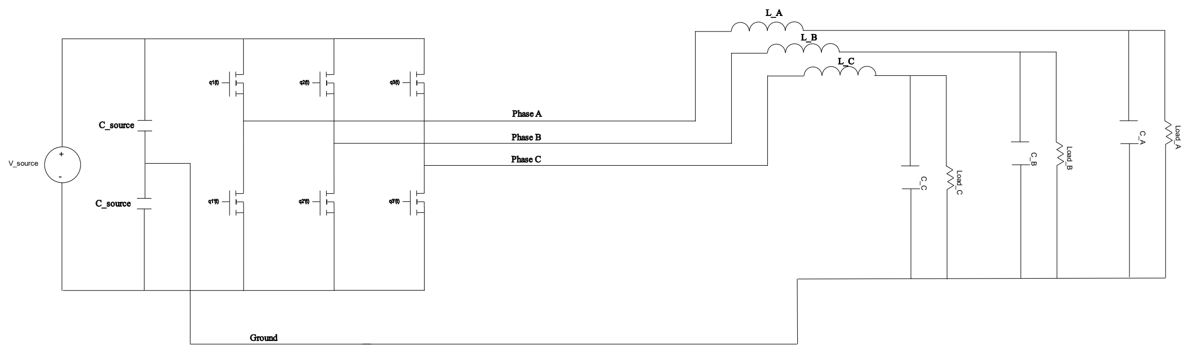

Figure 5.1. 3 Phase Half wave Inverter

There are three individual half bridge inverter that obtain the inverter's out signal

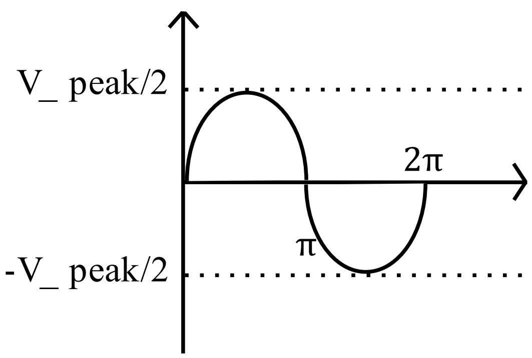

Figure 5.2. Half Wave Sinus wave form

One period of the sinus wave form is shown. The period is 0-2π.

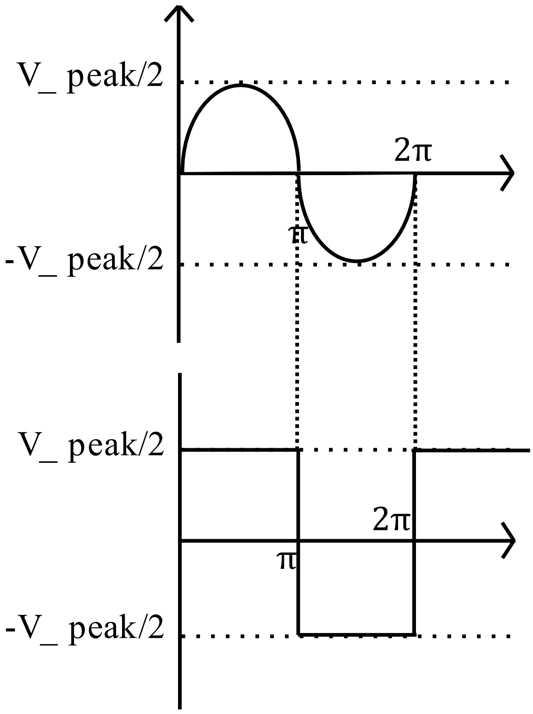

Figure 5.3. Half Wave Sinus wave form and Switching

In the system the DC voltage is supplied the three different half bridge converters. The half bridge topology produces the AC signal with half value of the DC voltage. For obtaining the sinus wave form the special control techniques are used. These controls are Sinusoidal Pulse Width Modulation, Space Vector Pulse Width Modulation and the other methods.

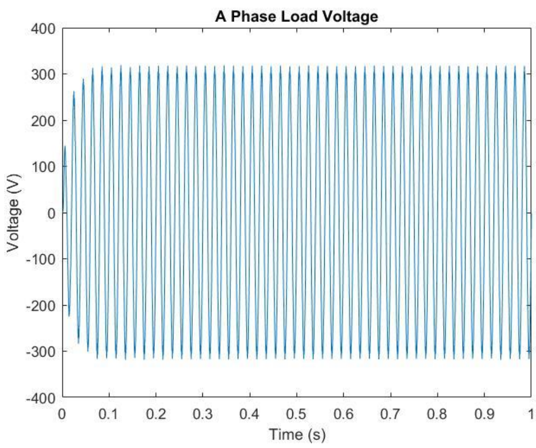

Figure 5.4. Phase A Load voltage

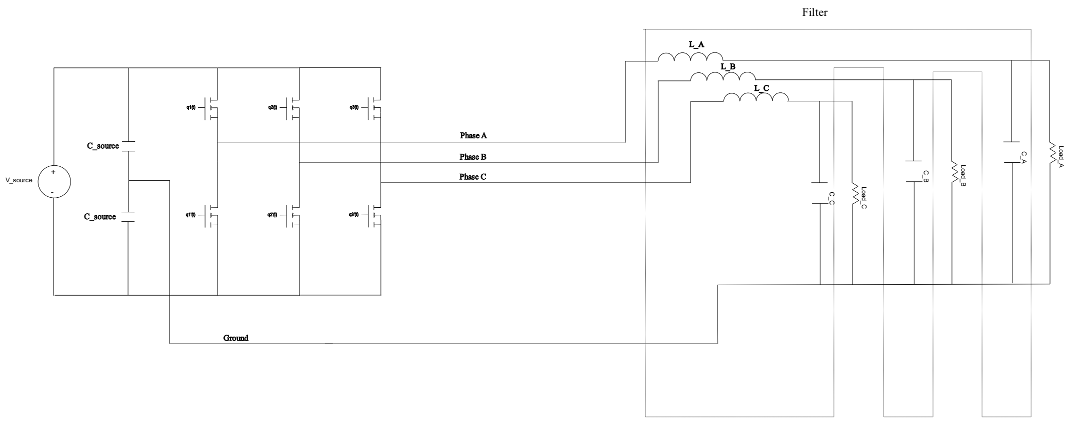

Figure 5.5. 3 Phase Half Bridge and Filter

For each phase the pure wave form is obtained for using LC filter combination.

$$2\pi f = w \quad (5.1)$$

$$w * L = \frac{1}{w*C} \quad (5.2)$$

If L value is known:

$$w^2 * L = \frac{1}{C} \quad (5.3)$$

$$(2\pi f)^2 * L = \frac{1}{C} \quad (5.4)$$

$$C = \frac{1}{(2\pi f)^2 * L} \quad (5.5)$$

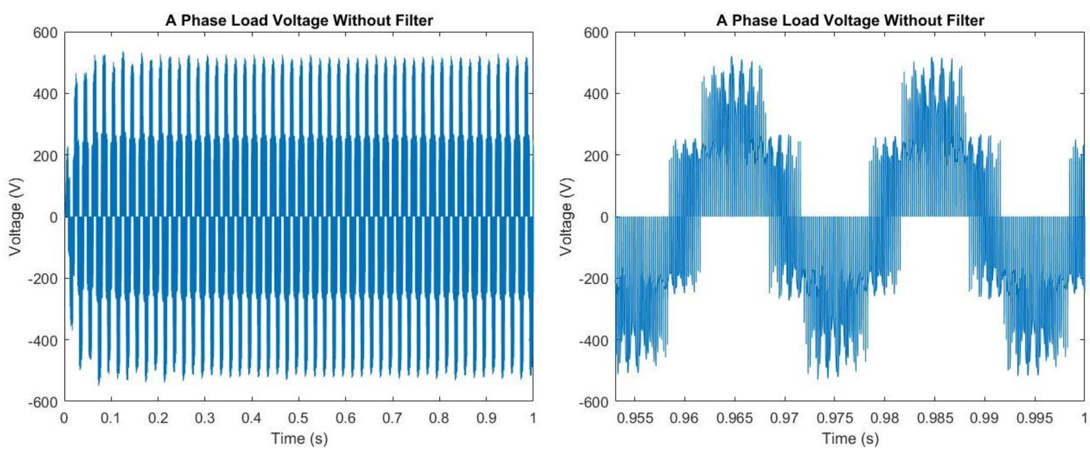

Figure 5.6. Before Filter

In these results, the obvious thing is that the DC voltage is switched from using MOSFET and using half bridge inverter topology for three phase inverters. The result is not Sinus wave without filtering. If the Fourier analysis is done, the result has 50 Hz's (the 50 Hz assumed to be base frequency) dominant component, but the other component is also written in the analysis. From using filter, the main aim is to eliminate some of the frequency part of the signal. For using this elimination, the result is more like to the sinus wave form. The only disadvantage is for this filter if the base frequency or near frequencies are selected, the main wave form is started to distort.

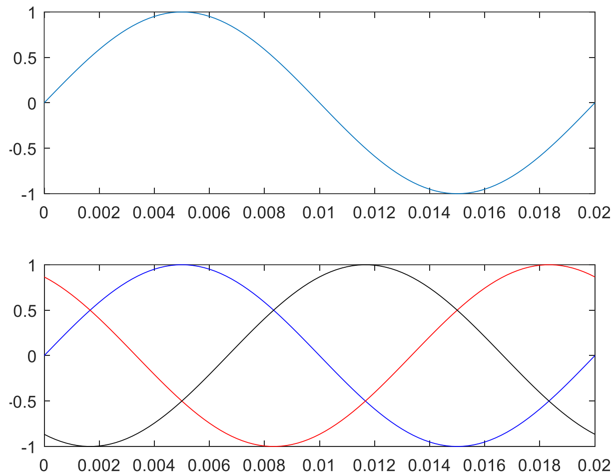

Figure 5.7. 3 Phase Sinus Wave 50Hz

The figure 5.7 shows ideal sinus wave form.

In the control part especially the Sinusoidal Pulse Width Modulation use above reference for obtaining sinus signal.

The sinus wave form is obtained for 2π. If desired wave form is related to time period the below calculation must done.

For 10000Hz

$$f = 10000 \tag{5.6}$$

$$T = \frac{1}{f} = \frac{1}{10000} = 1 * 10^{-4}\text{s} \tag{5.7}$$

2π angle must be equal to $1 * 10^{-4}$ s

$$2\pi = 1 * 10^{-5} * angle \tag{5.8}$$

$$angle = mod\left(\frac{2\pi}{10^{-4}} * currenttime, 2\pi\right) \tag{5.9}$$

Is the wanted angle function. Mod function is allow to control the angle value must be in the range of 0 to 2π.

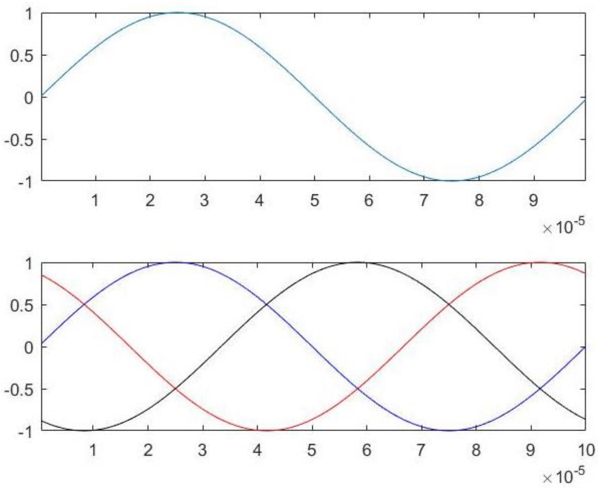

Figure 5.8. 3 Phase sinus wave form 10000Hz

For 50 Hz the function will be written as

$$\text{Angle}=100\,\pi * currenttime \tag{5.10}$$

The output is:

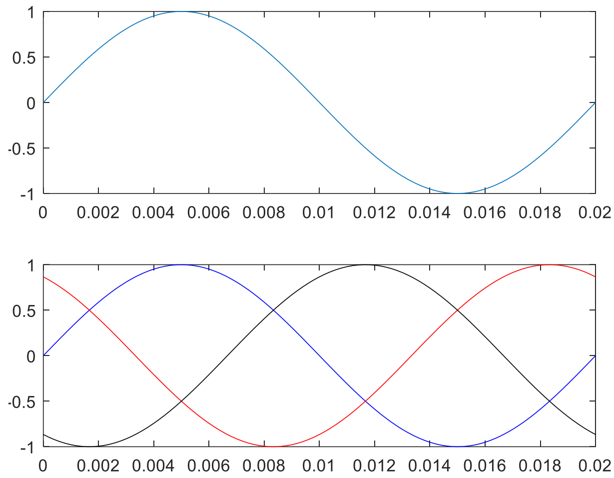

Figure 5.9. 3 Phase sinus wave form 50Hz

Positive cycle

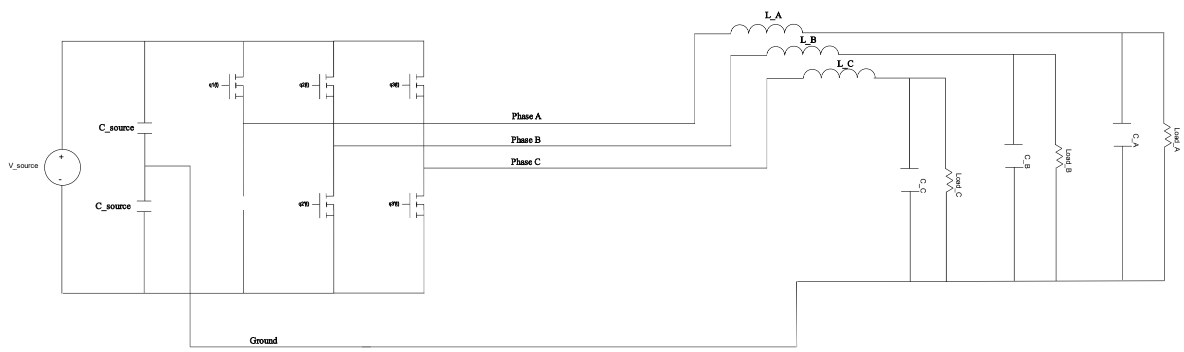

Figure 5.10. Stage 1 A Phase Half Wave inverter

Negative cycle

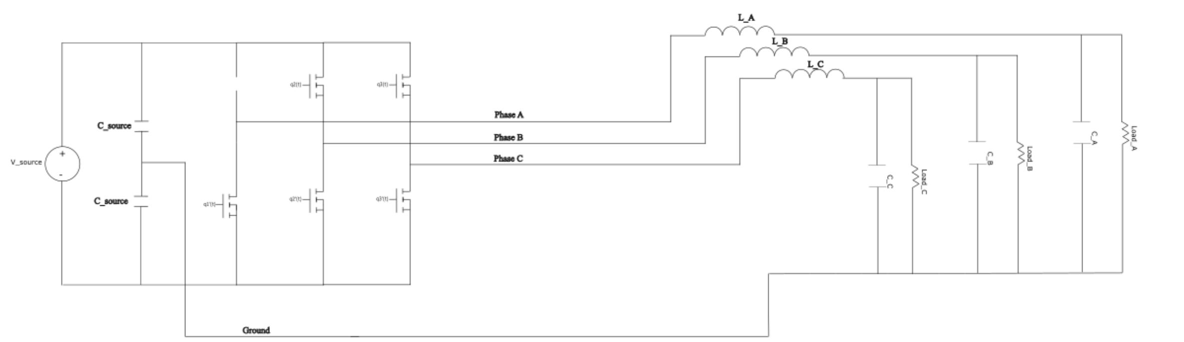

Figure 5.11. Stage 2 A Phase Half Wave inverter

In the Figure 5.12 and 5.13 the systems control signals are shown. In the Figure 5.13 The control signals are sinus wave form and they does not converted to the Pulse Wave model

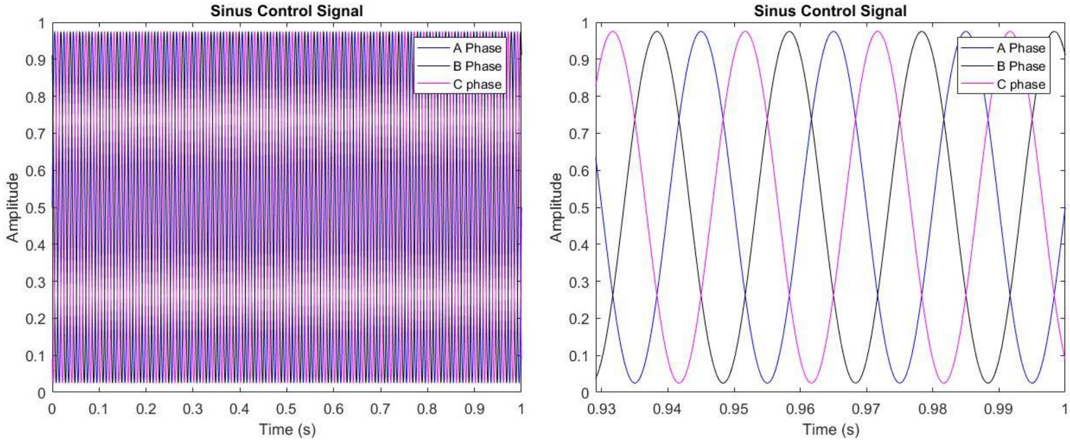

Figure 5.12. The Sinus waveform of Control Signal

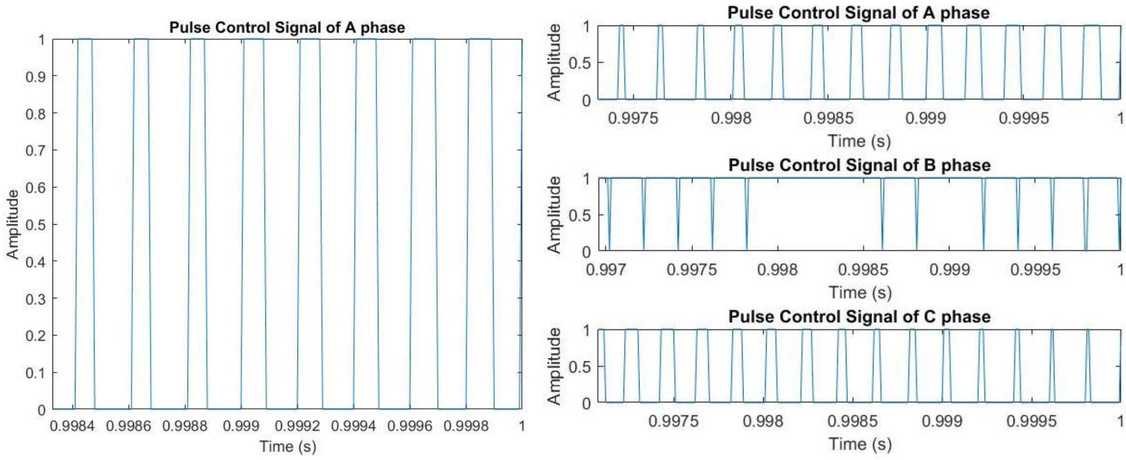

Figure 5.13. 3 Phase Pulse Control Signal

The total power of the 3 legs.

$$v_1 = v_{ac_{peak}} * cos\ (\alpha) \tag{5.11}$$

$$v_2 = v_{ac_{peak}} * cos\ (\alpha + 120) \tag{5.12}$$

$$v_3 = v_{ac_{peak}} * cos(\alpha + 240) \tag{5.13}$$

$$i_1 = i_{ac_{peak}} * cos\ (\beta) \tag{5.14}$$

$$i_2 = i_{ac_{peak}} * cos\ (\beta + 120) \tag{5.15}$$

$$i_3 = i_{ac_{peak}} * cos\ (\beta + 240) \tag{5.16}$$

$$power_{total} = power_1 + power_2 + power_3 \tag{5.17}$$

$$power_{total} = v_1 * i_1 + v_2 * i_2 + v_3 * i_3 \tag{5.18}$$

$$\cos(\alpha)\cos(\beta) = \frac{1}{2}(\cos(\alpha - \beta) + \cos(\alpha + \beta)) \tag{5.19}$$

$power_{total} = v_{ac_{peak}} * i_{ac_{peak}}(co\,s(\alpha)\,co\,s(\beta) + co\,s(\alpha+120) * co\,s(\beta+120) +$
$cos(\alpha+240) * co\,s(\beta+240))$ (5.20)

$\Sigma power = \frac{1}{2} * power * (\cos(\alpha-\beta) + \cos(\alpha+\beta) + \cos(\alpha-\beta) + \cos(\alpha+\beta+240) +$
$\cos(\alpha-\beta) + \cos(\alpha+\beta+480))$ (5.21)

$\cos(\alpha+\beta) + \cos(\alpha+\beta+240) + \cos(\alpha+\beta+480) = 0$ (5.22)

So,

$\Sigma power = \frac{1}{2} * power(\cos(\alpha-\beta) + \cos(\alpha-\beta) + \cos(\alpha-\beta))$ (5.23)

$\Sigma power = \frac{3}{2} * power * \cos(\alpha-\beta)$ (5.24)

(Irwin, Nelms and Patnaik, 2015: 481)

Finally, 3 Phase Behavior of the proposed control is shown in Figure 5.14.

α, β is equal to wt values of the system, power values are instantaneous power values.

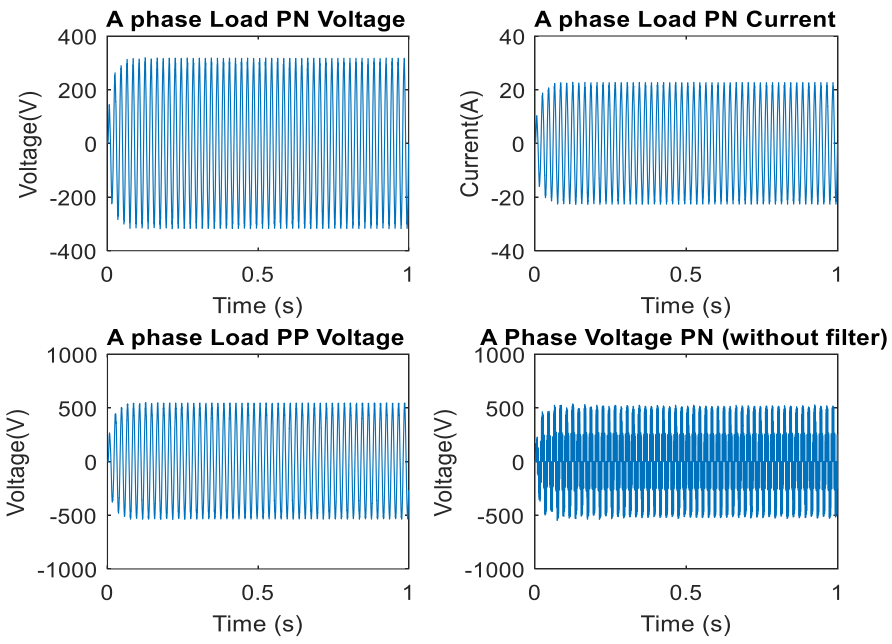

Figure 5.14. A Phase Output Behavior

In the 5.14 Figure A Phase Voltage PN (without filter) title the unfiltered voltage is contain other frequency values, so the voltage maximum value is nearly equal to 500V, however the 50 Hz component value is nearly 302V. The filter is filtered the other frequency values and the AC voltage is obtained.

6. SIMULATION STUDIES

In this thesis, three different type RESs are used as PV, TEG and Fuel Cell. The designed system, RESs and the control method are examined under two different types of models; mathematical model and circuit Model. In the design part, the all switching components are ideal and the used MPPT method is STSMC method. In the simulation and real system, there must be one energy converter to adapt the RESs' produced energy to the load side. For this reason, in PV, TEG and Fuel Cell sources converter is selected as boost converter. In the thesis, the electrolyser is used as DC Load. For electrolyser system, the selected converter is buck converter. These boost and buck converters control signal is produced by STSMC. For using mathematical model, the system behavior is shown and it can be optimized. The block diagram of the proposed system is shown below.

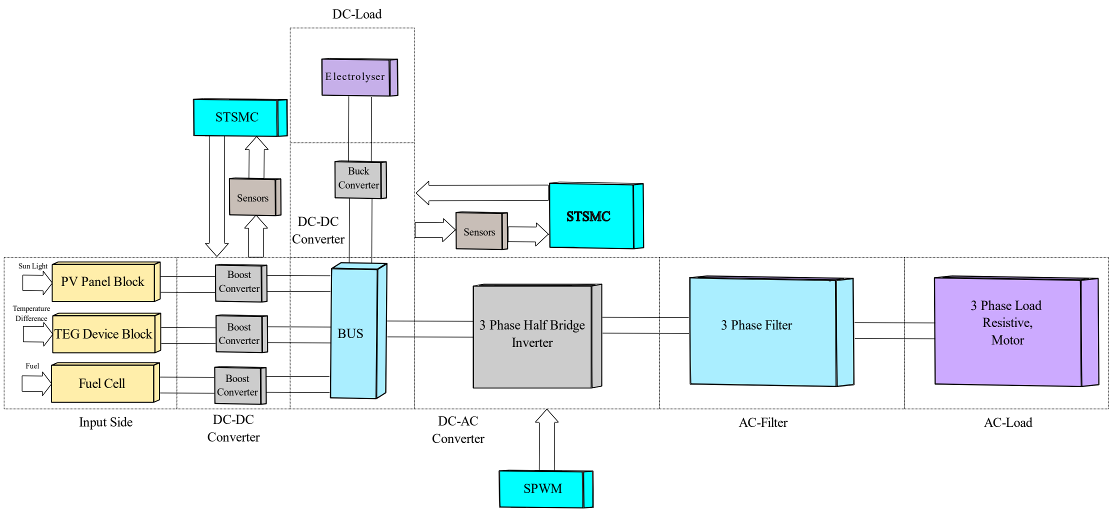

Figure 6.1. Block Diagram of Proposed System

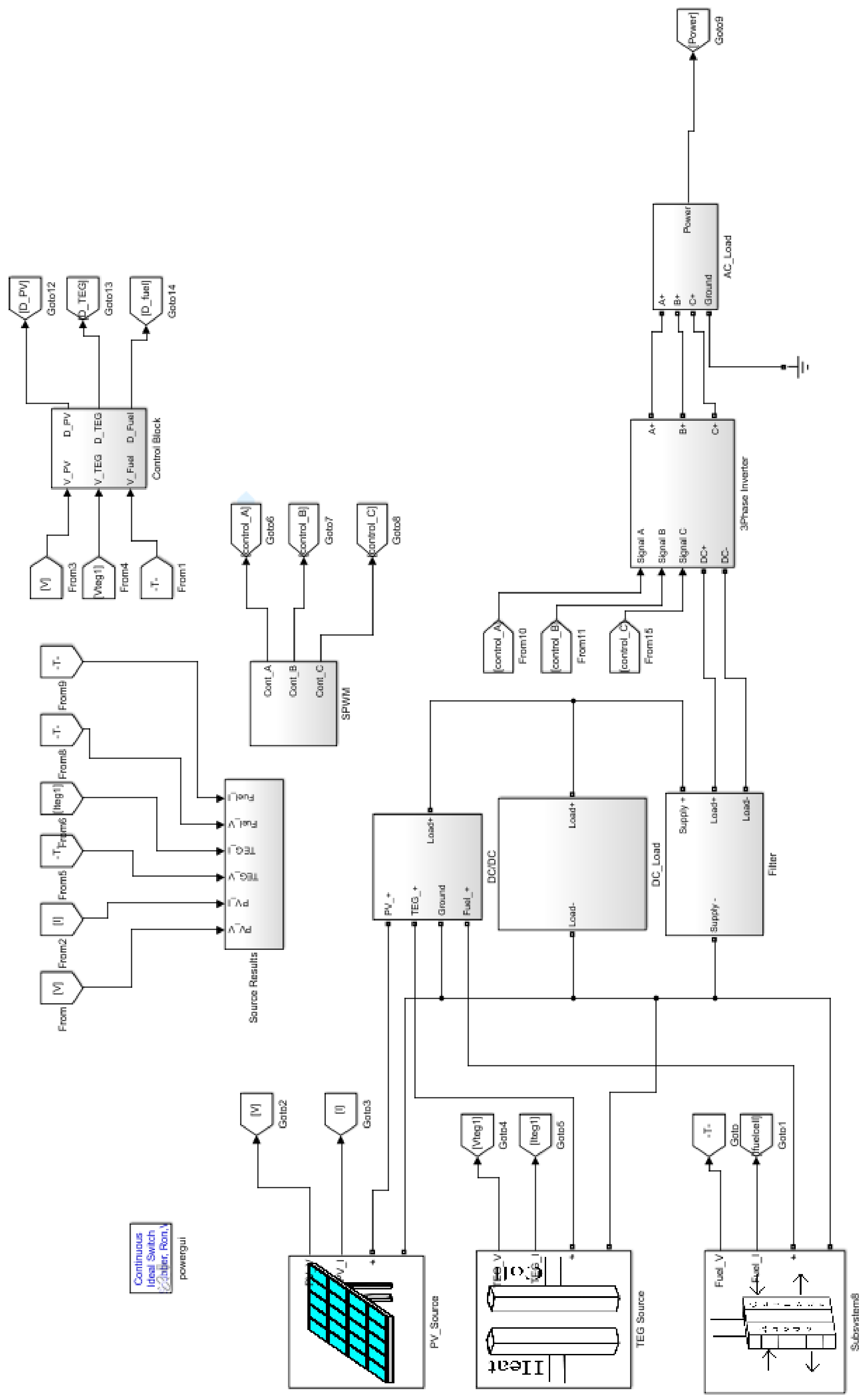

Figure 6.2. The Proposed System

6.1. PV System

The Simulation single diode equivalent circuit model PV is used. In the ideal case, the diode is working only a switch, so in the model diode is modelled as controlled current source to simulate the diode behavior properly,

<u>*PV model*</u>

The used PV panel parameters and the behavior of the PV panels Voltage - Power, Voltage – Current is shown. The Figure 6.3. is shown the selected panel values.

Table 6.1. PV Panel's Parameters

PV Panel Parameters	
Parameter Symbol	Value
V_{oc}	40V
V_{mppt}	20V
V_{coeff}	$-0,36428$
I_{short}	$7A$
I_{mppt}	$6A$
I_{coeff}	$\frac{0,03}{100}$
I_{sat}	$2,533 * 10^{-10}$
$ideal$	1,13
R_s	0,31105
R_p	28,4988
N	36
T	$27^o C, 298^o K$
Sun	$1000 \frac{W}{m^2}$

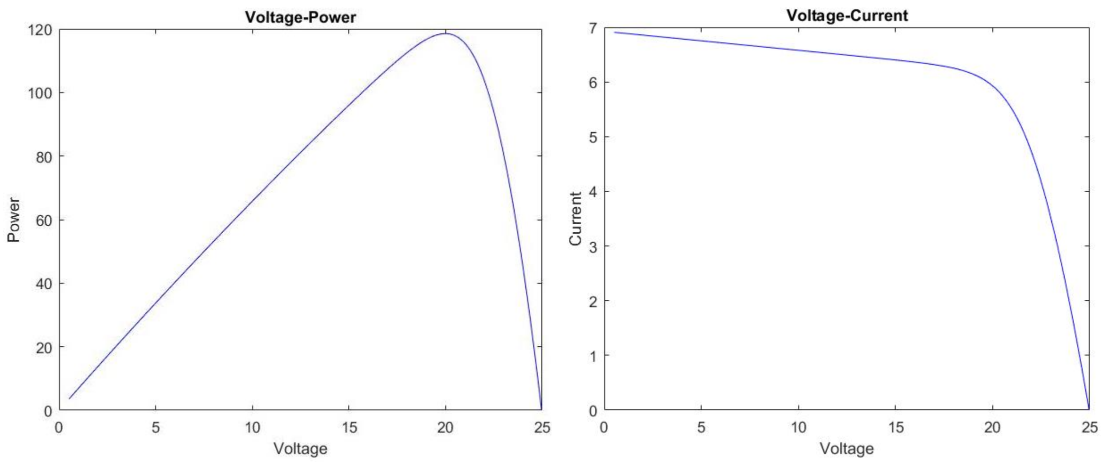

Figure 6.3. PV Voltage-Power and Voltage-Current graphics

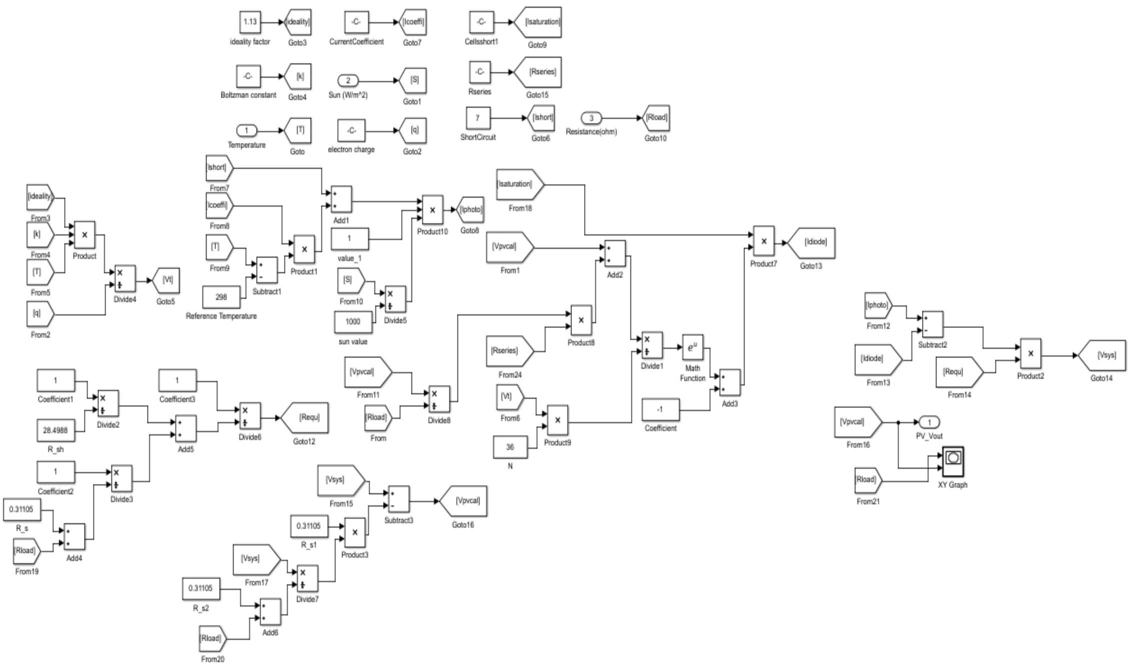

Figure 6.4. Model of PV based mathematical equivalent

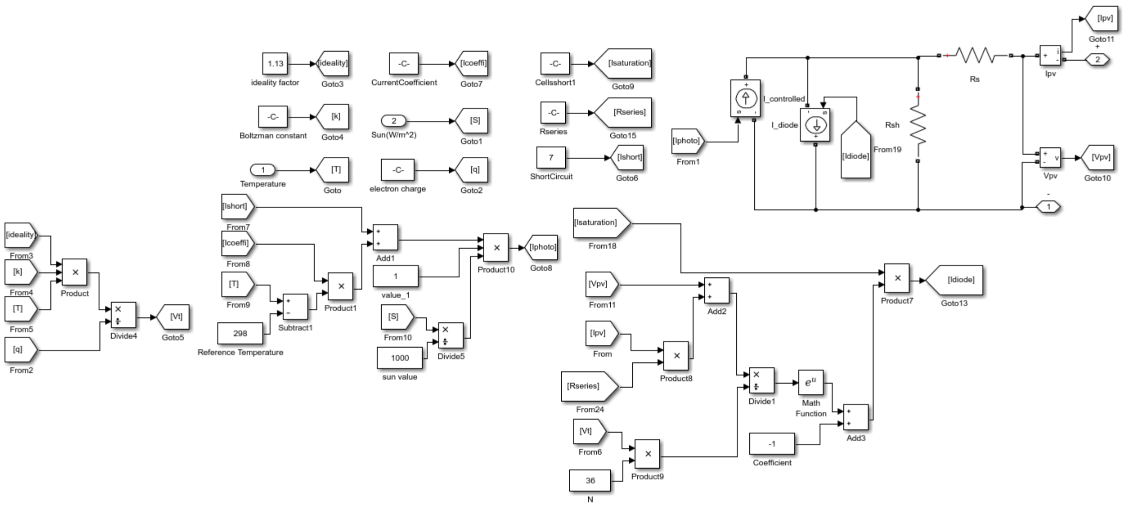

Figure 6.5. PV Circuit Model

<u>PV panel that 4 series panel as one PV panel</u>

From the design, the PV panel model is simplified to following panel. Because of the recursive calculation of the PV panel's Diode voltage and current the system needs to combine PV panel models.

Table 6.2. 4 Series PV Panel as one Panel Parameters

4 Series PV Panel Parameters	
Parameter Symbol	Value
V_{oc}	100V
V_{mppt}	80V
V_{coeff}	$-0,36428$
I_{short}	$7A$
I_{mppt}	$6A$
I_{coeff}	$\frac{0,03}{100}$
I_{sat}	$2,7656 * 10^{-10}$
$ideal$	1,134
R_s	1,2434
R_p	122,9058
N	144
T	$27^oC, 298^oK$
Sun	$1000\frac{W}{m^2}$

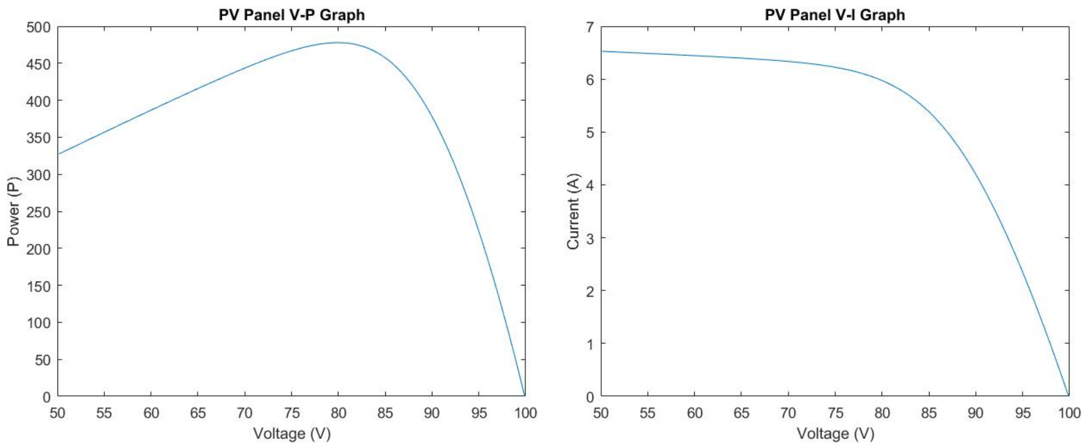

Figure 6.6. PV Behavior 4 Series Panel as one Panel

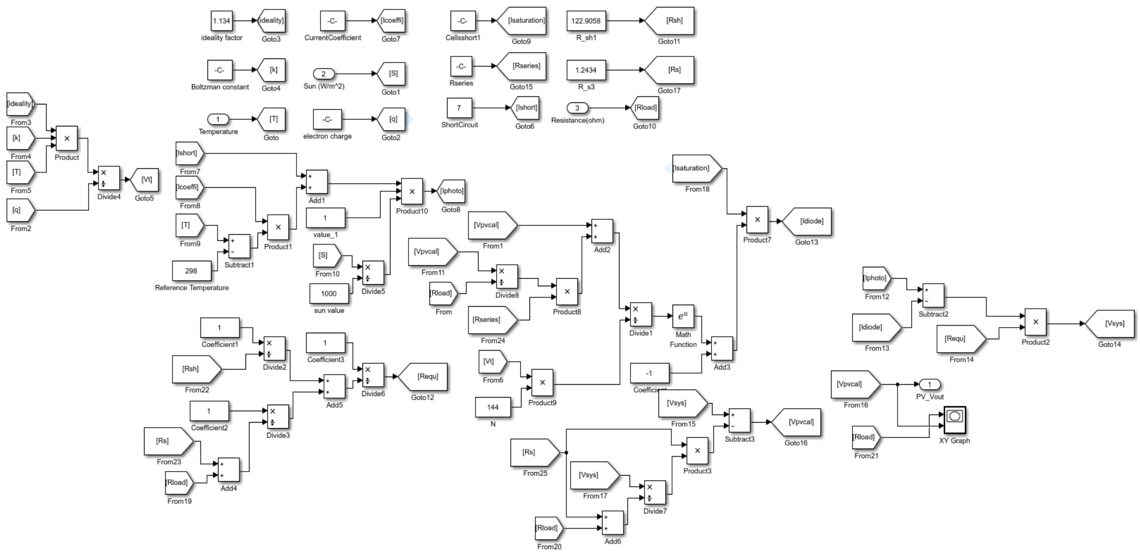

Figure 6.7. PV Mathematical Model

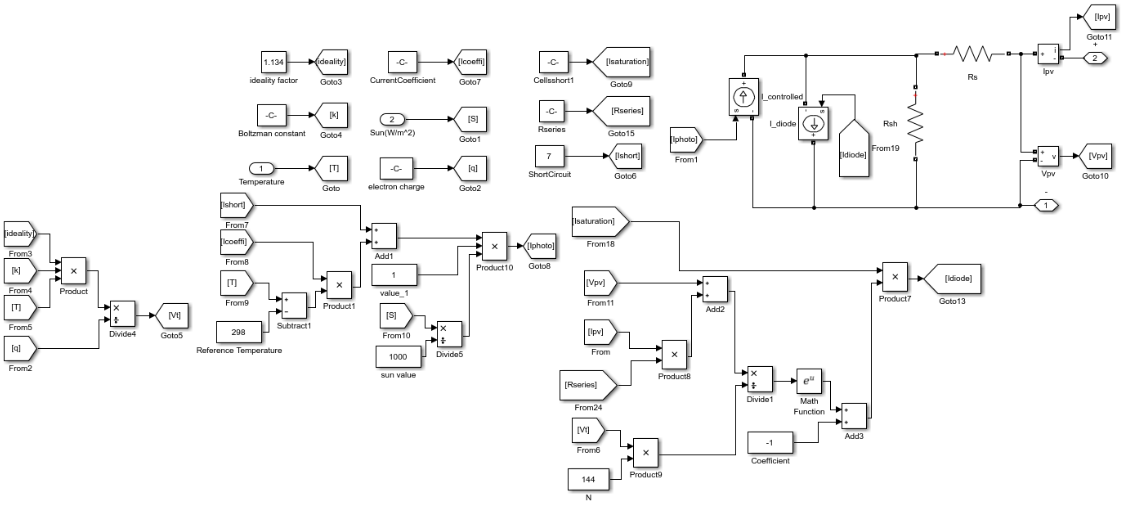

Figure 6.8. PV Circuit Model

<u>Total circuit</u>

In this part, the used PV panel, boost converter and STSMC system is explained. The mathematical model is designed to optimize system. The PV model is 320 V 6A (4 series 80V 6A). For using the mathematical model, STSMC behavior is optimized according to obtained results. The used formulas and device parameters are shown in this part.

<u>Mathematical model</u>

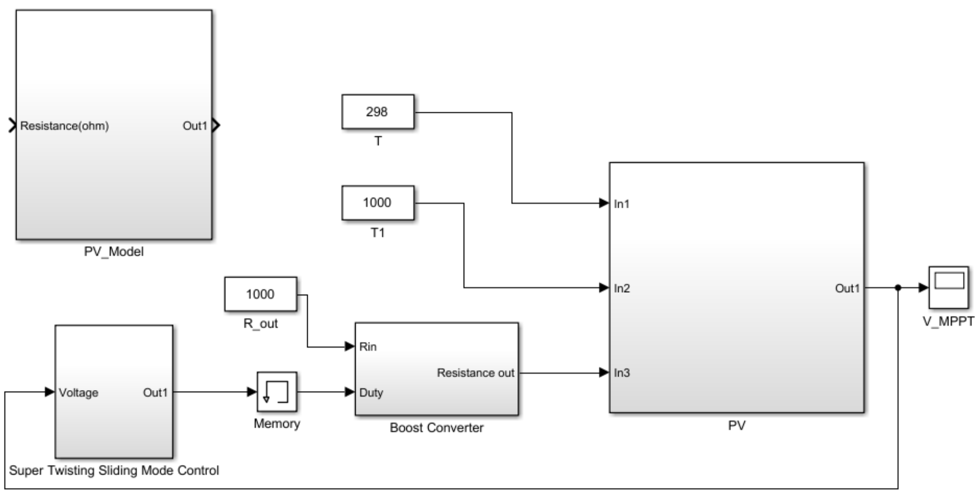

Figure 6.9. Standalone PV with Boost Converter

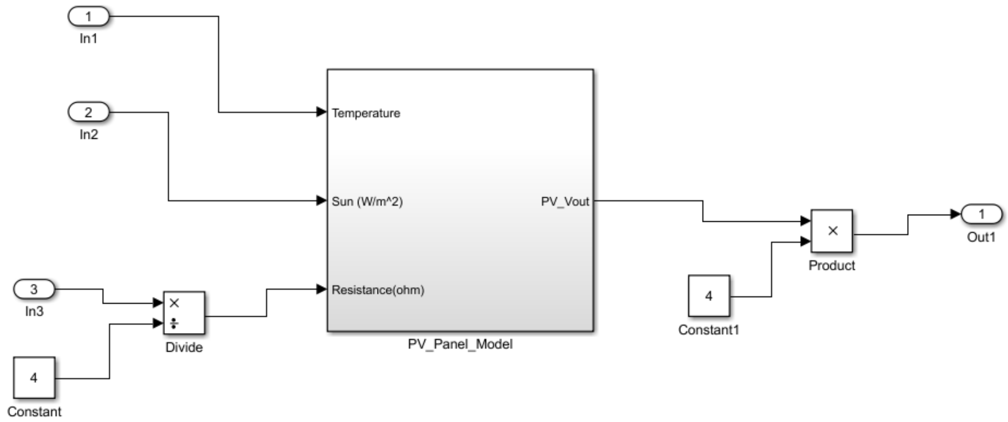

Figure 6.10. Equivalent Model of 4 Series PV

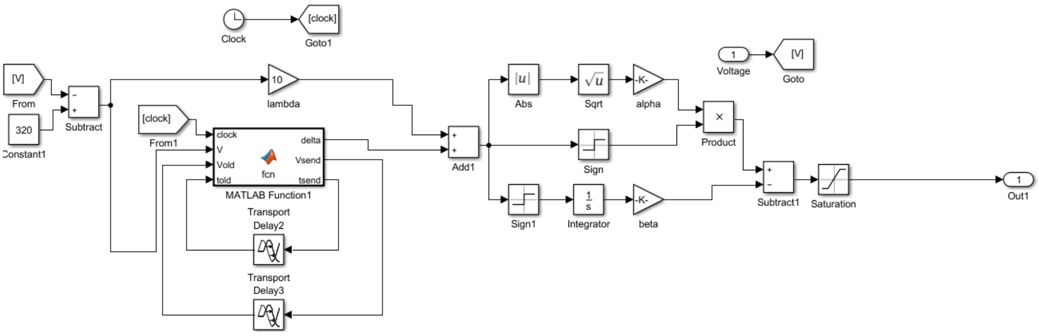

Figure 6.11. Super Twisting Sliding Mode Control

The mathematical model is shown in Figure 6.9, Figure 6.10, Figure 6. 11.

Table 6.3. PV System's Boost Converter

Boost Converter Parameters	
Parameter Symbol	Value
L	0,05H
C	$3* 10^{-4}$ F

The boost converter model is ideal in this simulation study.

Table 6.4. PV System's STSMC Parameters

STSMC Parameters	
Parameter Symbol	Value
V_{ref}	320V
Lambda	10
Alpha	0,00001
Beta	200

From 2.1.3.

$$I_{pv} = I_{ph} - I_{diode} - I_{R_p} \quad (6.1)$$

$$V_{diode} = R_p * \left(I_{ph} - I_{diode} - I_{PV}\right) = I_{PV} * \left(R_s + R_{Load_{in}}\right) = (I_{source} - I_{PV}) * \left(\frac{1}{\frac{1}{R_p} + \frac{1}{R_S + R_{load_{in}}}}\right) \quad (6.2)$$

$$R_{eq} = \frac{1}{\frac{1}{R_p} + \frac{1}{R_S + R_{load_{in}}}} \quad (6.3)$$

$$V_{PV_{system}} = (I_{Ph} - I_{diode}) * R_{eq} \quad (6.4)$$

$$V_{PV} = V_{PV_{system}} - R_S * \frac{1}{R_S + R_{load_{in}}} \quad (6.5)$$

<u>PV panels boost converter</u>

From 4.1

$$P_{in} = P_{out} \text{ ideally } V_{in} * I_{in} = V_{out} * I_{out}$$

$$V_{out} = \frac{V_{in}}{1-D} \quad (6.6)$$

$$V_{in} = I_{in} * R_{in} \quad (6.7)$$

$$V_{out} = I_{out} * R_{out} \quad (6.8)$$

$$V_{in} * I_{in} = \frac{V_{in}}{1-D} * I_{out} \quad (6.9)$$

$$I_{in} = \frac{1}{1-D} * I_{out} \quad (6.10)$$

$$I_{in} * R_{in} * I_{in} = I_{out} * R_{out} * I_{out} \quad (6.11)$$

$$\frac{1}{1-D} * I_{out} * R_{in} * \frac{1}{1-D} * I_{out} = I_{out} * R_{out} * I_{out} \quad (6.12)$$

$$R_{in} * \left(\frac{1}{1-D}\right)^2 = R_{out} \quad (6.13)$$

$$R_{in} = (1-D)^2 * R_{out} \quad (6.14)$$

Super twisting sliding mode control of PV panel

$$\Delta = 320 - V_{PV_{MPPT}} \tag{6.15}$$

$$e = 10 * \Delta + \frac{d\Delta}{dt} \tag{6.16}$$

$$d = \alpha\sqrt{|e|} * \text{signum}(e) - \beta\int \text{signum}\ (e)dt \tag{6.17}$$

$$d = \alpha\sqrt{\left|10\Delta + \frac{d\Delta}{dt}\right|} * \text{signum}\left(10\Delta + \frac{d\Delta}{dt}\right) - \beta\int \text{signum}\ (10\Delta + \frac{d\Delta}{dt})dt \tag{6.18}$$

for model

$$R_{in} = (1 - d)^2 * R_{out} \tag{6.19}$$

The model of the system is shown simply in the figure 6.12.

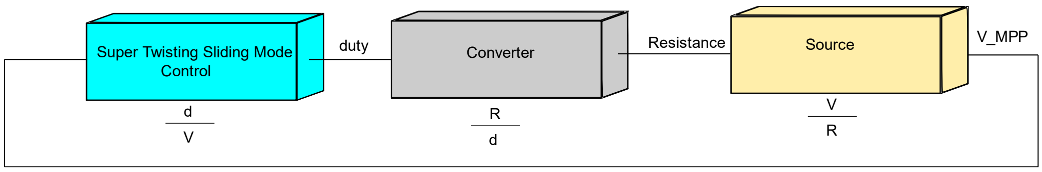

Figure 6.12. Control Model of Standalone PV

PV circuit standalone model

The standalone PV panel is shown this part. In this part, The standalone model is designed, and behavior of the output is obtained.

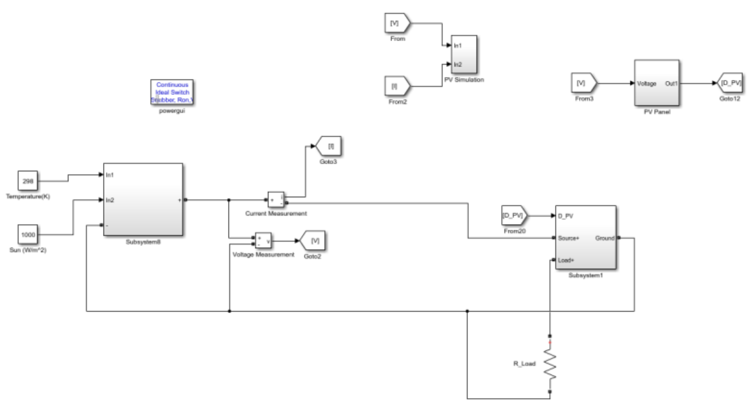

Figure 6.13. PV Standalone Model

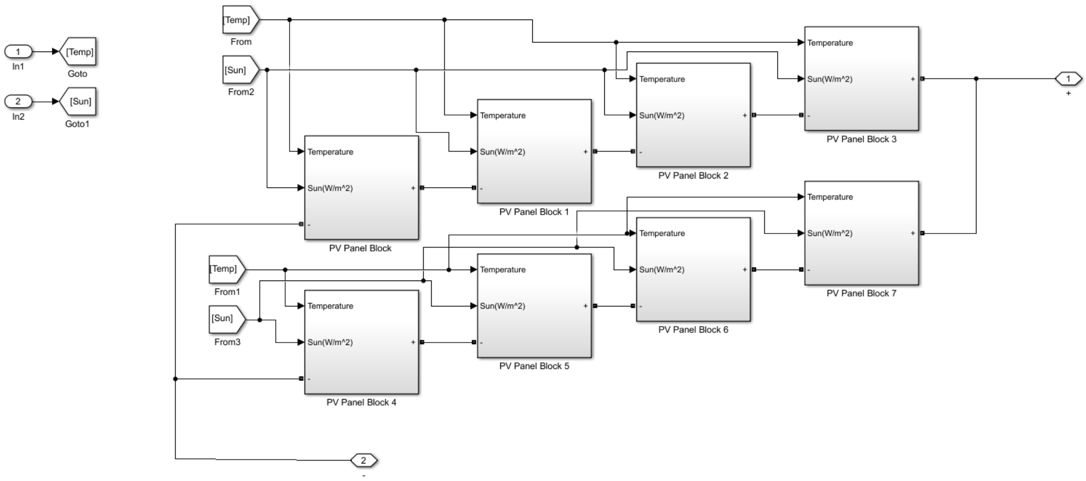

Figure 6.14. Total PV Panel model

8 Panel is connected, 4 of them series, 4 of them parallel

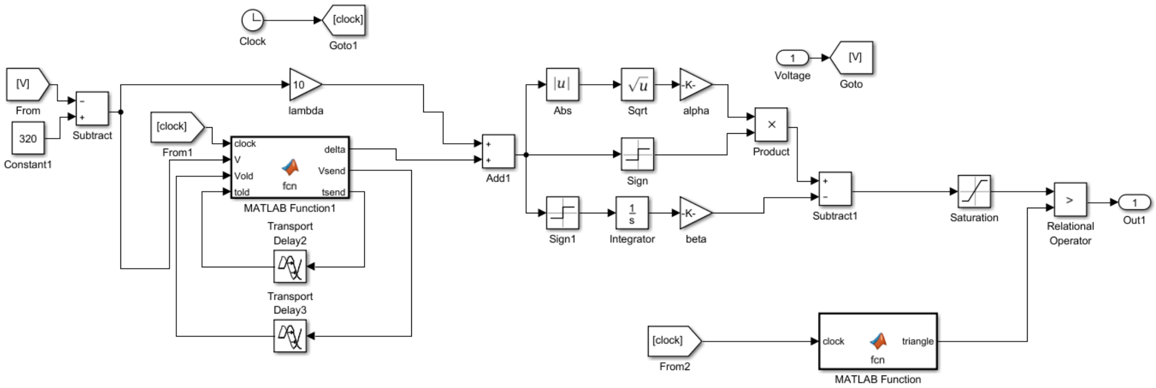

Figure 6.15. Super Twisting Sliding Mode Control Model

For minimize the algebraic Loop Behavior 4 panel is combined as one panel. For initial condition, there are 16 panel as series connected two panel series as parallel connected to obtain 320V 12A for obtaining nearly 50% duty cycle worked boost converter that obtain $440\sqrt{2}$ V as a AC side voltage in 3 phase half bridge based inverter system. These means that there is 32 algebraic loops for only PV panel of simulation. The system gets more slower than the other systems. 4 Panel as one model is reduce this number to 4 series connected two parallel series to obtain same values.

6.2. TEG System

In this part TEG system is designed and the results are shown. The TEG device model has two components; one controlled voltage source and one resistance.

TEG model

In this part, selected TEG device parameters and behavior is shown. Mathematical model is used for the optimization the STSMC behavior.

Table 6.5. TEG Device's Parameters

TEG Device Parameters	
Parameter Symbol	Value
V_{oc}	40V
V_{mppt}	20V
$Alpha$	0,2
I_{short}	8,08A
I_{mppt}	4,04A
R_{teg}	$\frac{500}{101}$ ohm
ΔT	200

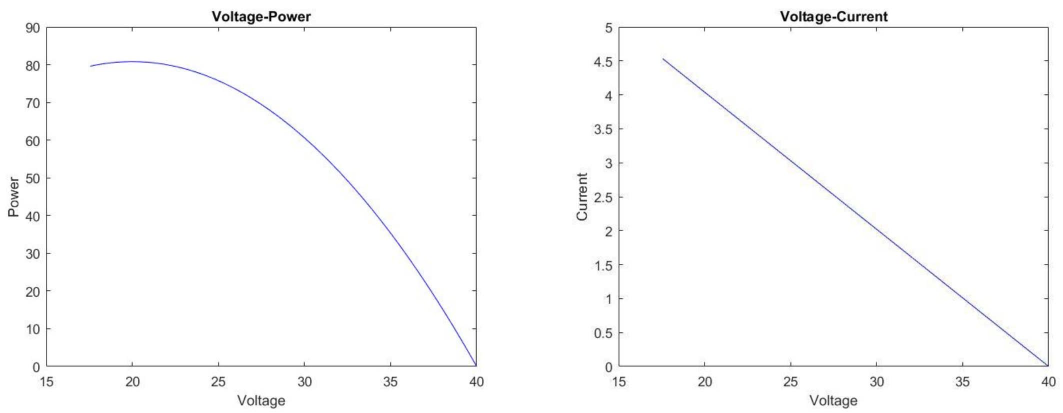

Figure 6.16. TEG Device

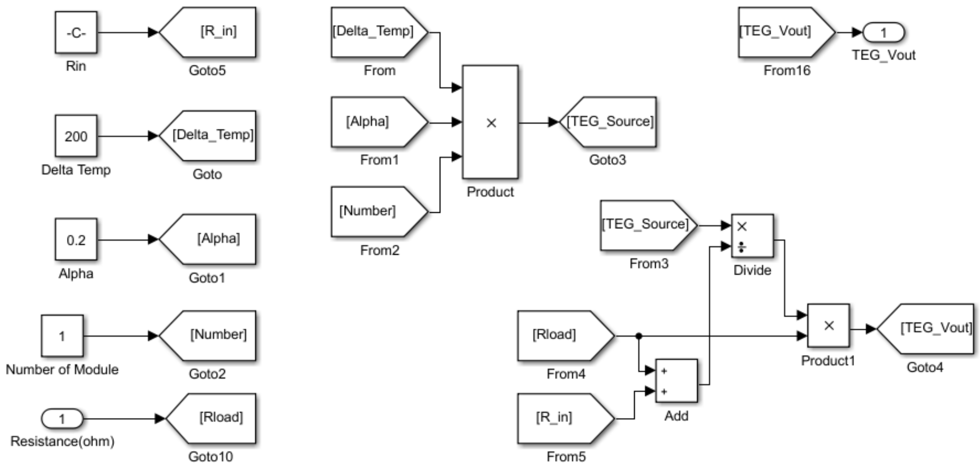

Figure 6.17. Mathematical Model of TEG

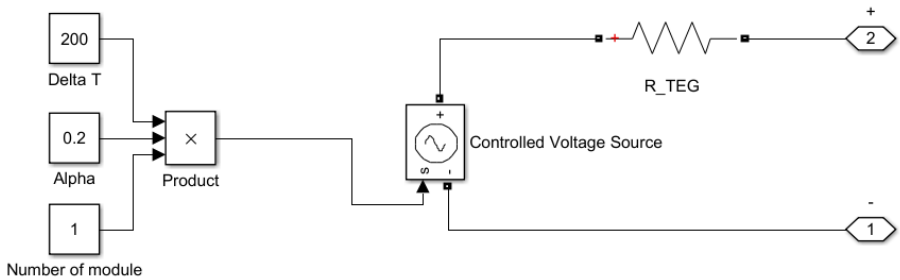

Figure 6.18. Circuit Model of TEG

$$V_{MPPT} = \frac{V_{oc}}{R_{in} * R_{load}} * R_{Load} \tag{6.20}$$

<u>Total circuit</u>

The used TEG block standalone Mathematical model is shown in Figure 6.17. In this part the TEG block is produced 320V 4,04A electricity. The mathematical model is used to optimize the system according to obtained results.

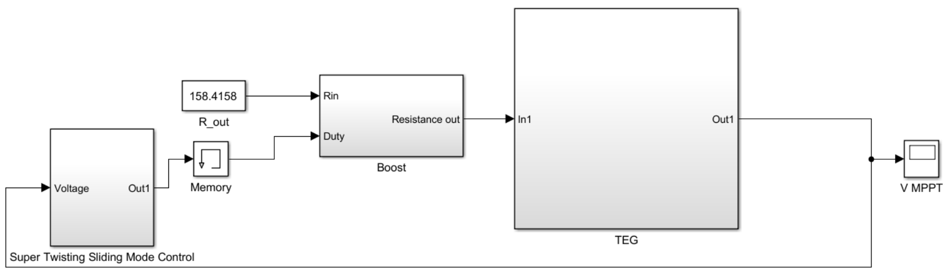

Figure 6.19. Mathematical Model of TEG

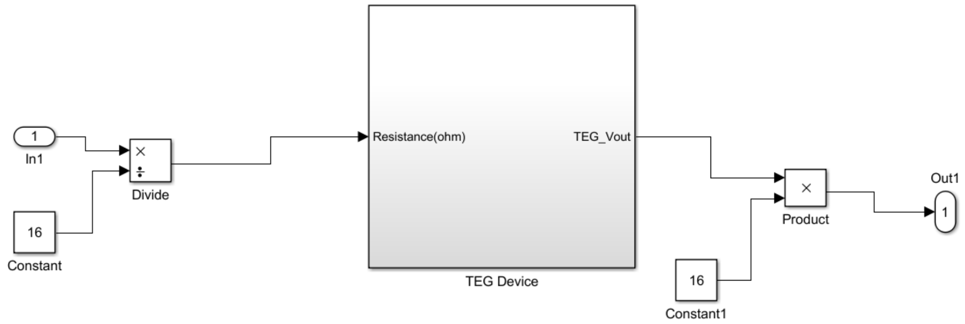

Figure 6.20. TEG device 16 TEG as Series

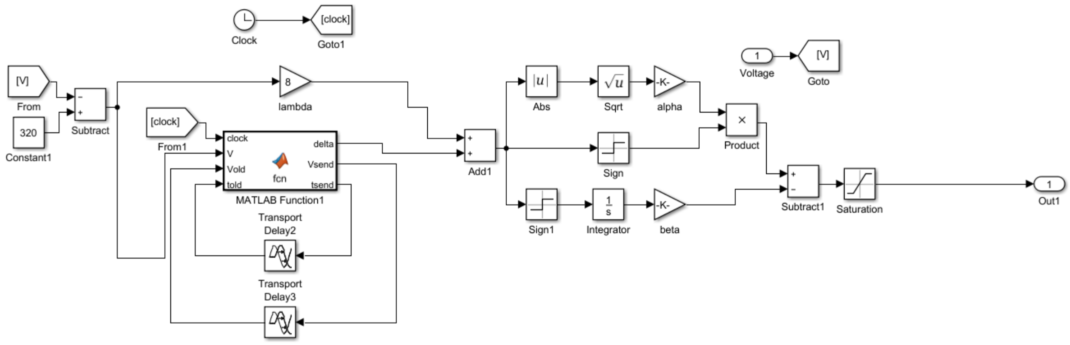

Figure 6.21. Super Twisting Sliding Mode Control

<u>TEG devices boost converter</u>

From 4.1

$P_{in} = P_{out}$ ideally $V_{in} * I_{in} = V_{out} * I_{out}$

$$V_{out} = \frac{V_{in}}{1-D} \tag{6.21}$$

$$V_{in} = I_{in} * R_{in} \tag{6.22}$$

$$V_{out} = I_{out} * R_{out} \tag{6.23}$$

$$V_{in} * I_{in} = \frac{V_{in}}{1-D} * I_{out} \tag{6.24}$$

$$I_{in} = \frac{1}{1-D} * I_{out} \tag{6.25}$$

$$I_{in} * R_{in} * I_{in} = I_{out} * R_{out} * I_{out} \tag{6.26}$$

$$\frac{1}{1-D} * I_{out} * R_{in} * \frac{1}{1-D} * I_{out} = I_{out} * R_{out} * I_{out} \tag{6.27}$$

$$R_{in} * \left(\frac{1}{1-D}\right)^2 = R_{out} \tag{6.28}$$

$$R_{in} = (1-d)^2 * R_{out} \tag{6.29}$$

Super twisting sliding mode control of TEG panel

$$\Delta = 320 - V_{TEG_{MPPT}} \tag{6.30}$$

$$e = 8 * \Delta + \frac{d\Delta}{dt} \tag{6.31}$$

$$d = \alpha\sqrt{|e|} * \text{signum}(e) - \beta\int \text{signum}\,(e)dt \tag{6.32}$$

$$d = \alpha\sqrt{\left|8\Delta + \frac{d\Delta}{dt}\right|} * \text{signum}\left(8\Delta + \frac{d\Delta}{dt}\right) - \beta\int \text{signum}\,(8\Delta + \frac{d\Delta}{dt})dt \tag{6.33}$$

The system is simply shown in figure 6.22.

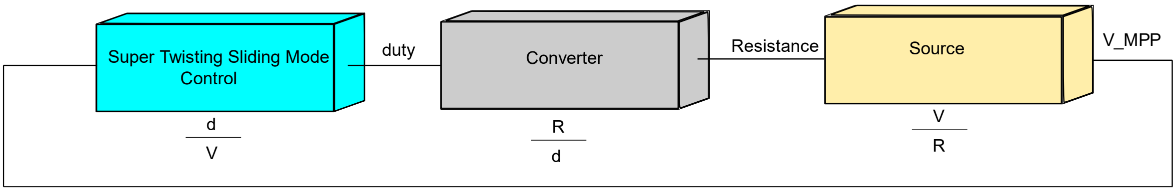

Figure 6.22. Control System

TEG device standalone

The standalone model is shown this part. In this part the TEG system is designed and the wanted values are obtained.

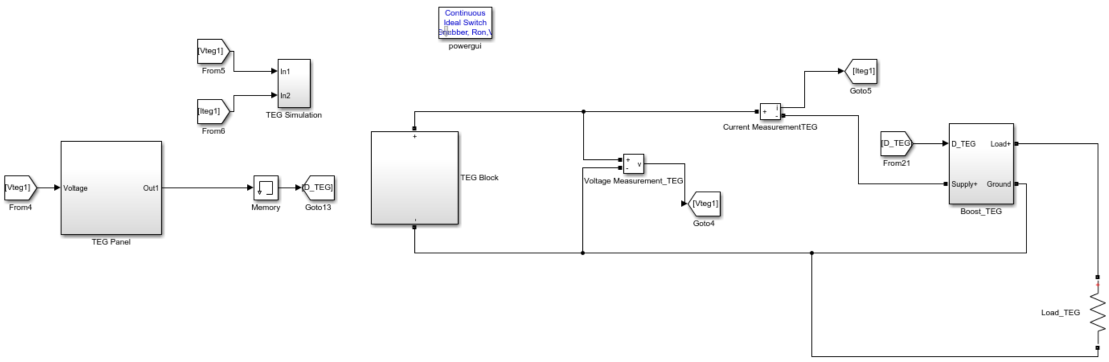

Figure 6.23. Standalone TEG System

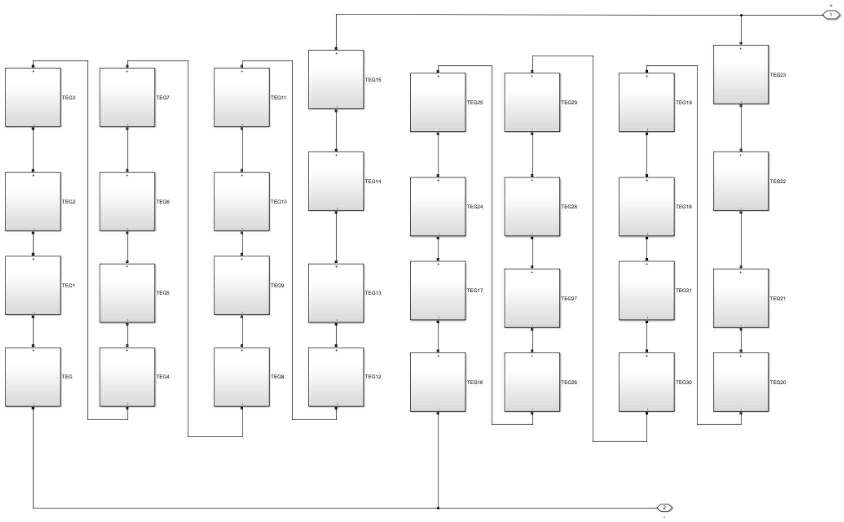

Figure 6.24. TEG total Model

32 TEG Device is connected, 16 Series Connected, 16 Parallel connected.

Boost converter

Table 6.6. TEG System's Boost Converter

Boost Converter Parameters	
Parameter Symbol	Value
L	0,013H
C	$0{,}8 * 10^{-5}$ F

The Boost Converter model is ideal

Super twisting sliding mode control

Table 6.7. TEG Device's STSMC Parameters

STSMC Parameters	
Parameter Symbol	Value
V_{ref}	320V
Lambda	8
Alpha	0,00001
Beta	500

6.3. Fuel Cell

The fuel cell is very complicated system, In the model there are one voltage source, two diode and one resistance. In this thesis, the concentration polarization part is neglected. The system is worked under ideal conditions. This means that the diode is worked like switch, so the activation losses is subtracted by the fuel cell voltage, and calculated voltage send to the controlled voltage source. The behavior of the system is shown in figure 6.25. The parameters of Fuel Cell is given as:

Table 6.8. Fuel Cell's Parameters

Fuel Cell Parameters	
Parameter Symbol	Value
V_{oc}	42V
V_{max}	20,85V
V_{mppt}	24,23V
I_{max}	61,54A
I_{mppt}	51A
I_{sat}	0,027318
gas constant	8,3145
Temperature	328^{o}K
alpha	0,308
$e^{-}num$	2
$Faraday_{cons}$	96485
R_{inner}	0,33 ohm

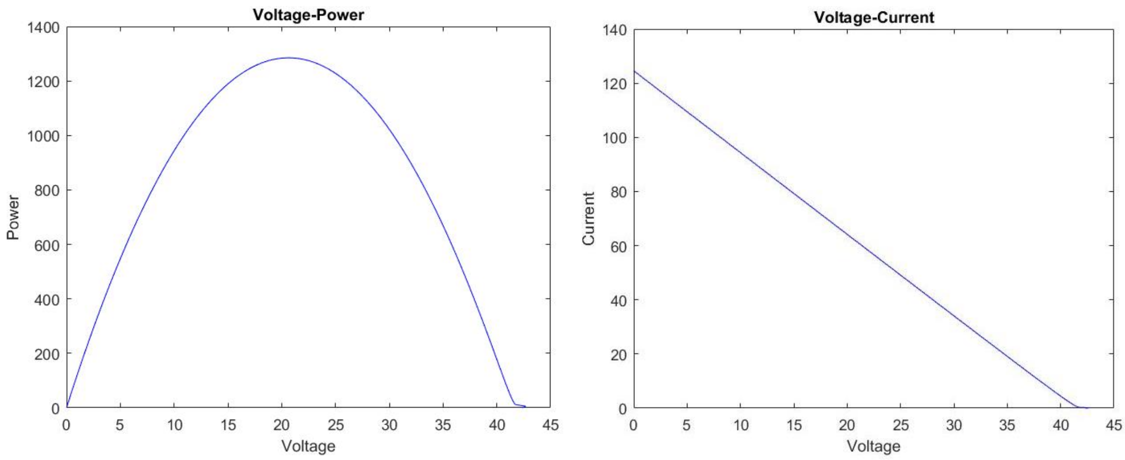

Figure 6.25. Fuel Cell Voltage-Power and Voltage- Current

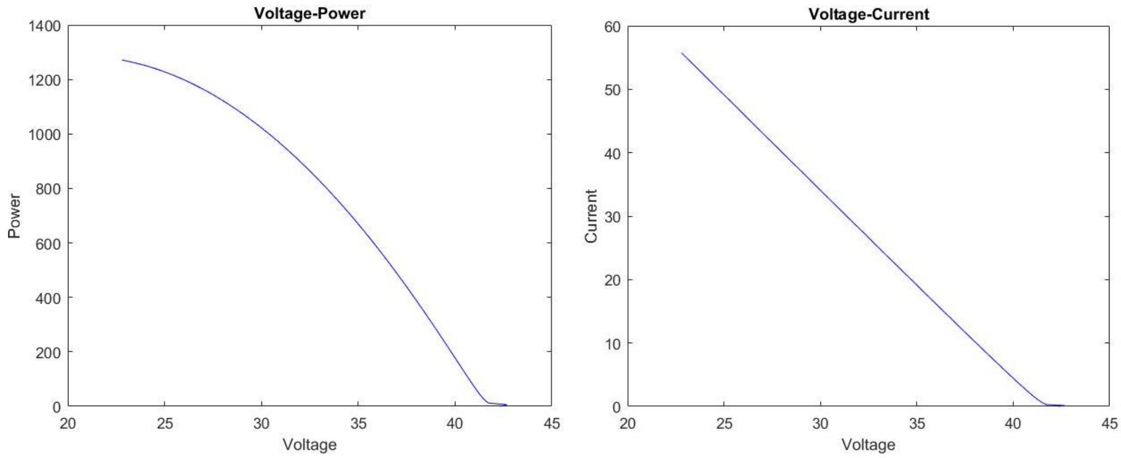

Figure 6.26. Maximum Values of Fuel Cell

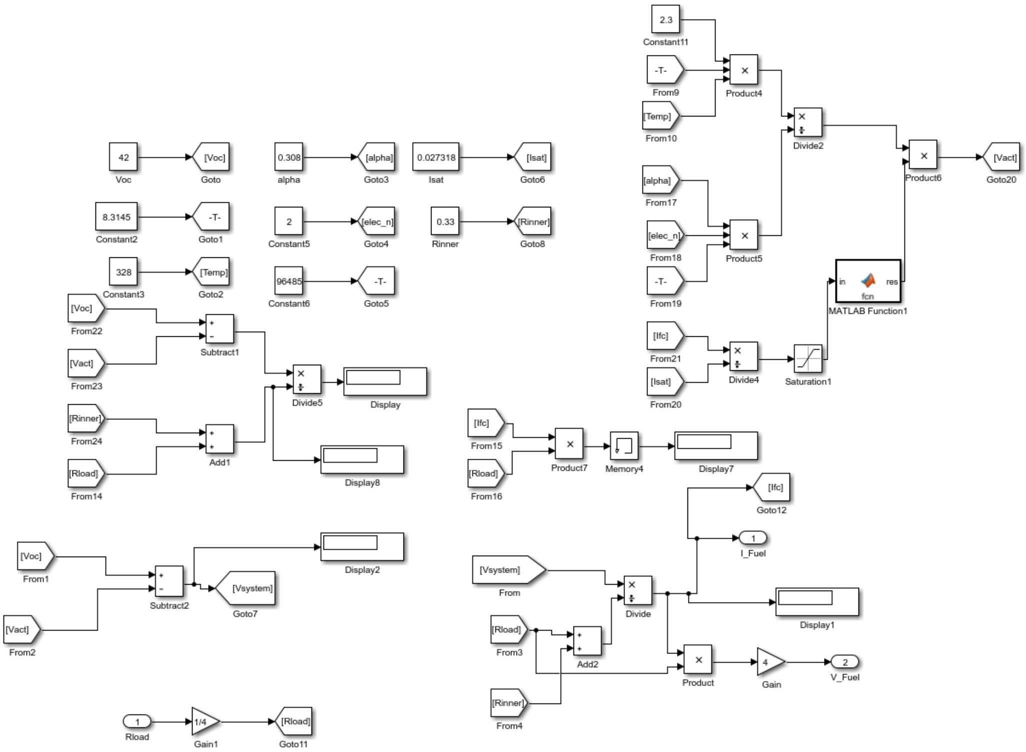

Figure 6.27. Fuel Cell Mathematical Model

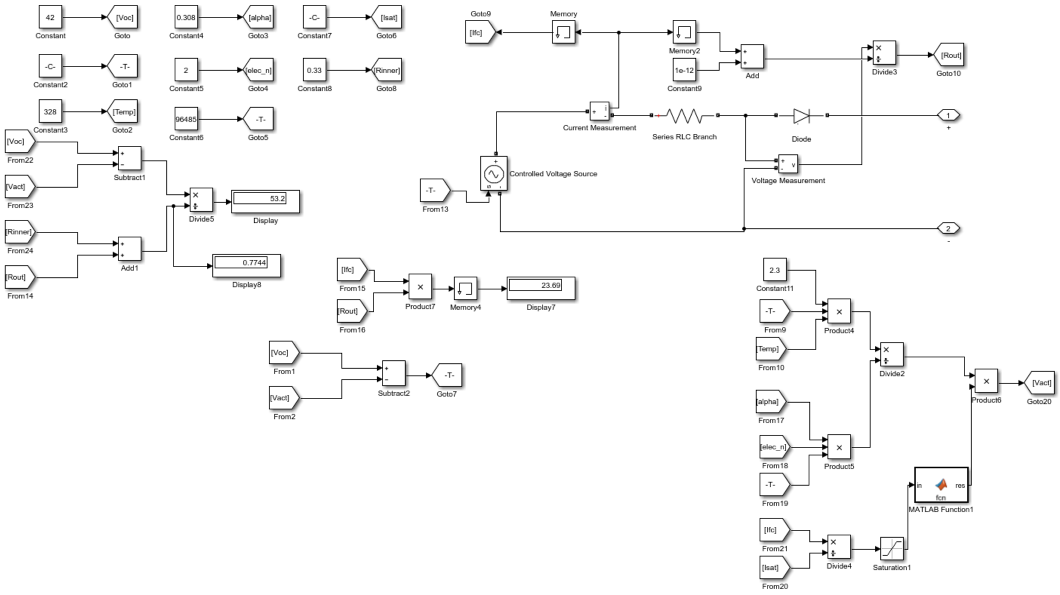

Figure 6.28. Fuel Cell Circuit Model

Total circuit

The mathematical model of the system is shown in the Figure 6.29, Figure 6.30. The mathematical model is used for the optimization of the STSMC behavior. According to obtained results the behavior is optimized.

Mathematical model

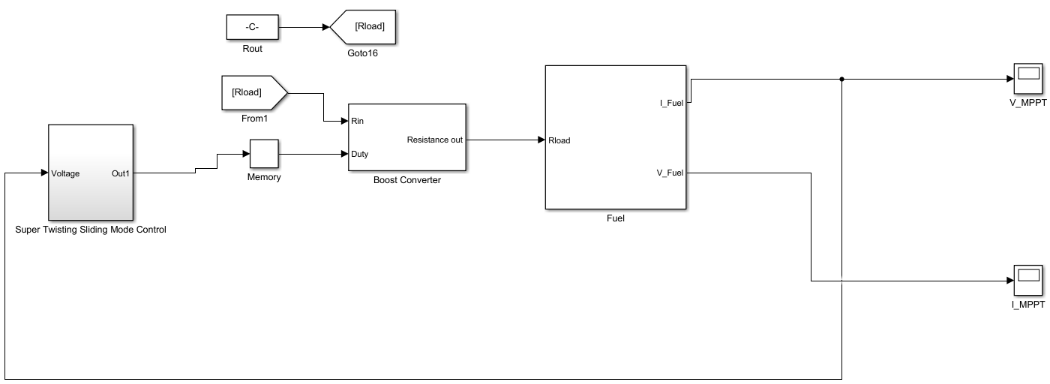

Figure 6.29. Fuel Cell Mathematical Model

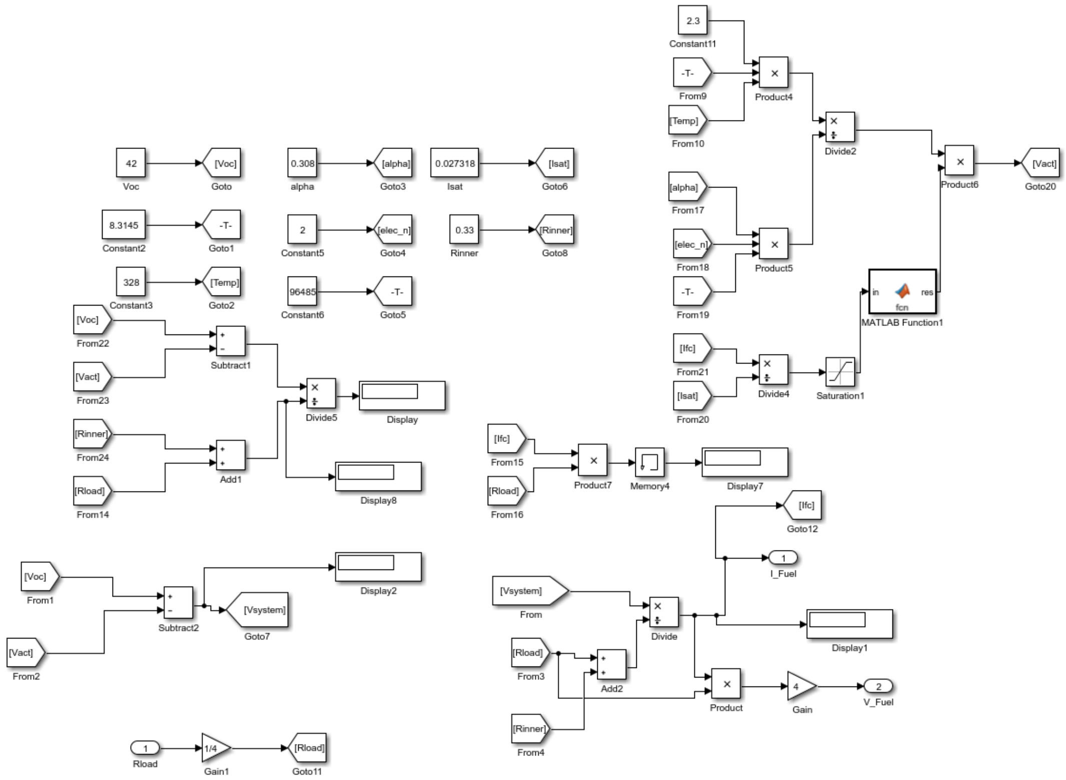

Figure 6.30. Fuel Cell Mathematical Model

From Part 2.3.3.

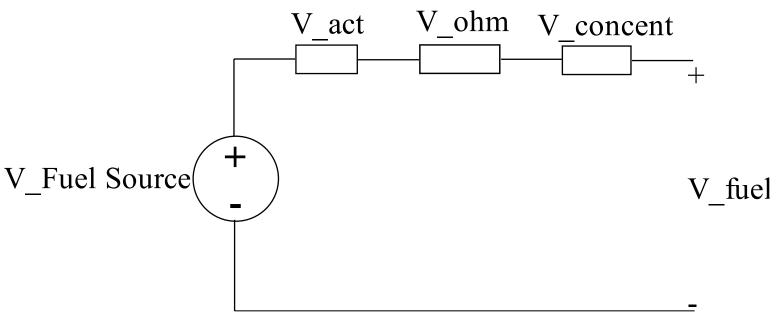

Figure 6.31. Fuel Cell Circuit

$$V_{Fuel\ Source} = \frac{-\Delta G}{2*F} + \frac{R*T}{2*F} In(\frac{P_{H_2}\sqrt{P_{O_2}}}{P_{H_2O}}) \quad (6.34)$$

$$V_{act} = \frac{2{,}3*R*T}{\alpha*n_{elec}*F} * In(\frac{I_{FC}}{I_o}) \quad (6.35)$$

$$V_{ohm} = I_{FC} * R_{in} \quad (6.36)$$

$$V_{concent} = -\frac{R*T}{n_{elec}*F} * In(1 - \frac{I_{FC}}{I_L}) \quad (6.37)$$

Open circuit voltage

$$E_{open} = \frac{-\Delta G}{2*F} + \frac{R*T}{2*F} In\left(\frac{P_{H_2}\sqrt{P_{O_2}}}{P_{H_2O}}\right) - \frac{\Delta S}{2*F} * (T - 298{,}15) \tag{6.38}$$

$$\Delta G = G_{H_2} + G_{O_2} - G_{H_2O} = 0 + 0 - (-237{,}13) = 237{,}13 \tag{6.39}$$

$$\Delta S = 131 + 205 - 69{,}9 = 266{,}1 \tag{6.40}$$

In the model I used V_{oc}, V_{Act} as primary design the resistance is placed to adjust voltage and current values of the fuel as simulate according to real values. The diode is ideal diode and it's duty is to prevent reverse current condition. For reverse current the electrolyser is used. Reverse modelling of Fuel cell.

<u>Fuel cell standalone model</u>

The standalone model is used for design the Fuel Cell system and obtain the wanted behaviors.

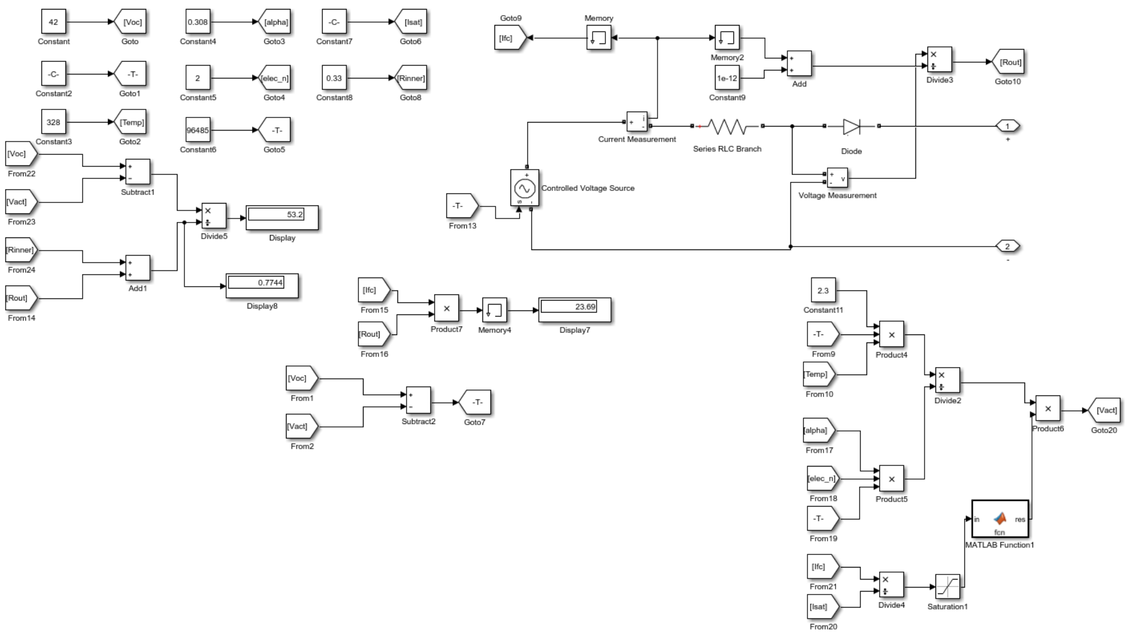

Figure 6.32. Standalone Fuel Cell

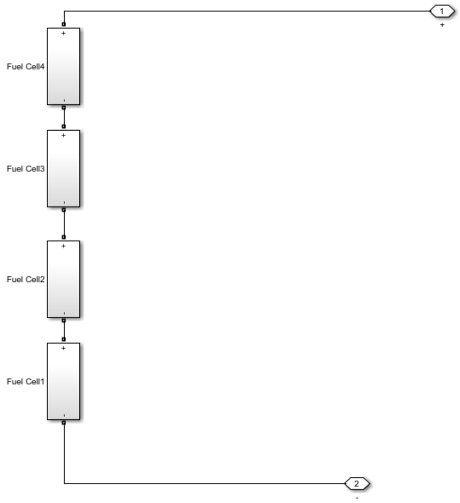

Figure 6.33. Total Fuel Cell Circuit

4 Panel are connected series.

Boost converter

Table 6.9. Fuel Cell System’s Boost Converter

Boost Converter Parameters	
Parameter Symbol	Value
L	0,003H
C	$1 * 10^{-5}$ F

The boost converter model is ideal.

Super twisting sliding mode control

Table 6.10. Fuel Cell’s STSMC Parameters

STSMC Parameters	
Parameter Symbol	Value
V_{ref}	96,92V
Lambda	20
Alpha	0,0001
Beta	200

6.4. Electrolyser

The electrolyser is used to convert the extra energy (if the produce energy is higher than the load demand) to the fuel of the fuel cell device. The aim is to convert extra energy to the fuel of the fuel cell.

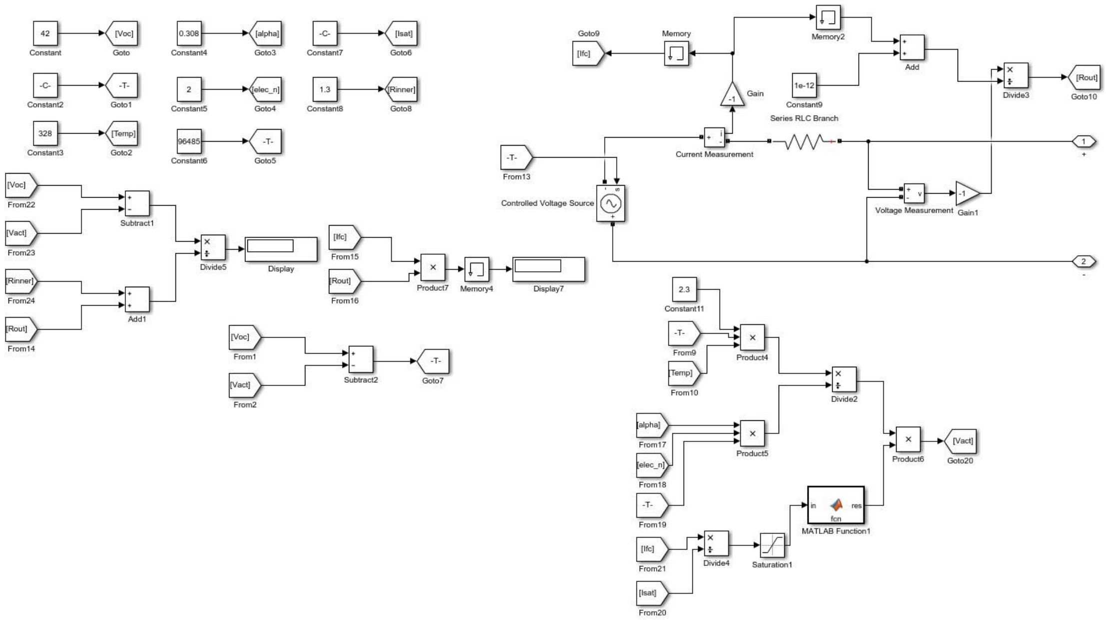

Figure 6.34. The model of Electrolyser

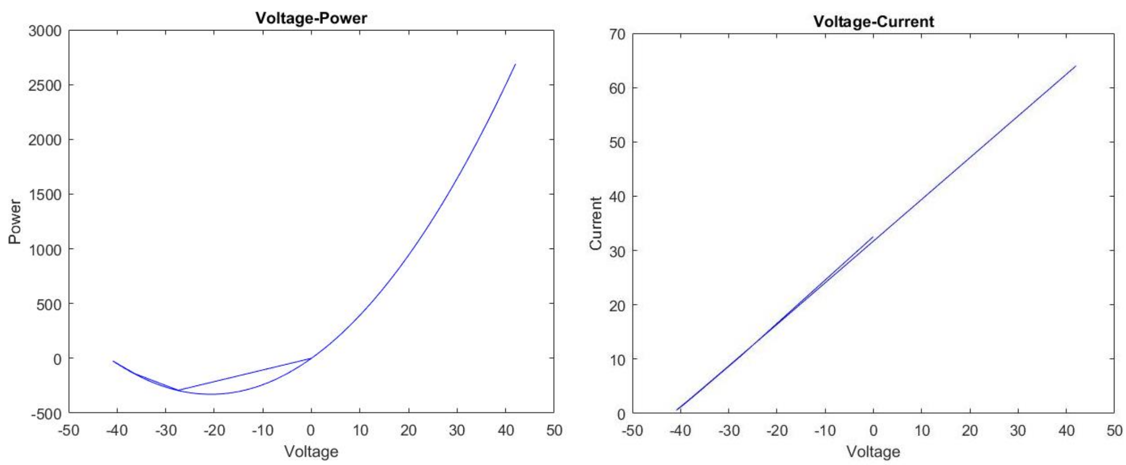

Figure 6.35. 42 V input variable Duty cycle 0-1

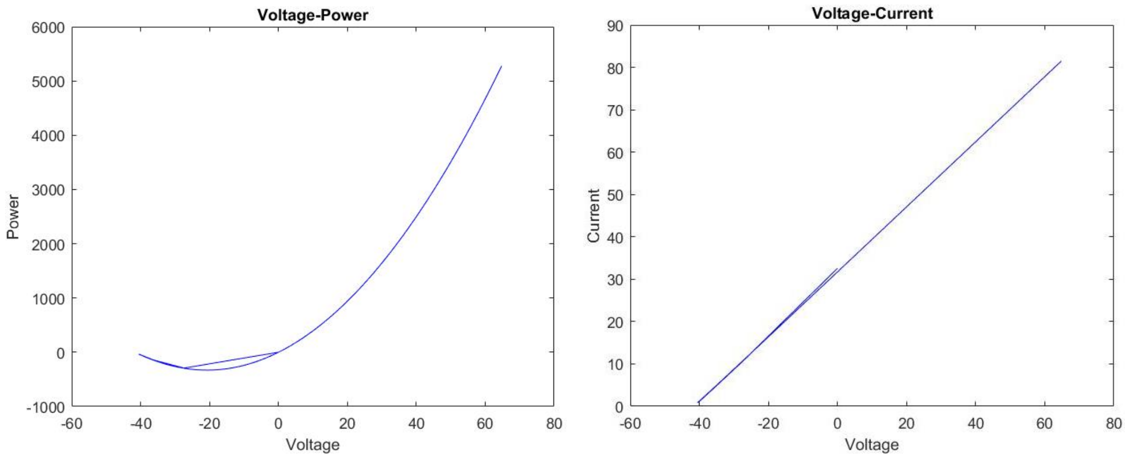

Figure 6.36. 24,23-640 V changing voltage

The reverse system of the Fuel Cell is used for electrolyser. In the thesis if the energy level is higher than the wanted value. The electrolyser is started to work and the energy is balanced. Positive side working principle is because of the initial conditions, the important part is Negative cycle.

In this part the used converter is Buck Converter.

Electrolyser devices buck converter

From 4.2

$\mathrm{P_{in}} = \mathrm{P_{out}}$ ideally $\mathrm{V_{in}} * \mathrm{I_{in}} = \mathrm{V_{out}} * \mathrm{I_{out}}$

$$V_{out} = V_{in} * D \tag{6.41}$$

$$\mathrm{V_{in}} = \mathrm{I_{in}} * \mathrm{R_{in}} \tag{6.42}$$

$$\mathrm{V_{out}} = \mathrm{I_{out}} * \mathrm{R_{out}} \tag{6.43}$$

$$\mathrm{P_{in}} = \mathrm{P_{out}} = \mathrm{V_{in}} * \mathrm{I_{in}} = \mathrm{V_{out}} * \mathrm{I_{out}} \tag{6.44}$$

$$\mathrm{V_{in}} * \mathrm{I_{in}} = V_{in} * D * \mathrm{I_{out}} \tag{6.45}$$

$$\mathrm{I_{in}} = D * \mathrm{I_{out}} \tag{6.46}$$

$$\mathrm{I_{in}} * \mathrm{R_{in}} * \mathrm{I_{in}} = \mathrm{I_{out}} * \mathrm{R_{out}} * \mathrm{I_{out}} \tag{6.47}$$

$$D * \mathrm{I_{out}} * \mathrm{R_{in}} * D * \mathrm{I_{out}} = \mathrm{I_{out}} * \mathrm{R_{out}} * \mathrm{I_{out}} \tag{6.48}$$

$$\mathrm{R_{in}} = \frac{R_{out}}{D^2} \tag{6.49}$$

Super twisting sliding mode control of electrolyser

$$\Delta = -24{,}23 + V_{PV_{MPPT}} \quad (6.50)$$

$$e = 20 * \Delta + \frac{d\Delta}{dt} \quad (6.51)$$

$$d = \alpha\sqrt{|e|} * \text{signum}(e) - \beta\int \text{signum}\,(e)dt \quad (6.52)$$

$$d = \alpha\sqrt{\left|20\Delta + \frac{d\Delta}{dt}\right|} * \text{signum}\left(20\Delta + \frac{d\Delta}{dt}\right) - \beta\int \text{signum}\,(20\Delta + \frac{d\Delta}{dt})dt \quad (6.53)$$

It is also controlled by the Super Twisting Sliding Mode Controller.

7. SIMULATION RESULTS

In this part the proposed system is tested under defined conditions and the results are shown. There are Subtitle Under STSMC control and non-ideal condition the overall system efficiency test for using R or Motor load, and The comparison part that testing under three different condition advantages and disadvantages of the STSMC compare to P&O control.

7.1. STSMC

In this part, the system is tested under non ideal condition and the control method is STSMC control.

7.1.1. Nonideal condition resistive load

In this part, the used control is STSMC control, however the system is tested under nonideal condition to obtain the efficiency of the system. The system is tested under resistive load.

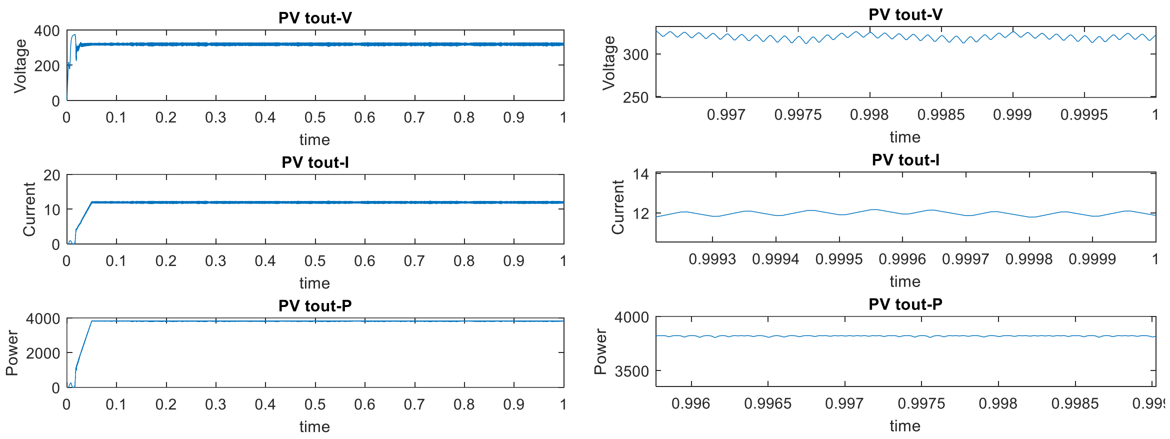

Figure 7.1. PV Panel Behavior

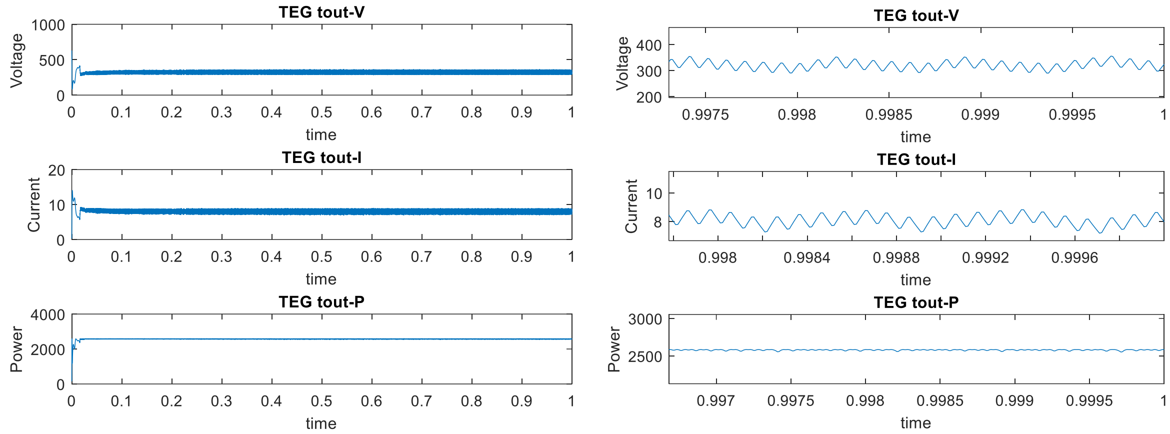

Figure 7.2. TEG Panel Behavior

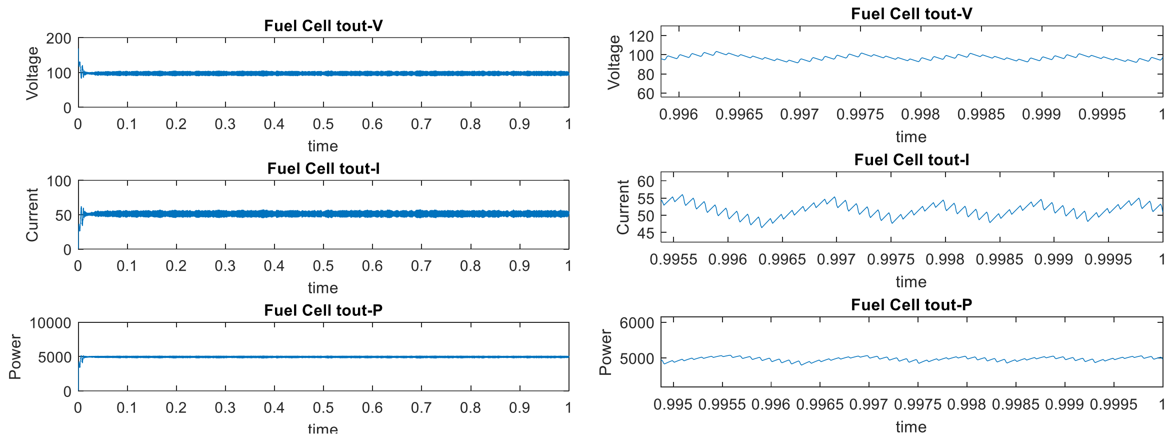

Figure 7.3. Fuel Cell Behavior

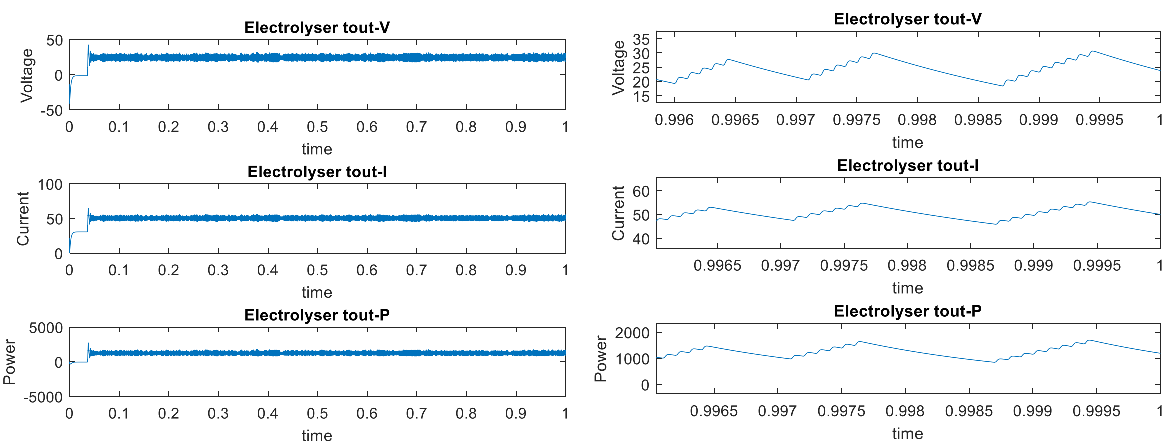

Figure 7.4. Electrolyser Behavior

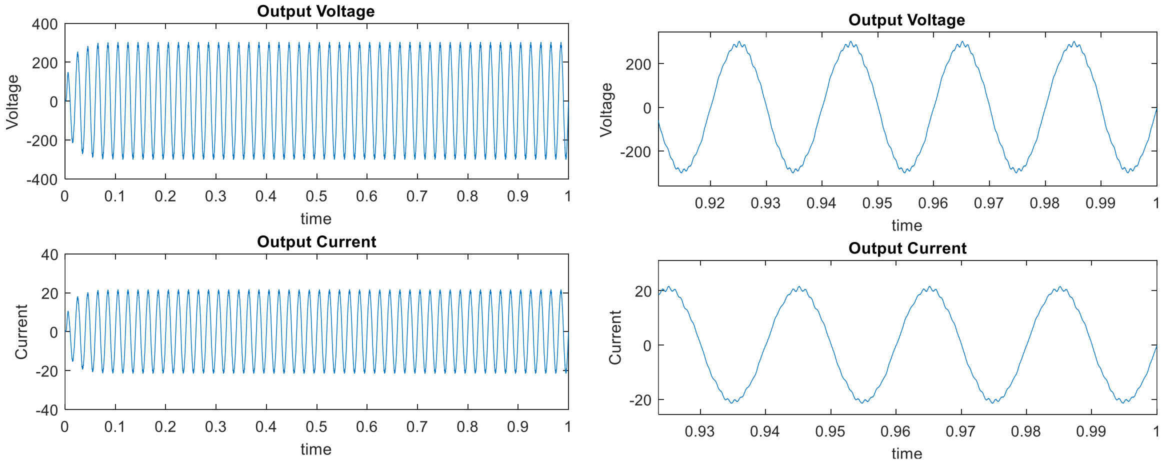

Figure 7.5. Output waveforms of inverter

The result efficiency is higher than 99% according to ratio of total produce power and total power of the DC and AC load (DC load electrolyser, AC load is resistive load)

7.1.2. Nonideal condition motor load

In this part, the used control is STSMC control, however the system is tested under nonideal condition to obtain the efficiency of the system. The system is tested under motor as a load.

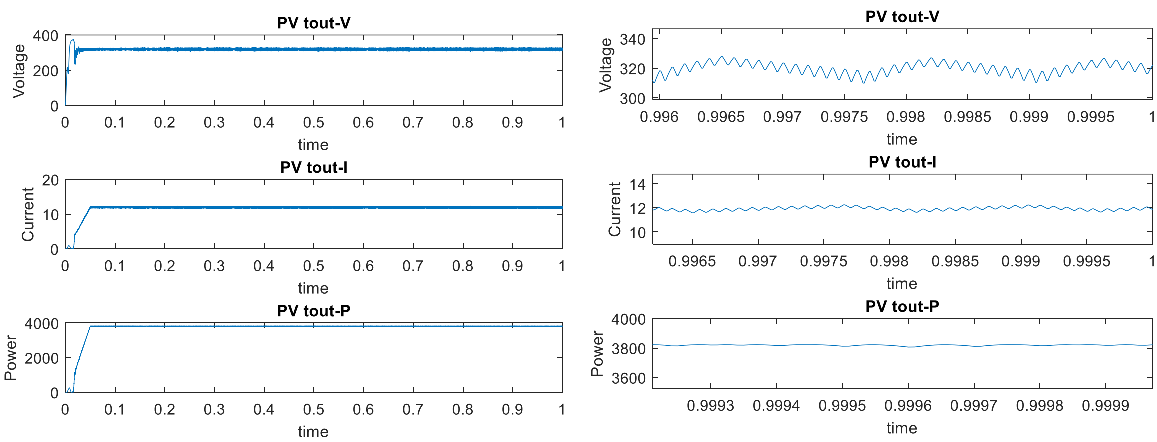

Figure 7.6. PV Panel Behavior

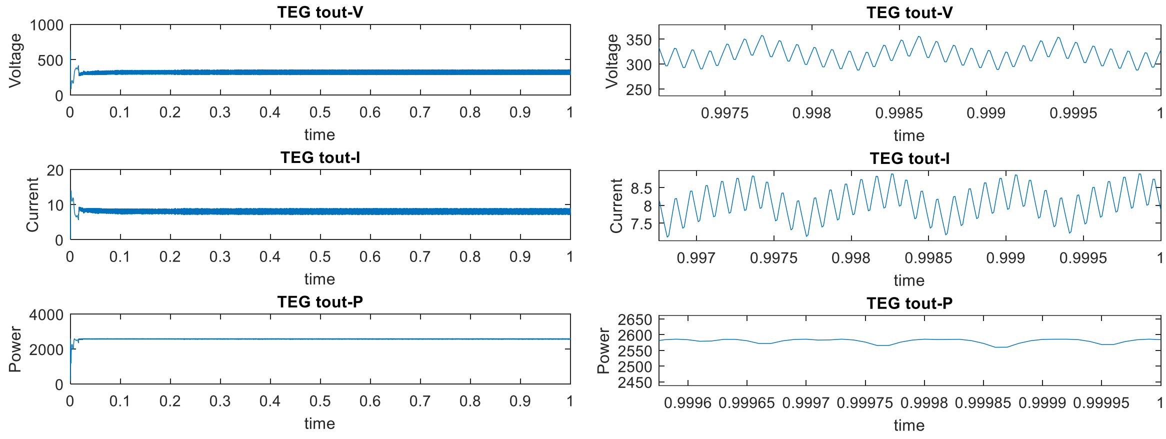

Figure 7.7. TEG Panel Behavior

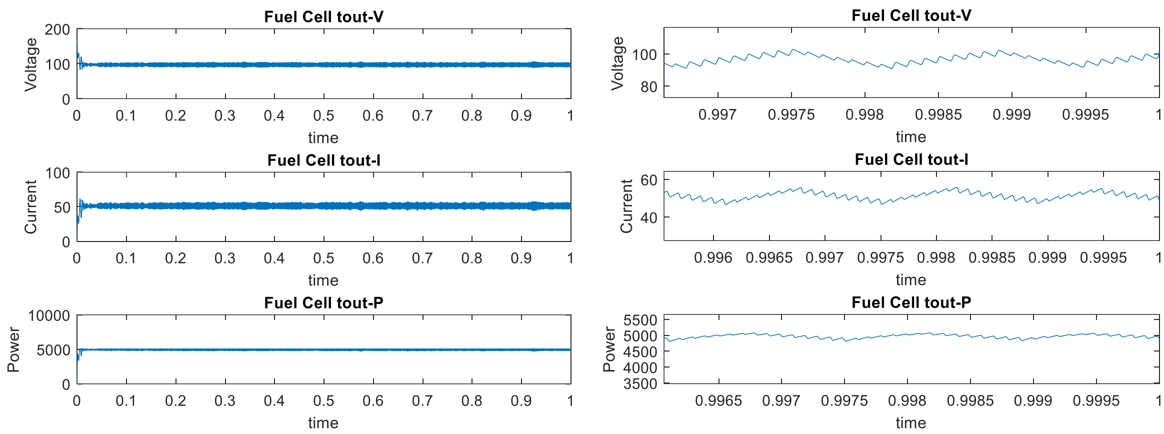

Figure 7.8. Fuel Cell Behavior

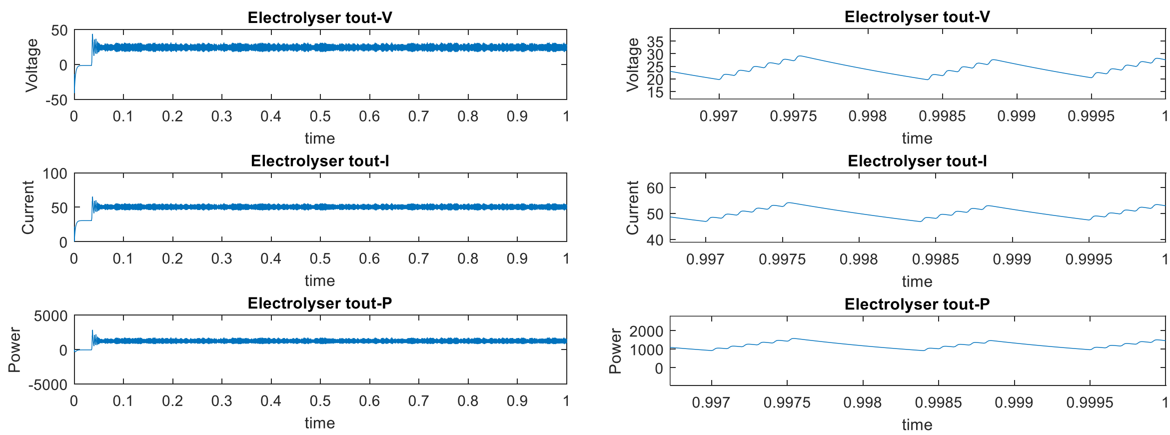

Figure 7.9. Electrolyser Behavior

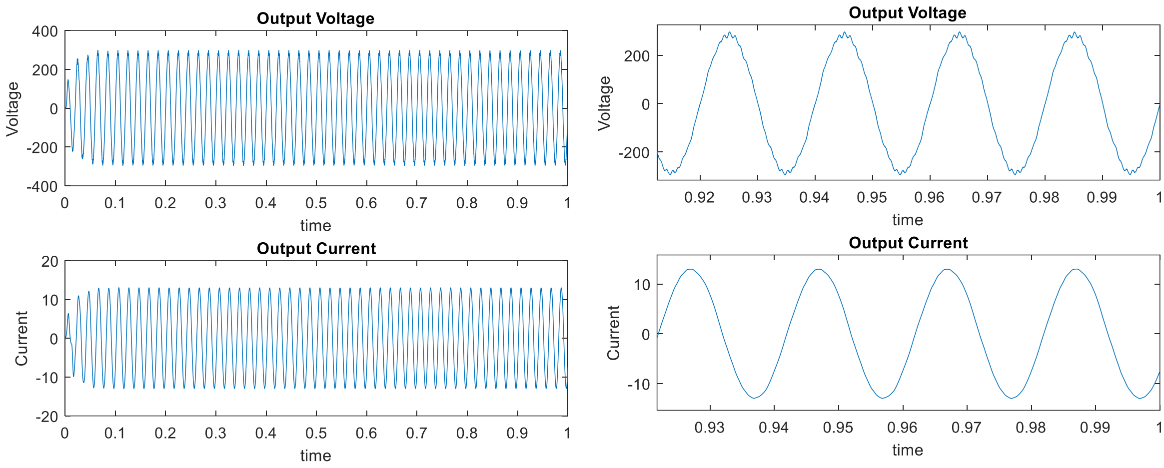

Figure 7.10. Output waveforms of inverter

The efficiency is higher than 99% according to ratio of total produce power and total power of the DC and AC load (DC load electrolyser, AC load is motor as load). From the Input and the Output Power values of nonideal condition comparison the power transmission is greater than 99%. The system will work with PV, TEG, Fuel Cell components under 8000W input power. Above this value the Electrolyser unit started to work with controlled to STSM controller. The system tested under R, and Motor Load.

The used MOSFET and Diodes are:

MOSFET for PV Panel Boost Converter, TEG Device Boost Convert and 3 Phase Half Bridge Inverter (Infineon, 2021)

Diode for PV Panel Boost Converter, TEG Device Boost Convert (Infineon, 2018)

MOSFET for Fuel Cell Boost Converter and Electrolyser Buck Converter (Microsemi, 2020)

Diode for Fuel Cell Boost Converter and Electrolyser Buck Converter (ROHM SEMICONDUCTOR, 2021)

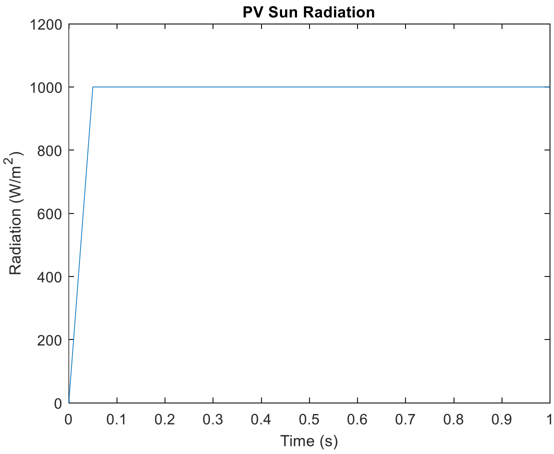

Figure 7. 11. PV Sun Radiation

In the test the Sun Radiation is given like figure 7.11.

7.2. Comparison

In this part the comparison between STSMC and P&O controlled system behavior is done. The working condition is the ideal condition. The results are compared from some wanted features of the system. These criterions:

- The load power values
- The RES's voltage and current behavior
- The behavior of the system's RESs, electrolyser part, and the load behavior under resistive, motor-based load.

There are three test conditions:

- Under ideal source and constant load (the sun light radiation is constant 1000)
- Under changing Sun radiation and TEG's temperature difference
- Under ideal source and changing Load condition.

7.2.1. Comparison of STSMC and P&O under constant ideal condition

<u>Resistive load</u>

The Test is done by using resistive load.

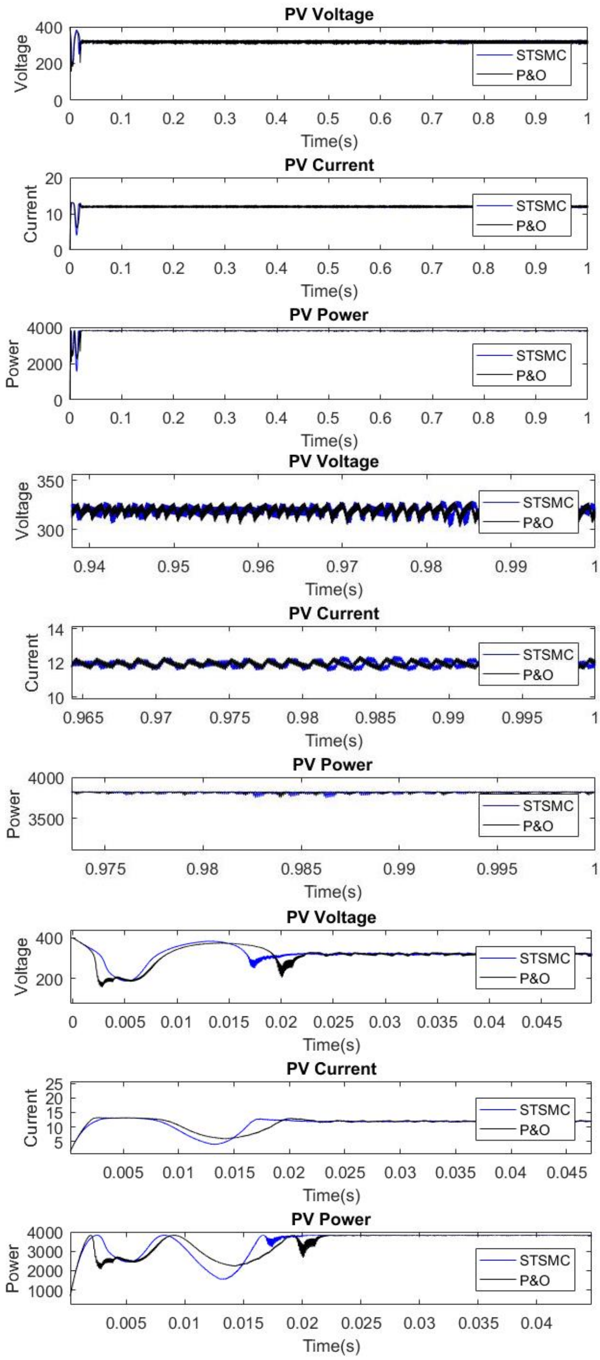

Figure 7.12. PV panel behavior under resistive load (Test 1)

In Figure 7.12, The results shown that the STSMC system find stable point faster than the P&O control and additionally the P&O wave form has fluctuation according to Figure 7.12 second figure. The Black one more fluctuated than the Blue one.

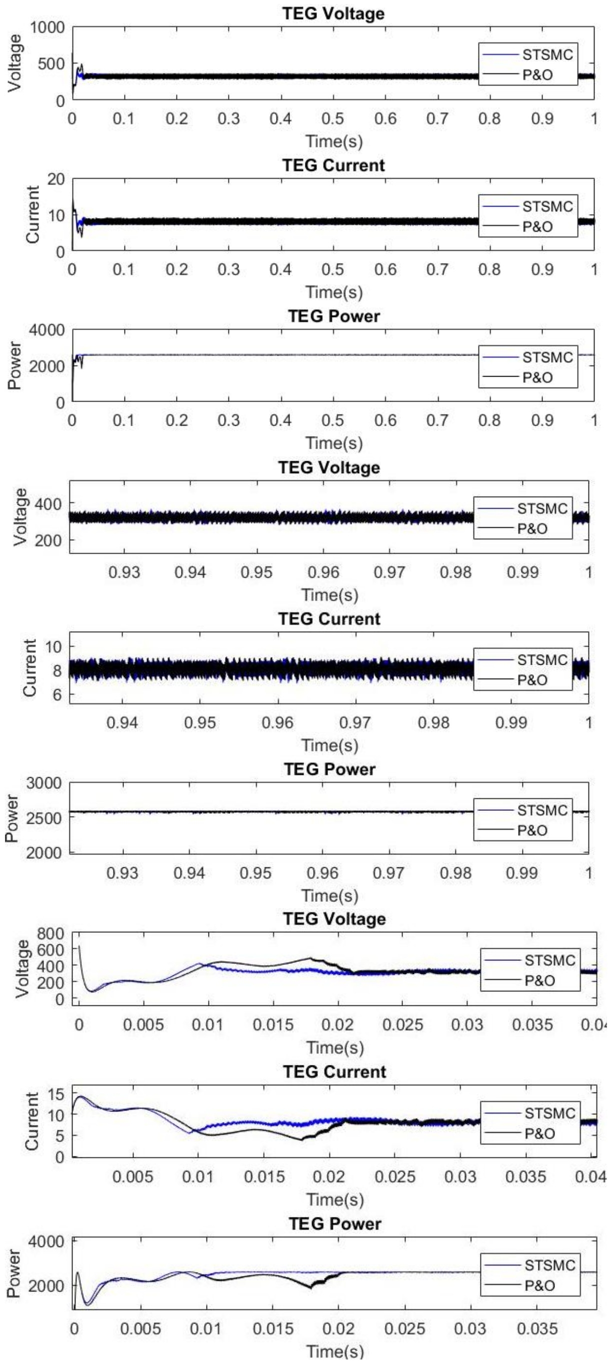

Figure 7.13. TEG Device behavior under resistive load (Test 1)

In Figure 7.13, The results shown that the STSMC system find stable point faster than the P&O control and additionally the P&O wave form has fluctuation according to Figure 7.13 second figure. The Black one more fluctuated than the Blue one.

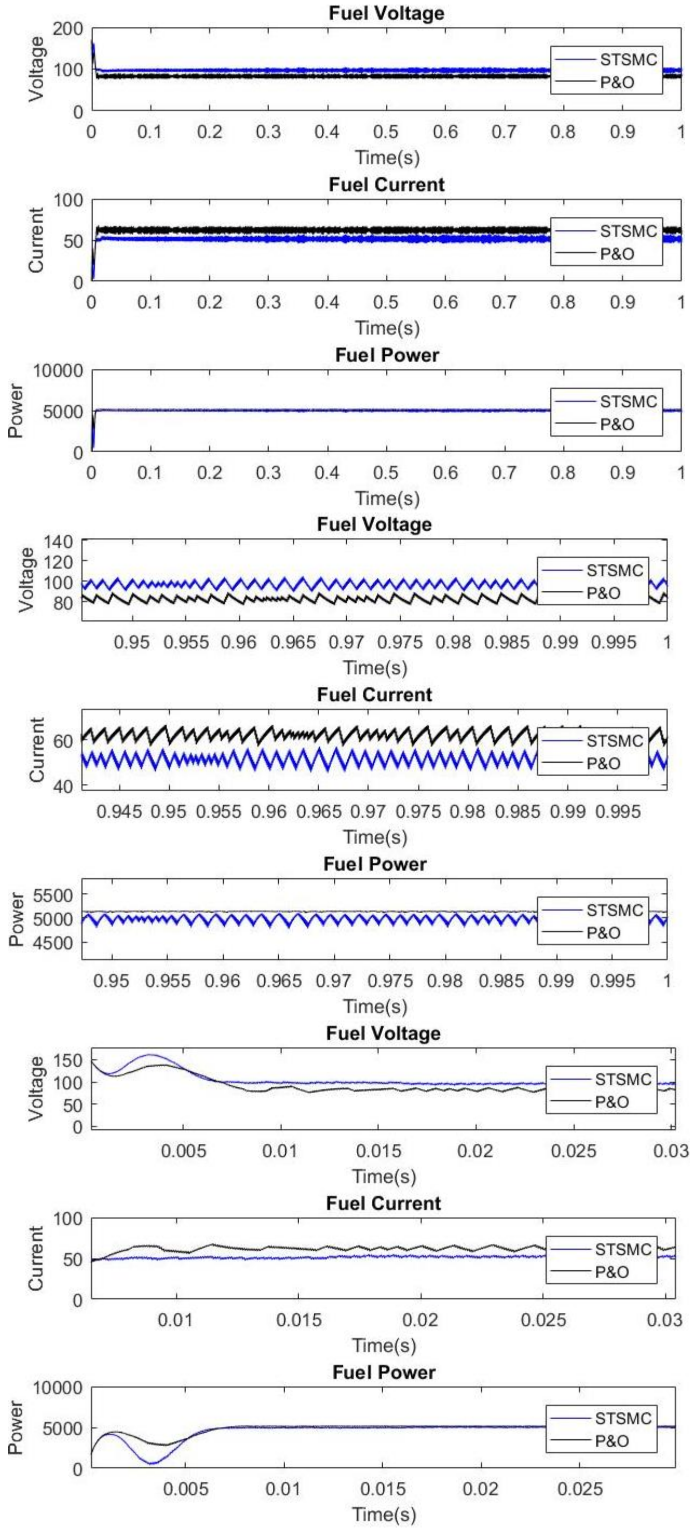

Figure 7.14. Fuel Cell behavior under resistive load (Test 1)

From the Fuel Cell system, the aim is to detect nominal working condition. In our system the nominal working condition is 96.92V at 51A. The MPP is 83.4 V at 62.54A. The two-control mechanism is working and found different points. The STSMC obtained the nominal working place correctly, however the P&O found maximum values.

In the thesis (Çavuşoğlu, 2006), the reason that why the fuel cell doesn't work at MPP is detailly explained. Briefly the main reason of the tracking nominal point is in the maximum condition, the unwanted conditions will obtain, so the P&O is not suitable for Fuel Cell Application.

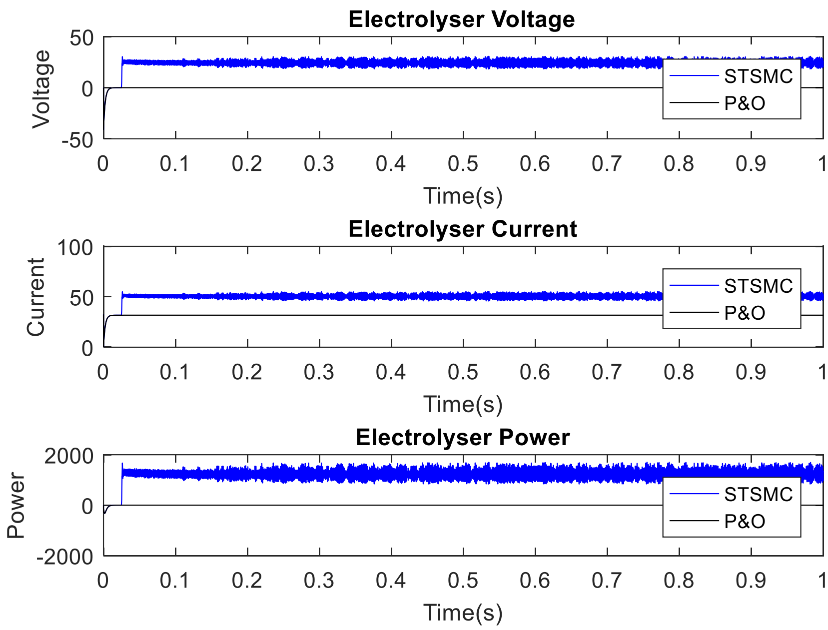

Figure 7.15. Electrolyser behavior under resistive load (Test 1)

In the system scenario, the input sources are produced 8000W power, after than if the system's power value is continued to increase the Electrolyser part started to work. The Electrolyser convert nearly 1300 W power to fuel of the system. For this reason, the Buck Converter control is started after some time, but the P&O system is not suitable for this condition. There are two options; one of them it started to work but the input part is not stable, or is not working. So, the P&O control is not suitable for Electrolyser part.

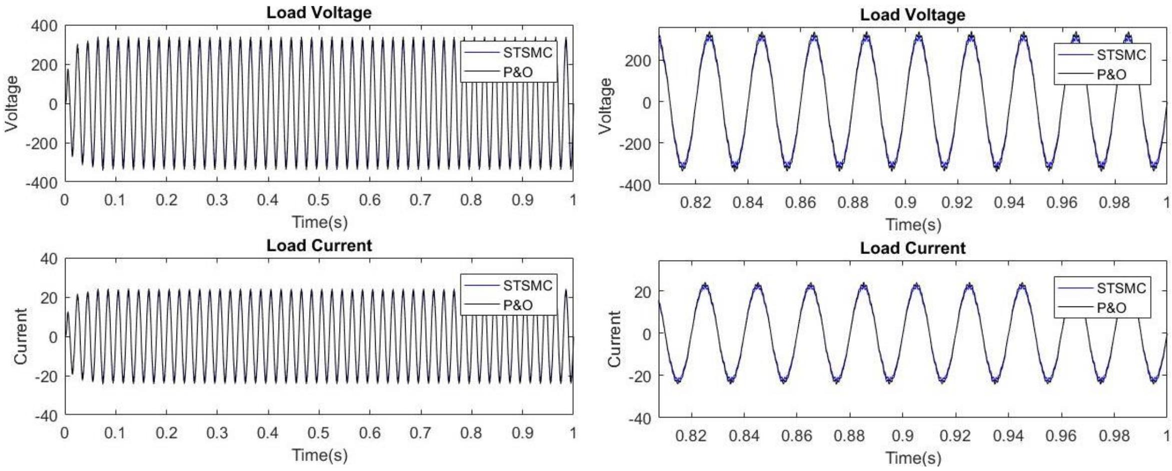

Figure 7.16. Output behavior under resistive load (Test 1)

From electoryser analyses, the electrolyser is not working on P&O control and the P&O control is forced the fuel cell that worked the maximum operation. This must be reflected that the output voltage and current must be higher than the STSM control.

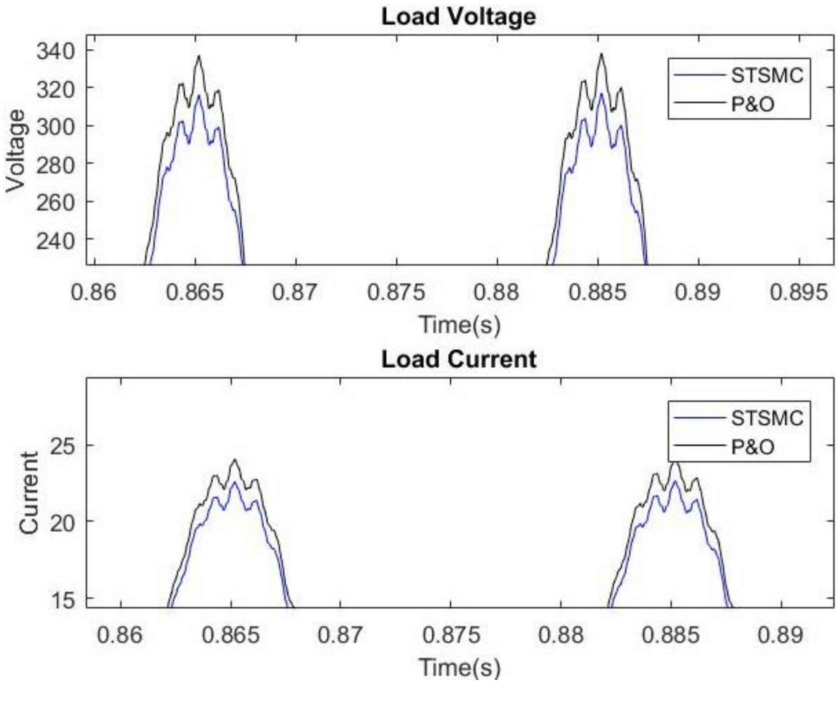

Figure 7.17. Output peak values under resistive load (Test 1)

From figure 7.17, the STSMC works under 3680W (from RMS values) at one phase. However, the P&O control is 4080W from one phase. Total difference 1200W for three phases. It is lower than the Electrolyser compensated power, so the STSM control has higher efficiency than P&O control in ideal conditions.

<u>Motor load</u>

The Test is done from using motor as a load.

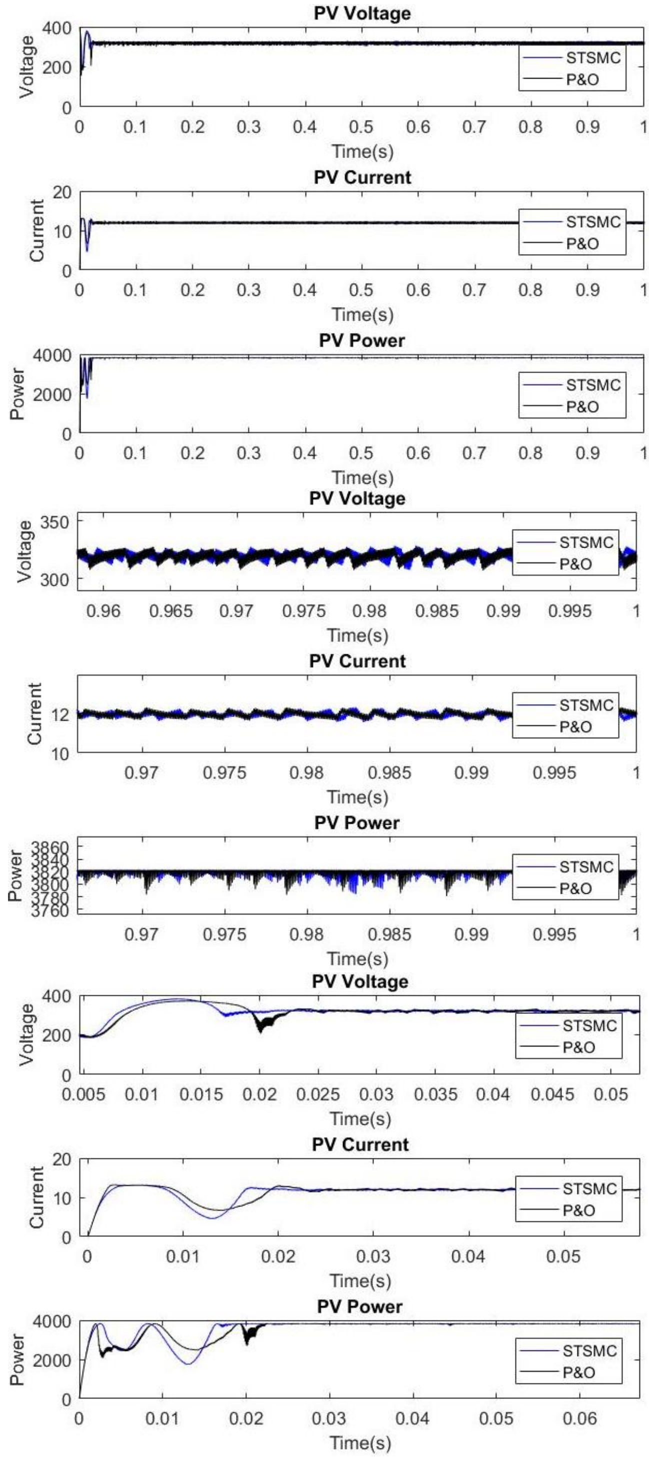

Figure 7.18. PV Panel behavior under motor load (Test 1)

In Figure 7.18, the results show that the STSMC find stable point faster than the P&O control and additionally the P&O wave form has fluctuation according to Figure 7.18. The Black one more fluctuated than the Blue one.

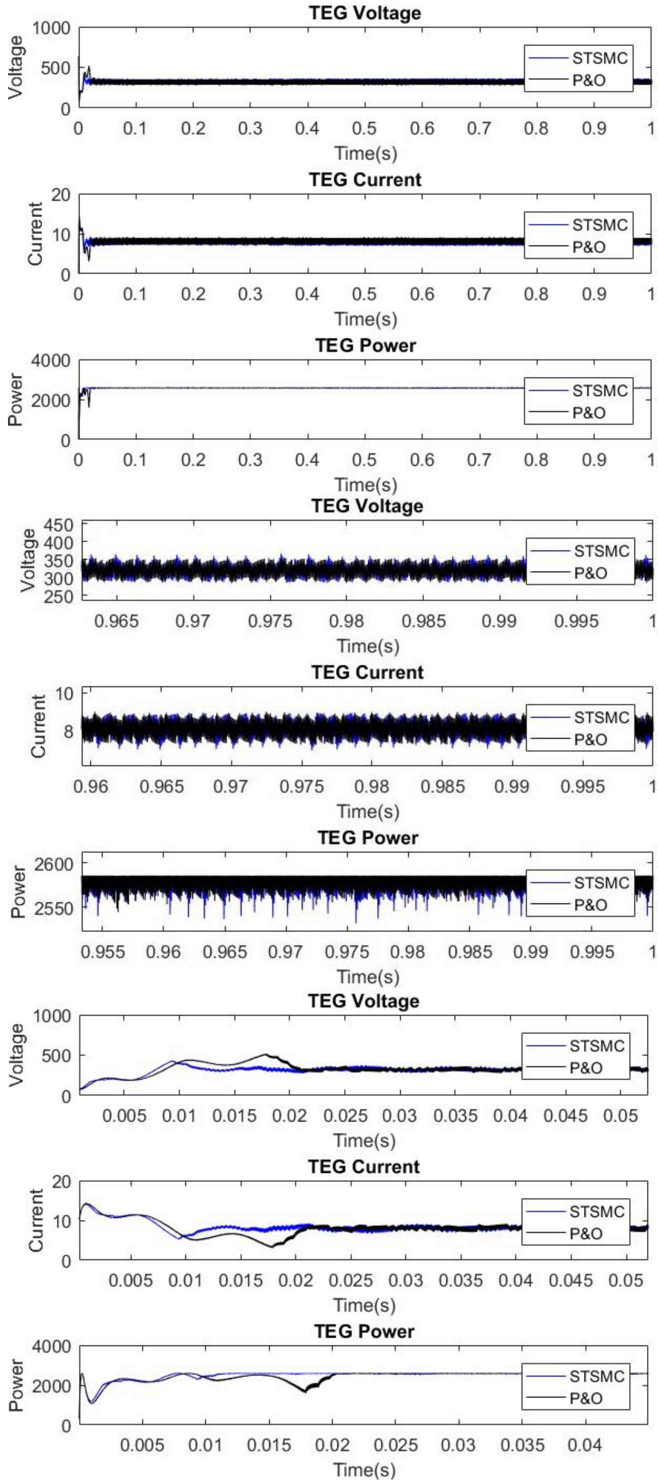

Figure 7.19. TEG device behavior under motor load (Test 1)

In Figure 7.19, the results show that the STSMC find stable point faster than the P&O control and additionally the P&O wave form has fluctuation according to Figure 7.19. The Black one more fluctuated than the Blue one.

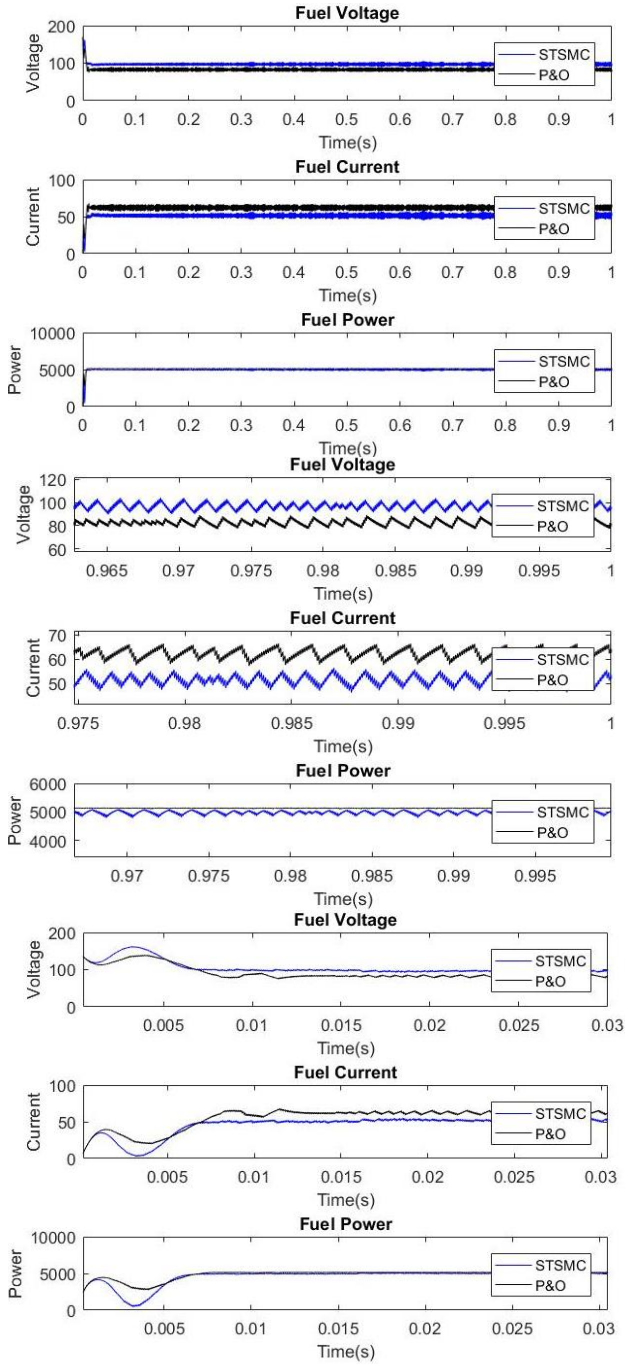

Figure 7.20. Fuel Cell device behavior under motor load (Test 1)

From the Fuel Cell system, the aim is to detect nominal working condition. In the proposed system, the nominal working condition is 96,92V at 51A. MPP is obtained at 83,4 V and

62,54A. The two-control mechanisms are working and found different MPPs. The STSMC obtain the nominal working place correctly, however the P&O found maximum values.

In the thesis (Çavuşoğlu, 2006), the reason that why the fuel cell is not work Maximum Point is detailly explained. Briefly the main reason of the tracking nominal point is in the maximum condition, the unwanted conditions will obtain, so the P&O is not suitable for Fuel Cell Application.

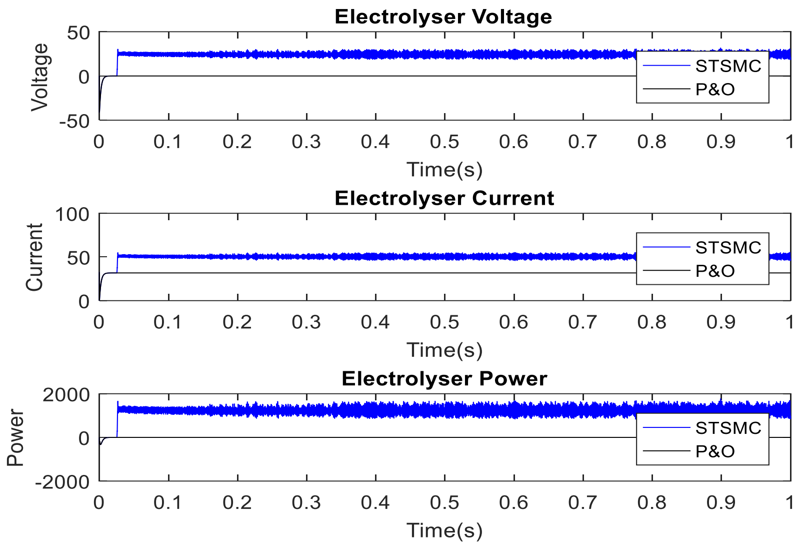

Figure 7.21. Electrolyser behavior under motor load (Test 1)

In the system scenario, the input sources produce 8000W power, after than if the system's power value continue to increase the electrolyser part start to work. The electrolyser converts nearly 1300 W power to fuel of the system. For this reason, the buck converter control is started after some time, but the P&O system is not suitable for this condition. There are two options; one of them it started to work but the input part is not stable, or is not working. So, the P&O control is not suitable for electrolyser part.

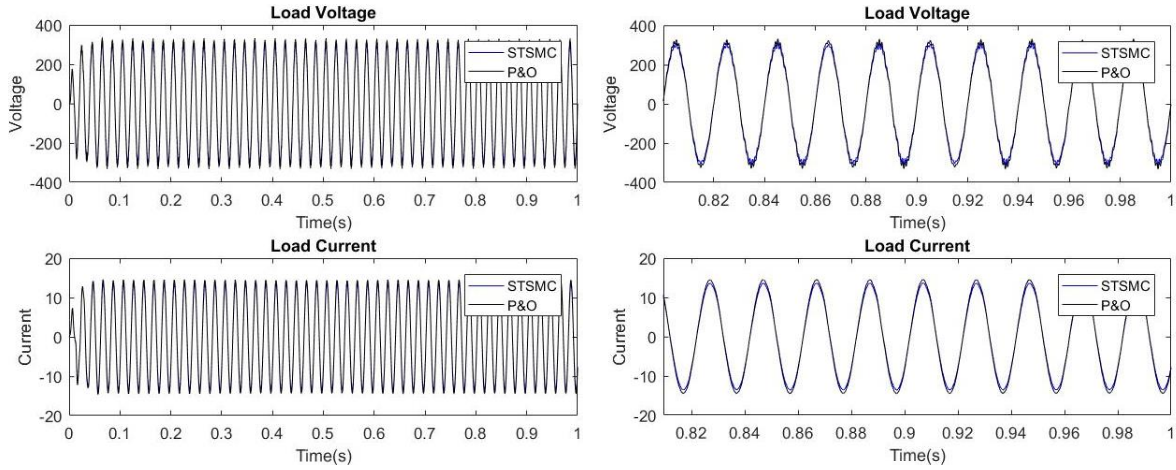

Figure 7.22. Output behavior under motor load (Test 1)

From electoryser analyses, the electrolyser is not working on P&O control and the P&O control is forced the fuel cell that worked the maximum operation. This must be reflected that the output voltage and current must be higher than the STSM control.

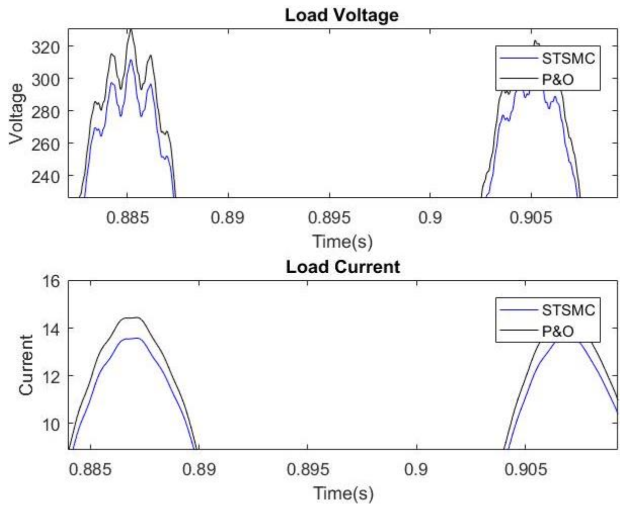

Figure 7.23. Output Peak Values under motor load (Test 1)

From figure 7.23, the STSMC works under 2015W (from RMS values) at one phase. However, the P&O control is 2240W from one phase. Total difference 225W for three phase one motor. In the system, there are two motor loads. It is lower than the electrolyser compensated power, so the STSMC has higher efficiency than P&O control in ideal conditions. The both control motor is high load than the resistive condition so the source side reflected resistance is higher. According to peak voltage and current, the motor load is nearly equal to 22,85714286 ohm, however from the other loads the equivalent load is nearly 14Ω. The difference is nearly the double resistive load condition.

7.2.2. Comparison of STSMC and P&O under variable irradiation and temperature differences

In this test the Load is constant, however the Sun radiation and the TEG device's temperature difference is changing the graphs are shown below. (The TEG device voltage is change so the reference voltage is also change)

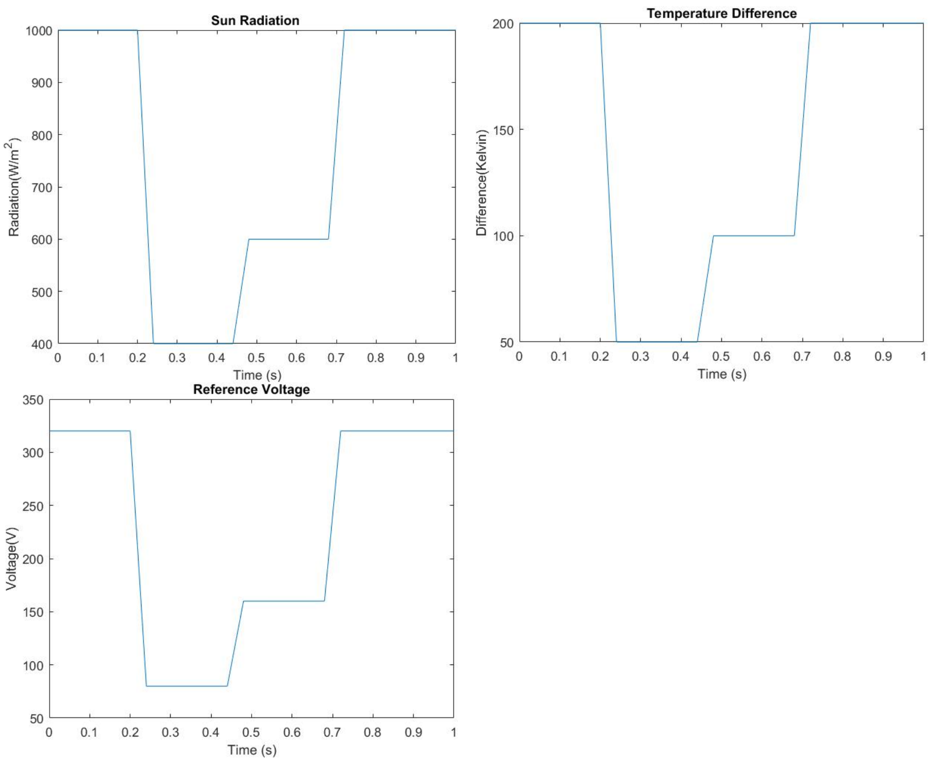

Figure 7.24. Source Parameter Signal (Test 2)

Resistive load

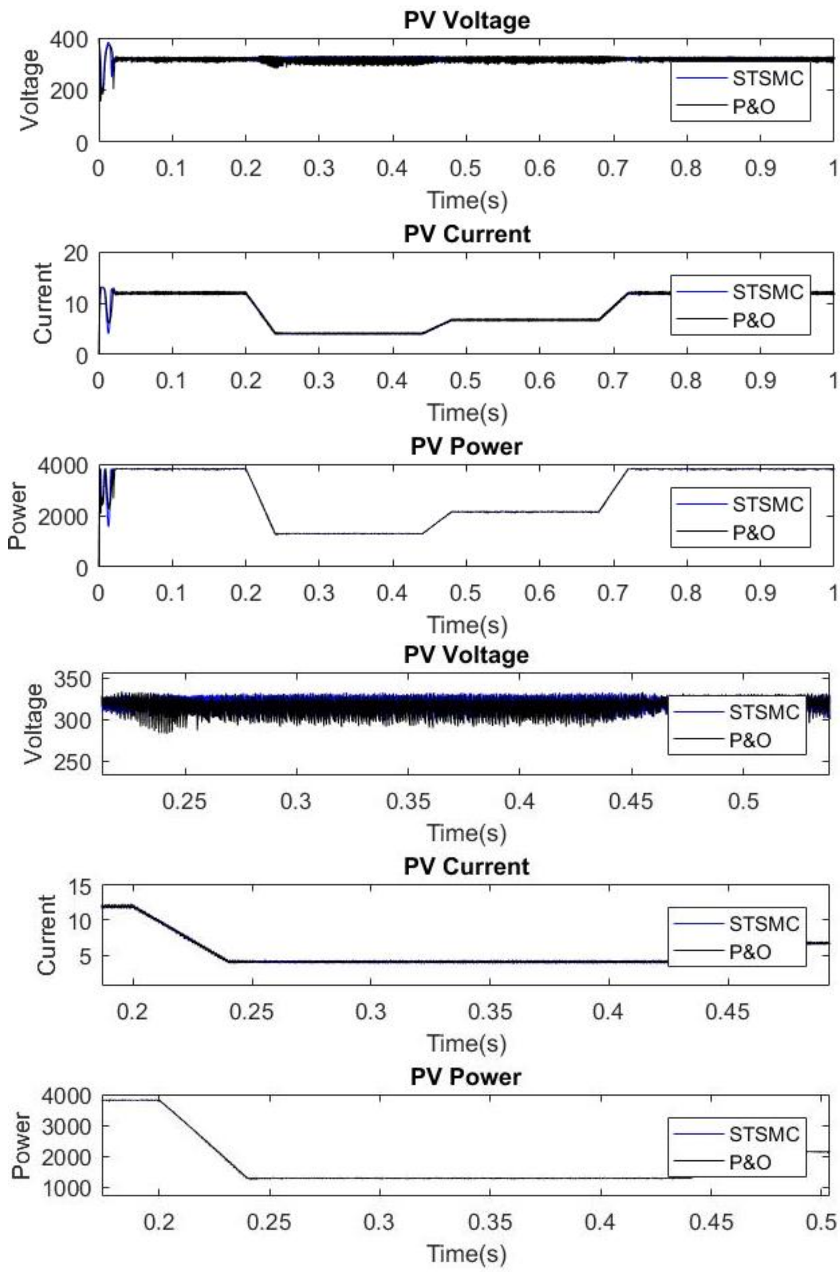

Figure 7.25. PV panel behavior under resistive load (Test 2)

According to Figure 7.25, the two MPPT system follow the changing the response time is nearly is the same, but 400 $\frac{W}{m^2}$ the STSMC control signaled peak value is slightly higher than the P&O controlled signal.

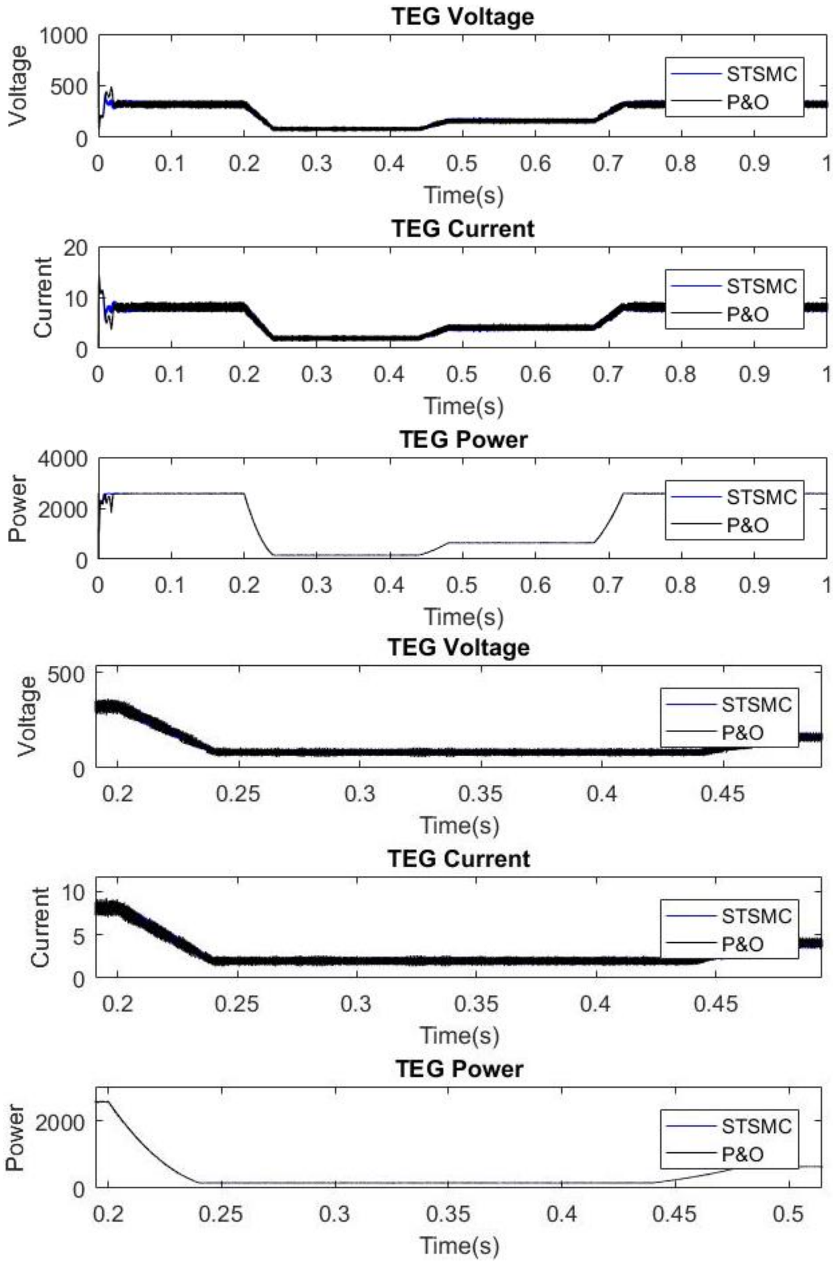

Figure 7.26. TEG behavior under resistive load (Test 2)

According to the Figure 7.26, the two PPT signal is flows the MPP point the results are nearly is the same of two MPPT signal controlled wave form.

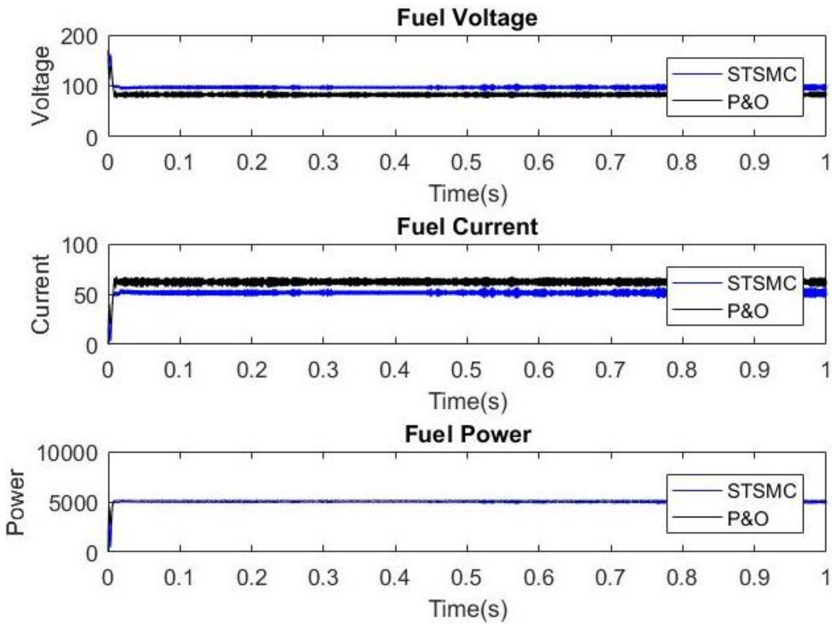

Figure 7.27. Fuel Cell behavior under resistive load (Test 2)

The wave form is nearly the same as figure 7.15. The P&O controlled system the electrolyser unit does not integrate, because the changing source is change the voltage, current and power values from that the electrolyser control is produced error in the MATLAB system this is a big disadvantages of the P&O control because the system has electrolyser unit and the electrolyser unit is not worked on this test.

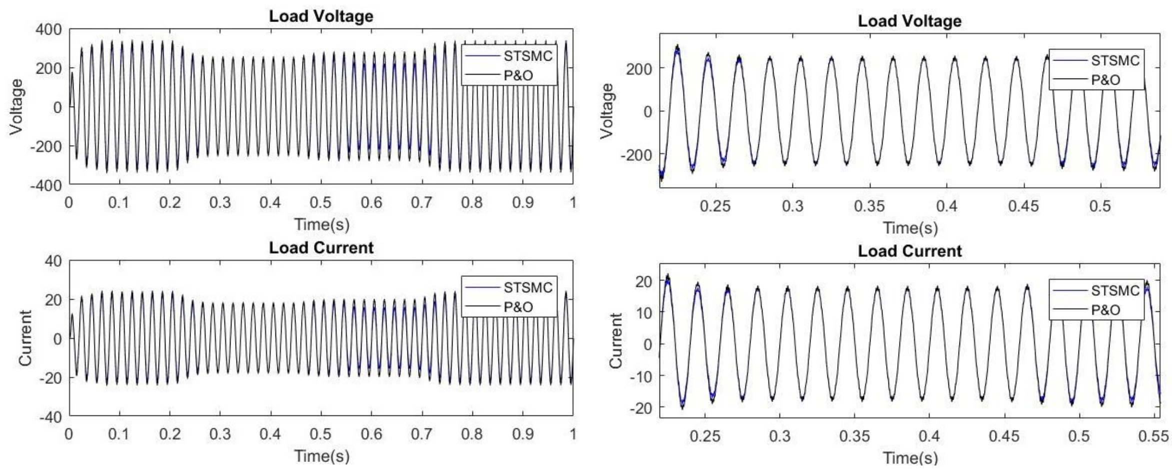

Figure 7.28. Load Output under resistive load (Test 2)

The two MPPT signal controlled wave forms are nearly similar, the only difference is the electrolyser is not worked on the P&O control. From the result, the P&O is one of the old, reliable and common control method. The proposed STSMC control is relatively new, robust control. In this part the results shown that the STSMC control is as reliable as the P&O control in this system, additionally, the system requirements are defined as DC Load (Electrolyser) should be added. According to tests the P&O is failed to start the Electrolyser unit, and because of the source condition change the electrolyser control produce error during the operation. The result of test is The STSMC is completed of all the goals of thesis, however the P&O control is failed some of them. The STSMC is true chose of control according to this result.

Motor load

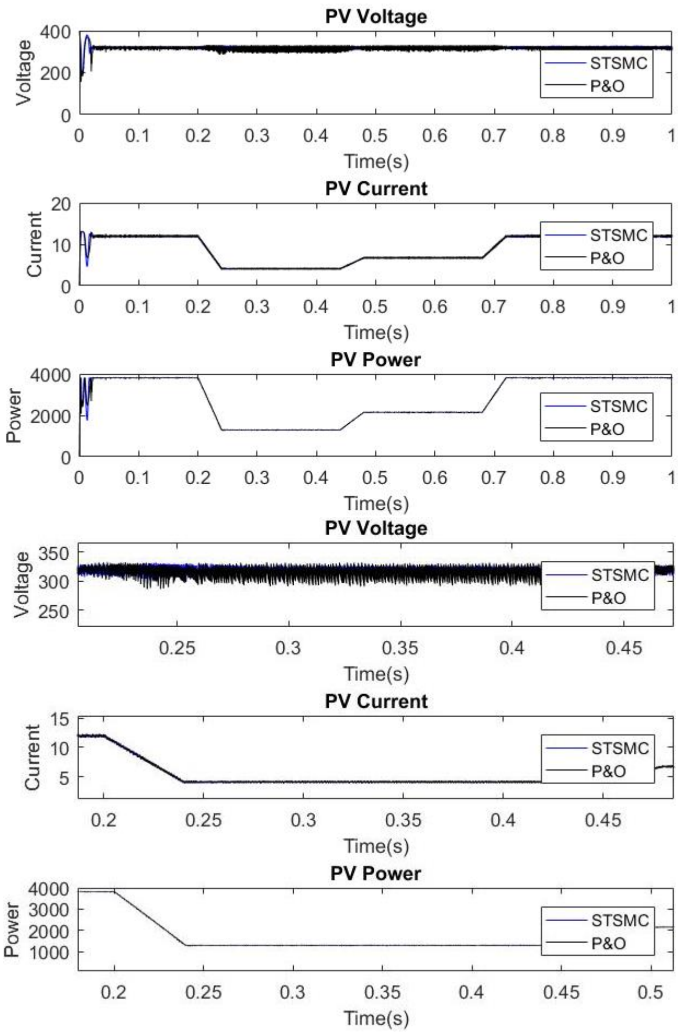

Figure 7.29. PV panel behavior under motor load (Test 2)

According to Figure 7.29, the two MPPT system follow the changing the response time is nearly is the same. The ripple of the P&O control is higher than PV at 400 $\frac{\mathrm{W}}{\mathrm{m}^2}$ radiation.

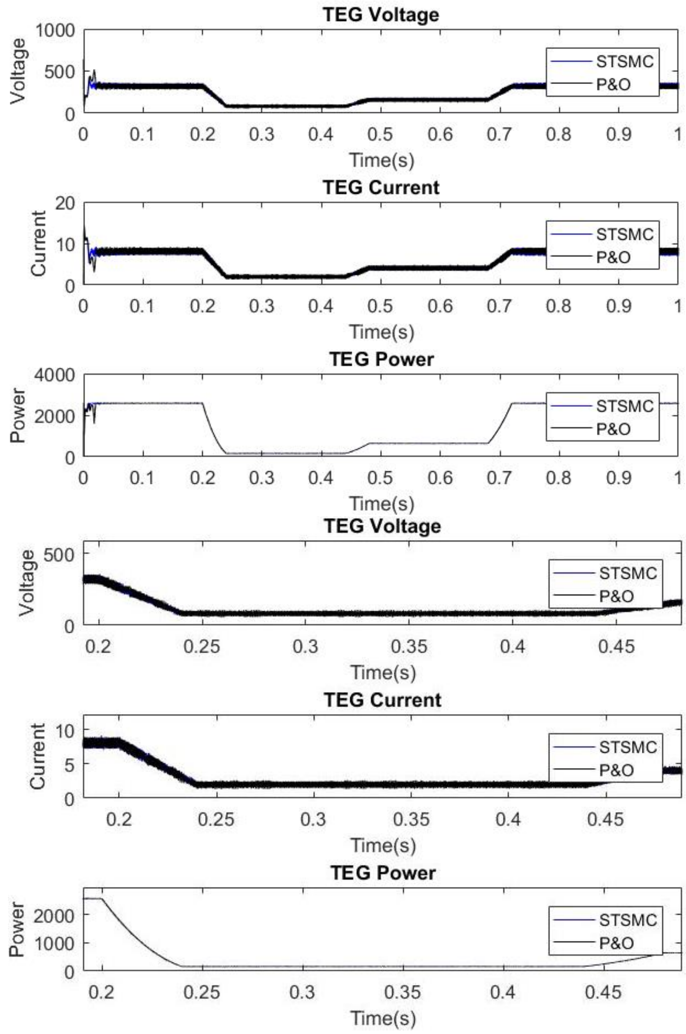

Figure 7.30. TEG behavior under motor load (Test 2)

According to the Figure 7.30, the two PPT signal is flows the MPP point the results are nearly is the same of two MPPT signal controlled wave form.

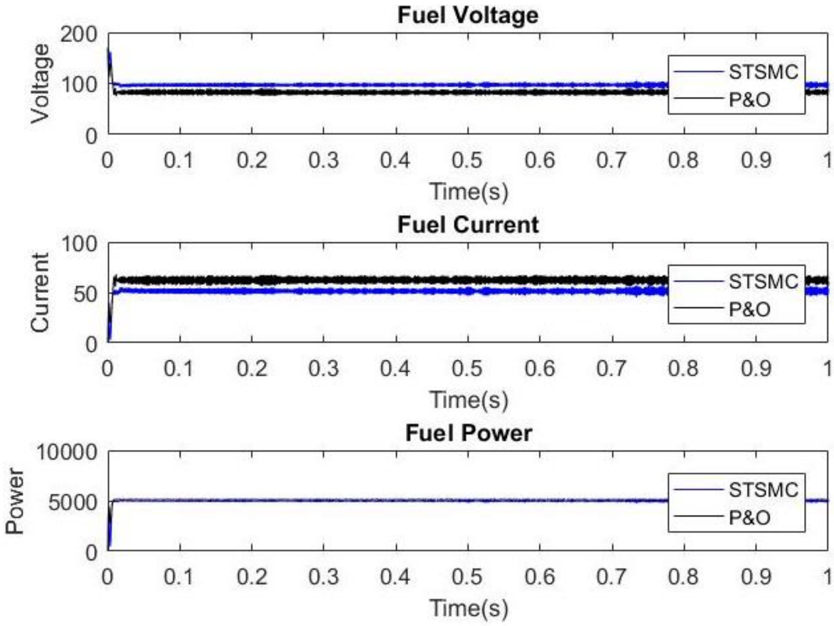

Figure 7.31. Fuel Cell behavior under motor load (Test 2)

The wave form is nearly the same as figure 7.21. the P&O controlled system the electrolyser unit does not integrate, because the changing source is change the voltage, current and power values from that the electrolyser control is produced error in the MATLAB system this is a big disadvantages of the P&O control because the system has electrolyser unit and the electrolyser unit is not worked on this test.

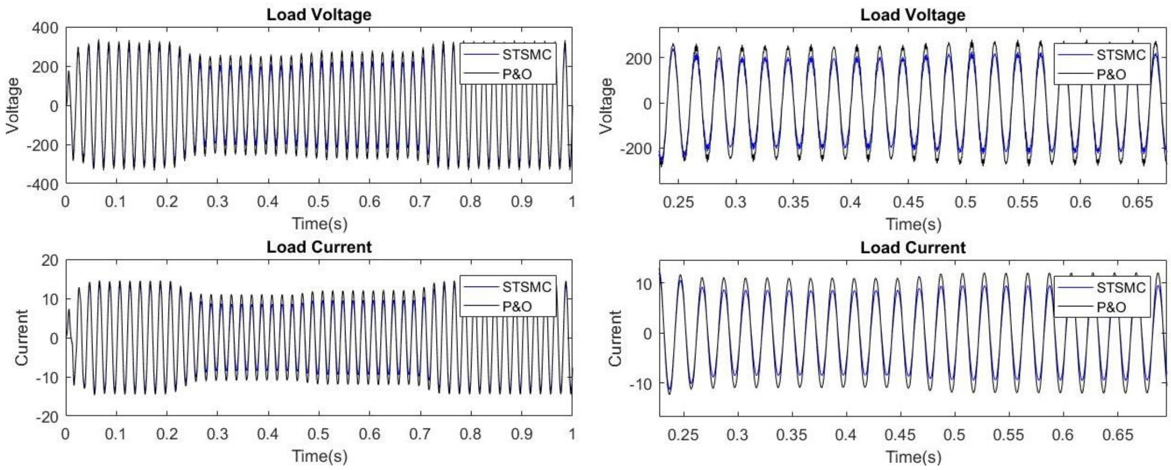

Figure 7.32. Load Output behavior under motor load (Test 2)

The two MPPT signal controlled wave forms are nearly similar, the only difference is the electrolyser is not worked on the P&O control. From the result, The P&O is one of the old, reliable and common control method. The proposed STSMC control is relatively new, robust control. In this part the results shown that the STSMC control is as reliable as the

P&O control in this system, additionally, the system requirements are defined as DC Load (Electrolyser) should be added. According to tests the P&O is failed to start the Electrolyser unit, and because of the source condition change the electrolyser control produce error during the operation. The result of test is The STSMC is completed of all the goals of thesis, however the P&O control is failed some of them. The STSMC is true chose of control according to this result.

7.2.3. Comparison of STSMC and P&O under variable load condition

In this test, the load values are changing (the resistance is 14 ohm and 28 ohm and motor is two paralleled motor and one motor) and sources conditions are constant (constant temperature difference of TEG, constant Sun radiation). For resistive case the load changing to 14 ohm – 28 ohm, for motor case two parallel motor is started to working one motor is stopped. After some time, the stopped motor is starting to work again.

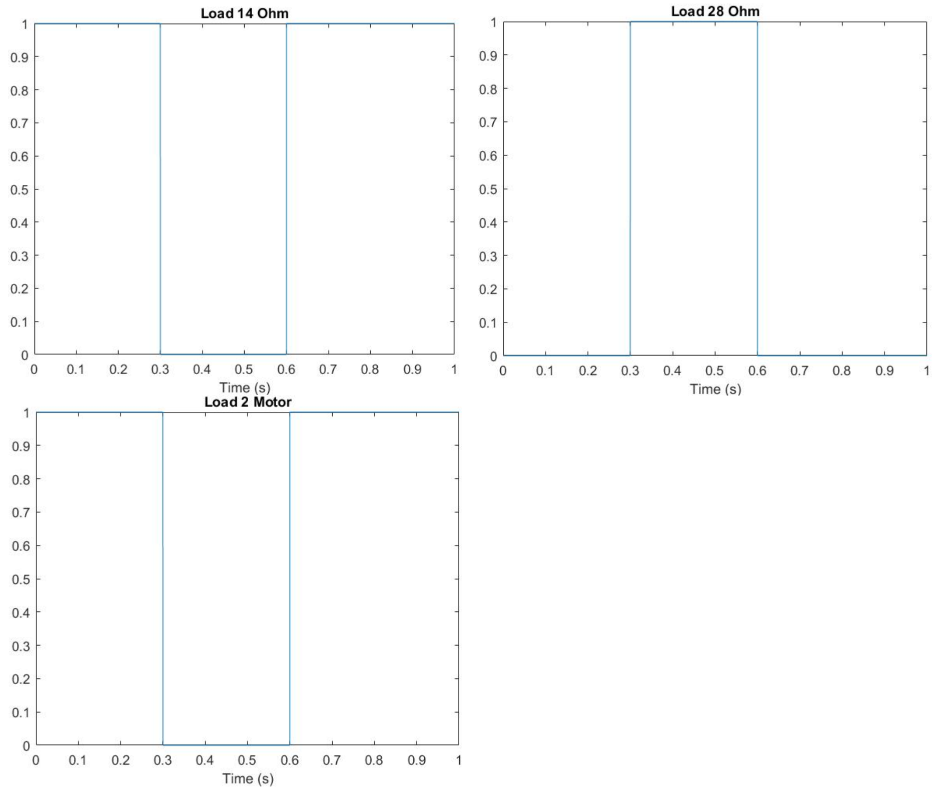

Figure 7.33. Load Side Control Signal (Test 3)

<u>Resistive load</u>

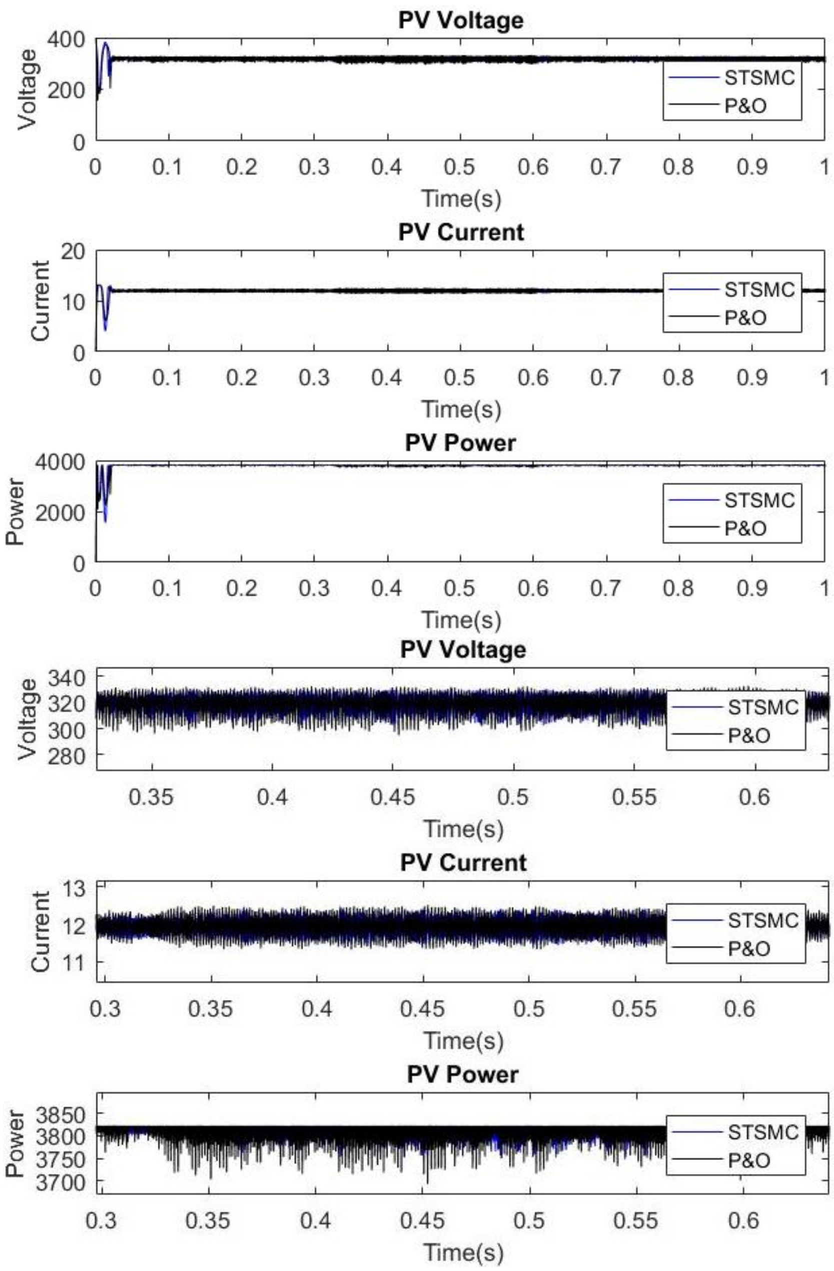

Figure 7.34. PV panel behavior under resistive load (Test 3)

According to Figure 7.34 the two MPPT signal control system follows the MPP Point, however the ripple of the P&O controlled signal is higher than the STSMC controlled signal.

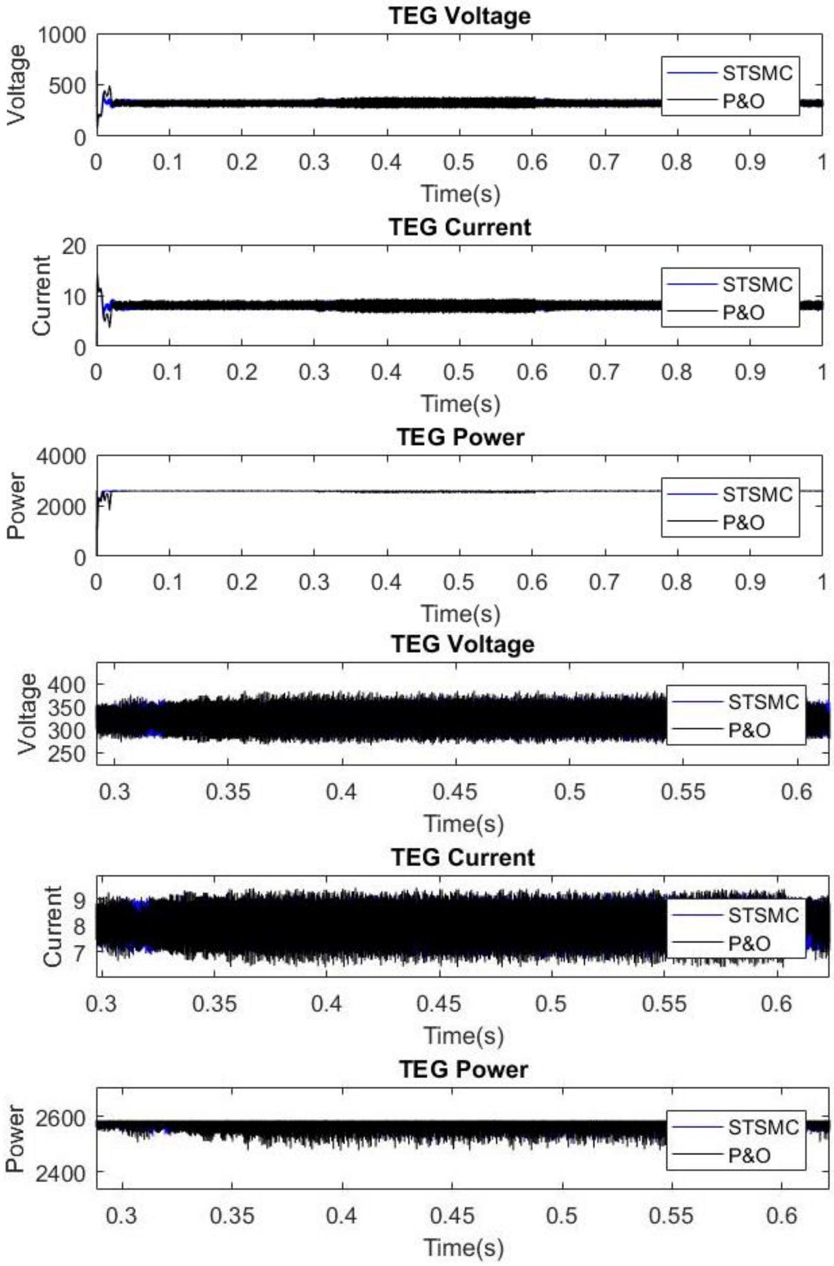

Figure 7.35. TEG behavior under resistive load (Test 3)

According to Figure 7.35 the two MPPT signal control system follows the MPP Point, however the ripple of the P&O controlled signal is higher than the STSMC controlled signal.

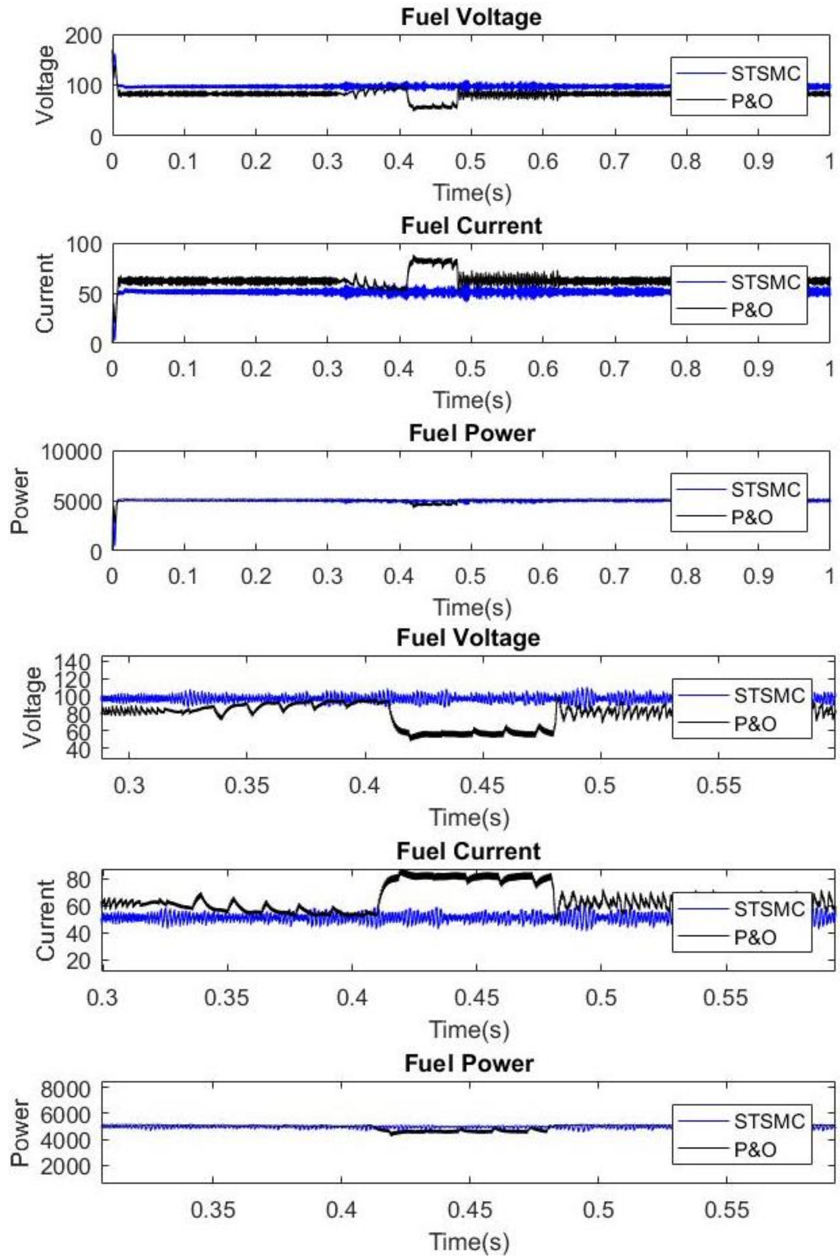

Figure 7.36. Fuel Cell behavior under resistive load (Test 3)

In the Figure 7.36, the results shown that the STSMC control is follows the changing correctly, however the P&O control is not following the change correctly. The P&O controlled signal is distorted between 0,34 second and 0,6236 second.

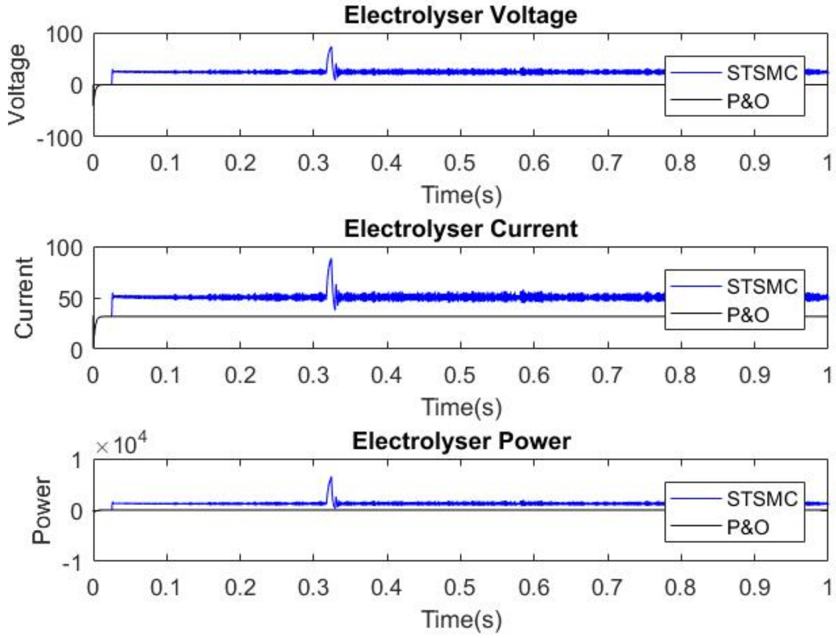

Figure 7.37. Electrolyser behavior under resistive load (Test 3)

According to Figure 7.37, the STSMC controlled system follows the changing the load change is occurred at 0,3 second, and from the figure the changing is detected.

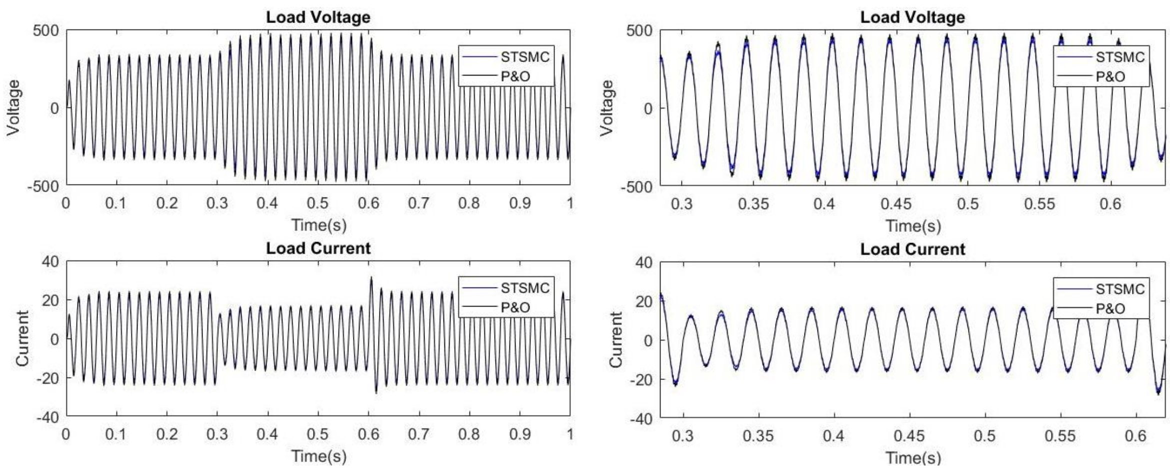

Figure 7.38. Load Output behavior under resistive load (Test 3)

The two MPPT signal controlled wave forms are nearly similar, the only difference is the electrolyser is not worked on the P&O control. From the result of the system, the STSMC controlled signal is follow the load change. According to the figure 7.37, the changing is done at 0,3 second. The P&O control is following the changing of the load according to figure 7.34, and figure 7.35. In these figures, the ripple of the P&O is higher than STSMC controlled signals. According to 7.36 the P&O controlled system is distorted on operation time. The results of the test shown that the STSMC control behavior much better than P&O control.

Motor load

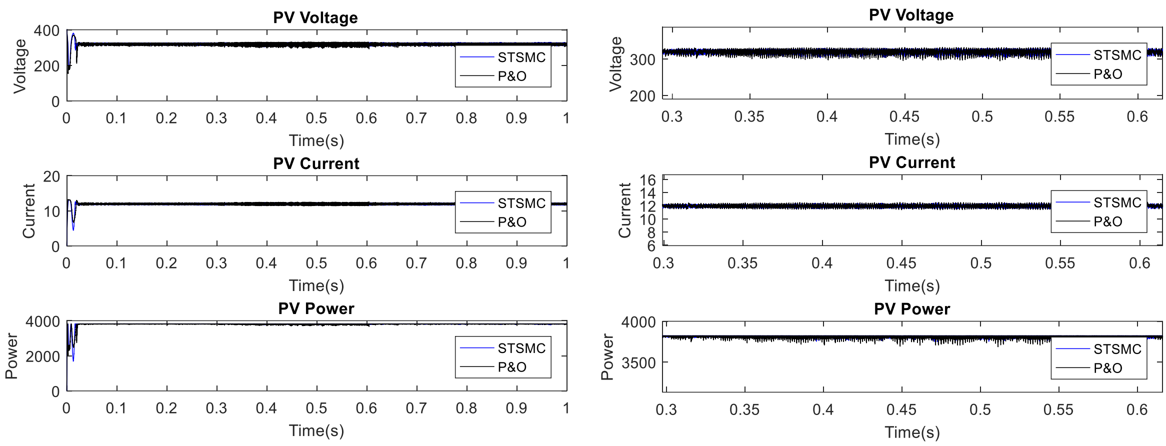

Figure 7.39. PV panel behavior under motor load (Test 3)

According to Figure 7.39 the two MPPT signal control system follows the MPP Point, however the ripple of the P&O controlled signal is higher than the STSMC controlled signal.

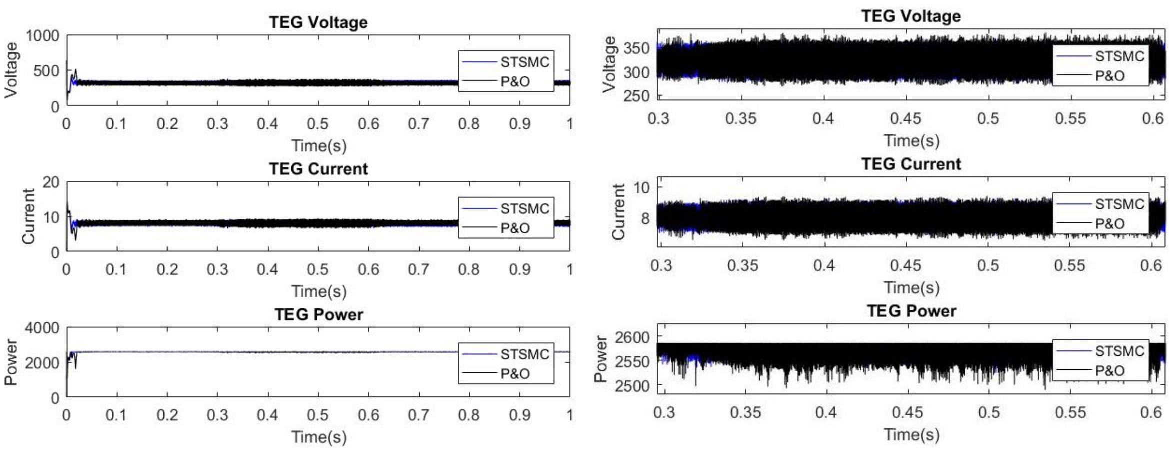

Figure 7.40. TEG panel behavior under motor load (Test 3)

According to Figure 7.40 the two MPPT signal control system follows the MPP Point, however the ripple of the P&O controlled signal is higher than the STSMC controlled signal.

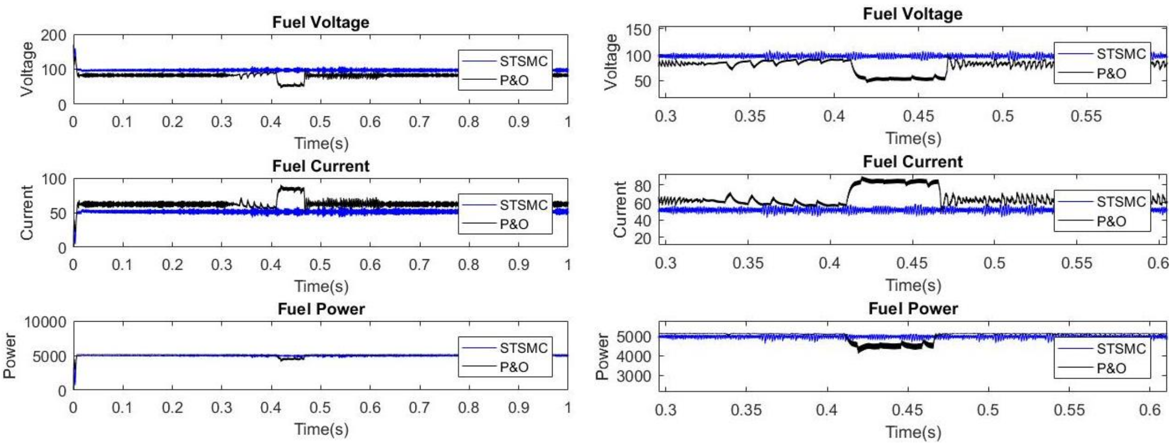

Figure 7.41. Fuel Cell panel behavior under motor load (Test 3)

In the Figure 7.41, the results shown that the STSMC control is follows the changing correctly, however the P&O control is not following the change correctly. The P&O controlled signal is distorted between 0,34 second and 0,614 second.

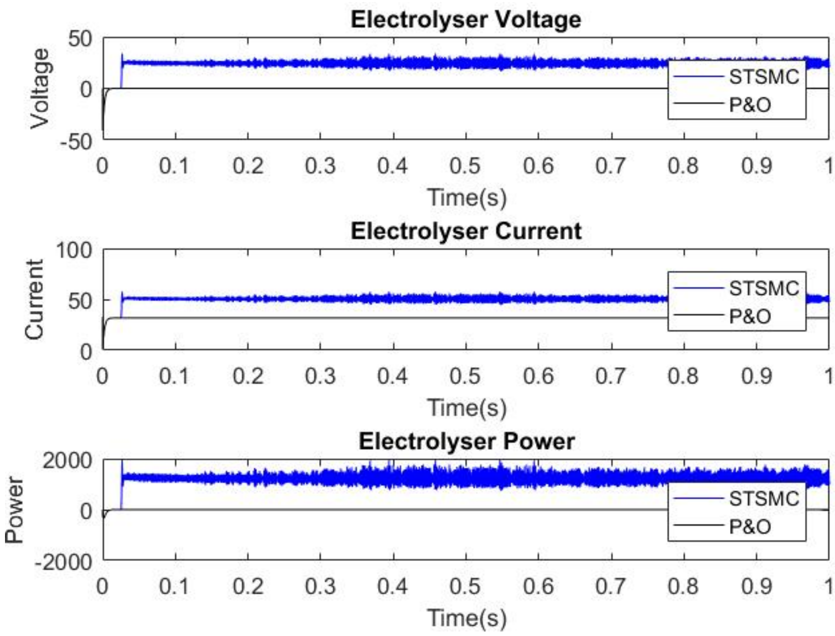

Figure 7.42. Electrolyser panel behavior under motor load (Test 3)

According to Figure 7.42, the STSMC controlled system follows the changing the load changing is increase the ripple according to Figure 7.42.

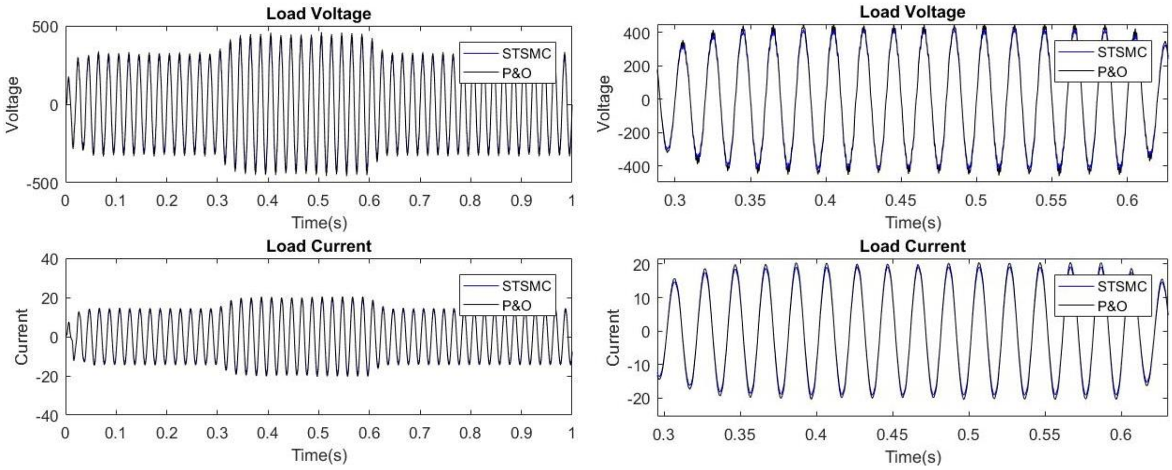

Figure 7.43. Load Output behavior under motor load (Test 3)

The two MPPT signal controlled wave forms are nearly similar, the only difference is the electrolyser is not worked on the P&O control.

From the result of the system, The STSMC controlled signal is follow the load change. According to the figure 7.41, the ripple slightly increases after 0,3 second. The P&O control is following the changing of the load according to figure 7.37, and figure 7.40. In these figures the ripple of the P&O is higher than STSMC controlled signals. According to figure 7.41 the P&O controlled system is distorted on operation time. The results of the test shown that the STSMC control behavior much better than P&O control.

8. CONCLUSION

The energy production is very important issue to continue the technological devices to work. Today most of the devices use electrical energy to the working or tried to supplied by electrical energy. For that reason, the electrical energy demand is increasing. There are several electrical energy production ways such as Fossil fuel-based systems, nuclear energy-based systems, hydroelectrical energy-based systems etc. Each source has limits, advantages and disadvantages. Some of the systems produce byproduct. Some byproducts are damaging the environment or will damage the environment if it is not stored proper conditions. On the other hand, some of the sources will be efficiently use very limited areas. From these conditions, new ways, combinations, or techniques must be found to maintain electrical energy production save and efficiently.

In this thesis the aim is to design system that using MPPT control high efficiency and robustness is ensure, and also the design must have more than one different type of sources. From that reason three different RES is selected and the system control method is selected according to usage frequency. The main proposes is to obtain high efficiency (higher than 98% to nonideal condition), robustness (according to the popular control methods), and show the advantages according to the popular control method.

In this thesis there are three RESs; PV, TEG, Fuel Cell. The sources energy is converted to another energy level by using Boost Converter. The energy is connected each other with using 2 capacitor and inductor. The load side is AC load, from obtaining the AC power 3 phase Half Bridge topology is used. The examination is done for 2 different source type. Resistive Load, and Motor Load. The Design has also additional part, if the energy demand is lower than the produced energy. In this condition one electrolyser is placed and supplied by the system from using Buck Converter Topology.

The other important part is the control method selection. The renewable energy systems are nonlinear systems, so from finding the maximum power (except fuel cell. In Fuel cell nominal condition should be found) is the aim. The selected control technique is called MPPT technique. This type techniques are aimed to find maximum power point of the system. From controlling the PV, TEG, Fuel Cell and Electrolyser the STSM control is selected. For PV and TEG system the aim is to find MPP, however, for Fuel Cell, and

Electrolyser the aim is to obtain nominal working point finding. DC part control is important, but the AC part control as important as DC type control. For the controlling AC part, the Sinusoidal Pulse Width Modulation (SPWM) is selected. The main power limit is 8000W above. Above 8000W, Electrolyser started the work.

The first test is the nonideal efficiency of the STSMC controlled system. The PV, TEG, Fuel Cell's behavior is obtained, and the DC-Load (Electrolyser), and AC-Load (Resistive Load or Motor) behavior is obtained. According to the system output and input values, the efficiency is higher than 99%. The system worked properly under STSMC and nonideal switching components.

The second test is Ideal Source (1000 $\frac{W}{m^2}$, and constant temperature difference). According to the results the STSMC controlled signal has lower fluctuation on PV, and TEG system. The signal is found the stable point faster in STSMC controlled signal in PV and TEG. The STSMC is found nominal point, however P&O found Maximum Point. The behavior Fuel Cell of nominal condition is more optimize than behavior of MPP. In this test the electrolyser unit control is not working stable so the electrolyser closed. The Load part the one of the important unit is electrolyser, so this is disadvantages of the P&O system. For this reason the power difference is seen. According to calculation the power difference is higher than the obtained difference. This means that P&O controlled system efficiency of power production is lower than the STSMC controlled system.

The Third Test is variable radiation and variable temperature difference. Under the variable source condition (radiation for PV, temperature difference for TEG) the electrolyser control produces errors on MATLAB simulation this is one of the important disadvantages of P&O control. The both system follows the changing values, however in PV system the ripple is slightly higher on P&O controlled system. The TEG, and Fuel Cell results are the same as each other.

The Last Test of comparison is variable load condition. According to results of PV and TEG behavior of the higher load, The P&O controlled system has significant ripple than STSMC system. In the Fuel Cell graphs, there is distorted part (the signal is increased and not follow the MPP) both loads. In the Resistive Load the first load changing is detected on Electrolyser unit, the overshoot is obtained. In the motor load this overshoot is not seen in the electrolyser only the ripple is increased.

According to the test result, The STSMC's efficiency is higher than 99%. The P&O system is relatively older and more common control, so the from testing part the P&O is selected as a reference control. According to the following test results, the STSMC has advantages on the results. The Electrolyser system is not stably working of P&O system, so in the tests of P&O the Electrolyser is closed. From Ideal Source test the power production value of STSMC is higher than P&O. In the variable source condition test, the main disadvantage of P&O is the produced error on the Electrolyser control, so the Electrolyser is disconnected to the system. In the thesis the electrolyser is one of the important DC loads. The Electrolyser cannot work during P&O control, but the disconnect means that in the test the P&O is failed according to the results. On the other hand, the STSMC is started and worked the electrolyser system. According to the test STSMC is passed the test. In the third test (Variable Load Test), The results shown that the ripple is higher on P&O controlled PV and TEG behavior than STSMC Controlled PV and TEG. The Fuel Cell behavior is distorted on P&O controlled system. In electrolyser behavior, the resistive load effected the occurs overshoot, however in the motor load this change is shown as small ripple on STSMC. In summary, the STSMC is passed all the tests according to results. Using STSMC some ripples and behavior distortions are prevented. The all goals that mentioned in hypothesis is obtained.

REFERENCES

AbdelHady, R. (2017). Modeling and simulation of a micro grid-connected solar PV system. *Water Science*, 31(1), 1-10.

Abukan, Y., and Almalı, M. N. (2023). İki serbestlik dereceli TRMS MIMO sistemin FOPID ve FOSTSMC yöntemi kullanılarak kontrolü . *Gazi Üniversitesi Mühendislik Mimarlık Fakültesi Dergisi*, *38*(1) ,605-616 .

Algowairi, A.B. (2017). *Modelling and simulation of microgrid using photovoltaic and battery based power generation.* Master's thesis, Graduate School of Natural And Applied Sciences Of Karabük University, Karabük.

Alhammad, Y.A., Al-Azzawi, W.F., and Tutunji, T.A. (2016, March 21-24). *Current control to improve COP of thermoelectrical generator and cooler for PV panel cooling.* Paper presented at the 2016 13th International Multi-Conference on Systems, Signal & Devices (SSD), Leipzig.

Alkan, A. (2016). *Yenilenebilir hibrit enerji kaynakları ile beslenen konutlarda akıllı enerji depolama ve yönetim sistemi*. Master's thesis, Graduate School of Natural and Applied Sciences of Kocaeli University, Kocaeli.

Altanneh, N . (2012). *Güneş pili ve hidrojen yakıt pilinden beslenen küçük bir elektrikli araç için batarya şarj sistemi tasarımı ve gerçekleştirlmesi*. Master's thesis, Graduate School of Natural and Applied Sciences of Gazi University, Ankara.

Altun, A. F. and Kılıç, M. (2019). Dynamic simulation of a PV/wind hybrid power generation system: case study of bursa province . *Uludağ Üniversitesi Mühendislik Fakültesi Dergisi ,* 24(2) , 571-582 .

Ammar, M.A., Chaabene, M., and Chtourou, Z. (2013). Artificial neural network based for PV/T panel to rack optimum thermal and electrical power. *Energy Conversion and Management,* 65, 372-380.

Ammari, C., Belatrache, D., Touhami, B., and Makhloufi, S. (2022). Sizing, optimization, control and energy management of hybrid renewable energy system—A review. *Energy and Built Environment,* 3(4), 399-411.

Ang, T-Z., Salem, M., Kamarol, M., Das H.S., Nazari, M.A., and Prabaharan, N. (2022). A comprehensive study of renewable energy sources: Classification, challenges and suggestions. *Energy Strategy Reviews,* 43(100939), 1-27.

Aoun, N., Chenni, R., Nahman, B., and Bouchouicha, K. (2014). Evaluation of validation of equivalent five-parameter model performance for photovoltaic panels using only reference data. *Energy and Power Engineering,* 6(9), 235-245.

Arıcı, N. and İskender, A. (2020). Fotovoltaik güneş santrallerinde şebeke bağlantı sorunları ve çözümleri. *Journal of Polytechnic,* 23(1), 215-222.

Ataol, M.T. (2021). *TEG yoğunluğunun sıcak hava akışı olan kapalı geometrilerde elektrik gücü üretimi ve evrimine etkisi: 3 boyutlu nümerik hesaplama yaklaşımı*. Doctoral dissertation, Graduate School of Natural and Applied Sciences of Kırıkkale University, Kırıkkale.

Baba, A.O., Liu, G., and Chen, X. (2020). Classification and evaluation review of maximum power point tracking methods. *Sustainable Futures*, 2.

Bandara, K., Sweet, T., and Ekanayake, J. (2012). Photovoltaic applications for off-grid electrification using novel multi-level inverter technology with energy storage. *Renewable Energy,* 37(1), 82-88.

Barrios, M.A., Cardenas, V., Sandoval, J.M., Guerrero, J.M., and Vasquez, J.C. (2021). A cascaded DC-AC-AC grid-tied converter for PV plants with AC-link. *Electronics,* 10(4), 1-21.

Başoğlu, M.E. (2021). Comparison of different maximum power point tracking strategies with zeta converter. *Balkan Journal of Electrical & Computer Engineering,* 9(3), 221-228.

Başoğlu, M.E., and Çakır, B. (2015). An improved incremental conductance based MPPT approach for PV modules. *Turkish Jounral of Electrical Engineering & Computer Sciences,* 23(6), 1687-1697.

Bekele, G., and Tadesse, G. (2012). Feasibility study of small hydro/PV/wind hybrid system for off-grid rural electrification in Ethiopia. *Applied Energy,* 97, 5-15.

Bekker, B., and Beukes, H.J. (2004, September 15-17). *Finding an optimal PV panel maximum power point tracking method.* Paper presented at 2004 IEEE Africon. Conference in Africa (IEEE Cat. No. 04CH37590), Gaborone.

Belkaid, A., Colak, I., and Kayisli, K. (2016). Implementation of a modified P&O-MPPT algorithm adapted for varying solar radiation conditions, *Electrical Engineering,* 99, 839-846.

Belkaid, A., Colak, I., and Kayisli, K. (2016, September 25-28). *Optimum control strategy based on an equivalent sliding mode for solar systems with battery storage*. Paper presented at 2016 IEEE International Power Electronics and Motion Control Conference (PEMC), Varna.

Belkaid, A., Colak, I., and Kayisli, K. (2017, November 05-08). *A comprehensive study of different photovoltaic peak power tracking methods*, Paper presented at 2017 IEEE 6th Inetrnational Conference on Renewable Energy Research and Applications (ICRERA), San Diego.

Belkaid, A., Colak, I., and Kayisli, K. (2017, November 05-08). *Modeling and simulation of thermos electrical generator with MPPT.* Paper presented at 2017 IEEE 6th International Conference on Renewable Energy Research and Applications (ICRERA), San Diego.

Belkaid, A., Colak, I., Kayisli, K., and Bayındır, R. (2019). Design and implementation of a cuk converter controlled by a direct duty cycle INC-MPPT in PV battery system. *International Journal of Smart Grid- (IJSMARTGRID),* 3(1), 19-25.

Belkaid, A., Colak, I., Kayıslı, K., and Bayındır, R. (2020, June 17-19). *Improving PV system performance using high efficient fuzzy logic control.* Paper presented at 2020 8th International Conference on Smart Grid (icSmartGrid), Paris.

Belkaid, A., Colak, I., Kayıslı, K., Bayındır, R., and Bulbul H.B. (2018, 04-06 December). *Maximum power extraction from a photovoltaic panel and a thermoelectric generator constituting a hybrid electrical generation system.* Paper presented at the 6th IEEE International Conference on Smart Grid (icSmartGrid), Nagasaki.

Belkaid, A., Colak, I. Kayisli, Sara, M., and Bayindir, R. (2019, December 9-11). *Modeling and simulation of polycrystalline silicon photovoltaic cells.* Paper presented at 2019 7th International Conference on Smart Grid (icSamrtGrid), Newcastle.

Beyarslan, S. (2021*). Yenilenebilir enerji kaynakları ile mikro şebeke tasarımı ve optimum çözümünün Homer ile incelenmesi*. Master's thesis, Graduate School of İstanbul Technical University, İstanbul.

Bijkumar, B., Raam, A.G.K., Ganesan, S.I., and Nagamani C. (2020). Adaptability of grid connected PV inverters with thermoelectric generator as power source: a performance comparison. *The Institution of Engineering and Technology (IET) Power Electronics,* 13(5), 981-990.

Bilen, G.H. (2011). *Termoelektrik modüllerden oluşan bir sistemin yapay sinir ağları ile Modellenmesi*. Master's thesis, Graduate School of Natural and Applied Sciences of Gazi University, Ankara.

Bishnoi, D. and Chaturvedi, H. (2022). Optimised site selected of hybrid renewable installations for flare gas reduction using multi-criteria decision making. *Energy Conversion and Management: X,* 13, 1-13.

Bıyıkoğlu, A. (2003). Historical Development, working principles and state of the art fuel cell. *Gazi University Journal of Science,* 16(3), 523-542.

Bhuyan, A.K.C., Sao ,B.S.K., and Mahapatra, K. (2012, March 16-18). *Fuel cell connected to grid through inverter.* Paper presented at 2012 Students Conference on Engineering and systems, Allahabad.

Boylestad, R., and Nashelsky, L. (1998). *Electronic devices and circuit theory* (7th edition). Upper Saddle River, New Jersey, and Columbus, Ohio : Prentice Hall. 908.

Brent, A.C., and Rogers, D.E. (2010). Renewable rural electrification: Sustainability assessment of mini-hybrid off-grid technological systems in the African context. *Renewable Energy,* 35(1), 257-265.

Caamano, E., and Lorenzo, E. (1996). Modelling and financial analysis tolls for PV grid-connected systems. *Progress in Photovoltaics: Research and Applications,* 4(4), 295-305.

Caglayan, R.Z., Kayisli, K., Zhakiyev, N., Harrouz, A.,and Colak, I. (2022, September 18-21). *A case study: Standalone hybrid renewable energy systems.* Paper presented at 11th IEEE International Conference on Renewable Energy Research and Application (ICRERA), İstanbul.

Caglayan, R.Z., Kayisli, K., Zhakiyev, N., Harrouz, A., and Colak, I. (2022). A review of hybrid renewable energy systems and MPPT methods. *International Journal of Smart Grid,* 6(3), 72-82.

Cao, D. and Peng, F.Z. (2011). Multiphase multilevel modular DC-DC converter for high-current high-gain TEG application. *IEEE Transactions on Industry Applications,* 47(3), 1400-1408.

Can, Ö. (2016). *Yenilenebilir microgrid systemin meta-sezgisel bir yöntem ile optimal güç Planlaması.* Master's thesis, Graduate School of Natural and Applied Science of Düzce University, Düzce.

Canada, S., Moore, L., Post, H., and Strachan, J. (2004). Operation and maintenance field experience for off-grid residential photovoltaic systems, *Progress in Photovoltaics: Research and Applications,* 13(1), 67-74.

Chakir, A., Abid, M., Tabaa, M., and Hachimi, H. (2022). Demand-side management strategy in a smart home using electric vehicle and hybrid renewable energy system. *Energy Reports*, 8(9), 383-393.

Choudhury, S., and Rout, P.K. (2015). Adaptive fuzzy logic based MPPT control PV system under partial shading condition. *International Journal of Renewable Energy Research*, *5*(4), 1252-1263.

Conn, R.W. (Ed.) (2023). *nuclear fusion*. Encyclopedia Britannica

Coppola, M., Daliento, S., Guerriero, P., Lauria, D., and Napoli, E. (2012, June 20-22). *On the design and the control of a coupled-inductors boost dc-ac converter for an individual PV panel.* Paper presented at International Symposium on Power Electronics, Electrical Drives, Automation and motion, Sorrento.

Cotfas, D.T., Cotfas, P.A., Mahmoudinezhad, S., and Louzazni, M. (2022). Critical factors and parameters for hybrid photovoltaic-thermoelectric systems; review. *Applied Thermal Engineering,* 215, 1-23.

Çalışkan, E. (2011). *Fotovoltaik sistemler için DSP temelli güneş çeviricisi tasarımı ve Uygulaması.* Master's thesis, Graduate School of Natural and Applied Sciences İstanbul Technical University, İstanbul.

Çavuşoğlu , A. (2006). *Yakıt pilleri ve kullanım alanları.* Master's thesis, Graduate School of Natural and Applied Science of Uludağ University, Bursa.

Çelikel, R. and Gündoğdu, A. (2021). Comparison of PO and INC MPPT methods using fpga in-the-loop under different radiation conditions . *Balkan Journal of Electrical and Computer Engineering* , 9(2) , 114-122 .

Çiçek, N. (2013). *Demand response and supply optimization in smart grids with renewable energy sources* (Master's thesis, Institute for Graduate Studies in Science and Engineering of Boğaziçi University, İstanbul.

Diemuodeke, O. , Agbalagba, E. O. and Okorho, M. İ. (2014). Building integrated hybrid pv-battery-diesel generator energy system for oil producing communities in niger-delta region of nigeria . *International Journal Of Renewable Energy Research* , 4(2) , 286-293.

Djoudi, A., Chekireb, H., Berkouk, E.M., and Bacha, S. (2015). Low-cost sliding mode control of WECS based on DFIG with stability analysis. *Turkish Journal of Electrical Engineering & Computer Sciences,* 23(6), 1698-1714.

Dongmei, Z., Nan, Z., and Yanhua, L. (2012, May 21-24). *Micro-grid connected/islanding operation based on wind and PV hybrid power system.* Paper presented at IEEE PES Innovative Smart Grid Technologies, Tianjin.

Drake, G.W.F., Schreiber, B.A., Gaur, A., Gregersen, E, Hosch, W.L., Lotha, G., Manchanda, K., and The Editors of Encyclopedia Britannica. (2023). *entropy*. Encyclopedia Britannica.

Dris, M., and Djilani, B. (2013). Comparative study of algorithms (MPPT) applied to photovoltaic systems. *International journal of renewable energy research*, 3(4), 872-879.

Edouard, M. and Njomo, D. (2013). Mathematical modelling and digital simulation of PV solar panel using MATLAB software. *International Journal of Emerging Technology and Advance Engineering*, 3(9), 24-32.

Ekşi, E. (2019). *Akıllı şebekelerin mikro güneş santralleri ile entegrasyonu.* Master's thesis, Graduate School of Science and Engineering of Yıldız Technical University, İstanbul.

Eldessouky, A.S., Mahmoud, I.M., and Abdel-Salam, T.S. (2023). MPPT based on a novel load segmentations structure for PV applications. *Ain Shams, Engineering Journal*, 14(4), 1-12.

Erdoğan, Y., Dinçler, T., Kuncan, M., and Ertunç, H.M. (2014, September 11-13). *Güneş panelleri için yüksek verimli maksimum güç noktası izleyici (MPPT) tasarımı.* Proceedings of the TOK 2014, Kocaeli.

Fara, L. and Craciunescu, D. (2017). Output analysis of stand-alone PV systems: Modelling, simulation and control. *Energy Porcedia,* 112, 595-605.

Farhat, O., Khaled, M., Faraj, J., Hachem, F., Taher, R., and Castelain, C. (2022). A short recent review on hybrid energy systems: Critical analysis and recommendations. *Energy Reports,* 8(9), 792-802.

Fawzy, T., Premm, D., Bletterie, B., and Gorsek, A. (2011). Active contribution of PV inverters to voltage control – from a smart grid vision to full-scale implementation. *e & i Elektrotechnik und Informationstechnik,* 128, 110-115.

Fazalyar, W. (2021). *Control of power flow in large-scale PV microgrid with load control and energy storage system.* Master's thesis, Institute of Graduate Studies of İstanbul Aydın University, İstanbul.

Fini, M.A., Gharapetian, D., and Asgari, M. (2022). Efficiency improvement of hybrid PV-TEG system based on an energy, exergy, energy-economic and environmental analysis; experimental, mathematical and numerical approaches. *Energy Conversion and Management*, 265, 1-28.

Ganesan, E., Dash, S.S., and Samanta, C. (2016). Modeling, control and power management for a grid-integrated photo voltaic, fuel cell, and wind hybrid system. *Turkish Journal of Electrical Engineering and Computer Sciences,* 24(6), 4804-4823.

Ghoddami, H., Delghavi, M.B., and Yazdani, A. (2012). An integrated wind-photovoltaic-battery system with reduced power-electronic interface and fast control for grid-tied and off-grid applications. *Renewable Energy*, 45, 128-137.

Goel, S., and Ali, S.M. (2013). Feasibility study of hybrid energy systems for remote area electrification in odisha, india by using HOMER . *International Journal Of Renewable Energy Research* , 3(3) , 666-672 .

Gözlükaya, H.G. (2018). *Mikro şebekeye bağlı fotovoltaik panelden beslenen lityum batarya sisteminin farklı yük durumlarına göre enerji yönetimi*. Master thesis, Graduate School of Natural and Applied Science of İstanbul Technical University, İstanbul.

Gupta, A., Saini, and Sharma, M.P. (2010). Steady-state modelling of hybrid energy system for off grid electrification of cluster of villages. *Renewable Energy*, 35(2), 520-535.

Güler, N. (2021). 9-Seviyeli paket e-hücreli eviriciler için üstün burulma algoritması tabanlı kayan kipli kontrol tasarımı, *Gazi University Jounral of Science Part C: Design and Technology*, 9(1), 57-70.

Internet: Hydrogen and Fuel Cell Technologies Office. (n.d.). *Fuel Cells.* Web: https://www.energy.gov/eere/fuelcells/fuel-cells, Date of access: 21.11.2022.

Internet: Hydrogen and Fuel Cell Technologies Office. (n.d.). *Types of Fuel Cells.* Web: https://www.energy.gov/eere/fuelcells/types-fuel-cells, Date of access: 21.11.2022.

Internet: Infineon. (2021). *MOSFET 650V CoolMOS^{TM} CFD7 SJ Power Device.* Web: https://eu.mouser.com/datasheet/2/196/Infineon_IPW65R018CFD7_DataSheet_v02_00_EN-3165662.pdf, Date of access 21.11.2022.

Internet: Infineon. (2018). *6th Generation CoolSiCTM 650V SiC Schottky Diode.* Web: https://www.infineon.com/dgdl/Infineon-IDDD06G65C6-DS-v02_00-EN.pdf?fileId =5546d462625a528f01628f86ff8c0e09, Date of access 21.11.2022

Internet: Kanimba, E., and Tian, Z . (2016). *Thermoelectrics for Power Generations*. Web: https://www.researchgate.net/publication/312277890_Modeling_of_a_Therm oelectric_Generator_Device. 479, Date of access 21.11.2022

Internet: Microsemi. (2020). *MSC035SMA070S Silicon Carbide N-Channel Power MOSFET.* Web: https://eu.mouser.com/datasheet/2/268/Microsemi_MSC035SM A070S_SiC_MOSFET_Datasheet_B-2934508.pdf, Date of Access: 21.11.2022

Internet: Office of Energy Efficiency & Renewable Energy. (n.d.). *Solar Radiation Basics.* Web: https://www.energy.gov/eere/solar/solar-radiation-basics, Date of Access: 21.11.2022

Internet: ROHM SEMICONDUCTOR (2021). *RFL60TZ6S Ultra Fast Recovery Diode.* Web: https://fscdn.rohm.com/en/products/databook/datasheet/discrete/diode/fast_ recovery/rfl60tz6sgc13-e.pdf, Date of Access:21.11.2022

Internet: Zaitsu, R. (2009). *Voltage Mode Boost Converter Small Signal Control Loop Analysis Using the TPS61030.* Web: https://www.ti.com/lit/an/slva274a/ slva274a.pdf?ts=1678346681737&ref_url=https%253A%252F%252Fwww.google. com%252F, Date of Access:21.11.2022

Hafez, A.A.A. (2015). Multi-level cascaded DC/DC converters for PV applications. *Alexandria Engineering Journal*, 54(4), 1135-1146.

Hakimizad, S., Asl, S.R., and Ghiai, M.M. (2015). A review on the design approaches using renewable energies in urban parks. *International Journal of Renewable Energy Research*, 5(3), 686-693.

Hasanzadehfard, H., Moghaddas-Tafreshi, M., and Hakimi, S.M. (2015). Optimization of grid connected micro-grid consisting of PV/FC/UC with considered frequency control. *Turkish Journal of Electrical Engineering and Computer Sciences*, 23(1), 1-16.

Hatlehol, M.U., and Zadeh, M. (2022). Super-twisting algorithm second-order sliding mode control of a bidirectional DC-to-DC converter supplying a constant power load. *IFAC- PapersOnLine,* 55(31), 287-294.

Hatzikraniotis, E., Zorbas, K.T., Samaras, I., Kyratsi, Th., and Paraskevopoulos, K.M. (2009). Efficiency study of a commercial thermoelectric power generator (TEG) under thermal cycling. *Journal of Electronic Materials,* 39(9), 2112-2116.

He, W. (1997). Numerical analysis of molten carbonate fuel cell systems. *International Journal of Energy Research,* 21(1), 69-76.

He, W. (1998). An investigation on the dynamic performance of molten carbonate fuel-cell power- generation system. *International Journal of Energy Research,* 22(4), 355-362.

He, Z.Y., and Chen H. (2011). Integrated solar controller for solar powered of grid lighting system. *Energy Procedia,* 12 , 570-577.

Hong, G.W., and Abe, N. (2012). Sustainability assessment of renewable energy projects off-grid rural electrification: The pagan- and island case in Philippines. *Renewable and Sustainable Energy Reviews,* 16(1), 54-64.

Hoang, P., Bourdin, V., Liu, Q., Caruso, G., and Archambault, V. (2014). Coupling optical and thermal models to accurately predict PV panel electricity production. *Solar Energy Materials and Solar Cells*, 125, 325-338.

Holweg, G.V., Evald, P.J.D. de O., Milbradt, D.M.C., Tambara, R.V., and Gründling H.A. (2022). Design of continuous-time model reference adaptive and super-twisting sliding mode controller. *Mathematics and Computers in Simulation,* 201, 215-238.

Hyunh, D.C., Dunnigan, M.W. (2016). Development and comparison of an improved incremental conductance algorithm for tracking the MPP of a solar PV panel. *IEEE Transactions on Sustainable Energy,* 7(4), 1421-1429.

Irwin, J.D., Nelms, R.M. and Patnaik, A. (2015). *Engineering Circuit Analysis* (11th edition), Asia: John Wiley & Sons (Asia) Pte Ltd, 716.

Jiang, S., Cao, D., Peng F.Z., and Li, Y. (2012). Grid-connected boost-half-bridge photovoltaic micro inverter system using repetitive current control and maximum power point tracking. *IEEE Transactions on Power Electronics,* 27(11), 4711-4722.

Jouhara, H., Zabnienska-Gora, A., Khordahgah, N., Doraghi, Q., Ahmad, L., Norman, L., Axcell, B., Wrobel, B., Wrobel, L. and Dai, S. (2021). Thermoelectric generator (TEG) technologies and applications. *International Journal of Thermofluids,* 9(100063), 1-18.

Kale, R., Thale, S., and Agarwal, V. (2013, June 16-21). *Design implementation of a solar PV panel integrated inverter with multi-mode-operation capability.* Paper presented at 2013 IEEE 39th Photovoltaic specialists conference (PVSC), Tampa.

Kartite, J. and Cherkaoui, M. (2019). Study of the different structures of hybrid systems in renewable in renewable energies: A review. *Energy Procedia,* 157, 323-330.

Kasper, M., Bortis, D., Friedli, T., Kolar, W. (2013). Classification and comparative evaluation of PV panel integrated DC-DC converter concepts. *IEEE Transactions on Power Electronics*, 29(4), 2511-2526.

Kasper, M., Herden, S., Bortis, D., and Kolra, J.W. (2014, August 26-28). *Impact of PV string shading conditions on panel voltage equalizing converters and optimization of a single converter system with overcurrent protection.* Paper presented at 2014 16th European Conference on Power Electronics and Applications, Lappeenranta.

Karanfil, G. (2020). Proton değişim membran yakıt hücreleri: termodinamiği, bileşenleri ve uygulama alanları . *Mühendis ve Makine,* 61(698), 57-76.

Kayisli, K. (2023). Super twisting sliding mode-type 2 fuzzy MPPT control of solar PV system with parameter optimization under variable irradiance conditions. *Ain Shams Engineering Journal,* 14(1), 1-14.

Kayışlı, K. and Caglayan, R.Z. (2022). Twisting sliding mode control based maximum power point tracking . *Balkan Journal of Electrical and Computer Engineering* , 10(4) , 356-362.

Keleş C. (2017). *Akıllı şebekelerde yenilenebilir enerji üretimine sahip akıllı evlerin enerji ve yük yönetimi*. Doctoral dissertation, Graduate School of Natural and Applied Science of İnönü University, Malatya.

Kim, H.-s., Kim, J.-H., Min, B.-D., Yoo, D.-W., and Kim, H.-J. (2009). A highly efficient PV system using a series connection of DC-DC converter output with a photovoltaic panel. *Renewable Energy,* 34(11), 2432-2436.

Khan, A.A. (2019), *Investigation of new control methods for hybrid AC/DC microgrid.* Master’s thesis, Institute of Science and Technology of İstanbul Aydın University, İstanbul.

Koca, Ö. (2017). *Güneş panellerinin şebeke bağlantısının kaskat H-köprü çok seviyeli evirici topolojisiyle gerçekleştirilmesi*. Master’s thesis, Graduate School of Natural and Applied Sciences of Gazi University, Ankara.

Kocabaş, A. (2017). *Design and optimization of a fuzzy logic based maximum power point tracker for PV panel*. Master's thesis, Graduate School of Natural and Applied Sciences of Karadeniz Technical University, Trabzon.

Korodi, A. (2012, October 03-05). *Building a knowledge base to obtain the maximum power point for a PV panel.* Paper presented at 2012 IEEE International Conference on Control Applications, Dubrovnik.

Koyi, O.O. (2019). *Improving the reliability of Nigeria's electricity grid with renewable energy microgrids.* Master's thesis, Graduate School of Natural and Applied Sciences of Karadeniz Technical University, Trabzon.

Koyuncuoğlu, A.S. (2019). *Blockchain applications on smart grid: a review.* Master's thesis, School of Graduate Studies Kadir Has University, İstanbul.

Kurak, E., Erdemir, V. and Dursun, B. (2016). PV sistemin için maksimum güç noktası izleyicisi tasarımı ve uygulaması. *Düzce Üniversitesi Bilim ve Teknoloji Dergisi,* 4(2), 581-592.

Latif, S. (2019) *Control microgrid with renewable energy source and multiple converters.* Master's thesis, Institute of Graduate Studies of Istanbul Aydın University, İstanbul.

Levron, Y., and Shmilovitz, D. (2013). Maximum power point tracking employing sliding mode control. *IEEE Transactions on Circuits and Systems I: Regular Papers,* 60(3), 724-732.

Li, C., Zhou, D., Zhang, L., and Shan, Y. (2022). Exploration on the feasibility of hybrid renewable energy generation in resource- based areas of China: Case study of a regeneration city. *Energy Strategy Reviews,* 42, 1-15.

Liu, C., Chau, K.T., Diao, C., Zhong, J., Zhang, X., Gao, S., and Wu D. (2010,September 01-03). *A new DC micro-grid system using renewable energy and electric vehicles for smart energy delivery.* Paper presented at 2010 IEEE Vehicle Power and Propulsion Conference, Lille.

Lloret, A., Andreu, J., Merten, J., Puigdollers, J., Aceves, O., Sabata, L., Chantant, M., and Eicker, U. (1998). Large grid-connected hybrid PV system integrated in a public building. *Progress in Photovoltaics: Research and Applications,* 6(6), 453-464.

Loba, T.H., and Salim, K.M. (2013, May 17-18). *Design and implementation of a micro-inverter for single PV panel based solar home system.* Paper presented at 2013 International Conference on Informatics, Electronics and Vision (ICIEV), Dhaka.

Maleki, A. and Askarzadeh, A. (2013). optimum configuration of fuel cell-b PV/wind hybrid system using a hybrid metaheuristic technique . *International Journal of Engineering and Applied Sciences,* 5(4), 1-12.

Mamur, H., and Çoban, Y. (2020). Detailed modelling of a thermoelectric generator for maximum power point tracking. *Turkish Journal of Electrical Engineering & Computer Sciences,* 28(1), 124-139.

Mao, M., Cui, L., Zhang, Q., Guo, K., Zhou, L., and Huang, H. (2020). Classification and summarization of solar photovoltaic MPPT techniques: A review based on traditional and intelligent control strategies. *Energy Reports,* 6, 1312-1327.

Marti-Arbona, E., Mandal D., Bakkaloglu, B., and Kiaei, S. (2015, March 15-19). *PV panel power optimization using sub-panel MPPT.* Paper presented at 2015 IEEE Applied Power Conference and Exposition (APEC), Charlotte.

Mayer, M.J., Szilagyi, A., and Grof, G. (2020). Environmental and economic multi-objective optimization of a household level hybrid renewable energy system by genetic algorithm. *Applied Energy,* 269(115058), 1-16.

McGrayne, S.B., Bertsch, G.F., Trefil, J., Albert, M., Augustyn, A., Chauhan, Y., Gaur, A Gregersen, E., Higgins, J., Hosh, W.L., Lotha, G., Metych, M., Parwani, N., Petruzzello, M., Promeet, D., Rodriguez E., Rogers, K., Sampaolo, M, Shukla, G., Singh S., Tikkanen, Young, G., and The Editors of Encyclopedia Britannica (Ed.). (2023). *atom*. Encyclopedia Britannica.

Mehdipour, A., Majdinasab, H., Khazraj, H., and Kumar, A.V. (2012, December 17-19). *Voltage -Fed trans Z source inverter in PV solar panel.* Paper presented at 2012 5th International Conference on Computers and Devices for Communication (CODEC), Kolkata.

Meyer, E.I. (2017). Extraction of saturation current and ideality factor form measuring V_{oc} and I_{sc} of photovoltaic modules. *International Journal of Photoenergy,* 2017, 1-9.

Mnati, M.J., Araujo, V.G.M., Abed, J.K., and den Bossche, A.V. (2018, June). *Review different types of MPPT techniques for photovoltaic systems.* Paper presented at International Conference on Sustainable Energy and Environment Sensing (SEES 2018). Cambridge City

Mo, Q., Chen M., Zhang, Z., Zhang, Y., and Qian, Z. (2012, February 05-09). *Digitally controlled active clamp interleaved flyback converters for improving efficiency in photovoltaic grid-connected micro-inverter.* Paper presented at 2012 Twenty-Seventh Annual IEEE Applied Power Electronics Conference and Exposition (APEC), Orlando.

Moghanlou, S.N. (2020). *Yenilenebilir enerji kaynaklarının ve enerji depolama sistemlerinin yer aldığı, akıllı dc mikroşebeke*. Master's thesis, Graduate School of Natural and Applied Science of Kocaeli University, Kocaeli.

Mortimer, C.E. (1999). *Modern Üniversite Kimyası Cilt 2* (T. Altınata, H. Akçay, H. Anıl, H. Avcıbaş, D. Balköse, S. Çelebi, E. Henden, G. Nişli, M. Toprak, D. Tosçalı, B. Yenigül, Trans.). İstanbul: Çağlayan Kitabevi. 464.

Mortimer, C.E. (2004). *Modern Üniversite Kimyası Cilt 1* (T. Altınata, H. Akçay, H. Anıl, H. Avcıbaş, D. Balköse, S. Çelebi, E. Henden, G. Nişli, M. Toprak, D. Tosçalı, B. Yenigül, Trans.). İstanbul: Çağlayan Kitabevi. 522.

Mosteiro, P., Bellini, G., Benziger, J., Bick, D., Bonfini, G. Bravo, D., Caccisnigs, B. Cadonati, L., Calaprice, F., Caminata, A., Cavalcante, P., Chavarria, A., Chepurnov, A., D'Angelo, D., Davini, S., Derbin, A., Empl, A., Etenko, A., Fomenko, k., Franco, K., Franco, D., Gabriele, F., Galbiti, C., Gazzana, S., Ghino, C., Giamamrchi, M., Göger-Neff, M., Goertti, A., Gromov, M., Hagner, C., Hungerfold, E., Al. lanni, An. lanni, Kobychev, V., Korablev, D., Korga, G., Kryn, D., Laubenstein, M., Lehnert, B., Lewke, T., Litvinovich, E., Lombardi, F., Lombardi, P., Ludhova, L., Lukyanchenko, G., Machulin, I., Manecki, S., Maneschg, W., Marcocci, S., Meindl, Q., Meroni, E., Meyer, M., Miramonti, L., Misiaszek, M., Mountuschi, M., Muratova, V., Oberauer, L., Obonlensky, M., Ortica, F., Otis, K., Pallavicini, M., Papp, L., Perasso, L., Pocar, A., Ranucci, G., Razeto, A., Re, A., Romani, A., Rossi, N., Saldanha, R., Salvo, C., Schönert, S., Simgen, H., Skorokhvatov, M., Smirnov, O., Sotnikov, A., Sukhotin, S., Suvorov, Y., Tarraglia, R., Testera, G., Vignaud, D., Vogelaar, R.B., von Feilitzsch, F., Wang, H., Winter, J., Wojcik, M., Wright, A., Wurn M., Zaimidoroga, O., Zavatarelli, S., Zuber, K., Zuzel, G., Zuzel, G. (2015). Low-energy (anti)neutrino physics with borexino: Neutrinos from the primary proton-proton fusion process in the Sun. *Nuclear and Particle Physics Proceedings*, 265-266, 87-92.

Nagayoshi, H., Nakabayashi, T., Maiwa, H., and Kajikawa, T. (2011). Development of 100-w high-efficiency MPPT power conditioner and evaluation of TEG system with battery load. *Journal of Electronic Materials*, 40(5), 657-661.

Nayar, C.V. (2020, July 16-20). *Control and interfacing of bi-directional inverters for off-grid and weak grid photovoltaic power systems.* Paper presented at the 2000 Power and Engineering Society Summer Meeting (Cat. No.00CH37137), Seattle.

Naz, M.Y., Bou-Rabee, M., Shukrullah, S., Ghaffar, A., Gungor, A., and Sulaiman, S.A. (2021). A review of hybrid energy technologies tenets, controls and combinational strategies. *Cleaner Engineering and Technology,* 5, 1-11.

Nguyen, T.N., and Luo, A. (2014). Multifunction converter based Lyapunov function used in a photovoltaic system. *Turkish Journal of Electrical Engineering and Computer Sciences,* 22(4), 893-908.

Nour, M., and Rohani, G. (2014). Prospect of stand-alone PV-diesel hybrid power system for rural electrification in UAE . *International Journal Of Renewable Energy Research* , 4(3) , 749-758.

Nur, A. (2022). *Akıllı şebekelerde AC/DC hibrit enerji sistemlerinin güç akış analizi*. Doctoral dissertation, Graduate School of Natural and Applied Science İnönü University, Malatya.

Obara, S. (2007). Power characteristics of a fuel cell micro-grid with wind power generation. *International Journal of Energy Research*, 31(11), 1064-1075.

Obara, S. (2008). Equipment plan of compound interconnection micro-grid composed from diesel power plants and solid polymer membrane-type fuel cell. *International Journal of Hydrogen Energy*, 33(1), 179-188.

Oğuz, Y. , Oğuz, H. , Yabanova, İ. , Oguz, E. and Kırkbaş, A. (2012). Efficiency Analysis of Isolated Wind-Photovoltaic Hybrid Power System With Battery Storage for Laboratory General Illumination for Education Purposes . *International Journal Of Renewable Energy Research* , 2(3) , 440-445.

Omran, A., Lucchesi, A., Smith, D., Alaswad, A., Amiri, A., Wilberforce, T., Sodre, J.R., and Olabi, A.G. (2021). Mathematical model of proton-exchange membrane (PEM) fuel cell. *International Journal of Thermofluids,* 11, 1-10.

Onat, N., and Ersöz, S. (2009). *Fotovoltaik sistemlerde maksimum güç noktası izleyici algoritmalarının karşılaştırılması.* Paper presented at 5th Yenilenebilir Enerji Kaynakları Sempozyumu 2009, Diyarbakır.

Özdemir, İ.B. (2021). *Reliability characteristics of a renewable hybrid energy system.* Master’s thesis,Graduate School of Natural and Applied Sciences of Atılım University, Ankara.

Özden, E. (2015). *PEM fuel cell degradation: numerical investigation and effects on the performance of solar-hydrogen based renewable energy systems.* Doctoral dissertation, Graduate School of Natural and Applied Sciences of Middle East Technical University, Ankara.

Palizban, O., Rezaei, M.A., and Mekhilef, S. (2011). *Active and reactive power control for a hybrid system with photovoltaic panel, wind turbine fuel cells, electrolyzer and super capacitor in off-grid mode.* Paper presented at 2011 IEEE International Conference on Control Systems, Computing and Engineering, Penang.

Pendem, S.R., and Mikkili, S. (2018). Modeling, simulation and performance analysis of solar PV array configurations (series, series-parallel and honey-comb) to extract maximum power under partial shading conditions. *Energy Reports, 4* , 274-287.

Qadir, Z., Khan, S.I., Khalaji, E., Munawar, H.S., Al-Turjman, F., Mahmud, M.A.P., Kouzani, A.Z., and Le, K. (2021). Predicting the energy output of hybrid PV-wind renewable energy system using feature selection technique for smart grids. *Energy Reports,* 7, 8465-8475.

Qi, C., and Ming, Z. (2012). Photovoltaic module Simulink model of a stand-alone PV system. *Physics Procedia,* 24(A), 94-100.

Qoaider, L., and Steinbrecht, D. (2010). Photovoltaic systems: A cost competitive option to supply energy to off-grid agricultural communities in arid regions. *Applied Energy,* 87(2), 427-435.

Raj ,J.S.S.S., Pounraj, P., Winston, Dr. D.P., Ramaraj, R., and Christabel, S.C. (2015). Intelligent MPPT control techniques for solar PV system. *International Journal of Applied Engineering Research,* 10(55), 3386-3391.

Rahman, A.S.F., Razak, A.R.A., and Hassan, S.I.S. (2016). A conceptual implementation of a buck converter of an off-grid hybrid system consisting of solar and wind turbine sources. *Turkish Journal of Electrical Engineering & Computer Sciences,* 24(5), 3781-3791.

Rahman, S.A., Varma, R.K., and Vanderheide, T. (2014). Generalised model of a photovoltaic panel. *IET Renewable Power Generation,* 8(3), 217-229.

Raof, A.A. (2020). *A comparative study of MPPT methods for PV array under partial shading condition in MATLAB/Simulink.* Master's thesis, Institute of Natural and Applied Sciences of Çukurova University, Adana.

Rao, S.N., Kumar, D.V.A., and Babu, Ch. S. (2018). Grid connected distributed generation system with high voltage gain cascaded DC-DC converter fed asymmetric multilevel inverter topology. *International Journal of Electrical and Computer Engineering (IJECE),* 8(6), 4047-4059.

Rastogi, M., Ahmad, A., and Bhat, A.H. (2021). Performance investigation of two-level reduced-switch D-STATCOM in grid-tied solar-PV array with stepped P&O MPPT algorithm and modified SRF strategy. *Journal of Kind Saud University-Engineering Sciences,* not pressed.

Reinders, A.H.M.E, van Dijk, V.A.P, Wiemken, E., and Turkenberg, W.C. (1999). Technical and economic analysis of grid-connected PV systems by means of simulation. *Progress in Photovoltaics: Research and Applications,* 7(1), 71-82.

Rhaman, M.M. (2013). Hybrid renewable energy system for sustainable future of bangladesh . *International Journal Of Renewable Energy Research* , 3(4) , 777-780.

Ropp, M.E., Begovic, M., and Rohatgi, A. (1999). Prevention of islanding in grid-connected photovoltaic systems. *Progress in Photovoltaic Research and Applications,* 7(1), 39-59.

Roshau, C., Yuvarajan, S., and Schulz, D. (2009, June 07-12). *Modeling and hardware implementation of VMPPT for a PV panel with a reference cell*. Paper presented at 2009 34th IEEE Photovoltaic Specialists Conference (PVSC), Philadelphia.

Saheb, S.S., and Gudey, S.K. (2020). Robust fractional order sliding mode control for solar based DC-AC inverter. *Journal of Energy Systems*, 4(4), 161-178.

Sahoo, N.C., Elamvazuthi, I., Nor, N.M., Sebastian, P., and Lim, B.P. (2011, December 28-30). *PV panel modelling using simscape.* Paper presented at 2011 International Conference on Energy, Automation and Signal, Bhubaneswar.

Saranrom, W., and Polmai, S. (2011, May 17-19). *The efficiency improvement of series connected PV panels operations under partial shading condition by using per-panel DC/DC converter*. Paper presented at the 8th Electrical Engineering/ Electronics, Computer, Telecommunications and Information Technology (ECTI) Association of Thailand – Conference 2011, Khon Kean.

Schumm, B., Schreiber, B.A., Albert, M., Augustyn, A., Gaur, A., Hosch, W.L., Lotha,G. , Rodriguez, E., Singh, S., Sinha, S., Young, G., and The Editors of Encyclopaedia Britannica (Ed.), (2023). *fuel cell*. Encyclopedia Britannica.

Sera, D., Teodorescu, R., and Rodriguez, P. (2007, June 04-07). *PV panel model based on datasheet values.* Paper presented at 2007 IEEE International Symposium on Industrial Electronics, Vigo.

Serway, R.A. and Beichner (2011). *Fen ve Mühendislik için Fizik Model Fizik Cilt 3* (K. Çolakoğlu, Trans.), Ankara:Palme Yayıncılık. 1551.

Sezen, S. (2015). *Üç fazlı şebeke bağlantılı çok seviyeli evirici kullanarak aktif filtreleme yeteneğine sahip fotovoltaik systemin tasarımı ve uygulanması.* Doctoral dissertation, Graduate School of Natural and Applied Science of Kocaeli University, Kocaeli.

Simmons, A.D., and Infield, D.G. (1996). Grid-connected amorphous silicon photovoltaic Array. *Progress in Photovoltaics: Research and Applications,* 4(5), 381-388.

Shaahid, S.M., and El-Amin, I. (2009). Techno-economic evaluation of off-grid hybrid photovoltaic-diesel-battery power systems for rural electrification in Saudi Arabia-a way forward for sustainable development. *Renewable and Sustainable Energy Reviews* , 13(3), 625-633 .

Shah, K., Chen, P., Schwab, A., Shenai, K., S. Gouin-Davis, and Downey L . (2012, May 29-31). *Smart efficient solar DC micro-grid.* Paper presented at 2012 IEEE Energytech, Cleveland.

Sharma, R., and Suhag, S. (2017). Novel control strategy for hybrid renewable energy-based standalone system. *Turkish Journal of Electrical Engineering & Computer Sciences,* 25(3), 2261-2277.

Shen, C.-L., Lee, Y.-C., Su, J.-C., and Tsai, C.-T. (2014, April 26-28). *A high step-up DC/DC converter for PV panel application.* Paper presented at 2014 International Conference on Information Science, Electronics and Electrical Engineering, Sapporo.

Sohail, M., Afrouzi, H.N., Ahmed, J., Mehranzamir, K., Tabassum, M., and Siddique, Md. B. M. (2022). A comprehensive scientometric analysis on hybrid renewable energy systems in developing regions of the world. *Results in Engineering*, 16, 1-18.

Srikumar, K. and Saibabu, Ch. (2020). A system and novel methodology to track maximum power from photo voltaic system: A comparative an experimental analysis. *Journal of King Saud University- Engineering Sciences*, 32(7), 442-458.

Strohl, G.R., Harpester, J.W., President, Intek Inc., Westerville, Ohio, Hosch, W.L., and The Editors of Encyclopaedia Britannica (Ed.), (2007). *Thermoelectric power generator*. Encyclopedia Britannica.

Sutton, C., Invictus, S., Augustyn, A., Curley, R., Gaur, A., Gregersen, E., Jain, P. Hosch, W.L., Lotha, G., Cunningham J.M., Rogriguez, E., Setia, V., and The Editors of Encyclopedia Britannica. (2023) *subatomic particles*. Encyclopedia Britannica.

The Editors of Encyclopaedia Britannica, Gregersen, E., Hosch, W.L., and Young, G. (2022). *free energy*. Encyclopedia Britannica.

Tozlu, Ö.F., and Çalık, H. (2021). A review and classification of most used MPPT algorithms for photovoltaic systems. *Hittite Journal of Science and Engineering,* 8(3), 207-220.

Tuoi, T.T.K., Toan, N.V, and Ono T. (2020). Theorical and experimental investigation of a thermoelectric generator (TEG) integrated with a phase change material (PCM) for harvesting energy from ambient temperature changes. *Energy Reports,* 6, 2022-2029.

Ullah, Md. H. (2013). An Efficiency Solar-wind-diesel-battery hybrid power system for St. martin island of Bangladesh. *International Journal of Renewable Energy Research,* 3(3), 659-665.

Ural ,Z., and Gencoglu, M.T. (2010, June 27-30). *Mathematical models of PEM fuel cells.* Paper presented at 5th International Ege Energy Symposium and Exhibition (IEEESE-5), Denizli.

Vakili, S., Schönborn, A., and Ölçer, A.I. (2022). Techno-economic feasibility of photovoltaic, wind and hybrid electrification systems for stand-alone and grid-connected shipyard electrification in Italy. *Journal of Cleaner Production,* 366, 1-11.

Valcan, D.-M., Marinescu, C., and Kaplanis, S. (2008, May 22-24). *Connecting a PV supplied micro-grid to the public grid.* Proceedings of 2008 11th International Conference of Optimization of Electrical and Electronics Equipment, Brasov.

Vazquez, N., Azaf, Y., Cervantes, I., Vazques, E., and Hernandez, C. (2015). Maximum power point tracking based on sliding mode control. *International Journal of Photoenergy,* 2015, 1-8.

Vergragt, P., and van Noort, D. (1996). Sustainable technology development: The mobile hydrogen fuel cell. *Business Strategy and the Environment,* 5(3), 168-177.

Vick, B.D., and Neal, B.A. (2012). Analysis of off-gris wind turbine/solar PV water pumping systems. *Solar Energy,* 86(5), 1197-1207.

Vinod, Kumar, R., and Singh, S.K. (2018). Solar photovoltaic modeling and simulation: As a renewable energy solution. *Energy Reports,* 4, 701-712.

Wehbi, Z., Taher, R., Faraj, J., Castelain, C., and Khaled, M. (2022). Hybrid thermoelectric generators-renewable energy systems: A short review on recent developments. *Energy Reports,* 8(9), 1361-1370.

Yahya, K., Bilgin, M.Z., Erfidan, T., and Çakir, B . (2018, May 03-05). *Improving the performance of the MPPT for thermoelectric generator system by using Kalman filter.* Paper presented at 2018 5th International Conference on Electrical and Electronics Engineering (ICEEE), Istanbul.

Yamagueu, D., Azoumah, Y., Py, X., and Zongo, N. (2011). Experimental study of electricity generation by solar PV/diesel hybrid systems without battery storage for-off-grid areas. *Renewable Energy,* 36(6), 1780-1787.

Yapıcı, H. (2019). *Yenilenebilir enerji kaynaklarının akıllı şebekelere entegrasyonu için yeni bir optimizasyon metodunun geliştirilmesi*. Doctoral dissertation, Graduate Education Institute of Konya Technical University, Konya.

Yılmaz, M. (2019). *Akıllı şebekelerde güç kalitesinin optimizasyonu ve yenilenebilir enerji kaynakları ile entegrasyonu*. Doctoral dissertation, Graduate School of Natural and Applied Science of Karabük University, Karabük.

You, S., Marra, F., and Træholt, C. (2012, March 27-29). *Integration of fuel cell micro-chips on low voltage grid: A danish case study*. Paper presented at 2012 Asia-Pacific Power and Energy Conference, Shanghai.

Yu, D., and Yuvarajan, S. (2006, March 19-23). *Load sharing in a hybrid power system with a PV panel and a PEM fuel-cell*. Paper presented at Twenty-First Annual IEEE Applied Power Electronics Conference and Exposition, 2006.APEC'06, Dallas.

Zafar, M.H., Khan, N.M., Mansoor, M., Mirza, A.F., Moosavi, S.K.R., and Sanfilippo, F. (2022). Adaptive ML-based technique for renewable energy system power forecasting in hybrid PV-wind farms power conversion systems. *Energy Conversion and Management*, 258, 1-15.

Zakharchenko, R., Licea-Jimenez, L., Perez-Garcia, S.A., Vorobiev, P., Dehesa-Carrasco, U., Perez-Robles, J.F., Gonzalez-Hernandez, J., and Vorobiev, Y. (2004). Photovoltaic solar panel for a hybrid PV/Thermal system. *Solar Energy materials and solar cells*, 82(1-2), 253-261.

Zebra, E.I.C., van der Windt, H.J., Nhumaio, G., and Faaij, A.P.C. (2021). A review of hybrid renewable energy systems in mini-grids for off-grid electrification in development countries. *Renewable and Sustainable Energy Reviews,* 144, 1-23.

Zhang, S., Oclon, P., Klemes, J.J., Michorczyk, P., Pielichowska, & Pielichowski, K. (2022). Renewable energy systems for building heating, cooling and electricity production with thermal energy storage. *Renewable and Sustainable Energy Reviews*, 165, 1-22.

APPENDIX

Appendix - 1. PV Panel Drawing

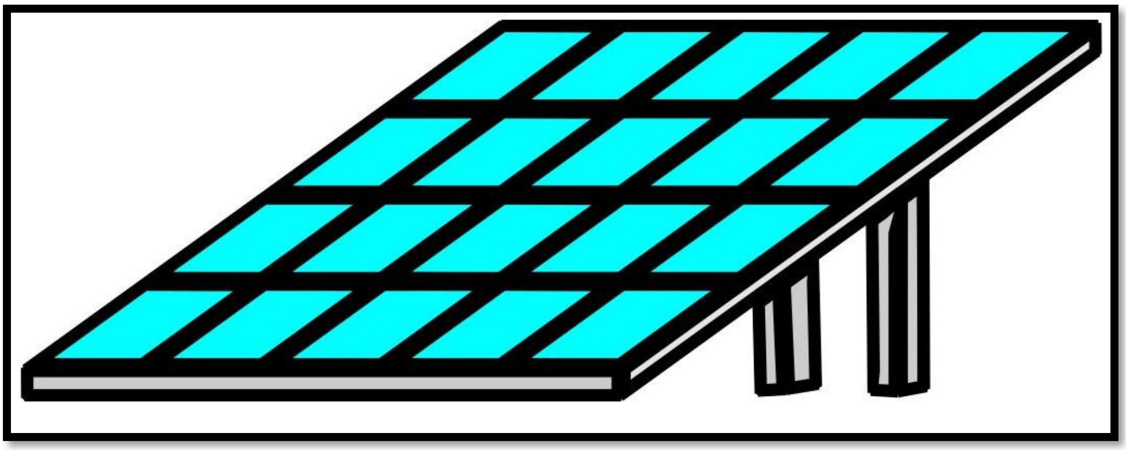

Figure 1.1.: PV Panel Drawing

Gazili olmak ayrıcalıktır